

UNIVERSITAT ROVIRA I VIRGILI

GOLD(I)-CATALYZED CYCLIZATIONS OF 1,6- AND 1,7-ENYNES: NEW GOLD COMPLEXES AND CYCLOPROPANATION REACTIONS

Elena Herrero Gómez

ISBN: 978-84-692-5924-5/DL:T-1663-2009

UNIVERSITAT ROVIRA I VIRGILI

GOLD(I)-CATALYZED CYCLIZATIONS OF 1,6- AND 1,7-ENYNES: NEW GOLD COMPLEXES AND CYCLOPROPANATION REACTIONS

Elena Herrero Gómez

ISBN: 978-84-692-5924-5/DL:T-1663-2009



# **Gold(I)-Catalyzed Cyclizations of 1,6- and 1,7-Enynes: New Gold Complexes and Cyclopropanation Reactions**

**MEMORIA que para optar al grado de  
DOCTORA EN QUÍMICA  
Presenta**

**ELENA HERRERO GÓMEZ**

**Tarragona**

**Julio 2009**

UNIVERSITAT ROVIRA I VIRGILI

GOLD(I)-CATALYZED CYCLIZATIONS OF 1,6- AND 1,7-ENYNES: NEW GOLD COMPLEXES AND CYCLOPROPANATION REACTIONS

Elena Herrero Gómez

ISBN: 978-84-692-5924-5/DL:T-1663-2009

El Prof. Dr. ANTONIO M. ECHAVARREN PABLOS, Catedràtic de la Universidad Autònoma de Madrid i Group Leader de l'Institut Català d'Investigació Química i el Prof. Dr. FELIU MASERAS CUNÍ, Professor Titular de la Universitat Autònoma de Barcelona i Group Leader de l' Institut Català d'Investigació Química,

CERTIFIQUEN:

Que la memòria que porta per títol "Gold(I)-Catalyzed Cyclizations of 1,6- and 1,7-Enynes: New Gold Complexes and Cyclopropanation Reactions", que presenta Elena Herrero Gómez per obtenir el grau de Doctora en Química, ha estat realitzada sota la nostra direcció en els corresponents grups de recerca de l'Institut Català d'Investigació Química.

Tarragona, Juliol de 2009

Prof. Dr. Antonio M. Echavarren

Prof. Dr. Feliu Maseras

UNIVERSITAT ROVIRA I VIRGILI

GOLD(I)-CATALYZED CYCLIZATIONS OF 1,6- AND 1,7-ENYNES: NEW GOLD COMPLEXES AND CYCLOPROPANATION REACTIONS

Elena Herrero Gómez

ISBN: 978-84-692-5924-5/DL:T-1663-2009

UNIVERSITAT ROVIRA I VIRGILI

GOLD(I)-CATALYZED CYCLIZATIONS OF 1,6- AND 1,7-ENYNES: NEW GOLD COMPLEXES AND CYCLOPROPANATION REACTIONS

Elena Herrero Gómez

ISBN: 978-84-692-5924-5/DL:T-1663-2009

*A mi familia*

UNIVERSITAT ROVIRA I VIRGILI

GOLD(I)-CATALYZED CYCLIZATIONS OF 1,6- AND 1,7-ENYNES: NEW GOLD COMPLEXES AND CYCLOPROPANATION REACTIONS

Elena Herrero Gómez

ISBN: 978-84-692-5924-5/DL:T-1663-2009

*“Porque te sé decir, que, aunque me costó algún trabajo componerla,  
ninguno tuvo por mayor que hacer esta prefacción que vas leyendo”*

Miguel de Cervantes

UNIVERSITAT ROVIRA I VIRGILI

GOLD(I)-CATALYZED CYCLIZATIONS OF 1,6- AND 1,7-ENYNES: NEW GOLD COMPLEXES AND CYCLOPROPANATION REACTIONS

Elena Herrero Gómez

ISBN: 978-84-692-5924-5/DL:T-1663-2009

Este trabajo de investigación ha sido realizado en el Institut Català d'Investigació Química (ICIQ) en Tarragona (noviembre 2004-marzo 2009) bajo la dirección del Prof. Antonio M. Echavarren y el Prof. Feliu Maseras. Al Prof. Antonio M. Echavarren quisiera agradecerle como nos transmite su pasión por la química, por su disponibilidad y todas las oportunidades que me ha brindado para ampliar mi formación. Al Prof. Feliu Maseras quisiera agradecerle también por todo lo aprendido, su disponibilidad y paciencia.

El trabajo recogido en esta memoria se ha llevado a cabo gracias a una Beca Predoctoral de Formación de Profesorado Universitario del Ministerio de Educación y Ciencia (FPU), a la financiación del Ministerio de Educación y Ciencia (Proyecto CTQ2004-02869), del Institut Català d'Investigació Química (ICIQ) y se ha desarrollado en el marco del proyecto Diseño de Catalizadores para una Química Sostenible: Una Aproximación Integrada (INTECAT) (CDS2006-0003) perteneciente al Programa Consolider-Ingenio 2010.

Durante mi Tesis Doctoral, he realizado una estancia de tres meses, gracias a la beca FPU del Ministerio de Educación y Ciencia, en el grupo del Prof. K. N. Houk (University of California, Los Angeles, agosto-octubre 2007). También he llevado a cabo una segunda estancia de tres meses en BASF (Ludwigshafen, Alemania, marzo-mayo 2009) bajo la supervisión del Dr. Klaas Lohmann. Me gustaría agradecer a ambos grupos de investigación la oportunidad de unirme a ellos, y la experiencia de trabajar ambientes tan distintos e interesantes.

Quería agradecer a las personas que han ayudado a que mi trabajo resultara más sencillo. En un lugar muy destacado a Sònia Gavalrà, asistente administrativa del grupo del Prof. Echavarren, por su ayuda, entusiasmo y cariño. Igualmente quiero agradecer todo su apoyo a Vanessa Martínez, nuestra técnico. También a Nùria Vendrell y Martín Gumbau, de los grupos de Química Computacional y a los servicios de investigación del ICIQ: Al Dr. Jonathan Barr, Joan Sallés y Dra. Noemí Cabello en el servicio de espectrometría de masas, al Dr. Gabriel González y a Kerman Gómez del servicio de RMN, y, especialmente, al Dr. Jordi Benet-Buchholz, Eduardo Escudero y Leire San Felices del servicio de rayos-X.

También quería expresar mi agradecimiento a las personas que han colaborado en desarrollar el trabajo que aquí presento. A Cristina Nieto-Oberhuber y a la Dra. Salomé López por su colaboración en la reacción de ciclopropanación intermolecular catalizada por oro así como en la síntesis de los complejos catiónicos con interacciones  $\pi$  oro-areno. Al Dr. Atahualpa A. C. Braga por iniciarme en el misterioso mundo de los cálculos y de Linux y a la Dr. Noemí Cabello por la ayuda prestada en la ciclación de 1,7-eninos catalizada por oro. También a Daniel T. Hog con quién fue un placer trabajar durante su estancia de tres meses en nuestro grupo de investigación.

Durante estos años he tenido ocasión de compartir laboratorio con muchos otros compañeros, a los que me gustaría hacer una pequeña mención aquí: Almudena Díaz, Susana Porcel, Eloísa Jiménez-Núñez, Dr. Domingo García, Dra. Christelle Claverie, Dra. Catelijne Amijs, Patricia Pérez-Galán, Paula de Mendoza, Mihai Raducan, Dr. Sergio Pascual, Dr. Antonio Rosellón, Dra. Cristina Rodríguez, Dr. Thorsten Lauterbach, Verónica López-Carrillo, Dr. Christophe Bour, Ana Escribano (mi “pequeña Ana”), Dr. Dominc Janssen, Dr. Kian Molawi, Nicolas Delpont, César Rogelio Solorio, Claudia de León, Dr. Dirk Spiegel, Nuria Huget, Dr. Julian Cecon y Dra. Norwenn Martin. Muchas gracias por vuestra ayuda y por los buenos momentos que hemos compartido estos años. También quisiera hacer extensivo este agradecimiento a los integrantes del laboratorio de Química Computacional (grupos de Maseras, Bo y López) porque, a pesar de haber pasado menos tiempo juntos, siempre me han hecho sentir como en casa.

De estos años en Tarragona me llevo un recuerdo imborrable (“espectacular”), gracias a los buenos amigos que he conocido estando aquí. Me alegra también que este grupo se está haciendo poco a poco mayor con nuevas y jovencísimas adquisiciones. Un agradecimiento especial a Natalia, Dani y Paula, a los que ahora de verdad podemos llamar la “familia Font”. Y por supuesto, a mi *editorial board*, Cati y Gerald. No me puedo olvidar mis amigos de Alcalá, que me han ido acompañando durante mis andanzas por el mundo. Y a Sergio, gracias por todo.

Y, como no, al pequeño “equipo” que me respalda: mi madre, mi padre y mi hermano Carlos. Sin su apoyo incondicional nada de esto hubiera sido posible.

Hasta el momento de redactar esta memoria, los resultados aquí descritos han dado lugar a las siguientes publicaciones:

**“Gold(I)-catalyzed cyclizations of 1,6-enynes: Alkoxycyclizations and Exo/Endo Skeletal Rearrangements”**

Nieto-Oberhuber, C.; Muñoz, M. P.; López, S.; Jiménez-Núñez, E.; Nevado, C.; Herrero-Gómez, E.; Raducan, M.; Echavarren, A. M. *Chem. Eur. J.* **2006**, *12*, 1677-1693.

**“Cationic  $\eta^1/\eta^2$ -Gold(I) complexes of simple arenes”**

Herrero-Gómez, E.; Nieto-Oberhuber, C.; López, S.; Benet-Buchholz, J.; Echavarren, A. M. *Angew. Chem. Int. Ed.* **2006**, *45*, 5455-5459.

**“Gold(I)-catalyzed intermolecular cyclopropanation of enynes with alkenes: Trapping of two different gold carbenes”**

López, S.; Herrero-Gómez, E.; Pérez-Galán, P.; Nieto-Oberhuber, C.; Echavarren, A. M. *Angew. Chem. Int. Ed.* **2006**, *45*, 6029-6032.

**“Gold(I)-catalyzed intramolecular [4+2] cycloadditions of arylalkynes or 1,3-enynes with alkenes: Scope and Mechanism”**

Nieto-Oberhuber, C.; Pérez-Galán, P.; Herrero-Gómez, E.; Lauterbach, T.; Rodríguez, C.; López, S.; Bour, C.; Rosellón, A.; Cárdenas, D. J.; Echavarren, A. M. *J. Am. Chem. Soc.* **2008**, *130*, 269-279.

**“Transition-metal catalyzed cycloisomerizations and nucleophilic cyclization of enynes”**

Herrero-Gómez, E.; Echavarren, A. M. *Handbook of Cyclization Reactions*, Wiley, **2008**. Chap. 12. Shemming Ma, Ed.

**“Bis(1,1-dimethylethyl)[2,4,6-tris(1-methylethyl)[1,1-biphenyl]-2-yl]-phosphine and Dicyclohexyl[2,4,6-tris(1-methylethyl)[1,1-biphenyl]-2-yl]-phosphine”**

Herrero-Gómez, E.; Echavarren, A. M. *Encyclopedia of Reagents in Organic Synthesis*, Wiley, **2008**.

UNIVERSITAT ROVIRA I VIRGILI

GOLD(I)-CATALYZED CYCLIZATIONS OF 1,6- AND 1,7-ENYNES: NEW GOLD COMPLEXES AND CYCLOPROPANATION REACTIONS

Elena Herrero Gómez

ISBN: 978-84-692-5924-5/DL:T-1663-2009



Consolider Ingenio 2010  
CSD2006-0003  
Diseño de Catalizadores  
para una Química Sostenible:  
una Aproximación Integrada

UNIVERSITAT ROVIRA I VIRGILI

GOLD(I)-CATALYZED CYCLIZATIONS OF 1,6- AND 1,7-ENYNES: NEW GOLD COMPLEXES AND CYCLOPROPANATION REACTIONS

Elena Herrero Gómez

ISBN: 978-84-692-5924-5/DL:T-1663-2009

	<b>Page</b>
<b>PRÓLOGO</b>	13
<b>RESUMEN</b>	15
<i>Abbreviations and Acronyms</i>	21
<b>INTRODUCTION</b>	23
1. <i>Theoretical Chemistry of Gold</i>	28
1.1. <i>Aurophilic Interactions</i>	28
1.2. <i>Computational Methods for Studying Gold-Catalyzed Reactions</i>	29
2. <i>Gold Catalysts for the Selective Activation of Alkynes</i>	33
2.1. <i>Interaction between Gold and Alkynes. Gold-Alkyne Complexes</i>	34
<b>CHAPTER 1</b>	
<b>INTRODUCTION</b>	39
1. <i>Gold(I) Complexes for Homogeneous Catalysis</i>	41
2. <i>Gold(I) Linear Species. Activation of Gold(I) Neutral Complexes</i>	42
3. <i>Ligand Effects in Homogeneous Gold(I)-Catalyzed Activation of Alkynes</i>	43
3.1. <i>N-Heterocyclic Carbenes and Related Ligands</i>	43
3.2. <i>Phosphine Ligands</i>	47
3.3. <i>Chiral Ligands in Enantioselective Gold-Catalyzed Reactions</i>	48
3.4. <i>Gold(I) Complexes with Higher Coordination Numbers</i>	51
4. <i>Gold(I) Complexes of Bulky, Electron-Rich Biaryl Phosphines</i>	54
4.1. <i>Gold(I)-Arene Interactions</i>	55
4.2. <i>Related Silver and Copper Complexes</i>	59
<b>OBJECTIVES</b>	63
<b>RESULTS AND DISCUSSION</b>	67
1. <i>Computational Study of Group II Metal Complexes with Bulky, Biphenyl Phosphines</i>	69
2. <i>Cationic <math>\eta^1/\eta^2</math>-Gold(I) Complexes of Simple Arenes</i>	81
3. <i>Gold Complexes with <math>\pi</math>-Acceptors Ligands</i>	90
<b>CONCLUSIONS</b>	95
<b>EXPERIMENTAL SECTION</b>	99

**CHAPTER 2**

INTRODUCTION	163
1. <i>Gold(I)-Catalyzed Cycloisomerization of Enynes</i>	169
1.1. <i>Gold(I)-Catalyzed Cycloisomerization of 1,6-Enynes</i>	171
1.2. <i>Gold(I)-Catalyzed Cycloisomerization of 1,7-Enynes</i>	178
1.3. <i>Gold(I)-Catalyzed Cycloisomerization of 1,n-Enynes</i>	180
2. <i>Gold(I)-Catalyzed Cyclopropanations</i>	187
OBJECTIVES	195
RESULTS AND DISCUSSION	199
1. <i>Gold(I)-Catalyzed Intermolecular Cyclopropanation</i>	201
2. <i>Computational Study of the Gold(I)-Catalyzed Cyclization of 1,7-Enynes</i>	225
3. <i>Gold(I)-catalyzed [4+2]-cycloadditions of 1,7-enynes</i>	238
CONCLUSIONS	243
EXPERIMENTAL SECTION	247

Esta memoria del trabajo de la Tesis Doctoral se ha dividido en tres partes, una introducción general y dos capítulos, que constan cada uno de una introducción, unos objetivos, un apartado de resultados y discusión, conclusiones y finalmente la parte experimental.

En la introducción general se recogen aspectos generales de la catálisis con complejos de oro, así como los métodos computacionales utilizados para el estudio de estas reacciones.

El primer capítulo se ha dedicado al estudio de los complejos de oro en el contexto de la reacción de activación de alquinos. La introducción contiene una revisión de los complejos utilizados para este fin, haciendo mención especial a los complejos que contienen bifenilfosfinas voluminosas como ligandos. A continuación, se exponen los resultados obtenidos en un estudio teórico comparativo de este tipo de complejos con metales del grupo 11, la síntesis y caracterización estructural de complejos de oro que contienen interacciones  $\pi$  oro-anillo aromático sencillo, y la síntesis de un nuevo complejo de oro con un ligando fosfito voluminoso.

El segundo capítulo trata de la reacción de ciclación de eninos catalizada por oro, prestando especial atención a las reacciones de transposición de esqueleto, así como de reacciones de ciclopropanación catalizadas por oro. El material del artículo de revisión publicado en "*Handbook of Cyclization Reactions*" se ha incorporado a la introducción de este capítulo. No se han incluido las reacciones de hidroxil- y alcoxiciclación de eninos por no estar relacionadas con los resultados descritos en este capítulo. En el apartado de resultados y discusión, se recogen los resultados obtenidos en la reacción de ciclopropanación intermolecular de eninos catalizada por oro, el estudio teórico y computacional de la reacción de ciclación de 1,7-eninos catalizada por oro y los resultados de la cicloadición [4+2] en 1,7-eninos.

UNIVERSITAT ROVIRA I VIRGILI

GOLD(I)-CATALYZED CYCLIZATIONS OF 1,6- AND 1,7-ENYNES: NEW GOLD COMPLEXES AND CYCLOPROPANATION REACTIONS

Elena Herrero Gómez

ISBN: 978-84-692-5924-5/DL:T-1663-2009

UNIVERSITAT ROVIRA I VIRGILI

GOLD(I)-CATALYZED CYCLIZATIONS OF 1,6- AND 1,7-ENYNES: NEW GOLD COMPLEXES AND CYCLOPROPANATION REACTIONS

Elena Herrero Gómez

ISBN: 978-84-692-5924-5/DL:T-1663-2009

*Resumen*

UNIVERSITAT ROVIRA I VIRGILI

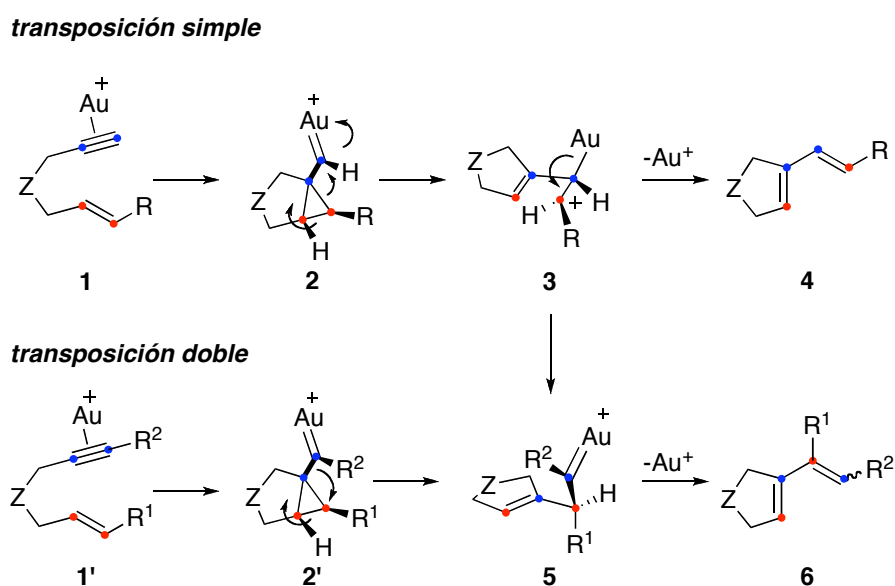
GOLD(I)-CATALYZED CYCLIZATIONS OF 1,6- AND 1,7-ENYNES: NEW GOLD COMPLEXES AND CYCLOPROPANATION REACTIONS

Elena Herrero Gómez

ISBN: 978-84-692-5924-5/DL:T-1663-2009

A pesar de ser un metal conocido desde la antigüedad, el uso de complejos de oro en catálisis homogénea es relativamente reciente. Sin embargo, durante estos años se ha demostrado su eficacia como catalizador para la activación de alquinos.<sup>1</sup>

Nuestro grupo de investigación se ha centrado en el estudio de la reacción de ciclación de eninos catalizada por oro, tanto en el desarrollo de nuevas metodologías sintéticas como en el estudio del mecanismo de la citada transformación. Para el caso concreto de 1,6-eninos, el uso de catalizadores de oro permite la obtención de un gran número de productos, de los cuales quizá los más representativos sean los dienos denominados de transposición simple **4** y doble **6**. Estudios computacionales proponen que la reacción transcurre a través de intermedios tipo carbeno de oro **2** y **5**,<sup>2</sup> tal como aparece representado en el Esquema 1.



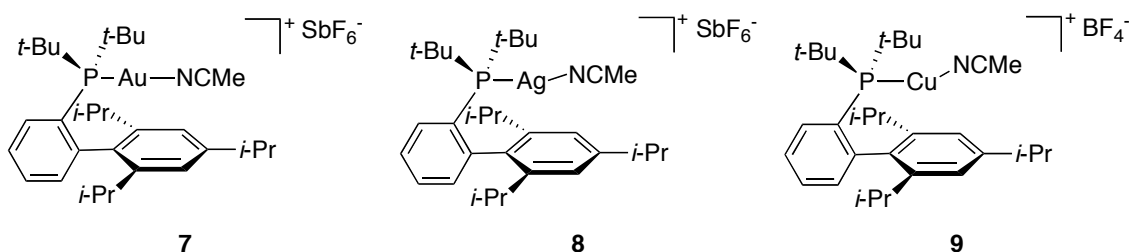
Esquema 1

En este contexto, el trabajo de esta tesis doctoral se ha dividido en dos grandes bloques. Por un lado, en el estudio y desarrollo de nuevos catalizadores de oro y, a continuación, en las aplicaciones catalíticas de los complejos de oro en reacciones de eninos.

El capítulo primero de esta memoria es el dedicado a los complejos de oro. En

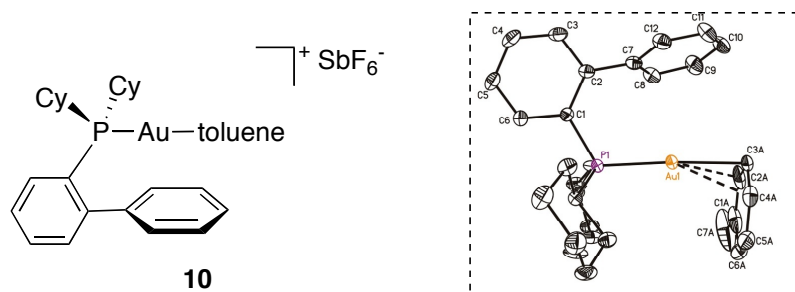
- 
- 1 (a) Jiménez-Núñez, E.; Echavarren, A. M. *Chem. Rev.* **2008**, *108*, 3326-3350. (b) Jiménez-Núñez, E.; Echavarren, A. M. *Chem. Commun.* **2007**, 333-346.
  - 2 Nieto-Oberhuber, C.; López, S.; Muñoz, M. P.; Cárdenas, D. J.; Buñuel, E.; Nevado, C.; Echavarren, A. M. *Angew. Chem. Int. Ed.* **2005**, *44*, 6146-6148.

éste se recogen los resultados correspondientes a un estudio computacional sobre una familia de complejos de metales del grupo 11 con fosfinas voluminosas. Las estructuras de rayos X de estos complejos con 2-di-*tert*-butil-2',4',6'-triiisopropilbifenilfosfina mostraban un evidente distorsión en el ángulo formado entre el fósforo, metal y nitrógeno (Esquema 2). Éste ángulo es prácticamente lineal para el complejo de oro (173.03°), mientras que en el caso del complejo de plata es 168.01° y para el complejo de cobre 148.79°. Nuestro estudio concluye que esta variación en el ángulo es debida a una interacción  $\pi$  con el anillo aromático que se encuentra situado sobre el metal, y que la intensidad de esta interacción varía de la siguiente manera Cu>Ag>Au, siendo prácticamente despreciable para el caso del oro.



Esquema 2

Siguiendo la línea del estudio de interacciones  $\pi$  entre el oro y anillos aromáticos, se llevó a cabo la síntesis y caracterización estructural mediante difracción de rayos X de los primeros complejos de oro que presentan esta interacción con anillos aromáticos sencillos (Esquema 3). Las distancias entre el oro y el anillo aromático coordinado varían entre 2.200(1) y 2.244(5) Å.

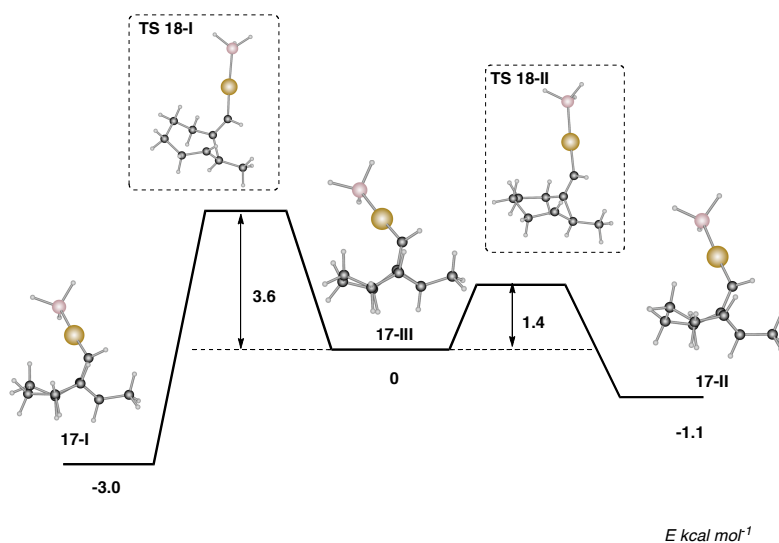


Esquema 3

También ha sido sintetizado un nuevo complejo de oro **11** con un ligando fosfito

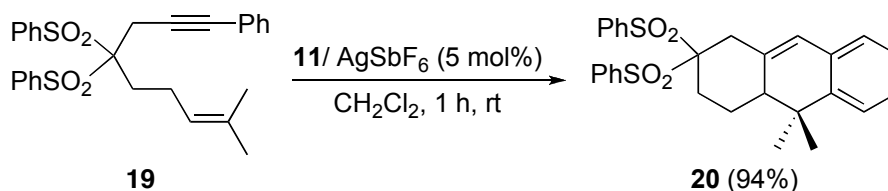


También se ha llevado a cabo un estudio computacional sobre la ciclación de 1,7-eninos catalizada por oro. Este trabajo se planteó con el objetivo de encontrar una explicación a la formación exclusiva de productos de transposición simple en esta reacción.<sup>3</sup> Los cálculos DFT señalan como elemento clave la conformación del anillo de seis miembros formado en el curso de la reacción. El equilibrio entre las distintas conformaciones **17-I**, **17-II** y **17-III** presenta una barrera energética menor para el camino que conduce a los productos de transposición simple (Esquema 6).



Esquema 6

Por último, y continuando el trabajo sobre cicloadiciones [4+2] catalizadas por oro, se ha logrado extender esta transformación a 1,7-eninos sustituidos **19** (Esquema 7). Estas reacciones también constituyen un ejemplo de la eficacia de nuevo catalizador **11**.



Esquema 7

3 Cabello, N.; Rodríguez, C.; Echavarren, A. M. *Synlett* **2007**, 1753-1758.

## Abbreviations and Acronyms

In this manuscript, the abbreviations and acronyms most commonly used in organic and organometallic chemistry have been used following the recommendations of “Guidelines for authors” from the *American Chemical Society* (ACS). Additionally, I have also used the following ones:

BHT:	Butylhydroxytoluene
Cy:	Cyclohexyl
DFT:	Density Funtional Theory
DTBM:	3,5-di- <i>tert</i> -butyl-4-methoxyphenyl
ECP:	Effective core potential
EDA:	Ethyldiazoacetate
GGA:	Generalized gradient approximation
H:	Enthalpy
HBHC:	Hydrogen bond supported heterocyclic carbene
LDA:	Local density approximation
LSDA:	Local spin density approximation
NHC:	<i>N</i> -Heterocyclic carbene
ORTEP:	Oac Ridge Thermal Ellipsoid Plot
PP:	Pseudopotential
S:	Entropy
TBAI:	Tetrabutylammonium iodide
Tf:	Triflate

UNIVERSITAT ROVIRA I VIRGILI

GOLD(I)-CATALYZED CYCLIZATIONS OF 1,6- AND 1,7-ENYNES: NEW GOLD COMPLEXES AND CYCLOPROPANATION REACTIONS

Elena Herrero Gómez

ISBN: 978-84-692-5924-5/DL:T-1663-2009

UNIVERSITAT ROVIRA I VIRGILI

GOLD(I)-CATALYZED CYCLIZATIONS OF 1,6- AND 1,7-ENYNES: NEW GOLD COMPLEXES AND CYCLOPROPANATION REACTIONS

Elena Herrero Gómez

ISBN: 978-84-692-5924-5/DL:T-1663-2009

*Introduction*

UNIVERSITAT ROVIRA I VIRGILI

GOLD(I)-CATALYZED CYCLIZATIONS OF 1,6- AND 1,7-ENYNES: NEW GOLD COMPLEXES AND CYCLOPROPANATION REACTIONS

Elena Herrero Gómez

ISBN: 978-84-692-5924-5/DL:T-1663-2009

Gold has been known and valued since prehistoric times due to its softness, stability against oxidation and unusual yellow color (Figure 1). However, it has not been until recent years that its applications in catalysis have been widely studied. The misconception of gold's inertness, based probably on the stability of native gold, explains this early lack of interest in the chemical community.



**Figure 1.** Gold is a usual material in ancient coins.

Nevertheless, in 1973, a contribution by Bond *et al.* on an efficient hydrogenation of olefins promoted by supported gold catalysts,<sup>1</sup> showed the interesting catalytic possibilities of this noble metal. Independent works by Haruta *et al.* and Hutchings highlighted the potential of gold heterogeneous catalysts by its successful

---

1 Bond, G. C.; Sermon, P. A.; Webb, G.; Buchanan, D. A.; Wells, P. B. *J. Chem. Soc., Chem. Commun.* **1973**, 444-445.

application in the oxidation of CO and the hydrochlorination of acetylene, respectively.<sup>2,3</sup> Advances in homogeneous catalysis followed these pioneer works. Contributions by Ito *et al.*,<sup>4</sup> Fukuda and Utimoto,<sup>5</sup> and especially by Teles *et al.* in a very efficient gold-catalyzed addition of alcohols to alkynes,<sup>6</sup> started a field of research that has experienced an outburst of activity in the present decade.<sup>7</sup>

Not only has gold a superior Lewis acidity compared with other metals, it also has some advantages that render it interesting for industrial purposes. Gold-catalyzed reactions are usually performed at room temperature and the catalyst loading is low. Of course, the high price of the metal catalyst can diminish these advantages. But, contrary to common belief, gold is not the most expensive metal. This element is produced in tons from mines every year and it is also recycled from stoichiometric technical applications. These facts lead to a high stability of its price, which is in fact lower than other commonly used metals such as rhodium or platinum.

Gold is an excellent soft Lewis acid that allows for the activation of carbon-carbon multiple bonds.<sup>8</sup> Gold catalysts have been successfully applied to nucleophilic additions (using hetero- or carbon nucleophiles), Friedel-Crafts reactions, C-H activation, hydrogenations, and oxidations.<sup>9</sup>

Gold owes its special properties to relativistic effects,<sup>10</sup> which are responsible, for example, of its yellow color. Relativistic effects are the result of considering both quantum mechanics and special relativity<sup>11</sup> and must be taken into account in systems in which the speed of the electrons is similar to the speed of light. This fact determines an

---

2 Haruta, M.; Kobayashi, T.; Sano, H.; Yamada, N. *Chem. Lett.* **1987**, *16*, 405-408.

3 Hutchings, G. J. *J. Catal.* **1985**, *96*, 292-295.

4 Ito, Y.; Sawamura, M.; Hayashi, T. *J. Am. Chem. Soc.* **1986**, *108*, 6405-6406.

5 Fukuda, Y.; Utimoto, K. *J. Org. Chem.* **1991**, *56*, 3729-3731.

6 Teles, H.; Brode, S.; Chabanas, M. *Angew. Chem. Int. Ed.* **1998**, *37*, 1415-1418.

7 For a review see: Hashmi, A. S. K.; Hutchings, G. J. *Angew. Chem. Int. Ed.* **2006**, *45*, 7896-7936.

8 Fürstner, A.; Davies, P. W. *Angew. Chem. Int. Ed.* **2007**, *46*, 3410-3449.

9 Recent reviews on gold-catalyzed organic reactions: (a) Li, Z.; Brouwer, C.; He, C. *Chem. Rev.* **2008**, *108*, 3239-3265. (b) Arcadi, A. *Chem. Rev.* **2008**, *108*, 3266-3325. (c) Hashmi, A. S. K. *Chem. Rev.* **2007**, *107*, 3180-3211.

10 Gorin, D. J.; Toste, F. D. *Nature* **2007**, *446*, 395-403.

11 (a) McKelvey, D. R. *J. Chem. Educ.* **1983**, *60*, 112-116. (b) Pitzer, K. S. *Acc. Chem. Res.* **1979**, *12*, 272-276.

increase in the mass of the electron and consequently, a decrease in the Bohr radius.<sup>12,13</sup> The electronic structure is obviously affected: *s* and *p* shells are stabilized and contracted while *d* and *f* orbitals are expanded and destabilized. The fact that relativistic effects are maximum in metals of group 11 (and, among them, in gold) is due to the overlap between the valence *ns* shell, which suffers a direct relativistic contraction, and the underlying (*n*-1) shell.<sup>14</sup>

The most common oxidation states in gold are +I and +III. Compounds of both oxidation states have a rich chemistry with applications in medicine, material science, nanoscience and both in homogeneous and heterogeneous catalysis.<sup>15</sup> Considering the wide variety of catalytic systems in which gold complexes have been successfully applied, the scarceness of cross coupling reactions is remarkable.<sup>16</sup> This limitation lays in the fact that gold is not easily oxidized. Theoretical studies explain this behavior by a decreased electron/electron repulsion in the more diffuse *5d* orbitals (compared with, for example, *3d* orbitals in copper). These electrons are consequently tightly bonded to the nucleus and thus oxidative additions are disfavored.<sup>17</sup> Nevertheless, the positive side is that gold complexes are air and moisture stable, which means that they can be handled without special precautions.

In general, coordination is linear in gold(I) and square-planar in gold(III) complexes. The preference of gold(I) for a linear coordination can be explained by the stabilization of the *6s* orbital, due to the relativistic effects on gold.<sup>12,13,18,19</sup> As the *5d*

- 
- 12 Pyykkö, P.; Desclaux, J. P. *Acc. Chem. Res.* **1979**, *12*, 276-281.  
13 Pyykkö, P. *Chem. Rev.* **1988**, *88*, 563-594.  
14 Autschbach, J.; Siekierski, S.; Seth, M.; Schwerdtfeger, P.; Schwarz, W. H. E. *J. Comput. Chem.* **2002**, *23*, 804-813.  
15 *Gold, Progress in Chemistry, Biochemistry and Technology*, Schmidbaur H. ed., Wiley-VCH, Weinheim, **1999**.  
16 (a) Zhang, X.; Corma, A. *Angew. Chem. Int. Ed.* **2008**, *47*, 4358-4361. (b) González-Arellano, C.; Abad, A.; Corma, A.; García, H.; Iglesias, M.; Sánchez, F. *Angew. Chem. Int. Ed.* **2007**, *46*, 1536-1538. (c) Corma, A.; González-Arellano, C.; Iglesias, M.; Pérez-Ferreras, S.; Sánchez, F. *Synlett* **2007**, *11*, 1771-1774.  
17 Nakanishi, W.; Yamanaka, M.; Nakamura, E. *J. Am. Chem. Soc.* **2005**, *127*, 1446-1453.  
18 Selected reviews: (a) Pyykkö, P. *Chem. Soc. Rev.* **2008**, *37*, 1967-1997. (b) Pyykkö, P. *Inorg. Chim. Acta* **2005**, *358*, 4113-4130. (c) Pyykkö, P. *Angew. Chem. Int. Ed.* **2004**, *43*, 4412-4456. (d) Pyykkö, P.; Li, J.; Runeberg, N. *Chem. Phys. Lett.* **1994**, *218*, 133-138. (e) Li, J.; Pyykkö, P. *Inorg. Chem.* **1993**, *32*, 2630-2634. (f) Li, J.; Pyykkö, P. *Chem. Phys. Lett.* **1992**, *197*, 586-590.

shell also undergoes an expansion, the energy gap between  $6s$  and  $5d$  is smaller. As a result, the  $s/p$  energy gap is larger, and only  $s/d$  hybridizations are made, explaining the tendency of gold(I) to form linear two-coordinate complexes. This tendency to the bicoordination is much stronger than for other isoelectronic metals, such as platinum(0), silver(I), copper(I), palladium(0) or mercury(II), in which compounds in higher coordination numbers are more common.

In addition, gold has also a negative oxidation state ( $\text{Au}^{-1}$ ) and, due to its high electron affinity (comparable to that of iodine) it is considered as a pseudohalogen.  $\text{Au}^{-1}$  forms a number of auride compounds, which are the subject of active research.<sup>20</sup>

## 1. Theoretical Chemistry of Gold

In parallel with the development of new methodologies based on gold, there is a need of an in-depth understanding of reaction mechanisms. Thus, theoretical chemistry of gold has also attracted great attention during these years.<sup>18</sup>

### 1.1. Auophilic Interactions

An intriguing aspect of this metal is the existence of auophilic interactions. This term refers to the tendency of gold(I) cations to form aggregates. Many computational efforts have been devoted to understand this counterintuitive attraction, which occurs between two closed-shell fragments of the same sign and that has a binding energy comparable to strong hydrogen bonding.

The possibility of forming a covalent bond is excluded, since there are no valence electrons available. In fact, auophilicity can be considered as a surprisingly strong van der Waals interaction, since it follows the London approximation, *i.e.* the attractive force decays with the sixth power of the intermolecular distance ( $R$ ).

$$V(R) = - (3/4) \alpha_A \alpha_B [I_A I_B / (I_A + I_B)] R^{-6}$$

---

19 (a) Schmidbaur, H. *Interdiscipl. Sci. Rev.* **1992**, *17*, 213-220. (b) Schmidbaur, H. *Gold Bull.* **1990**, *23*, 11-21.

20 Jansen, M. *Chem. Soc. Rev.* **2008**, *37*, 1826-1835 and references therein.

where  $\alpha$  is the electric polarizability,  $I$  is the ionization potential of the interacting systems A and B and  $R$  is the intermolecular distance.

This phenomenon can be envisioned as the attractive force between two instantaneous dipole moments, created by excitation of the two subsystems. The reason why the attraction is in fact so strong is related to the  $\alpha$  coefficient, the polarizability. Although the actual value for gold species is not very large, it comes from a compact volume that corresponds mainly to the  $5d^{10}$  shell. The overall effect is that is more difficult for gold to suffer interatomic Pauli repulsion.

## 1.2. Computational Methods for Studying Gold-Catalyzed Reactions

Density Functional Theory (DFT) provides a good and time-economic way to handle many electron systems.<sup>21</sup> Such methods were developed based on the Thomas-Fermi-Dirac model (1920's) and on the work of Slater in quantum chemistry (1950's). DFT methods are then similar to *ab initio* methods at a much less computational cost: they require roughly the same amount of computation sources as Hartree-Fock theory, the least expensive *ab initio* method.

Density Functional Theory methods are based on the calculation of electron density. This simplification is possible thanks to the development of the Hohenberg-Kohn theorems,<sup>22</sup> which demonstrate that the energy of a system can be expressed as a functional of the electron density. A functional is described as a function of a function, but the theorem does not provide the form of such functional. The most common implementation is the Kohn-Sham formalism<sup>23</sup> that obtains the electron density from a set of orbitals.

Compared to Hartree-Fock based methods, less computational resources are needed because it is not necessary to calculate the many electron wavefunction. Moreover, DFT calculations include electron correlation. This term, referring to instantaneous repulsive interactions, is absent from basic Hartree-Fock theory. In the Hartree-Fock framework, electron correlation has to be introduced through computationally demanding schemes as MP2 or configuration interaction.

---

21 Koch, W.; Holthausen, M. C. *A Chemist's Guide to Density Functional Theory*; Wiley-VCH: Weinheim, **2001**.

22 Hohenberg, P.; Kohn, W. *Phys. Rev.* **1964**, *136*, B864-B871.

23 Kohn, W.; Sham, L. J. *Phys. Rev.* **1965**, *140*, A1133-A1138.

The accuracy of a DFT calculation depends on the quality of the exchange-correlation functional. As the expression of this functional is not known, some approximations are therefore needed. The first generation of functionals is the local-density approximation (LDA), where the functional depends only on the density at the coordinate where it is evaluated. Local spin-density approximation (LSDA) also includes electron spin. These functionals were good for solid state physics, but failed when calculating chemical properties. Generalized gradient approximations (GGA) take into consideration the gradient of the density at the same coordinate. This type of functionals is required when working with transition metals. The accuracy of this functional can be improved by using meta-GGA approaches, in which the gradient of the density and its Laplacian (second derivative) are included.

However, all these functionals are local and the difficulty of defining the exchange part of the energy was still the major drawback. This problem was addressed by Becke with the development of hybrid functionals, which include a component of the exact exchange energy calculated from Hartree-Fock theory. Nowadays, hybrid functionals (such as B3LYP) are commonly used in Density Functional Theory-based calculations. In particular, B3LYP uses the hybrid three-term exchange functional developed by Becke<sup>24</sup> and the correlation functional proposed by Lee, Yang and Parr.<sup>25</sup> Nevertheless, it is worth mentioning that GGA-based functionals are still useful for certain studies.

Some considerations have to be made regarding the accuracy of the method. Three main shortcomings have to be considered when working with B3LYP functional. Firstly, it works better for main group elements than for transition metals. In addition, it systematically underestimates reaction barrier energies and it is inaccurate for weak interactions at a supramolecular level, such as aurophilic interactions. The difficulty to overcome these problems is based in the lack of hierarchy in DFT methods, which does not allow for systematic improvements. Consequently, the search for better functionals is an important field of research.<sup>26</sup> Nevertheless, B3LYP is still the most popular

---

24 Becke, A. D. *J. Chem. Phys.* **1993**, *98*, 5648-5652.

25 Lee, C.; Yang, W.; Parr, R. G. *Phys. Rev. B.* **1988**, *37*, 785-789.

26 Zhao, Y.; Truhlar, D. G. *Acc. Chem. Res.* **2008**, *42*, 157-167.

functional and its performance has shown to be sufficiently good, in particular, for the study of gold-catalyzed reactions.<sup>27</sup>

In gold-containing systems, it is highly important to consider relativistic effect when choosing the appropriate basis set. Benchmarking studies demonstrate that relativistic methods reproduce quite accurately experimental properties, such as first ionization potential or electron affinity (Table 1).

---

27 Recent examples of B3LYP studies of gold-catalyzed reactions: (a) Trillo, B.; López, F.; Montserrat, S.; Ujaque, G.; Castedo, L.; Lledós, A.; Mascareñas, J. L. *Chem. Eur. J.* **2009**, *15*, 3336-3339. (b) Nieto-Oberhuber, C.; Pérez-Galán, P.; Herrero-Gómez, E.; Lauterbach, T.; Rodríguez, C.; López, S.; Bour, C.; Rosellón, A.; Cárdenas, D. J.; Echavarren, A. M. *J. Am. Chem. Soc.* **2008**, *130*, 269-279. (c) Marion, N.; Carlqvist, P.; Gealageas, R.; de Frémont, P.; Maseras, F.; Nolan, S. P. *Chem. Eur. J.* **2007**, *13*, 6413-6451. (d) Lemiere, G.; Gandon, V.; Cariou, K.; Fukuyama, T.; Dhimane, A.-L.; Fensterbank, L.; Malacria, M. *Org. Lett.* **2007**, *9*, 2207-2209. (e) Comas-Vives, A.; González-Arellano, C.; Corma, A.; Iglesias, M.; Sánchez, F.; Ujaque, G. *J. Am. Chem. Soc.* **2006**, *128*, 4756-4765.

**Table 1.** Benchmark studies on gold-containing systems.

System	Property <sup>[a]</sup>	Exp.	R <sup>[b]</sup>	NR <sup>[b]</sup>	R-NR	Method
Au(atom)	<i>IPI</i> [eV]	9.22554(2)	9.197	7.057	2.140	CCSD <sup>28</sup>
	<i>EA</i> [eV]	2.30863 <sup>29</sup>	2.295	1.283	1.012	CCSD <sup>28</sup>
	<i>a</i>	30(4) <sup>30</sup>	36.06			CCSD(T) <sup>31</sup>
Au <sup>+</sup>	<i>a</i>		12.75			CCSD(T) <sup>31</sup>
AuH	<i>R<sub>e</sub></i> [pm]	152.4	152.5	175.0	-22.5	AE CCSD(T) <sup>32</sup>
			152.7	174.7	-22.0	PP CCSD(T) <sup>33</sup>

[a] Dipole polarizability, *a*, in atomic units and bond lengths *R<sub>e</sub>* in pm. [b] R = relativistic, NR = non-relativistic.

To calculate valence properties of molecules containing heavy atoms (such as gold), better efficiency is achieved when the core orbitals are replaced by an effective core potential (ECP), also known as pseudopotential (PP). By using this computational device, it is possible to avoid the inner electrons and their basis functions, keeping an *ab initio* treatment for the valence part. This approach has been extensively tested, and the agreement between all-electron methods (AE) and the methods that used pseudopotential (PP) is remarkable (see examples in Table 1).

When considering bulky systems, the use of hybrid calculations (QM:MM), such as ONIOM, dramatically reduces the computational cost.<sup>34</sup> In ONIOM calculations the

- 28 Eliav, E.; Kaldor, U.; Ishikawa, Y. *Phys. Rev. A* **1994**, *49*, 1724-1729
- 29 Miller, T. M. in *CRC Handbook of Chemistry and Physics*, CRC, Boca Raton: FL, **2002**, (Ed.:D. R. Lide), Vol. 83, chap. 10, pp. 147-162.
- 30 Henderson, M.; Curtis, L. J.; Matulioniene, R.; Ellis, D. G.; Theodosiu, C. E. *Phys. Rev. A* **1997**, *56*, 1872-1878.
- 31 Neogrády, P.; Kellö, V.; Urban, M.; Sadlej, A. J. *Int. J. Quantum Chem.* **1997**, *63*, 557-565.
- 32 Kaldor, U.; Hess, B. A. *Chem. Phys. Lett.* **1994**, *230*, 1-7.
- 33 Schwerdtfeger, P.; Brown, J. R.; Laerdahl, J. K.; Stoll, H. *J. Chem. Phys.* **2000**, *113*, 7110-7118.
- 34 (a) Vreven, T.; Morokuma, K. *J. Comp. Chem.* **2000**, *21*, 1419-1432. (b) Dapprich, S.; Komáromi, I.; Byun, K. S.; Morokuma, K.; Frisch, M. J. *J. Mol. Struct. (Theochem)* **1999**, *462*, 1-21. (c) Svensson, M.; Humbel, S.; Morokuma, K. *J. Chem. Phys.* **1996**, *105*, 3654-3661. (d) Svensson, M.; Humbel, S.; Froese, R. D. J.; Matsubara, T.; Sieber, S.; Morokuma, K. *J. Phys.*

molecular system is divided into two or three layers that are treated with different model chemistries. Molecular mechanics can be applied to the part of the system that it is not directly implied in the reaction, consequently diminishing the number of atoms considered by quantum mechanics. The results of the different layers are automatically combined in the final calculation.

As general consideration, the performance of theoretical calculations in gold-catalyzed reactions is calibrated using experimental results or, when not available, high-level wave-function-based calculations.

## 2. Gold Catalysts for the Selective Activation of Alkynes

Gold is known to be alkynophilic,<sup>35</sup> that is, gold activates selectively triple bonds in the presence of different insaturations. This selective activation occurs both in homogeneous and heterogeneous gold catalysis, although the reason of this behavior is found to be different.<sup>36</sup>

For heterogeneous catalysis, differential reactant adsorption on the catalysts surface is the key, leading to bonded, active species that give rise to fast hydrogenation or hydration reactions. In contrast, for homogeneous catalysts, alkenes are preferentially coordinated to gold,<sup>37</sup> but electro- and nucleophilic attacks are more thermodynamically favored for alkynes. As an example, enyne cyclizations in homogeneous systems are mainly driven by the exceptionally low energy LUMO of the coordinated C≡C (Figure 2).

---

*Chem.* **1996**, *100*, 19357-19636. (e) Matsubara, T.; Sieber, S.; Morokuma, K. *Int. J. Quant. Chem.* **1996**, *60*, 1101-1109. (f) Humbel, S.; Sieber, S.; Morokuma, K. *J. Chem. Phys.* **1996**, *105*, 1959-1967. (g) Maseras, F.; Morokuma, K. *J. Comp. Chem.* **1995**, *16*, 1170-1179.

35 Jiménez-Núñez, E.; Echavarren, A. M. *Chem. Commun.* **2007**, 333-346.

36 García-Mota, M.; Cabello, N.; Maseras, F.; Echavarren, A. M.; Pérez-Ramírez, J.; López, N. *ChemPhysChem* **2008**, *9*, 1624-1629.

37 (a) Hertwig, R. A.; Koch, W.; Schröder, D.; Schwarz, H.; Hrusak, J.; Schwerdtfeger, P. *J. Phys. Chem.* **1996**, *100*, 12253-12260. (b) Nechaev, M. S.; Rayón, V. M.; Frenking, G. *J. Phys. Chem. A* **2004**, *108*, 3134-3142.

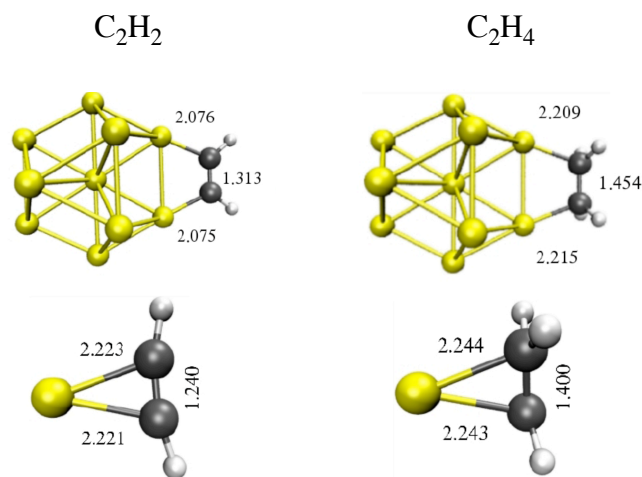


**Figure 2.** Acetylene and ethylene coordination to a gold nanoparticle and  $\text{Au}^+$ , respectively.

Therefore, the alkynophilicity in homogeneous systems is not related to the relative strength of the bonding of the active alkyne species but to its activation for a desired reaction. Experimentally, heterogeneous catalysts that are effective in CO oxidations and hydrogenation reactions have been shown to be inert in the activation of enynes.<sup>36</sup>

### 2.1. Interaction between Gold and Alkynes. Gold-Alkyne Complexes.

To understand the bonding situation in metal-alkyne complexes, the Dewar-Chatt-Duncanson<sup>38,39</sup> model provides a helpful tool. This model considers the bond as a donor-acceptor interaction between two closed-shell fragments.<sup>40,41</sup> In this way, the metal-acetylene bonding is described as the combination of a  $\sigma$ -interaction (donation of the unsaturated moiety to empty *dsp* orbitals of the metal), and a back-bonding  $\pi$ -interaction (donation of the metal to the  $\pi^*$  orbitals of the alkyne). Quantitative estimation of the contributions of the individual  $\sigma$  and  $\pi$  terms has been analyzed by means of high level computational methods.<sup>37</sup> In the simplified gold(I)-acetylene

38 Dewar, M. J. S. *Bull. Soc. Chim. Fr.* **1951**, *18*, C71-C79.

39 Chatt, J.; Duncanson, L. A. *J. Chem. Soc.* **1953**, 2939-2947.

40 Mingos, D. M. P. in *Comprehensive Organometallic Chemistry*, Vol. 3; Wilkinson, G.; Stone, F. G. A.; Abel, E. W. Eds.; Pergamon: Oxford, **1982**; pp. 1-88.

41 Recent reviews: (a) Frenking, G.; Fröhlich, N. *Chem. Rev.* **2000**, *100*, 717-774. (b) Dedieu, A. *Chem. Rev.* **2000**, *100*, 543-600.

complex  $[\text{Au}^+(\text{C}_2\text{H}_2)]$  the  $\sigma$ -interaction accounts for the largest contribution to the orbital term (*ca.* 65%), followed by the in-plane  $\pi$  back-donation (*ca.* 27%) and the orthogonal  $\pi$  back-donation (*ca.* 7%). In conclusion, alkynes are strong two electron  $\sigma$  donors but quite weak  $\pi$  acceptors towards gold(I), although some back-bonding occurs. On the other hand, electrostatic interactions between the substrate and the metal also have to be taken into consideration. In this direction, computational studies of  $[\text{M}^+(\text{C}_2\text{H}_4)]$  and  $[\text{M}^+(\text{C}_2\text{H}_2)]$  ( $\text{M} = \text{Cu}, \text{Ag}, \text{Au}$ ) performed at very advanced levels of theory indicate that roughly half of the total bonding force is electrostatic.<sup>37a,42</sup>

To further quantify the relative importance of these contributions, the study of X-ray structures of gold-alkyne complexes would be of interest. Such complexes are highly reactive intermediates in gold catalyzed reactions, and hence very difficult to isolate. Accordingly, gold-alkyne complexes are scarce in the literature, and only a handful of examples have been reported.<sup>43,44,45,46</sup>

For the particular case of strained alkynes, due to a strong interaction with the gold(I) center, thermally stable complexes can be formed.<sup>43</sup> More precisely, complexes **1** and **2** were reported (Figure 3). Complex **1** has a dimeric structure while complex **2** forms polymeric chains, but, in both of them, gold atoms are in trigonal planar environments. Carbon-gold distances, between 2.050(7) and 2.100(8) Å, indicate very strong alkyne-gold bonds, similar to the corresponding  $\sigma$  bond. The authors attribute these structural features to a high degree of gold-to-alkyne back-bonding that can also be envisioned as a partial oxidation of the metal from gold(I) to gold(III).

---

42 Ziegler, T.; Rauk, A. *Inorg. Chem.* **1979**, *18*, 1558-1565.

43 Schulte, P.; Behrens, U. *Chem. Commun.* **1998**, 1633-1634.

44 Shapiro, N. D.; Toste, F. D. *Proc. Nat. Ac. Sci.* **2008**, *105*, 2779-2782.

45 Wu, J.; Kroll, P.; Dias, H. V. R. *Inorg. Chem.* **2008**, *48*, 423-425.

46 Related gold-alkyne complexes: (a) Köhler, K.; Silverio, S. J.; Hyla-Kryspin, I.; Gleiter, R.; Zsolnai, L.; Driess, A.; Huttner, G.; Lang, H. *Organometallics* **1997**, *16*, 4970-4979. (b) Lang, H.; Köhler, K.; Zsolnai, L. *Chem. Commun.* **1996**, 2043-2044. (c) Mingos, D. M. P.; Yau, J.; Menzer, S.; Williams, D. J. *Angew. Chem., Int. Ed. Engl.* **1995**, *34*, 1894-1895. (d) Hüttel, R.; Forkl, H. *Chem. Ber.* **1972**, *105*, 1664-1673.

*Introduction*

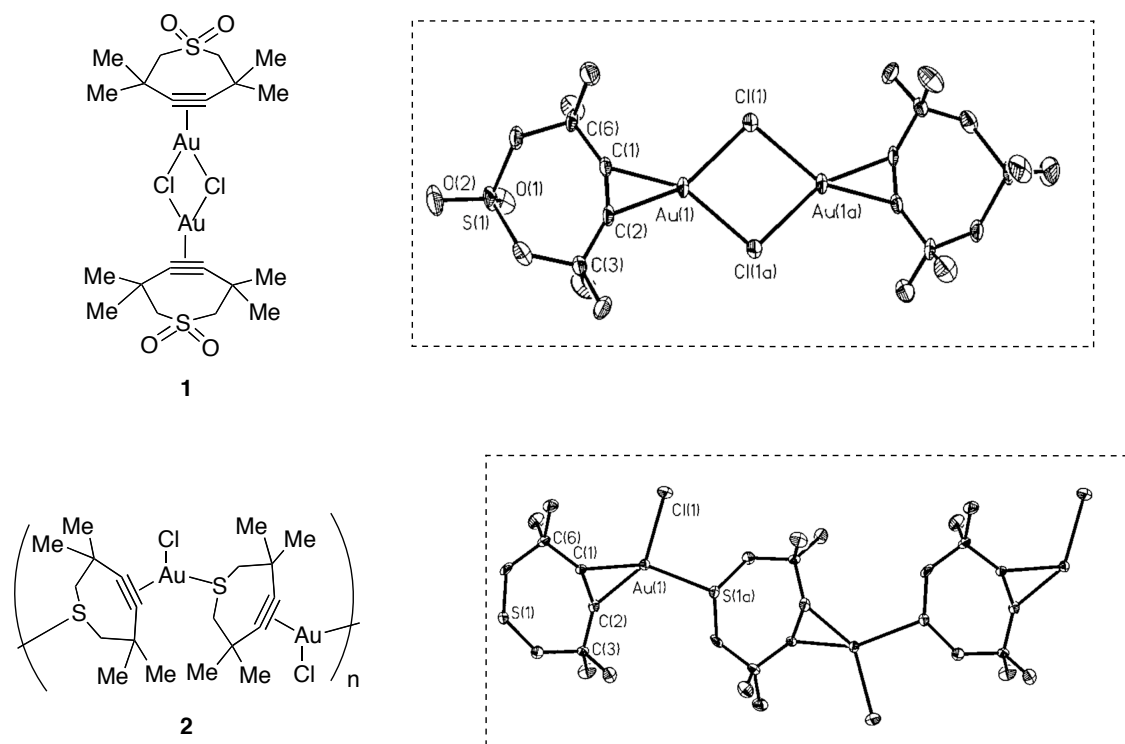


**Figure 3.** Gold complexes with strained alkynes.

Last year, a new complex **3** in which the alkyne is covalently attached to the phosphine ligand was described (Figure 4).<sup>44</sup> In this Au(I)-phosphine- $\eta^2$ -alkyne complex, the X-ray structure shows gold-carbon distances of 2.197(5) and 2.270(5) Å. The gold is then displaced towards one of the carbons of the insaturation.

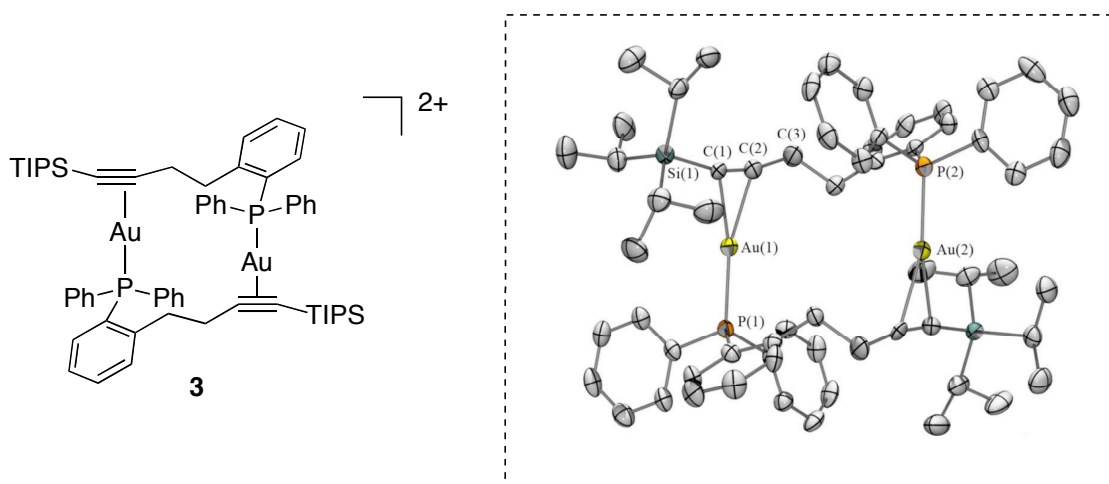


**Figure 4.** Gold complex with an alkyl-substituted phosphine.

Particularly interesting is the recent isolation of neutral gold complex **4** with a simple unstrained alkyne (Figure 5).<sup>45</sup> In this case, gold is coordinated in a  $\eta^2$  fashion,

with Au-C distances of 2.152(4) and 2.172(5) Å and a Cl-Au-centroid<sub>alkyne</sub> angle of 176.3°.

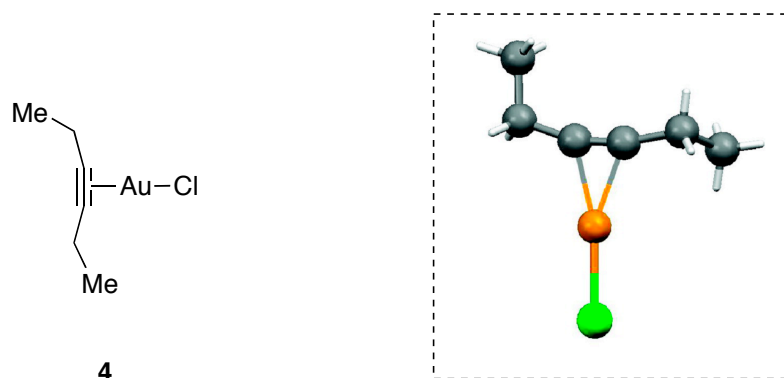


**Figure 5.** Gold complex with a simple alkyne.

A common feature of the latter complexes is the distortion observed in the alkyne moiety. Although small changes in the C-C distance caused by coordination to a metal are difficult to observe, deviations from linearity of this moiety are detected. The average  $C_{sp}-C_{sp}-C_{sp^3}$  angle in complex **4**<sup>45</sup> is 165.0(5)° and 167.2(6) in complex **3**<sup>44</sup>. However, the distortion of the alkyne bond does not provide any insight in the nature of the gold-alkyne bonding, due to the fact that both  $\pi$ -to-metal  $\sigma$ -donation and metal-to- $\pi^*$  back-bonding elongate and distort a coordinated  $\pi$ -bond. As a result, one cannot directly correlate the degree of alkyne distortion with the degree of metal-to- $\pi^*$  back-donation.

For this reason, DFT natural bond order calculations were performed for both **3** and **4** complexes. For a simplified version of complex **3**, second perturbative analysis reveals that  $\pi$ -to-metal  $\sigma$ -donation is the largest contribution (56.6 kcal/mol) followed by metal-to- $\pi^*$  back donation (13.3 kcal/mol).<sup>44</sup> The same trend was observed in the computed values for complex **4** (76.2 kcal/mol and 26.5 kcal/mol, respectively).<sup>45</sup> In both cases the results are in agreement with previous calculations and account for a high  $\sigma$ -donation from the alkyne to the metal. This increases the electrophilicity of this triple bond, supporting the experimentally observed high activity of gold catalysts towards nucleophilic additions to alkynes.

UNIVERSITAT ROVIRA I VIRGILI

GOLD(I)-CATALYZED CYCLIZATIONS OF 1,6- AND 1,7-ENYNES: NEW GOLD COMPLEXES AND CYCLOPROPANATION REACTIONS

Elena Herrero Gómez

ISBN: 978-84-692-5924-5/DL:T-1663-2009

UNIVERSITAT ROVIRA I VIRGILI

GOLD(I)-CATALYZED CYCLIZATIONS OF 1,6- AND 1,7-ENYNES: NEW GOLD COMPLEXES AND CYCLOPROPANATION REACTIONS

Elena Herrero Gómez

ISBN: 978-84-692-5924-5/DL:T-1663-2009

*Chapter 1. Introduction*

UNIVERSITAT ROVIRA I VIRGILI

GOLD(I)-CATALYZED CYCLIZATIONS OF 1,6- AND 1,7-ENYNES: NEW GOLD COMPLEXES AND CYCLOPROPANATION REACTIONS

Elena Herrero Gómez

ISBN: 978-84-692-5924-5/DL:T-1663-2009

## 1. Gold(I) Complexes for Homogeneous Catalysis

When dealing with the chemistry of this noble metal, one cannot forget that mankind has always wanted to possess gold, King Midas legend being a beautiful illustration. On the other hand, at the early beginnings of chemistry, the esoteric Alchemy focused its effort on converting lead into gold. For many years gold compounds were seen only as intermediates to recover this precious metal. As gold(0) is only soluble in cyanide and aqua regia (mixture of nitric and hydrochloric acid), gold cyanide compounds were used to recover gold from its ores. When treated with aqua regia, tetrachloroauric acid is formed. Nowadays, this complex and its salts are commonly used for the preparation of different gold complexes.<sup>1</sup>

This introduction will show an overview of gold(I) complexes, paying special attention to the complexes most commonly used in homogeneous catalysis. Gold(I) compounds are, generally speaking, linear, bi-coordinated, 14-electron species. However, a small number of other complexes with higher coordination numbers have also been reported.<sup>2</sup>

---

1 Schmidbaur, H. *Interdiscipl. Sci. Rev.* **1992**, *17*, 213-220.

2 Gimeno, M. P.; Laguna, A. *Chem. Rev.* **1997**, *97*, 511-522.

Gold(III) complexes are known to be harder Lewis acids than their gold(I) counterparts, and thus, to show a preference for harder nucleophiles such as carbonyl groups. Although catalytic applications of gold(III) have been disclosed,<sup>3</sup> such complexes will not be covered in this introduction. A great number of gold clusters, formed by aurophilic interactions, have also been described.<sup>4</sup>

## 2. Gold(I) Linear Species. Activation of Gold(I) Neutral Complexes

The vast majority of catalytic applications have been developed using gold(I) linear complexes.<sup>3a,5,6</sup> When neutral complexes are employed, it is necessary to abstract one of the ligands in order to get the catalytic active species. This has been performed *in situ* by cleavage of the Au-Me bond in [AuMe(PPh<sub>3</sub>)] complexes with a protic acid<sup>7,8,9,10</sup> or by the use of a silver(I) salt (for example, AgSbF<sub>6</sub>) as a chloride scavenger in [AuLCl].<sup>7,8,11</sup>

- 
- 3 Recent reviews on gold catalysis, which include gold(III)-catalyzed reactions: (a) Gorin, D. J.; Sherry, B. D.; Toste, F. D. *Chem. Rev.* **2008**, *108*, 3351-3378. (b) Zhang, L.; Brouwer, C.; He, C. *Chem. Rev.* **2008**, *108*, 3239-3265. (c) Hashmi, A. S. K.; Hutchings, G. J. *Angew. Chem. Int. Ed.* **2006**, *45*, 7896-7936.
  - 4 (a) Schier, A.; Schmidbaur, H. *Encyclopedia of Inorganic Chemistry*. King, R.B., Ed.; Wiley, 2005; Vol III, pp. 1688-1698. (b) Vittal, J. J.; Puddephat, R. J. *Encyclopedia of Inorganic Chemistry*. King, R.B., Ed.; Wiley, 2005; Vol III, pp. 1673-1687. (c) Gimeno, M. C.; Laguna, A. *Comprehensive Coordination Chemistry II*. McCleverty, J. A., Meyer, T. J., Fenton D. E., Eds.; Elsevier, 2004; Vol 6, pp 911-1145.
  - 5 Jiménez-Núñez, E.; Echavarren, A. M. *Chem. Commun.* **2007**, 333-346.
  - 6 Jiménez-Núñez, E.; Echavarren, A. M. *Chem. Rev.* **2008**, *108*, 3326-3350.
  - 7 Nieto-Oberhuber, C.; Muñoz, M. P.; Buñuel, E.; Nevado, C.; Cárdenas, D. J.; Echavarren, A. M. *Angew. Chem. Int. Ed.* **2004**, *43*, 2402-2406.
  - 8 Nieto-Oberhuber, C.; Muñoz, M. P.; López, S.; Jiménez-Núñez, E.; Nevado, C.; Herrero-Gómez, E.; Raducan, M.; Echavarren, A. M. *Chem. Eur. J.* **2006**, *12*, 1677-1693.
  - 9 Teles, J. H.; Brode, S.; Chabanas, M. *Angew. Chem. Int. Ed.* **1998**, *37*, 1415-1418.
  - 10 (a) Mizushima, E.; Hayashi, T.; Tanaka, M. *Org. Lett.* **2003**, *5*, 3349-3352. (b) Mizushima, E.; Sato, K.; Hayashi, T.; Tanaka, M. *Angew. Chem. Int. Ed.* **2002**, *41*, 4563-4565.
  - 11 Ferrer, C.; Raducan, M.; Nevado, C.; Claverie, C. K.; Echavarren, A. M. *Tetrahedron* **2007**, *63*, 6306-6316.

In order to avoid the use of a silver salt, which can lead to unwanted side reactions,<sup>12</sup> cationic gold(I) complexes were developed.<sup>8</sup> In this case, the coordination vacancy is already preformed and stabilized by a weakly coordinating ligand, usually a molecule containing a nitrile functionality, that can be easily displaced in the presence of the substrate.

### 3. Ligand Effects in Homogeneous Gold(I)-Catalyzed Activation of Alkynes

The role of the ligand of gold(I) is of great interest. Although AuCl or other commercially available salts such as NaAuCl<sub>4</sub> are active enough to catalyze many transformations, the use of different ligands allows to modify the electronic and steric properties of the metal center. Thus, the reactivity in the catalytic system can be effectively modified.

#### 3.1. *N*-Heterocyclic Carbenes and Related Ligands

Gold complexes **1a-d** with highly  $\sigma$ -donating ligands, such as *N*-heterocyclic carbenes have been described (Figure 1).<sup>13,14,15</sup> The electronic donation from the ligand determines a slightly lower reactivity of these complexes compared with their phosphine analogues. On the other hand, this fact, together with the bulkiness of these ligands, causes a higher selectivity.

---

12 Nevado, C.; Echavarren, A. M. *Chem. Eur. J.* **2005**, *11*, 3155-3164.

13 Nieto-Oberhuber, C.; López S.; Echavarren, A. M. *J. Am. Chem. Soc.* **2005**, *127*, 6178-6179.

14 de Frémont, P.; Scott, N. M.; Stevens, E. D.; Nolan, S. P. *Organometallics* **2005**, *24*, 2411-2418.

15 de Frémont, P.; Stevens, E. D.; Fructos, M. R.; Díaz-Requejo, M. M.; Pérez, P. J.; Nolan, S. P. *Chem. Commun.* **2006**, 2045-2047.

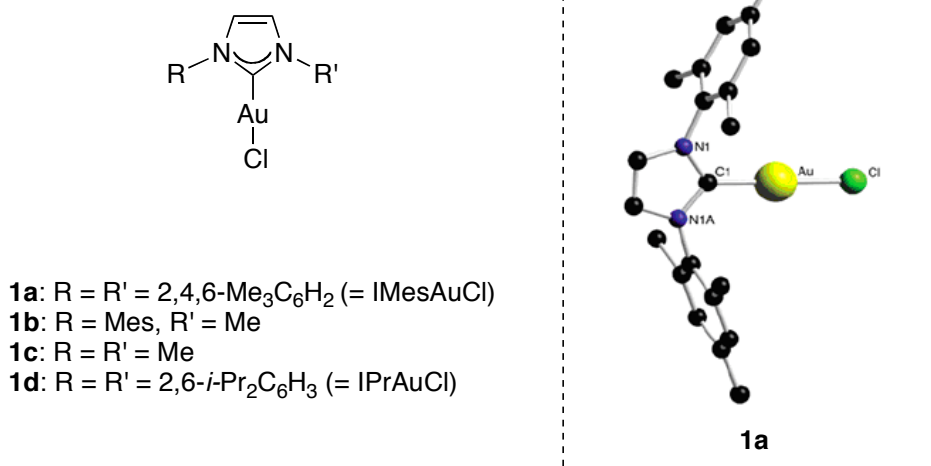


**Figure 1.** Examples of gold NHC-complexes together with X-ray structure of **1a**.

A cationic complex using acetonitrile as ligand **2** was reported to be unstable,<sup>15</sup> but this instability can be overcome by using more electron-rich nitrile ligands, such as benzonitrile or 2,4,6-trimethoxybenzonitrile (**3**, **4a-c**).<sup>16</sup> Related complexes **5a-b** with weakly coordinated bis(trifluoromethanesulfonyl)amide NTf<sub>2</sub> (Tf = CF<sub>3</sub>SO<sub>2</sub>) have also been prepared (Figure 2).<sup>17,18</sup>

- 
- 16 Amijs, C. H. M.; López-Carrillo, V.; Raducan, M.; Pérez-Galán, P.; Ferrer, C.; Echavarren, A. M. *J. Org. Chem.* **2008**, *73*, 7721-7730.
- 17 Li, G.; Zhang, L. *Angew. Chem. Int. Ed.* **2007**, *46*, 5156-5159.
- 18 Ricard, L.; Gagosz, F. *Organometallics* **2007**, *26*, 4704-4707.

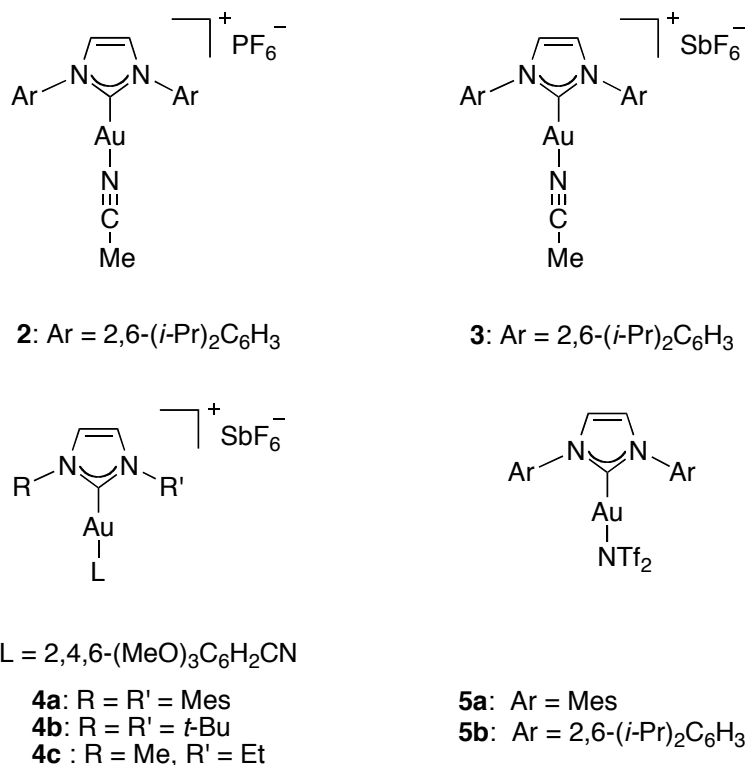


**Figure 2.** Cationic *N*-heterocyclic carbene gold(I) complexes.

Related to the gold(I) complexes with *N*-heterocyclic carbenes, gold(I) carbene complexes of the type AuCl{C(NHR)-(NHPy-*n*)} (where Py = pyridyl; and *n* = 2, 4) have been reported recently.<sup>19,20</sup> These complexes have been obtained by nucleophilic addition of primary amines to pyridylisocyanides coordinated to gold. Different structures are observed depending on the substitution of the pyridine moiety and subsequently, on the hydrogen bonds that exist in the final gold complex.

In the case of gold(I) carbene complexes **6a-e** and **7**, a strong intramolecular hydrogen bond produces a planar cycle, similar to the structure of the nitrogen heterocyclic carbenes (Figure 3). For this reason, these complexes were called hydrogen bond supported heterocyclic carbenes (HBHCs). The hydrogen-bond-supported cyclic structure is observed in the solid state and maintained in solution in CDCl<sub>3</sub> and acetone-*d*<sub>6</sub>, but broken in MeOH.<sup>19</sup>

19 Bartolomé, C.; Carrasco-Rando, M.; Coco, S.; Cordovilla, C.; Martín-Alvarez, J. M.; Espinet, P. *Inorg. Chem.* **2008**, *47*, 1616-1624.

20 Bartolomé, C.; Carrasco-Rando, M.; Coco, S.; Cordovilla, C.; Espinet, P.; Martín-Alvarez, J. M. *Dalton Trans.* **2007**, 5339-5345.

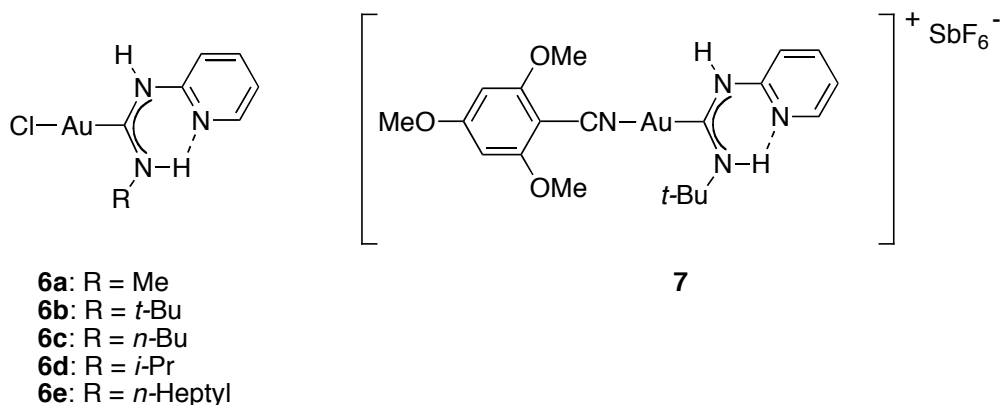
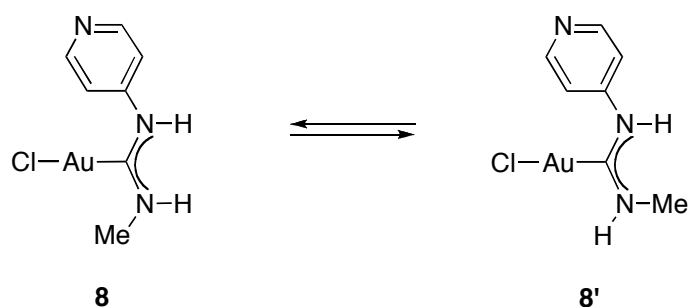


**Figure 3.** Hydrogen bond supported heterocyclic carbene gold complexes.

In complex **8** derived from 4-pyridyl isocyanide, the intermolecular hydrogen bonds are only present in the solid state, whereas in solution noncyclic structures are formed (Scheme 1).<sup>20</sup>



**Scheme 1**

These structural differences also correspond with a different reactivity. Complexes **6a-e** and **7** are good catalysts for the skeletal rearrangement and alkoxy cyclization of enynes.<sup>21</sup> In contrast, the complexes of type **8** are not active. The lack of reactivity can be attributed to the blocking effect of the nitrogen in the NHPy-4 group to the approach of the incoming reagent.

---

21 Bartolomé, C.; Ramiro, Z.; Pérez-Galán, P.; Bour, C.; Raducan, M.; Echavarren, A. M.; Espinet, P. *Inorg. Chem.* **2008**, *47*, 11391-11397.

### 3.2. Phosphine Ligands

Phosphines are the most popular ligands in organometallic chemistry, and the case of gold is not an exception. From very simple complexes, such as  $[\text{AuCl}(\text{PPh}_3)]$  to more sophisticated BINAP-Au-complexes have proven to be excellent catalysts for a number of reactions, in particular for the cyclization of enynes in the presence or absence of external nucleophiles. Gold-oxo complex  $[(\text{Ph}_3\text{PAu})_3\text{O}]\text{BF}_4$ <sup>22</sup> has also been introduced as a catalyst for the propargylic Claisen rearrangement of enynes.<sup>23</sup>

From all available phosphines, bulky biphenylphosphines have turned out to be privileged ligands for gold complexes.<sup>13</sup> This type of ligand was described in the context of palladium-catalyzed cross-coupling reactions, giving excellent results.<sup>24</sup> The activated neutral complexes **9a-d** and their cationic gold(I) counterparts **10a-d** are excellent catalysts for the cyclization of enynes and related reactions (Figure 4).<sup>7,8,13,25,26,27,28</sup> These complexes will be discussed in more detail in *Section 4* of this introduction.

- 
- 22 (a) Yang, Y.; Ramamoorthy, V.; Sharp, P. R. *Inorg. Chem.* **1993**, *32*, 1946-1950. (b) Nesmeyanov A. N.; Perevalova, E. G.; Struchkov, Y. T.; Antipin, M. Y.; Grandberg, K. I.; Dyadchenko, V. P. *J. Organomet. Chem.* **1980**, *201*, 343-349.
- 23 Sherry B. D.; Toste, F. D. *J. Am. Chem. Soc.* **2004**, *126*, 15978-15979.
- 24 (a) Barder, T. E.; Buchwald, S. L. *J. Am. Chem. Soc.* **2007**, *129*, 5096-5101. (b) Barder, T. E.; Walker, S. D.; Martinelli, J. R.; Buchwald, S. L. *J. Am. Chem. Soc.* **2005**, *127*, 4685-4696. (c) Walker, S. D.; Barder, T. E.; Martinelli, J. R.; Buchwald, S. L. *Angew. Chem. Int. Ed.* **2004**, *43*, 1871-1876. (d) Strieter, E. R.; Blackmond, D. G.; Buchwald, S. L. *J. Am. Chem. Soc.* **2003**, *125*, 13978-13980. (e) Kaye, S.; Fox, J. M.; Hicks, F. A.; Buchwald, S. L. *Adv. Synth. Catal.* **2001**, *343*, 789-794.
- 25 Nieto-Oberhuber, C.; López, S.; Muñoz, M. P.; Cárdenas, D. J.; Buñuel, E.; Nevado, C.; Echavarren, A. M. *Angew. Chem. Int. Ed.* **2005**, *44*, 6146-6148.
- 26 Nieto-Oberhuber, C.; López, S.; Jiménez-Núñez, E.; Echavarren, A. M. *Chem. Eur. J.* **2006**, *12*, 5916-5923.
- 27 Nieto-Oberhuber, C.; López, S.; Muñoz, M. P.; Jiménez-Núñez, E.; Buñuel, E.; Cárdenas, D. J.; Echavarren, A. M. *Chem. Eur. J.* **2006**, *12*, 1694-1702.
- 28 Ferrer, C.; Echavarren, A. M. *Angew. Chem. Int. Ed.* **2006**, *45*, 1105-1109.

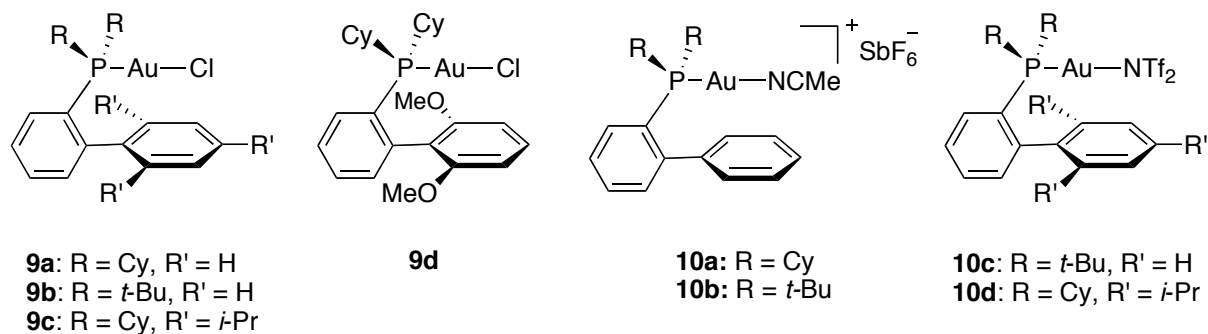


**Figure 4.** Gold(I) complexes with bulky biphenyl phosphines.

A different approach to decrease the electrophilicity on the gold center by non-covalent effects was tested in triphenylphosphine-based complexes. Therefore, an electron-donating group, such as a methoxy group, was placed in the *ortho*-position of one of the aromatic rings. Thus, a donation from the oxygen to the gold center was expected (Figure 5).<sup>29</sup> Complex **11** was tested in the gold(I)-catalyzed hydroamination of allenes, but no significant improvement was observed compared with simple [AuCl(PPh<sub>3</sub>)].

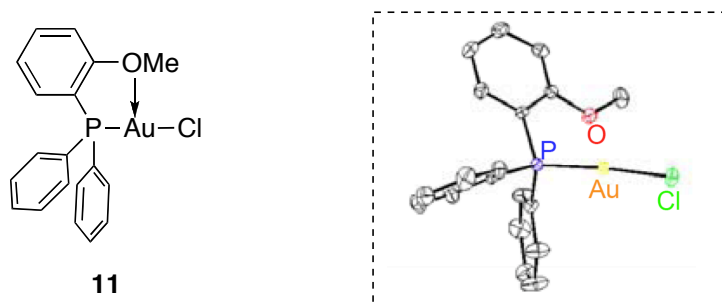


**Figure 5.** X-ray structure of complex **11**.

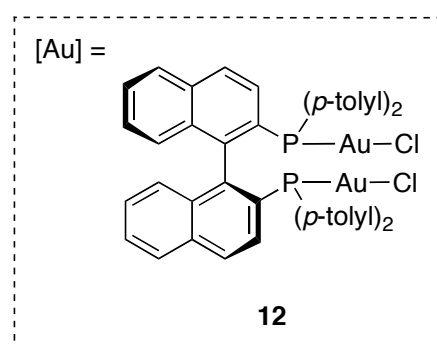
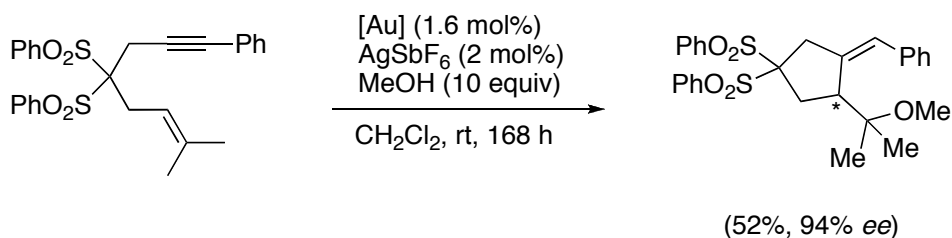
### 3.3. Chiral Ligands in Enantioselective Gold-Catalyzed Reactions

The development of highly enantioselective transformations still remains a challenge in many gold-catalyzed reactions.<sup>30</sup> The difficulty to get a high level of stereinduction lies in the already mentioned linear coordination of gold(I) complexes, that places the chiral ligand

29 Nishina, N.; Yamamoto, Y. *Tetrahedron* **2008**, *49*, 4908-4911.

30 Recent review in enantioselective gold(I) catalysis: Widenhoefer, R. A. *Chem. Eur. J.* **2008**, *14*, 5382-5391.

far from the reaction center. However, the first example of a gold(I)-catalyzed enantioselective alkoxy cyclization of 1,6-enynes was reported using a chiral bis(gold) complex **12** (Scheme 2).<sup>31,32</sup>



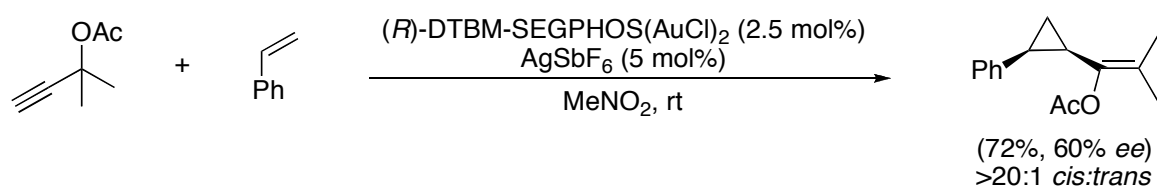
Scheme 2

Based on this promising result, some examples of enantioselective gold(I) transformations have been developed, mainly in the field of intramolecular hydrofunctionalization of allenes with carbo- and heteronucleophiles. Thus, examples have been reported in allene hydroarylation,<sup>33,34</sup> cycloisomerization of enallenes,<sup>35</sup> [2+2] cycloaddition of enallenes,<sup>36</sup> intramolecular hydroalkoxylation of allenes,<sup>37</sup> hydroamination

- 31 Muñoz, M. P.; Adrio, J.; Carretero, J. C.; Echavarren, A. M. *Organometallics* **2005**, *24*, 1293-1300.
- 32 In early examples of enantioselective gold(I)-catalyzed coupling of aldehydes with isocyanoacetate esters, gold acts as a traditional Lewis acid through carbonyl group activation: (a) Ito, Y.; Sawamura, M.; Hayashi, T. *J. Am. Chem. Soc.* **1986**, *108*, 6405-6406. (b) Hayashi, T.; Sawamura, M.; Ito, Y. *Tetrahedron* **1992**, *48*, 1999-2012.
- 33 Zhang, Z.; Liu, C.; Kinder, R. E.; Han, X.; Qian, H.; Widenhofer, R. A. *J. Am. Chem. Soc.* **2006**, *128*, 9066-9073.
- 34 Liu, C.; Widenhofer, R. A. *Org. Lett.* **2007**, *9*, 1935-1938.
- 35 Tarselli, M. A.; Chianese, A. R.; Lee, S. L.; Gagné, M. R. *Angew. Chem. Int. Ed.* **2007**, *46*, 6670-6673.
- 36 Luzung, M. R.; Mauleón, P.; Toste, F. D. *J. Am. Chem. Soc.* **2007**, *129*, 12402-12403.

of *N*-allenyl carbamates,<sup>38</sup> and hydroamination of allenyl sulfonamides<sup>39</sup> among others. Bis(gold)-phosphine complexes [(AuX<sub>2</sub>)(P-P)] (P-P = chiral biphosphine, X = anionic ligand or counteranion) are still the most employed catalysts for these transformations.

The combination of a chiral bis(gold)phosphine complex together with a silver salt has also been successfully applied to the enantio- and stereoselective gold(I)-catalyzed cyclopropanation of olefins (Scheme 3).<sup>40</sup> Gold(I)-catalyzed cyclopropanation reactions will be discussed in more detail in the introduction of *Chapter 2*.



**Scheme 3**

Recently, the first enantioselective [4+2]-cycloaddition of 1,6-enynes has been described using (*R*)-4-MeO-3,5-(*t*-Bu)<sub>2</sub>MeOBIPHEP(AuCl)<sub>2</sub> (**13**).<sup>41</sup> This result confirms the possibility of developing efficient enantioselective gold(I)-catalyzed transformations for enynes (Scheme 4).

---

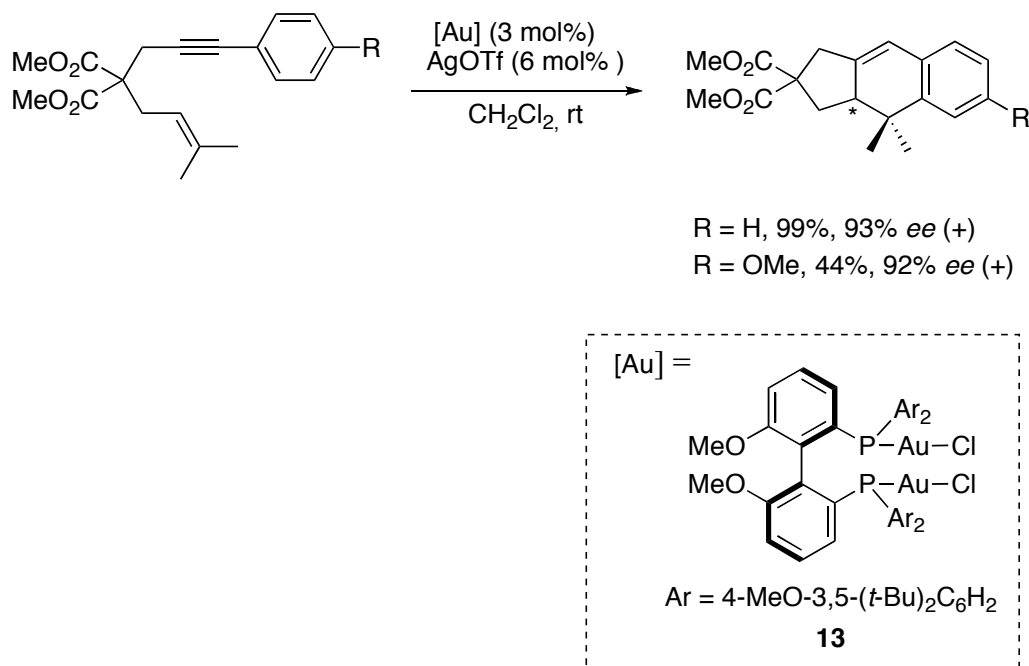
37 Zhang, Z.; Widenhofer, R. A. *Angew. Chem. Int. Ed.* **2007**, *46*, 283-285.

38 Zhang, Z.; Bender, C. F.; Widenhofer, R. A. *Org. Lett.* **2007**, *9*, 2887-2889.

39 LaLonde, R. L.; Sherry, B. D.; Kang, E. J.; Toste, F. D. *J. Am. Chem. Soc.* **2007**, *129*, 2452-2453.

40 Johansson, M. J.; Gorin, D. J.; Staben, S. T.; Toste, F. D. *J. Am. Chem. Soc.* **2005**, *127*, 18002-18003.

41 Chao, C.-M.; Vitale, M. R.; Toullec, P. Y.; Genêt, J.-P.; Michelet, V. *Chem. Eur. J.* **2009**, *15*, 1319-1323.



Scheme 4

Another strategy based on the use of non-chiral gold complexes in combination with a binaphthol-based chiral counteranion has proven to be useful in the case of hydroxy- and amino cyclizations of allenes.<sup>42</sup>

### 3.4. Gold(I) Complexes with Higher Coordination Numbers

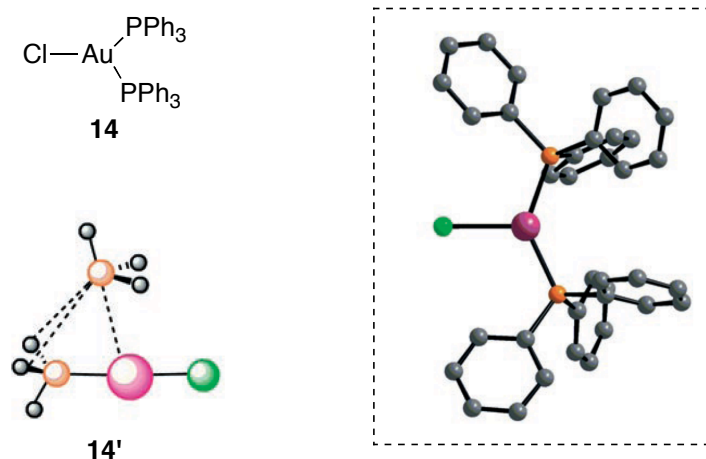
Despite being less common than linear gold compounds, gold(I) complexes with three ligands have been described and characterized by X-ray crystallography. Most of them are complexes containing two phosphines as ligands, and usually the interaction with the second phosphine ligand is weaker. As an example, in complex **14**<sup>43</sup> (Figure 6)  $r_{\text{Au-P1}}$  is 2.230 Å and  $r_{\text{Au-P2}}$  is 2.313 Å (for comparison, in [AuCl(PPh<sub>3</sub>)]  $r_{\text{Au-P}}$  is 2.235 Å). This preference for bicoordination is more evident in the simplified calculated structure **14'**,<sup>44</sup> where an almost

42 Hamilton, G. L.; Kang, E. J.; Mba, M.; Toste, F. D. *Science* **2007**, *317*, 496-499.

43 Khan, M.; Oldham, C.; Tuck, D. G. *Can. J. Chem.* **1981**, *59*, 2714-2718.

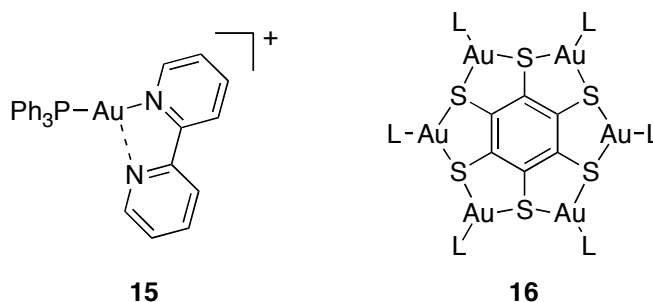
44 (a) Schwerdtfeger, P.; Hermann, H. L.; Schmidbaur, H. *Inorg. Chem.* **2003**, *42*, 1334-1342. (b) Bowmaker, G. A.; Schmidbaur, H.; Krüger, S.; Rösch, N. *Inorg. Chem.* **1997**, *36*, 1754-1757.

linear arrangement between the gold atom and one of the phosphines is observed, and can also be explained considering that  $[\text{AuL}]^+$  fragment is isolobal to  $\text{H}^+$  and  $\text{HgL}_2^+$ .<sup>45</sup>



**Figure 6.** X-Ray and computed structure of complex **14**.

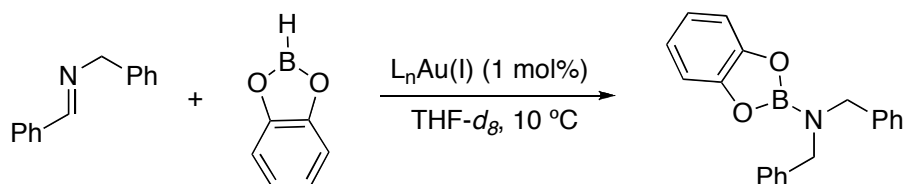
Therefore, the structures can vary from very distorted ones with an almost linear arrangement of the gold center with two of the three donor atoms<sup>46</sup> (T-shaped coordination) to a regular trigonal-planar geometry<sup>47</sup> (Figure 7). In addition, some examples of tetrahedral four coordinate complexes have also been reported.<sup>2</sup>

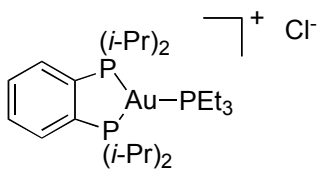
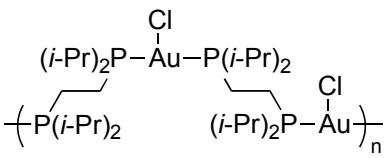


**Figure 7.** Examples of T-shaped (**15**) and trigonal-planar (**16**) gold complexes.

- 
- 45 (a) Schmidbaur, H. *Chem. Soc. Rev.* **1995**, 391-400. (b) Hall, K. P.; Mingos, D. M. P. *Prog. Inorg. Chem.* **1984**, *32*, 237-325. (c) Hoffmann, R. *Angew. Chem., Int. Ed. Engl.* **1982**, *21*, 711-724.
- 46 Selected example: Usón, R.; Laguna, A.; Navarro, A.; Parish, R. V.; Moore, L. S. *Inorg. Chim. Acta* **1986**, *112*, 205-208.
- 47 Selected example: Yip, H. K.; Schier, A.; Riede, J.; Schmidbaur, H. *J. Chem. Soc., Dalton Trans.* **1994**, 2333-2334.

The interest of these rather anomalous complexes is not only based on the novel structural situation, but also because of their potential applications. Interestingly, three-coordinate biphosphine gold(I) chloride complexes are effective catalysts for reduction and hydrogen atom transfer reactions (Scheme 5).<sup>48,49</sup>



catalyst	relative rate
none	1.0
(Et <sub>3</sub> P)AuCl	2.0
	3.7
	14.8
[AuCl(μ-dppf)] <sub>n</sub>	>40

Scheme 5

48 Baker, R. T.; Calabrese, J. C.; Westcott, S. A. *J. Organomet. Chem.* **1995**, 498, 109-117.

49 Baker, R. T.; Nguyen, P.; Marder, T. B.; Westcott, S. A. *Angew. Chem. Int. Ed.* **1995**, 34, 1336-1338.

## 4. Gold(I) Complexes of Bulky, Electron-Rich Biaryl Phosphines

The reason behind the stability and high activity of this family of biphenyl phosphine ligands, which are also referred to as Buchwald phosphines (Figure 8), has been the subject of numerous studies.<sup>24a,e</sup> They are believed to stabilize critical intermediates, such as three-coordinate palladium species, by an effective spatial shielding of the metal by the *ortho* phenyl substituent.<sup>50</sup> Palladium- $\pi$  aryl bonding interactions with the non-phosphorous containing aryl group have been proposed and confirmed by control experiments with a ligand bearing cyclohexyl instead of the pendant arene ring, molecular modeling, and structural studies of chemically competent palladium complexes.<sup>51</sup>

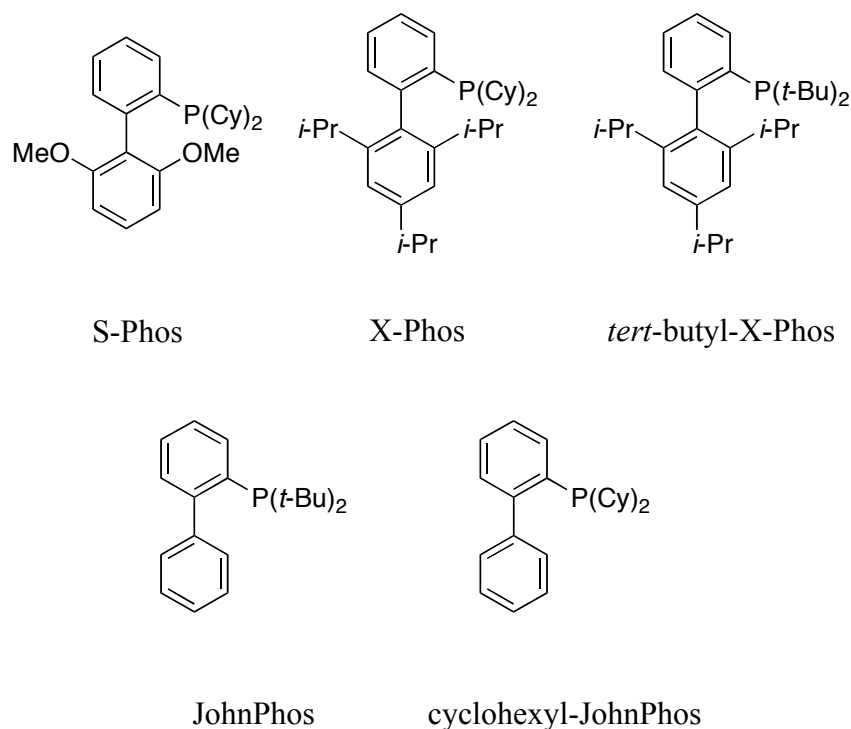


**Figure 8.** Representative examples of Buchwald phosphines.

---

50 Old, D. W.; Wolfe, J. P.; Buchwald, S. L. *J. Am. Chem. Soc.* **1998**, *120*, 9722-9723.

51 Wolfe, J. P.; Tomori, H.; Sadighi, J. P.; Yin, J.; Buchwald, S. L. *J. Org. Chem.* **2000**, *65*, 1158-1174.

The use of these ligands has also led to the isolation of new palladium(I) complexes such as **17**, which display unusual Pd-arene interactions (Figure 9).<sup>52</sup>

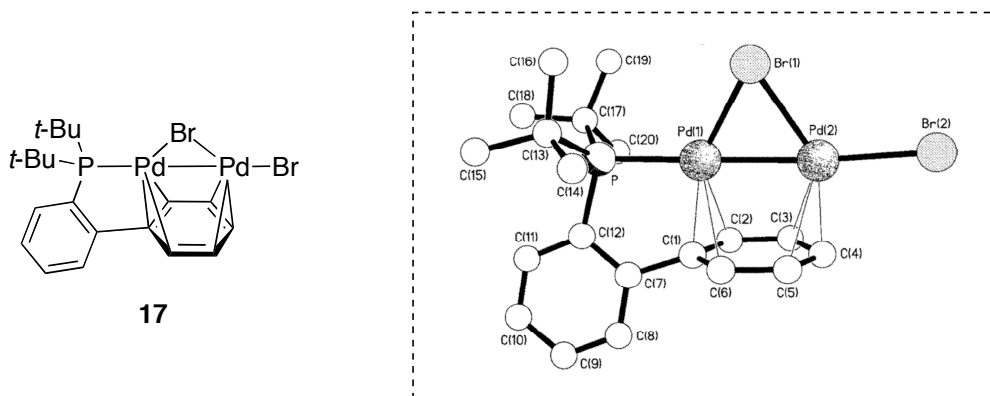


Figure 9. X-ray structure of dinuclear palladium complex **17**.

Gold(I) complexes with Buchwald phosphines are stable solids that are the catalysts of choice for the cyclization of 1,6- and 1,7-enynes,<sup>8,53</sup> intramolecular cyclopropanation of dienyne,<sup>27</sup> [2+2] cycloadditions of enynes,<sup>25</sup> [4+2] intramolecular cycloadditions of 1,3-enynes with olefins<sup>13</sup> and cyclization reaction of alkynes with indoles.<sup>28</sup>

#### 4.1. Gold(I)-Arene Interactions

The question if the gold center is stabilized by a  $\pi$  interaction with the covering arene is still open. Although some authors favor the involvement of gold(I)-arene interactions, the bonding distances do not lead to a definitive conclusion. Recently, Gray and coworkers have quantified the hapticity of this interaction in a family of gold(I) complexes with Buchwald phosphines.<sup>54</sup>

The hapticity ( $\eta^x$ ) indicates the connectivity between a ligand, usually a hydrocarbon, and a metal. That is, the superscripted number following the  $\eta$  denotes the number of carbon

- 
- 52 (a) Christmann, U.; Pantazis, D. A.; Benet-Buchholz, J.; McGrady, J. E.; Maseras, F.; Vilar, R. *J. Am. Chem. Soc.* **2006**, *128*, 6376-6390. (b) Barder, T. E. *J. Am. Chem. Soc.* **2006**, *128*, 898-904. (c) Christmann, U.; Vilar, R.; White, A. J. P.; Williams, D. J. *Chem. Commun.* **2004**, 1294-1295.
- 53 Cabello, N.; Rodríguez, C.; Echavarren, A. M. *Synlett* **2007**, 1753-1758.
- 54 Partyka, D. V.; Robilotto, T. J.; Zeller, M.; Hunter, A. D.; Gray, T. G. *Organometallics* **2008**, *27*, 28-32.

atoms of a ligand bound to the metal. It can be estimated taking into account the distances between the metal and the involved ligand atoms and comparing them with standard bond distances, although sometimes not well-defined situations are found. In order to have a more accurate value, Kochi and co-workers introduced a geometrical criterium in the context of silver(I)-arene complexes (Scheme 6).<sup>55</sup>

$$\eta^x; x = 1 + 2(d_1^2 - D^2)^{1/2} / [(d_1^2 - D^2)^{1/2} + (d_2^2 - D^2)^{1/2}]$$

### Scheme 6

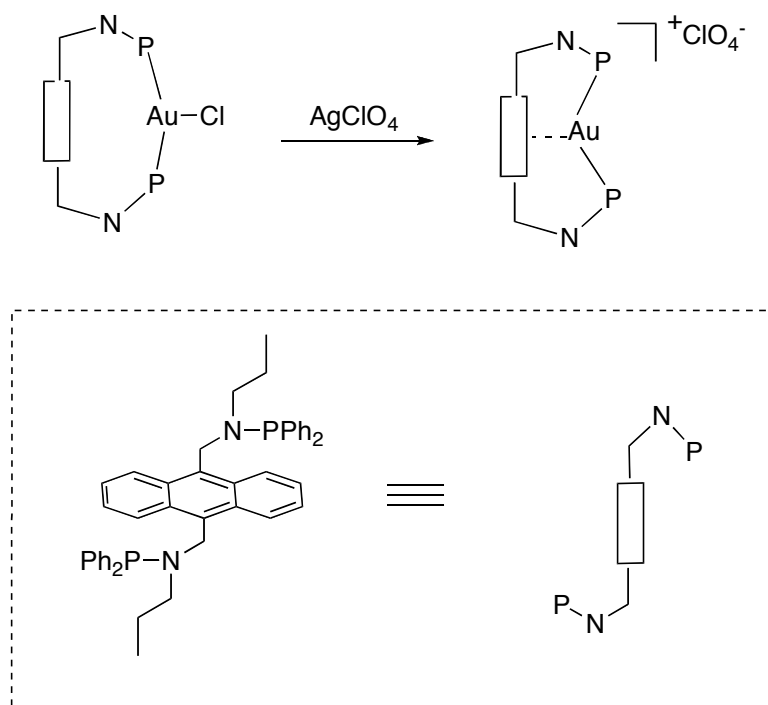
Where  $d_1$  and  $d_2$  are the closest and the second closest Ag-C distances, respectively, and  $D$  is the distance between the silver atom and the mean plane of the aromatic ring.

The reported values of hapticity ranged from  $\eta = 1.32$  to  $\eta = 1.95$ , being the average distance between gold and the mean plane of the covering arene 3.111 Å. This distance, although shorter than the sum of van der Waals radii of carbon and gold (3.36 Å),<sup>56</sup> seems too long for a real coordinative interaction. However, the scarceness of gold(I)-arene complexes in the literature left the question of the existence of gold-arene interactions open. This is in sharp contrast to silver(I), whose complexes with arenes have been thoroughly investigated.<sup>55a,57</sup> In fact, previous to our work, there were only four reported examples of complexes displaying such interactions.<sup>58,59</sup> In these compounds, studied by Zhang and

- 
- 55 (a) Ogawa, K.; Kitagawa, T.; Ishida, S.; Komatsu, K. *Organometallics* **2005**, *24*, 4842-4844. (b) Vasilyev, A. V.; Lindeman, S. V.; Kochi, J. K. *Chem. Commun.* **2001**, 909-910.
- 56 Bondi, A. *J. Phys. Chem.* **1964**, *68*, 441-451.
- 57 Leading references: (a) Rathore, R.; Chebny, V. J.; Abdelwahed, S. H. *J. Am. Chem. Soc.* **2005**, *127*, 8012-8023. (b) Laali, K. K.; Hupertz, S.; Temu, A. G.; Galembeck, S. E. *Org. Biomol. Chem.* **2005**, *3*, 2319-2326. (c) Lindeman, S. V.; Rathore, R.; Kochi, J. K. *Inorg. Chem.* **2000**, *39*, 5707-5716. (d) Munakata, M.; Wu, L. P.; Ning, G. L. *Coord. Chem. Rev.* **2000**, *198*, 171-203. (e) Munakata, M.; Wu, L. P.; Kuroda-Sowa, T.; Maekawa, M.; Suenaga, Y.; Ning, G. L.; Kojima, T. *J. Am. Chem. Soc.* **1998**, *120*, 8610-8618.
- 58 Xu, F.-B.; Li, Q.-S.; Wu, L.-Z.; Leng, X.-B.; Li, Z.-C.; Zeng, X.-S.; Chow, Y. L.; Zhang, Z.-Z. *Organometallics* **2003**, *22*, 633-640.
- 59 Li, Q.-S.; Wang, C.-Q.; Zou, R.-Y.; Xu, F.-B.; Song, H.-B.; Wan, X.-J.; Zhang, Z.-Z. *Inorg. Chem.* **2006**, *45*, 1888-1890.

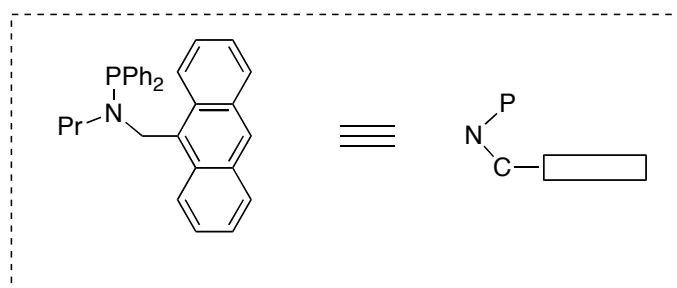
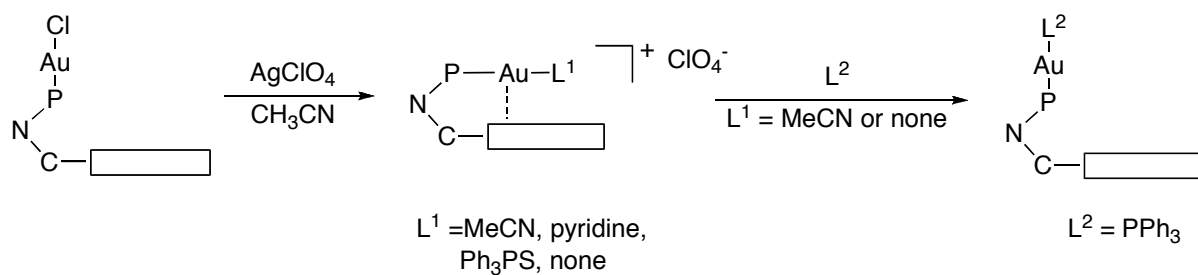
coworkers, the gold center interacts with an aromatic ring that is covalently attached to the ligand in the complex.

The first reported gold(I) complex has a bidentate 9,10-bis- $\{[N-n\text{-propyl-}N\text{-}(\text{diphenylphosphino})\text{amino}]\text{methyl}\}$ -anthracene ligand.<sup>58</sup> Upon reaction with  $\text{AgClO}_4$ , the cationic derivative is formed, which displays a  $\eta^6$ -gold(I)-arene interaction (Scheme 7). This complex, together with the  $\text{Ag}^+$  and  $\text{Cu}^+$  analogues, was structurally characterized by X-ray diffraction and confirmed using *ab initio* and density functional calculations. The distance of the gold ion to the centroid of the anthracene is 3.00 Å and the distance of the gold ion to the six carbon atoms of the middle ring in anthracene varies from 3.118 to 3.246 Å.



Scheme 7

Using a different ligand that also contains an anthracene moiety, 9- $\{[N-n\text{-propyl-}N\text{-}(\text{diphenylphosphino})\text{amino}]\text{methyl}\}$ -anthracene, the first gold(I) complexes displaying a  $\text{Au(I)-arene } \eta^2$  interaction were synthesized (Scheme 8).<sup>59</sup> Interestingly, as in the first example, the mentioned interaction is only present in the cationic complexes, in which the electron densities of gold atoms are less than in the corresponding neutral complexes.



**Scheme 8**

This conflicts with a  $\eta^2$ -bonding formed by  $\pi$  back donation from the metal to two carbons of the aromatic ring, which is predicted by the Dewar-Chatt-Duncanson<sup>60</sup> model for  $\text{Ag}^+$ -arene complexes. Thus, following Mulliken's assumption,<sup>61</sup> the  $\pi$ -interaction in complexes **18** is dominated by a charge transfer from the arene to the  $\text{Au}^+$  ion. The distances between the two carbons of the arene involved in the interaction with  $\text{Au}^+$  in complex **18** are comparable to those reported for the  $\eta^6$  gold(I)-arene complex depicted in Scheme 8 and vary from 2.958 and 3.163 Å (Figure 10).

60 (a) Chatt, J.; Duncanson, L. A. *J. Chem. Soc.* **1953**, 2939-2947. (b) Dewar, M. J. S. *Bull. Soc. Chim. Fr.* **1951**, 18, C71-C79.

61 Mulliken, R. S. *J. Am. Chem. Soc.* **1952**, 74, 811-824.

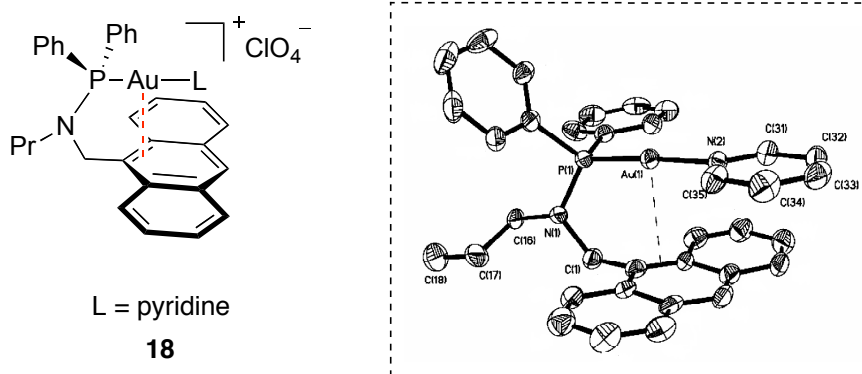


**Figure 10.** X-ray structure of complex **18**.

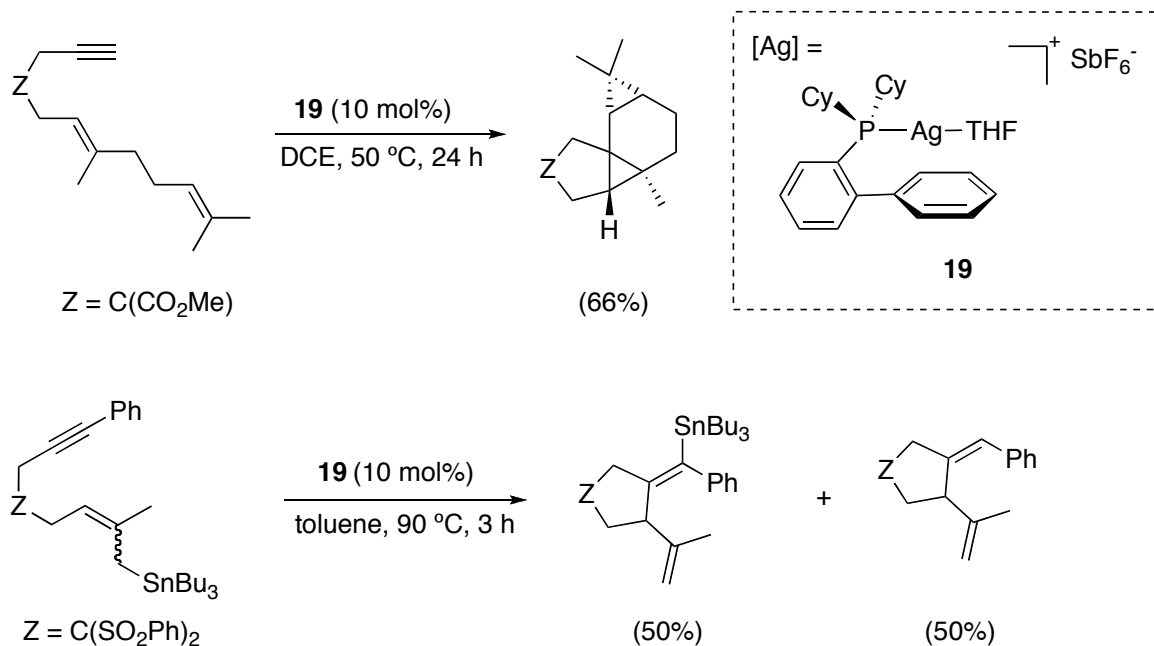
## 4.2. Related Silver and Copper Complexes

Although gold(I) complexes with biaryl phosphine have proven to be excellent catalysts for a variety of transformations, the use of such ligands with other metals from group 11 is not so common.

Cationic silver(I) complex **19** has shown to be an active catalyst for the intramolecular carbostannylation of alkynes as well as for the skeletal rearrangement and cyclopropanation reactions of 1,6-enynes (Scheme 9).<sup>62,63</sup>

62 Porcel, S.; Echavarren, A. M. *Angew. Chem. Int. Ed.* **2007**, *46*, 2672-2676

63 Related heterobimetallic [(*g*<sup>4</sup>-1,5-C<sub>8</sub>H<sub>12</sub>)Ir(1-Cl)<sub>2</sub>Ag(*t*-Bu<sub>2</sub>Pbiph<sup>Me</sup>)] complexes: Dahlenburg, L.; Menzel, R.; Puchta, R.; Heinemann, F. W. *Inorg. Chim. Acta.* **2008**, *361*, 2623-2630.



Scheme 9

Few examples of related copper complexes are reported in the literature.<sup>64</sup> The ability to form stable complexes with phosphines was exploited by using CuCl as scavenger and recovering agent of phosphines in palladium cross-coupling reactions.<sup>65</sup> The strategy was based on the addition of this cheap, commercially available copper salt to the reaction mixture. Upon filtration, the phosphine is isolated *via* the corresponding copper complexes. Free ligand can be recovered by treating the formed complexes with a simple dithiol. Although this protocol was applied mainly to chiral phosphines, an example with biphenyl-2-ylidicyclohexylphosphine is also reported.<sup>65</sup> The stoichiometry of CuCl and the mentioned phosphine was 1:1, although no further characterization of the formed copper complex was carried out.

In a different context, *o*-semiquinone copper(I) complexes with (2-dicyclohexylphosphino)biphenyl or (2-di-*tert*-butylphosphino)biphenyl were described

---

64 Related copper complexes and their use as coupling catalysts are patented: Scholz, U.; Kunz, K.; Gaertzen, O.; Benet-Buchholz, J.; Wesener, J. *Eur. Pat. Appl.* 1, 437, 356, **2004**.

65 Lipshutz, B. H.; Frieman, B.; Birkedal, H. *Org. Lett.* **2004**, 6, 2305-2308.

(Figure 11). These three-coordinated copper complexes species are remarkably stable and do not react when solvating solvents or neutral ligands are added.<sup>66</sup>

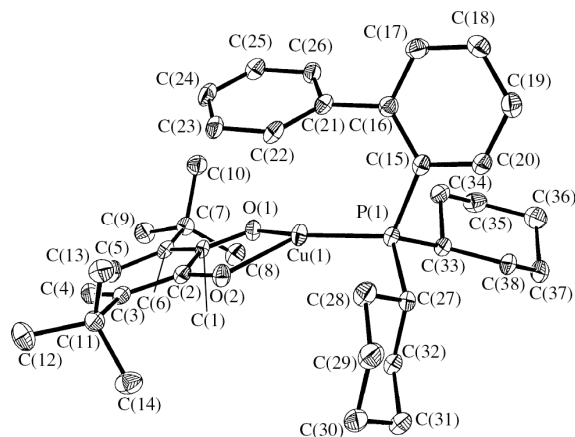
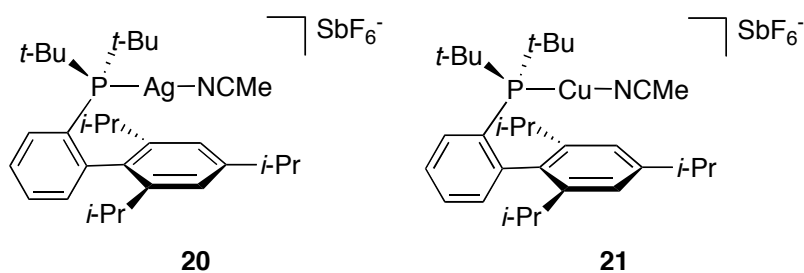
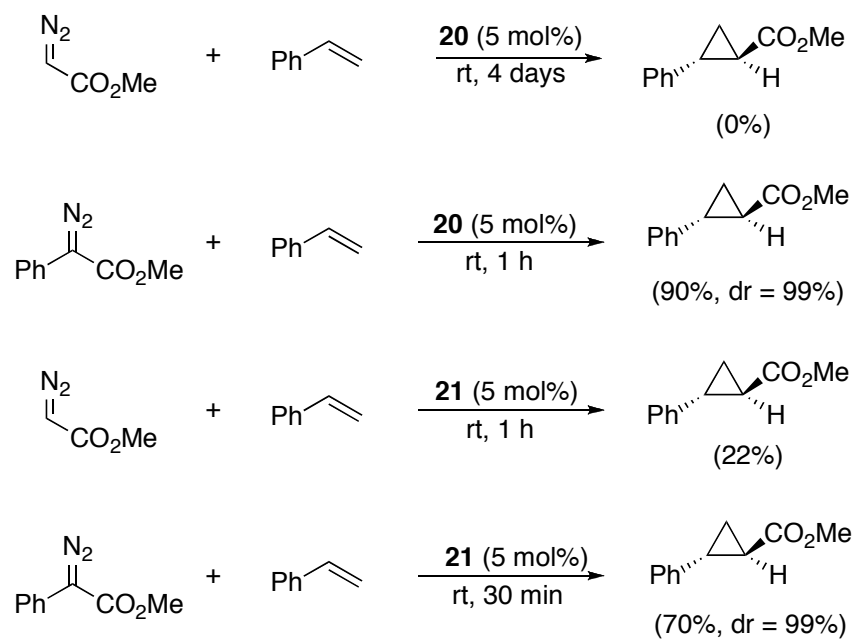


**Figure 11.** X-ray structure of an *o*-semiquinone copper complex with 2-(dicyclohexylphosphino)biphenyl phosphine.

Recently, silver and copper complexes **20** and **21** were employed as part of a study of the olefin cyclopropanation with a manifold of complexes of coinage metals.<sup>67</sup> The use of ethyldiazoacetate (EDA) as a carbene source led to low conversions using the copper catalyst **21** and was not successful with the silver counterpart **20**. Changing to phenyldiazoacetate led to a dramatic increase in reactivity (Scheme 10). These studies showed that gold- and copper-complexes with phosphine, phosphite and *N*-heterocyclic carbenes were suitable catalysts for these transformations. High conversion and diastereoselectivity towards the *trans* isomer was achieved. On the contrary, silver analogues were markedly less active in this reaction.

66 Abakumov, G. A.; Krashilina, A. V.; Cherkasov, V. K.; Zakharov, L. N. *Dokl. Chem.* **2003**, *391*, 343-345.

67 Prieto, A.; Fructos, M. R.; Díaz-Requejo, M. M.; Pérez, P. J.; Pérez-Galán, P.; Delpont, N.; Echavarren, A. M. *Tetrahedron* **2009**, *65*, 1790-1793.



Scheme 10

UNIVERSITAT ROVIRA I VIRGILI

GOLD(I)-CATALYZED CYCLIZATIONS OF 1,6- AND 1,7-ENYNES: NEW GOLD COMPLEXES AND CYCLOPROPANATION REACTIONS

Elena Herrero Gómez

ISBN: 978-84-692-5924-5/DL:T-1663-2009

## *Chapter 1. Objectives*

UNIVERSITAT ROVIRA I VIRGILI

GOLD(I)-CATALYZED CYCLIZATIONS OF 1,6- AND 1,7-ENYNES: NEW GOLD COMPLEXES AND CYCLOPROPANATION REACTIONS

Elena Herrero Gómez

ISBN: 978-84-692-5924-5/DL:T-1663-2009

Complexes of bulky biphenyl phosphines have been reported mainly in the context of Pd-catalyzed reactions.<sup>24</sup> However, the success of gold(I) complexes with these ligands has prompted the use of this type of phosphines with other metals of group 11. A number of new coinage metal-complexes were synthesized in our research group as a part of ongoing studies of new metal catalyzed reactions and their catalytic properties that have been reported elsewhere.<sup>67</sup> Interestingly, their X-ray diffraction characterization showed significant structural differences between these novel silver and copper complexes and their gold analogues. We envisioned that a combined X-ray and computational structural study of a group 11 family of related complexes was of interest as it will shed light into the debate about the possible interaction between the gold(I) and the covering arene of the biphenyl phosphine.

In addition, given the few literature precedents on gold-arene complexes, we were interested in preparing a new family of complexes that display novel gold-arene interactions. In particular, we focused on the study phosphine gold complexes that are commonly used in the group in the context in enyne cyclization reactions.

The use of gold catalysts has opened new possibilities for organic reactions. Thus, the development of new gold complexes will be interesting not only as a way to improve the outcome of known reactions but also to discover new transformations. Our goal in this field was to develop the synthesis of new gold catalysts with  $\pi$  acceptor ligands, as we predicted that greater electrophilicity on the gold center would give as a consequence a higher reactivity.

UNIVERSITAT ROVIRA I VIRGILI

GOLD(I)-CATALYZED CYCLIZATIONS OF 1,6- AND 1,7-ENYNES: NEW GOLD COMPLEXES AND CYCLOPROPANATION REACTIONS

Elena Herrero Gómez

ISBN: 978-84-692-5924-5/DL:T-1663-2009

UNIVERSITAT ROVIRA I VIRGILI

GOLD(I)-CATALYZED CYCLIZATIONS OF 1,6- AND 1,7-ENYNES: NEW GOLD COMPLEXES AND CYCLOPROPANATION REACTIONS

Elena Herrero Gómez

ISBN: 978-84-692-5924-5/DL:T-1663-2009

*Chapter 1. Results and discussion*

UNIVERSITAT ROVIRA I VIRGILI

GOLD(I)-CATALYZED CYCLIZATIONS OF 1,6- AND 1,7-ENYNES: NEW GOLD COMPLEXES AND CYCLOPROPANATION REACTIONS

Elena Herrero Gómez

ISBN: 978-84-692-5924-5/DL:T-1663-2009

## 1. Computational Study of Group 11 Metal Complexes with Bulky, Biphenyl Phosphines<sup>68</sup>

The excellent performance shown by gold complexes with Buchwald phosphines has allowed to perform certain reactions under milder conditions and with an increased selectivity.<sup>7,8,13,24,25,26,27,28</sup> However, a good understanding of their structural features will also provide the tools to design even more efficient catalysts. On the other hand, similar complexes containing silver or copper have a completely different reactivity in carbene transfer reactions from phenyldiazoacetate.<sup>67</sup> We envisioned that a comparative study of gold, silver and copper related complexes would be of interest since it would provide an insight on the different observed reactivity. In addition, the question of a possible  $\pi$  stabilization of the gold center by the pendant aromatic ring would be addressed by this study.

Firstly, the available experimental data were examined. In our research group, all three coinage metal complexes with 2-di-*tert*-butylphosphino-2',4',6'-triisopropylbiphenyl **20**, **21** and **22** were prepared in the context of the investigation on new cyclopropanation reactions *via* carbene transfer from diazo derivatives (Figure 12). Remarkably, they showed a very different activity towards the mentioned reaction. Crystallographic data were available for the three complexes.

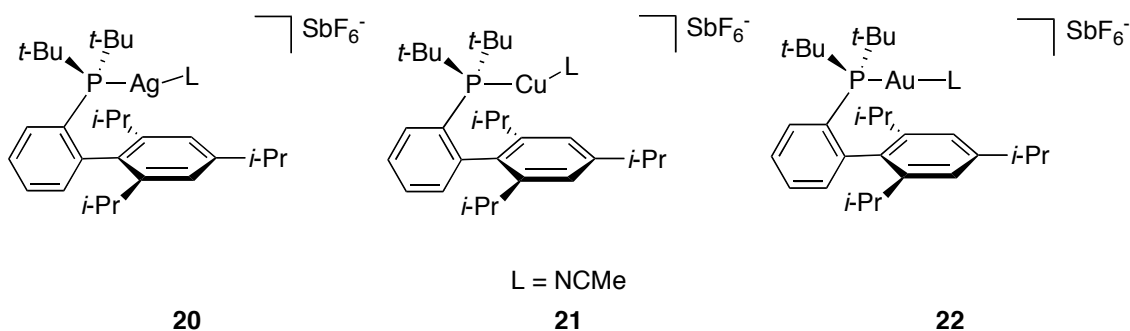


**Figure 12.** New group 11 complexes **20-22** with 2-di-*tert*-butylphosphino-2',4',6'-triisopropylbiphenyl.

68 Complexes **22** and **10b** were prepared by Cristina Nieto-Oberhuber, complex **20** was prepared by Patricia Pérez-Galán, and complex **21** was prepared by Nicolas Delpont.

To complement the information obtained by X-ray analysis, we carried out theoretical study, as gas-phase computational simulations allow to eliminate the distortion caused by constrains of crystal packing. Density Functional Theory (DFT) was the method of choice, as it had been successfully applied to similar studies.<sup>52a,69</sup> Hybrid functional B3LYP was used, and the basis set was 6-31G(d) (C, P, N, H) and SDD (Au, Ag, Cu) for the core and its associated double- $\zeta$  for the valence.

### 1.1. Information from X-ray Structures

Single crystal X-ray diffraction techniques are an invaluable tool in structural studies. The results obtained by this analytical technique are depicted as ORTEP diagrams, in which the position of the atoms are represented together with the thermal vibration ellipsoids, and they are still regarded as “photographs” of the molecules. They provide the most accurate way to measure intrinsic features of the compounds, such as angles and bond distances. Nevertheless, the most important drawback of this analytical method is, indeed, the difficulty to obtain a suitable crystal (bigger than 0.1 mm in each dimension) and to ensure its stability during the whole measurement. It is important to bear in mind that the results are solid state structures, which might not be the most stable in solution since crystal packing forces and solvation effects can be very important. On the other hand, it is not always possible to determine accurately the positions of hydrogens. Computational techniques are thus the perfect complement, since they allow to optimize the molecules in gas-phase, eliminating any kind of crystal constrains.

In this regard, a first look to the ORTEP diagrams of **20-22** indicates the most remarkable difference in this family of complexes: the angle between the phosphorus atom, the metal and the nitrogen of the acetonitrile moiety (Figure 13). This angle is close to the linearity in complex **22** ( $173.06(9)^\circ$ ), while is slightly bent for complex **20** ( $168.01(5)^\circ$ ). This bending is more evident for the copper complex **21** ( $148.79(3)^\circ$ ) (Table 1).

The bonding angle has an influence in the distances between the metal and the aromatic ring. In each case, there are two distances between the metal and the carbons

---

69 DFT-studies of Au(I)-alkyne complexes: (a) Wu, J.; Kroll, P.; Dias, H. V. R. *Inorg. Chem.* **2009**, *48*, 423-425. (b) Shapiro, N. D.; Toste, F. D. *Proc. Nat. Acad. Sci.* **2008**, *105*, 2779-2782.

of the pendant aromatic ring that are below the sum of van der Waals radii.<sup>70</sup> In complex **22** such distances are 3.038 and 3.284 Å, in complex **20** is 2.910 and 3.101 Å and in complex **21** 2.580 and 2.580 Å (sum of van der Waals radii for C-Au is 3.36 Å, C-Ag 3.42 Å and C-Cu 3.10 Å).

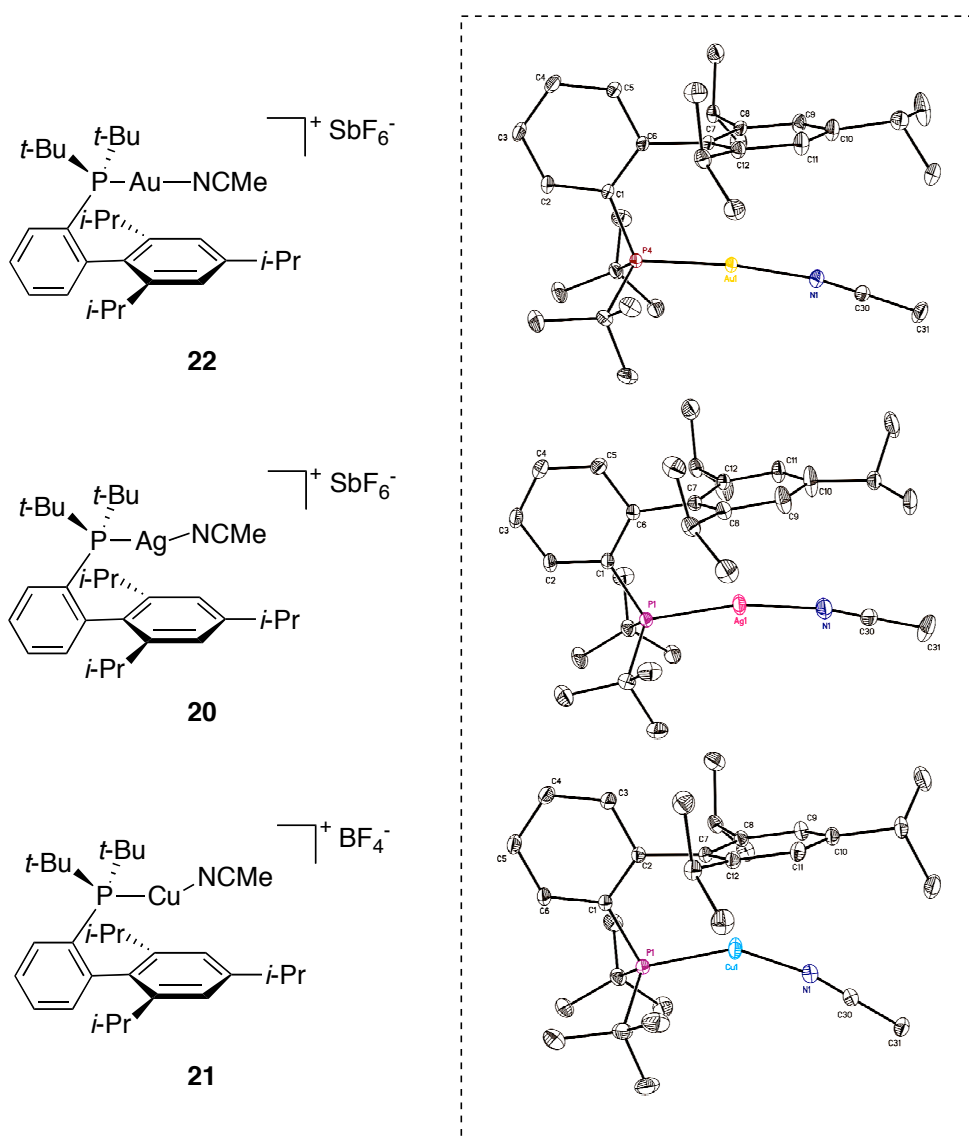


**Figure 13.** X-ray structures of complexes **20-22**. Counteranions ( $\text{SbF}_6^-$ ,  $\text{BF}_4^-$ ) were omitted for clarity.

70 Bondi, A. *J. Phys. Chem.* **1964**, *68*, 441-451.

**Table 1.** Selected calculated distances (Å) and angles (°) for complexes **22-24**.

Complex	[M]...P (Å)	[M]...N (Å)	[M]...plane Ph (Å) <sup>[a]</sup>	P-[M]-N (°)
<b>22</b>	2.2541(8)	2.046(3)	3.04	173.06(9)
<b>20</b>	2.3583(5)	2.1100(18)	2.89	168.01(5)
<b>21</b>	2.1961(3)	1.8853(10)	2.48	148.79(3)

[a] These distances are only approximations.

## 1.2. First Set of Calculations: Reproducing X-ray Structures

Despite the accuracy of X-ray diffraction techniques, it is important to keep in mind that the observed structures can be influenced by diverse factors. One of the most important is the effect of crystal packing, *i.e* the obtained structure is not the intrinsic structure of the molecule but the one that more efficiently fills the space in the crystal. Thus, this distortion effect has to be taken into account when examining crystallographic structures.

Consequently, starting with the X-ray coordinates, structures of the 2-di-*tert*-butylphosphino-2',4',6'-triisopropylbiphenyl family **20'-22'** were optimized as gas phase calculations allows to eliminate the constrains of crystal packing. The computed structures together with the X-ray structures are represented in Figure 14.

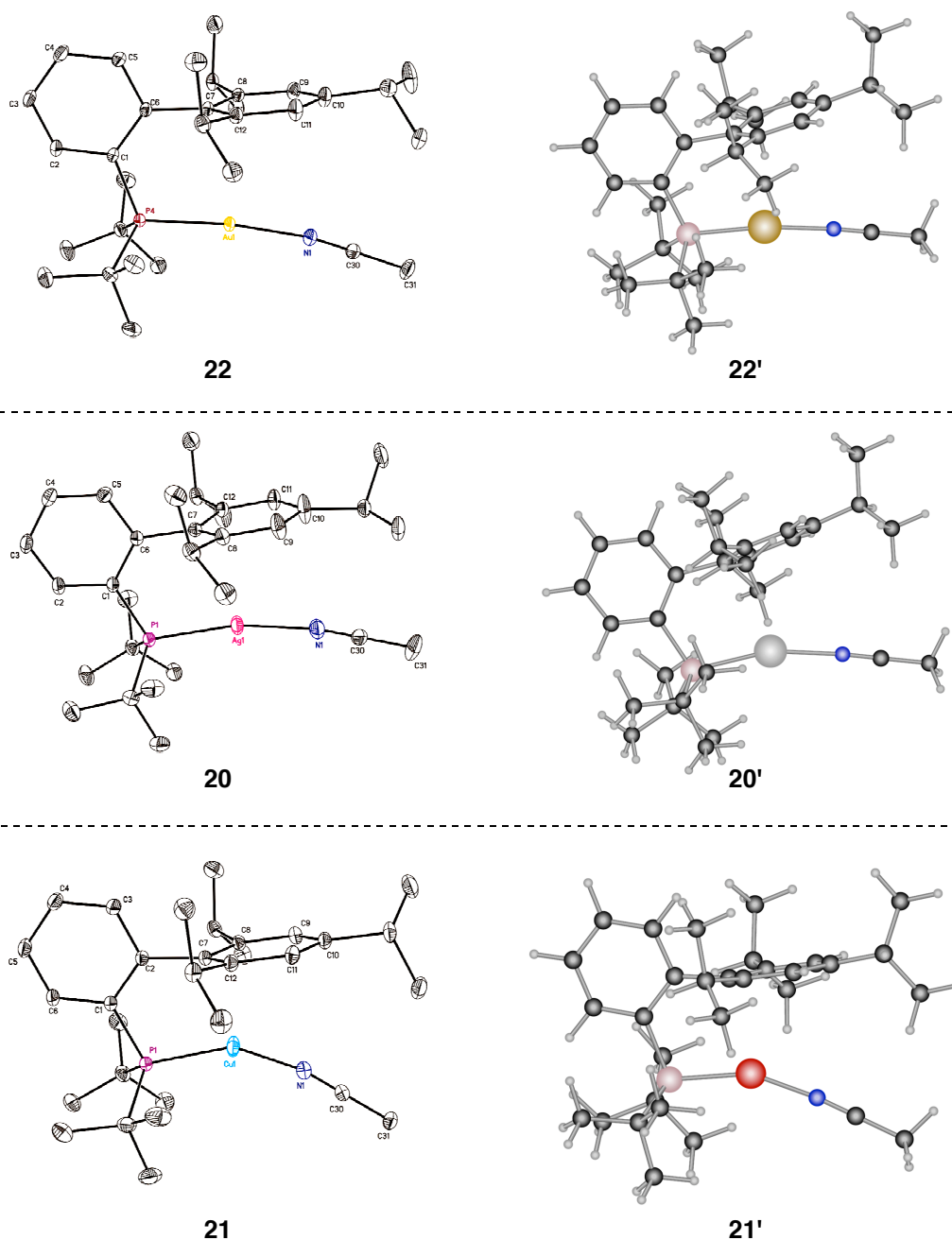


**Figure 14.** X-ray and computed structures of **20-22**. Counteranions were eliminated for clarity.

The distances in the aromatic ring as well as distances from the metal to the carbons of the arene were measured both in the X-ray and computed structures (Table 2). Selected angles are reported in Table 3.

**Table 2.** Selected calculated distances (Å) for complexes **20'**-**22'**.<sup>[a]</sup>

Complex	[M]...P (Å)	[M]...N (Å)	[M]...C <sub>ipso</sub> /C <sub>ortho</sub> /C <sub>ortho</sub>
<b>22'</b>	2.321 [2.254]	2.094 [2.047]	3.19/ 3.39/ 3.67 [3.04/ 3.28/ 3.38]
<b>20'</b>	2.413 [2.3583(5)]	2.161 [2.1100(18)]	3.01/3.10/ 3.50 [2.91/ 3.10/ 3.21] 2.70/ 2.87/ 2.87
<b>21'</b>	2.233 [2.1961(3)]	1.912 [1.8853(10)]	[2.58/ 2.58/ 3.21/ 3.156[meta]

[a] X-ray diffraction values are in brackets.

**Table 3.** Selected calculated angles (°) for complexes **20'**-**22'**.<sup>[a]</sup>

Complex	P-[M]-N	dihedral angle <sup>[b]</sup>
<b>22'</b>	172.68 [173.06(9)]	-86.14 [-87.98]
<b>20'</b>	163.83 [168.01(5)]	-87.84 [-86.91]
<b>21'</b>	155.87 [148.79(3)]	-86.84 [-88.81]

[a] X-ray diffraction values are in brackets.

[b] Dihedral angle between phenyl groups.

The computed structures showed the same tendency already observed in the experimental counterparts. The calculated angle in complex **22'** is 172.68°, quite similar to the experimental value (173.06(9)°). For complexes **20'** and **21'** calculated angles were 163.83° and 155.87°, being the experimental values 168.01(5)° and 148.79(3)°, respectively. Although DFT calculations failed to reproduce the exact value of the studied angle, they clearly reproduced the observed trend when moving from copper to gold. These results indicate that the crystal packing can be eliminated as one of the causes for the distortion of the structure in the studied complexes.

From this point, two other factors have to be carefully considered. On one hand, all the isolated compounds bear bulky isopropyl groups in *o*-, *m*-, *p*- position in the non-phosphorus bonded aromatic ring, that could be influencing the mentioned angle by steric hindrance. On the other hand and more interestingly, a possible  $\pi$ -interaction between the metal and the aromatic ring may exist (Figure 15).

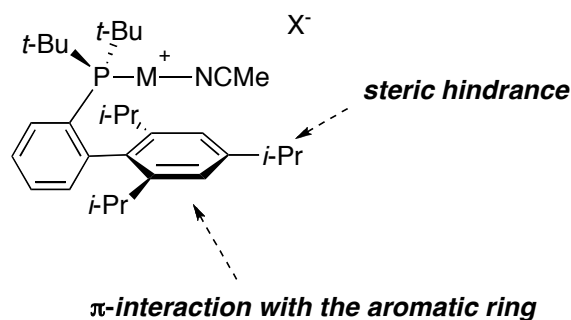


Figure 15. Possible causes of the bending of the P-[M]-N angle.

### 1.3. Second Set of Calculations: Evaluating the Steric Effect of the Isopropyl Groups

The second step consisted on eliminating the steric effect of the isopropyl groups. Compound **10b** is an air-, moisture-stable solid that presents a high activity in cyclization of enynes. X-ray structure of complex **10b** was available (Figure 16), although crystallographic structures of the corresponding silver- and copper-complexes have not still been reported. Complex **10b** has a structure closely related to complex **22**. The P-Au-N angle is  $174.44(3)^\circ$  and the distances to the closest carbons in the aromatic ring are 3.024 and 3.236 Å.

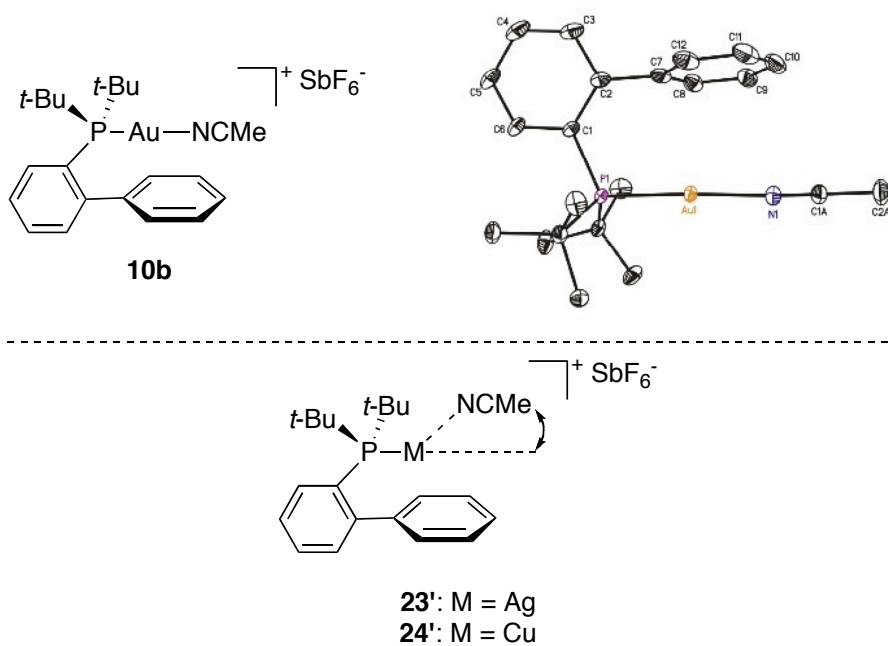


Figure 16. X-ray structure of complex **10b** and calculated structures **23'**-**24'**.

The corresponding silver(I) and copper(I) analogues **23'** and **24'** were computed. As input structures, crystallographic coordinates of **20** and **21** were used. A double check was made by starting with an input structure with a linear environment in the studied atoms. Identical structures were obtained in both cases, reproducing the experimentally observed P-[M]-N angle (Figure 17).

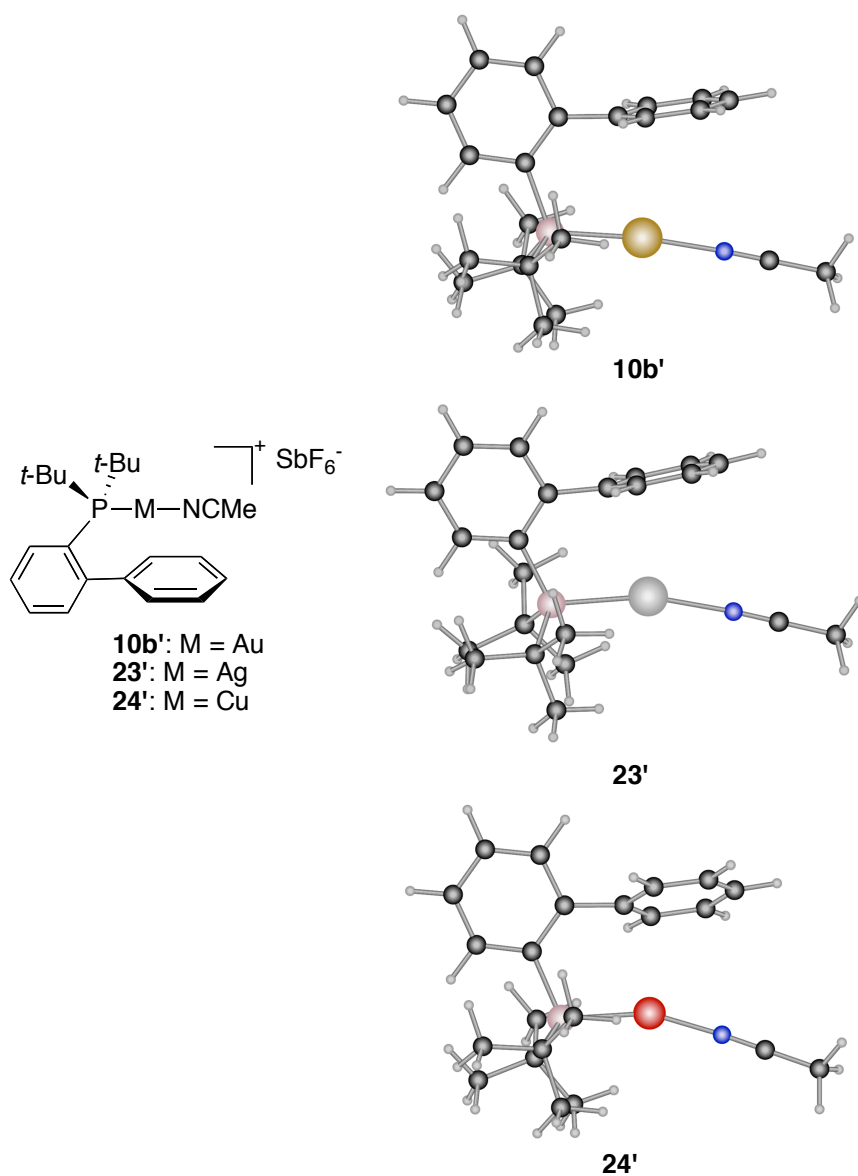


Figure 17. Computed structures of **10b'**, **23'**-**24'**.

**Table 4.** Selected calculated distances (Å) for complexes **10b'**, **23'**, **24'**.<sup>[a]</sup>

Complex	[M]...P (Å)	[M]...N (Å)	[M]...C <sub>ipso</sub> /C <sub>ortho</sub> /C <sub>ortho</sub>
<b>10b'</b>	2.326 [2.2465(3)]	2.093 [2.0338(9)]	3.11/ 3.42/ 3.35 [3.02/ 3.24/ 3.25]
<b>23'</b>	2.419	2.158	3.04/ 2.97/ 3.53/ 3.42 <sub>meta</sub>
<b>24'</b>	2.232	1.911	2.79/ 2.70/ 3.37/ 3.25 <sub>meta</sub>

[a] X-ray diffraction values are in brackets.

**Table 5.** Selected calculated angles (°) for complexes **10b'**, **23'**, **24'**.<sup>[a]</sup>

Complex	P-[M]-N	Dihedral angle <sup>[b]</sup>
<b>10b'</b>	174.2 [174.44(3)]	-79.38° [-95.69°]
<b>23'</b>	165.6	-100.24
<b>24'</b>	158.9	-105.39

[a] X-ray diffraction values are in brackets. [b] Dihedral angle between the phenyl groups.

Although these bulky substituents are influencing the dihedral angle between the two aromatic rings (Table 5), they do not seem to be the key factor that closes the P-M-N angle when the metal changes from gold to copper.

#### 1.4. Third set of calculations: $\pi$ -interactions between the metal and the aromatic ring?

A  $\pi$ -interaction between the metal and the aromatic ring could be the responsible of certain structural changes, which would result in an evident bending of the angle between the phosphorus, the metal and acetonitrile ligand. To further study the effect of such pendant aromatic group, simplified structures **25'**, **26'** and **27'** were computed. In them, the covering arene has been removed, while the other substituent remained unchanged (Figure 18).

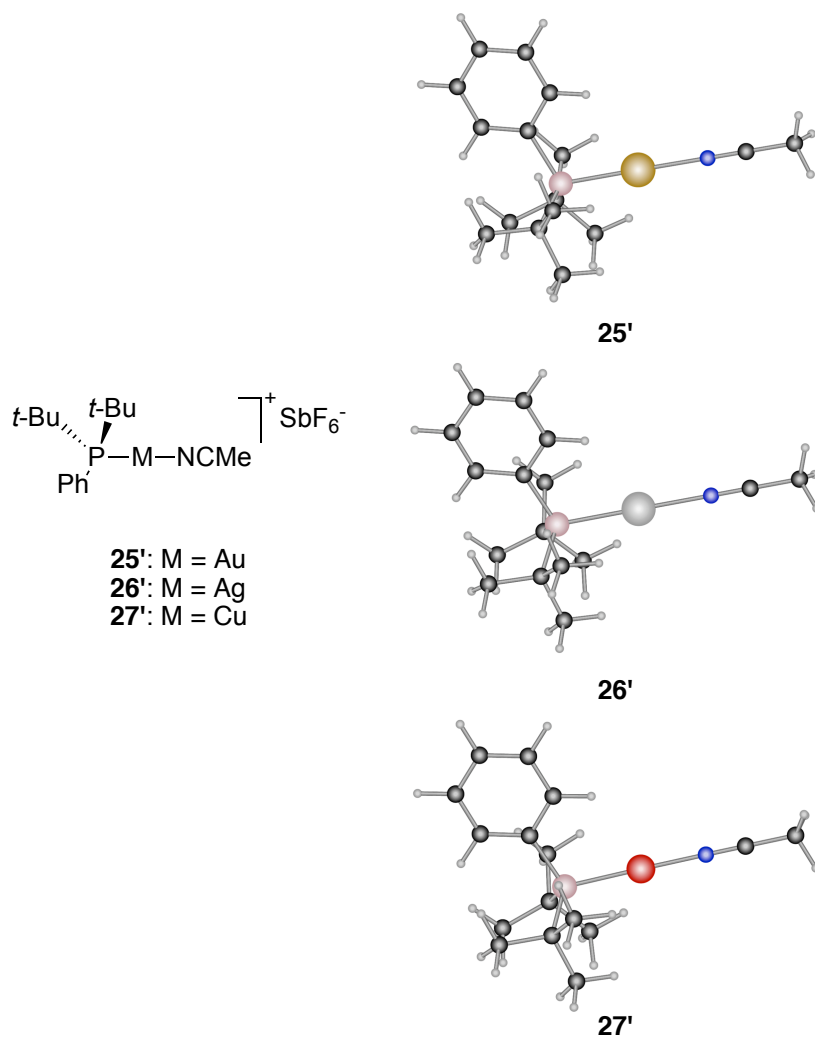


**Figure 18.** Computed structures of **25'**-**27'**.

**Table 6.** Selected calculated distances (Å) and angles (°) for complexes **25'**-**27'**.

complex	[M]...P	[M]...N	P-[M]-N
<b>25'</b>	2.331	2.094	179.3
<b>26'</b>	2.410	2.140	179.4
<b>27'</b>	2.230	1.895	179.0

Optimized compounds **25'**-**27'** presented a very similar structure, independently of the metal present in the molecule. This result showed that in these calculation we have finally removed the moiety that was differentiating these family of complexes. Therefore the  $\pi$ -interaction between the pendant phenyl ring and the metal was responsible for the observed distortions. The strength of this interactions followed the order  $\text{Cu} > \text{Ag} > \text{Au}$ .

## 1.5. Summary

The data of the computed 2-di-*tert*-butylphosphino-2',4',6'-triisopropylbiphenyl complexes (**20'**-**22'**) were in good agreement with the X-ray results (**20-22**, Figure 14). This agreement showed that there are no crystallographic constraints affecting the structure of these complexes. The trend in the P-[M]-N angle as well as the distances between the metal and the carbon atoms of the aromatic pendant ring were reproduced in all cases.

Then, the effect of the bulky isopropyl groups was examined. The computed structures of the (2-di-*tert*-butylphosphino)biphenyl family were good models for this purpose. In complexes **10b'**, **23'** and **24'** the same trend was found regarding the P-[M]-N angle that was already observed in complexes **20'**-**22'**. Thus, a steric effect of the *o*-, *m*-, *p*-isopropyl groups in the mentioned angle can be discarded. However, these bulky groups had an influence in the shape of the studied complexes. In complexes **20'**-**22'** the dihedral angle between the two aromatic rings stayed constant around 87.9°, that is, there is an almost perpendicular arrangement of the two phenyl rings. In complexes **10b'**, **23'** and **24'** a variation in this angle was observed. In complexes **23'**-**24'**, the dihedral angle decreased significantly, reaching the maximum value (-105.391°) in complex **24'**. Then, in the computed structures, the pendant ring turned in order to place two carbons closer to the metal center. This evidence agrees with the well-known preference of Ag(I) and Cu(I) for higher coordination numbers.<sup>71</sup>

The difference in the P-[M]-N angle seemed to be caused by a  $\pi$ -interaction of the metal with the covering arene. The results obtained for complexes **25'**-**27'**, in which this aromatic ring is not present, support this hypothesis. In the absence of the non-phosphorous containing aromatic ring, the arrangement of the P-[M]-N atoms was roughly linear in all three cases, indicating that this aromatic ring is the responsible for the structural modifications in these complexes. These results suggested that there was a significant interaction between the Ag(I) and Cu(I) and the aromatic ring. In contrast, Au(I) did not seem to have a meaningful interaction with the arene, since the mentioned angle remained unchanged in complexes **22'** and **25'**. The strength of this interactions in the computed complexes followed the order Cu > Ag > Au.

71 Carvajal, M. A.; Novoa, J. J.; Álvarez, S. *J. Am. Chem. Soc.* **2004**, *126*, 1465-1477.

The interaction between the metal center and the aromatic ring could also be quantified by the distortion of the C-C bond distances in the aromatic ring. However, as usual for this kind of situations, differences in bond distances are subtle and can be masked by large standard deviations. For this reason, we propose that, in these cases, the measurement of the P-[M]-N angle provides a useful tool to detect and quantify this interaction.

## 2. Cationic $\eta^1/\eta^2$ -Gold(I) Complexes with Simple Arenes<sup>72,73</sup>

The results presented in the former section indicate that a possible  $\pi$ -interaction between the gold center and the covering aromatic ring of the phosphine does not play an important role in stabilizing gold(I) complexes with biphenyl-based phosphines. But, undoubtedly the synthesis of a gold complex that displays such interactions would be of great interest as it could be used as a standard to compare this type of interaction.

Although complexes which presents a  $\sigma$ -interaction between gold and an arene have been widely reported,<sup>74</sup> the scarceness of the equivalent complexes showing  $\pi$ -interactions is remarkable. Only a few previous examples have been reported by Zhang and coworkers, in which the interacting arene is covalently attached to the ligand in the gold complex.<sup>58,59</sup>

Thus, in the context of the development of the gold-catalyzed cyclization of enynes, our interest was focused in the investigation of these novel gold-arene  $\pi$ -interactions. Neutral gold complexes **9a**, **9b**, [AuCl(PPh<sub>3</sub>)] and their corresponding cationic derivatives **10a**, **10b**, [Au(PPh<sub>3</sub>)(NCMe)]SbF<sub>6</sub> were selected as substrates for the present study (Figure 19). The choice of these complexes is based on their high catalytic activity in the cyclization of enynes and, very importantly, on the fact that they are air and moisture stable solids.

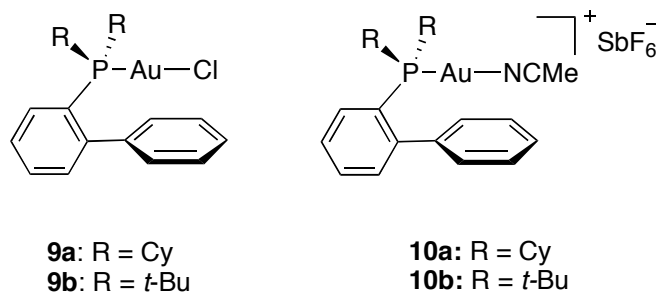


Figure 19. Gold complexes **9a-b** and **10a-b** selected for the study.

72 Taken from: Herrero-Gómez, E.; Nieto-Oberhuber, C.; López, S.; Benet-Buchholz, J.; Echavarren, A. M. *Angew. Chem. Int. Ed.* **2006**, *45*, 5455-5459.

73 This work has been done in collaboration with Cristina Nieto-Oberhuber.

74 Uson, R.; Laguna, A.; Vicente, J. *Syn. React. Inorg. Met.* **1977**, *7*, 463-496.

Starting gold complexes **9a-b** and **10a-b** were prepared according to reported procedures.<sup>13,27</sup> Neutral complexes **9a-b** were prepared in one step from NaAuCl<sub>4</sub>·2H<sub>2</sub>O by reduction with 2,2'-thiodiethanol and consecutive addition of the desired phosphine. Upon mixing with a stoichiometric amount of AgSbF<sub>6</sub> using acetonitrile as solvent, cationic derivatives **10a-b** were obtained.

NMR and HRMS data of these complexes were already available. The structures of complexes **9a-b** and **10a-b** were also confirmed by X-ray crystallography (see example of both neutral and cationic complexes **9a** and **10a** in Figure 20).

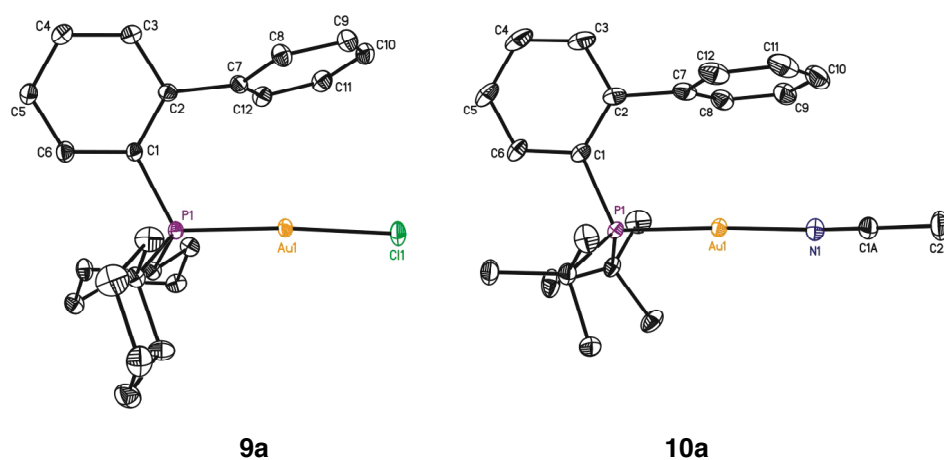


Figure 20. X-ray structures of complexes **9a** and **10a**.

Table 7. Selected distances (Å) and angles (°) for complexes **9a-b** and **10a-b**.

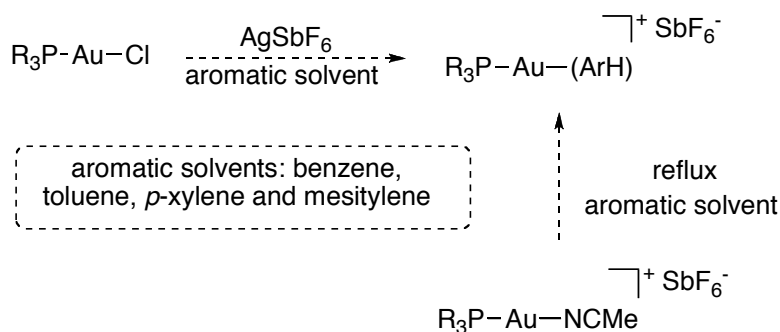
	Au...P	Au...Cl/N <sup>[a]</sup>	P-Au-Cl,N
<b>9a</b>	2.2364(6)	2.2912(6)	175.596(19)
<b>9b</b>	2.254(3)	2.303(4)	172.56(14)
<b>10a</b>	2.2466(3)	2.0338(9)	174.43(3)
<b>10b</b>	2.2539(7)	2.046(2)	173.06(7)

[a] Distances are from Au to Cl for **9a-b**, to N for **10a-b**.

Closely related structures were observed in both **9a** and **10a** gold complexes. Significant distances and angles are shown in Table 7. The angle between phosphorus, gold and chloride or nitrogen, respectively, is close to 180° in all cases. The two aromatic rings in the biphenyl moiety are arranged in a perpendicular fashion, being one of them located over the gold center. The average interatomic distance between gold

and the closest carbons of the aromatic ring was 3.15 Å for neutral complexes **9a-b**. This distance is slightly shorter in cationic complexes **10a-b** (3.03 Å). The values are very similar to the ones reported by Zhang and coworkers for gold-anthracene complexes,<sup>58,59</sup> in which the closest distances found were reported to be 2.958 and 3.097 Å, whereas values such as 3.020 and 3.246 Å were reported in other cases.

In order to prepare the new gold-arene cationic complexes, two strategies were pursued (Scheme 11). Firstly, the same protocol that was already established for preparing the acetonitrile containing cationic complexes **10a-b** could be applied. That is, starting from neutral complexes **9a-b** or [AuCl(PPh<sub>3</sub>)], the addition of a stoichiometric quantity of AgSbF<sub>6</sub> in the chosen aromatic solvent would provide the desired gold-arene cationic complexes. Nevertheless, as cationic complexes are known to be labile, the formation of the desired products could as well be accomplished by ligand exchange starting from compounds **10a-b** and [Au(PPh<sub>3</sub>)(NCMe)]SbF<sub>6</sub>.



Scheme 11

Aromatic solvents were selected among simple arenes. Benzene, toluene, *p*-xylene, and mesitylene were tested. The use of hetero-aromatic compounds or heteroatomic substituted arenes was avoided since the coordination is more likely to happen in this electron rich substituent. The selected solvents would help us to elucidate the steric and electronic effects involved in the coordination to the metal complexes.

Chloride abstraction by using of a silver(I) salt did not give satisfactory results in this reaction. In contrast, the second approach allowed for the synthesis of a number of novel gold-arene complexes **28a-d** (Figure 21).

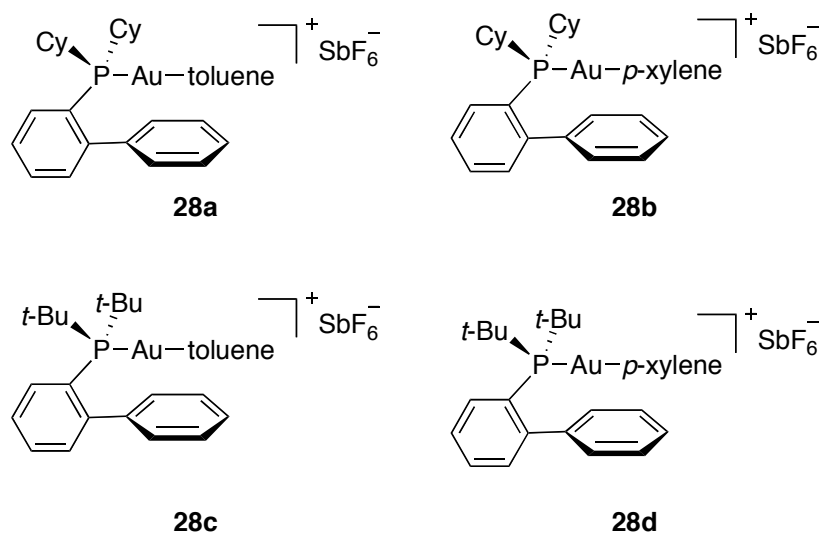


**Figure 21.** Novel cationic gold complexes **28a-d**.

Biaryl phosphines performed better in the stabilization of such complexes than triphenylphosphine, since no arene cationic derivatives were obtained with this ligand. The replacement of the acetonitrile ligand by an aromatic ligand is particularly interesting in these complexes **28a-d**. In them, two different aromatic moieties were present: the newly introduced aromatic ring and the one that it is covalently attached to the phosphine. This way, we can compare both interactions directly within the same substrate.

Regarding the aromatic solvents, no successful results were obtained when either benzene or mesitylene were employed. The lack of reactivity of the last one could be explained in terms of the steric hindrance of the three methyl substituents. More surprising is that benzene did not get coordinated in any case. It suggests that a compromise between electronic effects (electron richer rings) and steric bulkiness must be reached in order to get an effective coordination. Nevertheless, we can not forget that the fact of not having any benzene complex can be also caused by problems during crystallization.

The developed experimental procedure only allowed for the preparation of small amounts of the desired products, which were isolated as solids.  $^1\text{H}$  and  $^{31}\text{P}$  NMR experiments were carried out using  $\text{CD}_2\text{Cl}_2$ . NMR characterization of compounds **28a-d** was somehow difficult, due to its labile nature. However, characteristic  $^{31}\text{P}$  NMR signals were detected. In solution, broad signals were observed in the  $^{31}\text{P}\{^1\text{H}\}$  NMR (202.5 MHz) spectra of the arene-gold(I) complexes at room temperature. Upon lowering the temperature, the signals split up indicating the presence of an equilibrium

with other coordinating molecules such as water. Fluxional equilibrium in the coordinated arene could also be present. Therefore, in the case of **28c** the broad resonance signal around 64 ppm led to a sharp signal at 65.70 ppm (200 K). Addition of water to the  $\text{CD}_2\text{Cl}_2$  solution of **28c** led to a new signal at 60.40 ppm (300 K) corresponding to the aquo complex (Figure 22). As a comparison, the  $^{31}\text{P}$  NMR signal of acetonitrile complex **10a** was observed at  $\delta$  60.53 ppm (300 K).

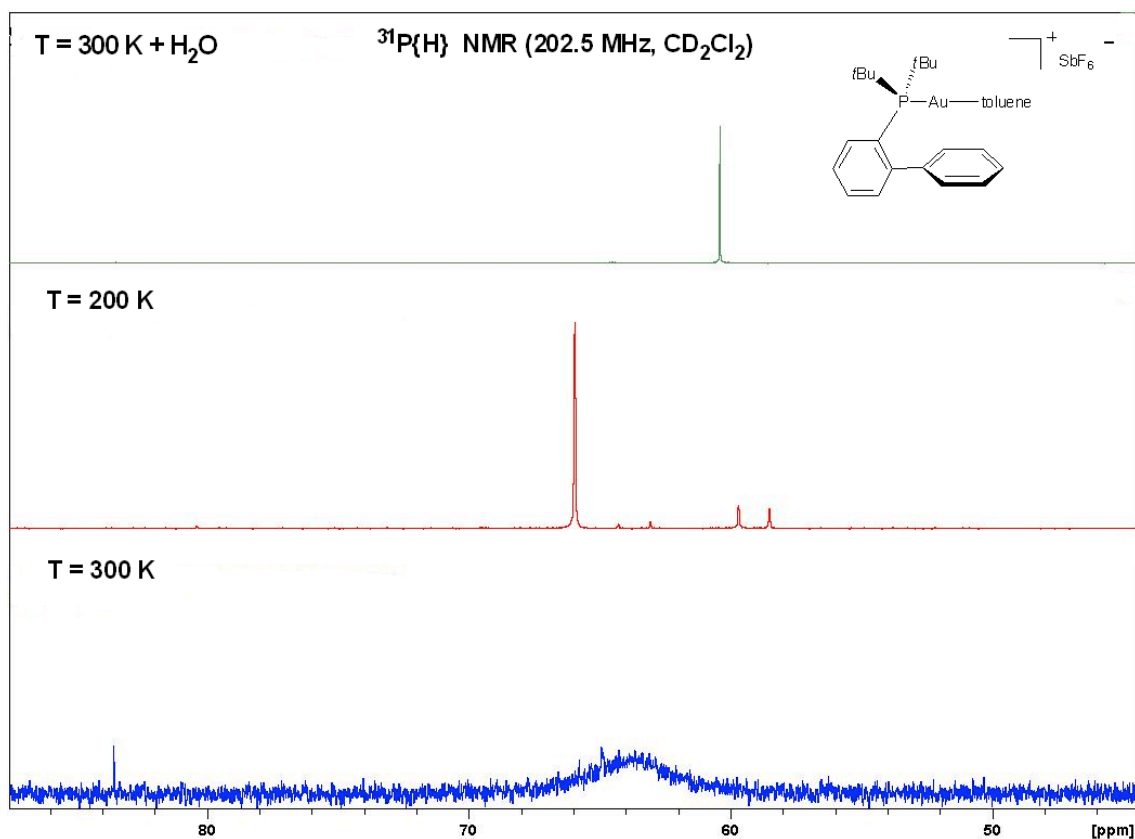
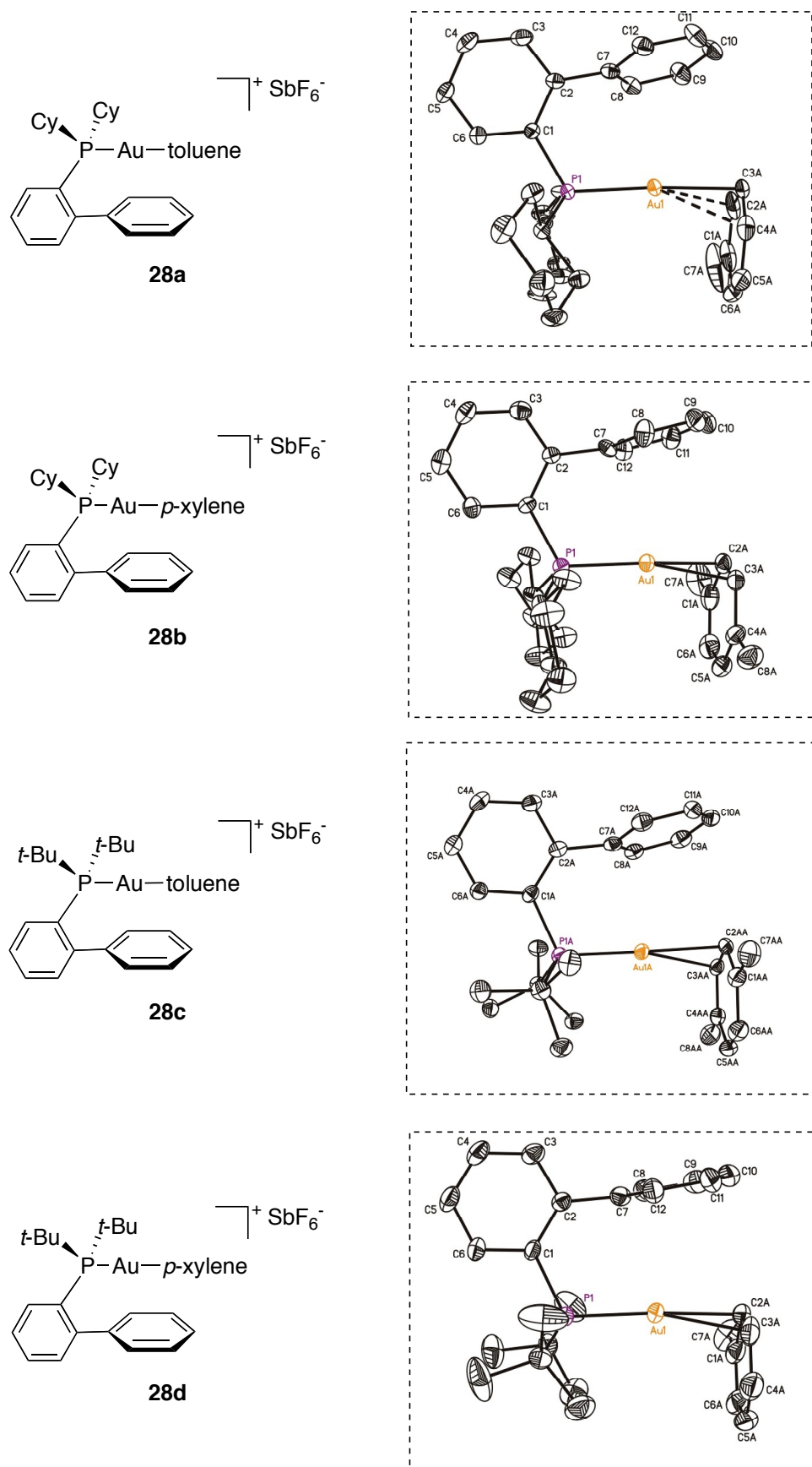


Figure 22.  $^{31}\text{P}$  NMR spectra of complex **28c**.

Infrared techniques were also employed to check the displacement of the acetonitrile ligand by the aromatic solvent. The characteristic IR signal of nitrile group around  $2100\text{ cm}^{-1}$ , disappeared when submitted to reaction conditions.

Remarkably, complexes **28a-d** were crystallized by slow evaporation of the aromatic solvent at room temperature and unequivocal characterization was achieved by means of X-ray diffraction techniques. ORTEP diagrams are depicted in Figure 23.



**Figure 23.** ORTEP (50%) of the cationic part of complexes **28a-d**. The hydrogens atoms have been omitted for clarity.

For complexes **28a-d**, the distances between gold and the covering arene ring are in the range of 3.03-3.22 Å. In contrast, the arene-gold(I) interactions with the coordinated toluene or *p*-xylene ligands in complexes **28a-d** are considerably stronger (Table 8). In all cases the plane of the aromatic ring forms an angle with the vector of the gold-phosphorus bond close to 90° (Table 9). The shortest distances between the gold atom and the plane of the aromatic ring of the  $\pi$ -complexed arenes are 2.20-2.24 Å (Table 8). These values are markedly shorter than those found for Ag(I)-arene complexes ( $2.41 \pm 0.05$  Å) which is probably due to rather large relativistic effects in gold.

**Table 8.** Selected distances (Å) for **9a-b**,<sup>[a]</sup> **10a-b** and **28a-d**.<sup>[b]</sup>

	Au-P	Au-Cl,N,C2A/C3A/C4A <sup>[c]</sup>	Au-Ar <sup>[d]</sup>	Au-C7/C8/C12 <sup>[e]</sup>
<b>9a</b>	2.2364(6)	2.2912(6)		3.15/3.55/3.83
<b>9b</b>	2.254(3)	2.303(4)		3.16/3.40/3.40
<b>10a</b>	2.2466(3)	2.0338(9)		3.02/3.25/3.24
<b>10b</b>	2.2539(7)	2.046(2)		3.04/3.28/3.38
<b>28a</b>	2.2459(13)	2.535(6)/2.263(5)/ 2.689(6)	2.244(5)	3.22/3.10/3.69
<b>28b</b>	2.2400(17)	2.338(7)/ 2.341(7)	2.229(7)	3.15/3.45/3.33
<b>28c</b>	2.2643(10)	2.299(5)/ 2.423(5)	2.233(5)	3.03/3.42/3.14
<b>28d A</b> <sup>[b]</sup>	2.2657(11)	2.300(4)/ 2.354(4)	2.200(4)	3.04/3.00/3.64
<b>28d B</b> <sup>[b]</sup>	2.2636(10)	2.308(4)/ 2.370(4)	2.221(4)	3.04/3.41/3.21

[a] Distances of complexes **9a-b** are included for comparison. [b] Compound **28d** has two independent molecules (A and B). [c] Distances are from Au to Cl for **9a-b**, to N for **10a-b**, and to C2A/C3A/C4A for **28a-d**. [d] Shortest distance between Au and the plane of the complexed arene. [e] These distances are only approximations.

**Table 9.** Selected angles (°) for **9a-b**,<sup>[a]</sup> **10a-b** and **28a-d**.<sup>[b]</sup>

	P-Au-Cl,N,XA <sup>[c]</sup>	Au1-P1-C2-C7	C1-C2-C7-C8[C12]	Au $\perp$ Ar <sup>[d]</sup>
<b>9a</b>	175.596(19)	14.2(1)	63.9(3)	
<b>9b</b>	172.56(14)	0.0	87.3	
<b>10a</b>	174.43(3)	9.1(1)	81.90(16)	
<b>10b</b>	173.06(7)	0.0(1)	86.8(3)	
<b>28a</b>	174.64(16)	7.8(1)	63.5(9)	6.32
<b>28b</b>	171.4 (approx.)	4.9(1)	77.6(9)	7.21
<b>28c</b>	171.2 (approx.)	1.7(1)	78.8(6)[-85.9(7)]	2.66
<b>28d A</b> <sup>[b]</sup>	173.7 (approx.)	0.9(1)	72.6(6)	0.62
<b>28d B</b> <sup>[b]</sup>	171.9 (approx.)	3.8(2)	79.8(5)	5.37

[a] Angles of complexes **9a-b** are included for comparison. [b] Compound **28d** has two independent molecules (A and B). [c] XA is C3A in **28a** and the point centered between C2A and C3A in the rest of molecules. [d] Angle formed between the vector of the Au-P bond and the normal of the aromatic plane C1A-C6A (arene).

Compound **28a**, which is complexed to a molecule of toluene, showed an  $\eta^1$ -arene interaction with the shortest atom-atom distance from gold to C3A (2.263 Å) and secondary interactions to C2A and C4A (2.535 and 2.689 Å). In *p*-xylene complex **28b** the gold atom shows an almost  $\eta^2$ -arene interaction (2.338 and 2.341 Å with C2A and C3A, respectively). Complex **28c** showed a distorted  $\eta^1$ -arene interaction with the shortest atom-atom distance from gold to C2A (2.299 Å) and a secondary interaction to C3A (2.423 Å). Curiously, in complex **28a** the gold atom is more strongly bonded to the *meta* position of the toluene ring, whereas in complex **28c** the strongest interaction occurs at the *ortho* position of toluene. Complex **28d**, which contains two independent molecules in the crystal packing, showed a distorted  $\eta^2$ -arene interaction with a stronger bond to C2 than to C3 of the aromatic ring. According to the criteria of Kochi,<sup>55b</sup> the hapticity of our complexes is  $\eta = 1.42$  (**28a**), 1.69 (**28b**), 1.41 (**28c**), and 1.52/1.56 (two independent molecules of **28d**).

Regarding to aurophilic interactions, the shortest intermolecular Au...Au distance was found for **9a** (5.4 Å), whereas for **9b**, **10a-b**, **28a-d** this distance ranges from 7.6 to 9.7 Å, all beyond the accepted contact limit of 3.6 Å. Thus, the presence of the biphenyl phosphine could isolate the gold center from the environment and prevents aggregation though aurophilic interactions. Then, the covering arene seems to be playing an important role in these gold complexes not because of a  $\pi$  interaction with the metal, but by being an effective way to prevent aggregation and, consequently, a loss of catalytic activity.

### 3. Gold Complexes with $\pi$ Acceptors Ligands

Ligand modification has been confirmed as an efficient way to modify the outcome of metal-catalyzed reactions, including the ones performed with gold catalysts. As an example, the use of bulky phosphines has improved the performance of gold-catalyzed reactions.

Our interest was now settled in the search of new complexes with increased activity. Since gold(I) is known to act as an electrophilic Lewis acid, the use of electron-withdrawing ligands would enhance the reactivity on the metal center by making it more electron deficient. Nevertheless, a compromise has to be found, since the ligand has also to be able to form stable gold complexes.

Organophosphite ligands fulfil all these requirements: they are strong  $\pi$ -acceptor ligands and can form stable complexes with electron rich transition metals. It is expected that they are also good  $\sigma$ -donors since stable complexes with electron-poor transition metals have been reported.<sup>75</sup> In addition, phosphites are commercially available and less expensive than the equivalent phosphines.

Some examples of gold complexes bearing phosphite ligands have been reported.<sup>9,76</sup> Interestingly, Teles et al. in one of the first published examples of an homogenous gold-catalyzed reaction, compared the performance of a number of gold catalysts with different ligands, including  $\text{P}(\text{OMe})_3$  and  $\text{P}(\text{OPh})_3$ .<sup>9</sup> They reported that higher activity was found using phosphite ligands compared to their phosphines analogues, but the turnover numbers were lower. Therefore, while gold complexes with phosphines have been widely employed as catalysts, there are scarce examples of the use of phosphite ligands in such context.

We envisioned that the use of a bulkier ligand would help to increase the stability of the resulting complex, since sterically hindered ligands are known to stabilize complexes of metals in low oxidation states, as they isolate the metal center

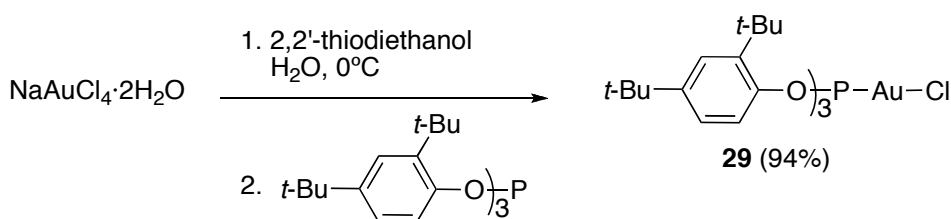
---

75 van Leeuwen, P. W. N. M. *Homogeneous Catalysis: Understanding the Art*, Kluwer Academic Publishers: The Netherlands, 2004, pp 10-11.

76 (a) Hollatz, C.; Schier, A.; Schmidbaur, H. *Inorg. Chim. Acta* **2000**, 300-302. (b) Mays, M. J.; Vergnano, P. A. *J. Chem. Soc., Dalton Trans.* **1979**, 6, 1112-1115. (c) Hitchcock, P. B.; Pye, P. L. *J. Chem. Soc., Dalton Trans.* **1977**, 15, 1457-1460. (d) Couch, D. A.; Robinson, S. D. *Inorg. Chim. Acta* **1974**, 9, 39-47. (e) Schmidbaur, H.; Franke, R. *Chem. Ber.* **1972**, 105, 2985-97. (f) Couch, D. A.; Robinson, S. D. *J. Chem. Soc., Chem. Commun.* **1971**, 23, 1508-1059.

from the environment and therefore prevent other ligands to get close to the coordination sphere of the metal.

Taking into account all these considerations, the ligand of choice was *tris*(2,4-*tert*-butylphenyl)phosphite. Neutral gold complex **29** was uneventfully prepared using a standard procedure: reduction of sodium tetrachloroaurate dihydrate with 2,2'-thiodiethanol using water as solvent, followed by addition the phosphite ligand in pentane (Scheme 12). Complex **29** was obtained as an air-, moisture-stable white solid.



Scheme 12

Novel complex **29** was characterized by means of HRMS and <sup>1</sup>H, <sup>13</sup>C and <sup>31</sup>P NMR. A characteristic signal at 103.78 was observed in the <sup>31</sup>P NMR in CDCl<sub>3</sub>. The X-ray structure of complex **29** confirmed the assigned structure (Figure 24).<sup>77</sup>

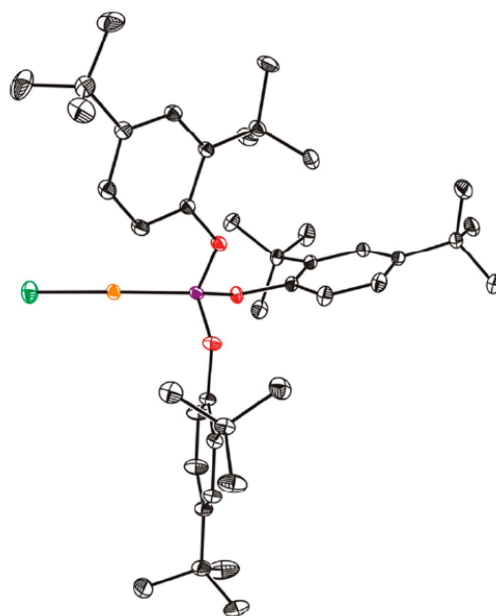
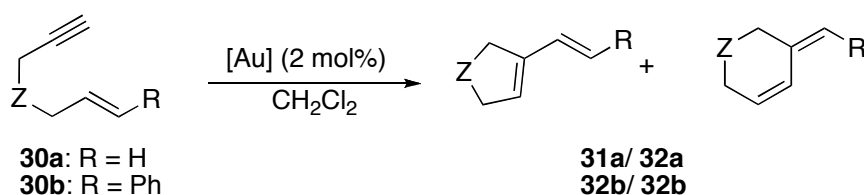


Figure 24. X-ray structure of complex **29**.

77 A suitable crystal for X-ray measurement of complex **29** was obtained by Eloísa Jiménez-Núñez.

The crystal structure of **29** displays a Au-P distance of 2.1940(6) Å and Au-Cl distance of 2.2676(5) Å. These distances, specially the one found in Au-P bond, are shorter than the ones reported for neutral phosphine gold complexes **9a-b** (Au-P = 2.23-2.25 Å, Au-Cl = 2.29-2.30 Å). The Cl-Au-P angle of 179.00(2)° agrees with the tendency of gold(I) to form linear complexes. The intermolecular Au...Au distance is 10.294 Å, much longer than the value established for significant aurophilic interactions (3.6 Å).

The catalytic performance of **29** was preliminary tested in the gold(I)-catalyzed skeletal rearrangement reaction, which is generally performed with phosphine containing complexes (Scheme 12, Table 10).



Scheme 12

Table 10. Gold(I)-catalyzed skeletal rearrangement of enynes **30a-b**.

entry	substrate	[Au]	time (min)	T (°C)	Yield (%) ratio <b>33/ 34</b>
1	<b>30a</b>	[AuCl(PPh <sub>3</sub> )]/AgSbF <sub>6</sub>	20	0	77 (1:7)
2	<b>30a</b>	<b>10a</b>	20	23	82 (1:2)
3	<b>30b</b>	[AuCl(PPh <sub>3</sub> )]/AgSbF <sub>6</sub>	5	23	100 (1.1:1) 16-26
4 <sup>[a]</sup>	<b>30a</b>	<b>29</b> /AgSbF <sub>6</sub>	5	0	(0.5:1- 1:2.3)
5 <sup>[b]</sup>	<b>30b</b>	<b>29</b> /AgSbF <sub>6</sub>	5	0	59 (1:2)

[a] Two results selected from four trials. [b] Yield is the average of two reactions.

Cyclization of substrates **30a-b** proceeded efficiently using gold(I)-phosphine catalysts. Enyne **30a** reacted with [AuCl(PPh<sub>3</sub>)]/AgSbF<sub>6</sub> (2 mol%) in 20 min at 0 °C to afford a 1:7 *exo:endo* mixture in 77% (Table 10, entry 1). This transformation can also be accomplished at room temperature in 20 min using catalyst **10a** (Table 10, entry 2).

In this case, lower selectivity was observed since the *exo:endo* ratio changed to 1:2. For the phenyl substituted enyne **30b**, the use of [AuCl(PPh<sub>3</sub>)]/AgSbF<sub>6</sub> allowed to achieve a complete conversion in 5 min at room temperature (Table 10, entry 3).<sup>8</sup>

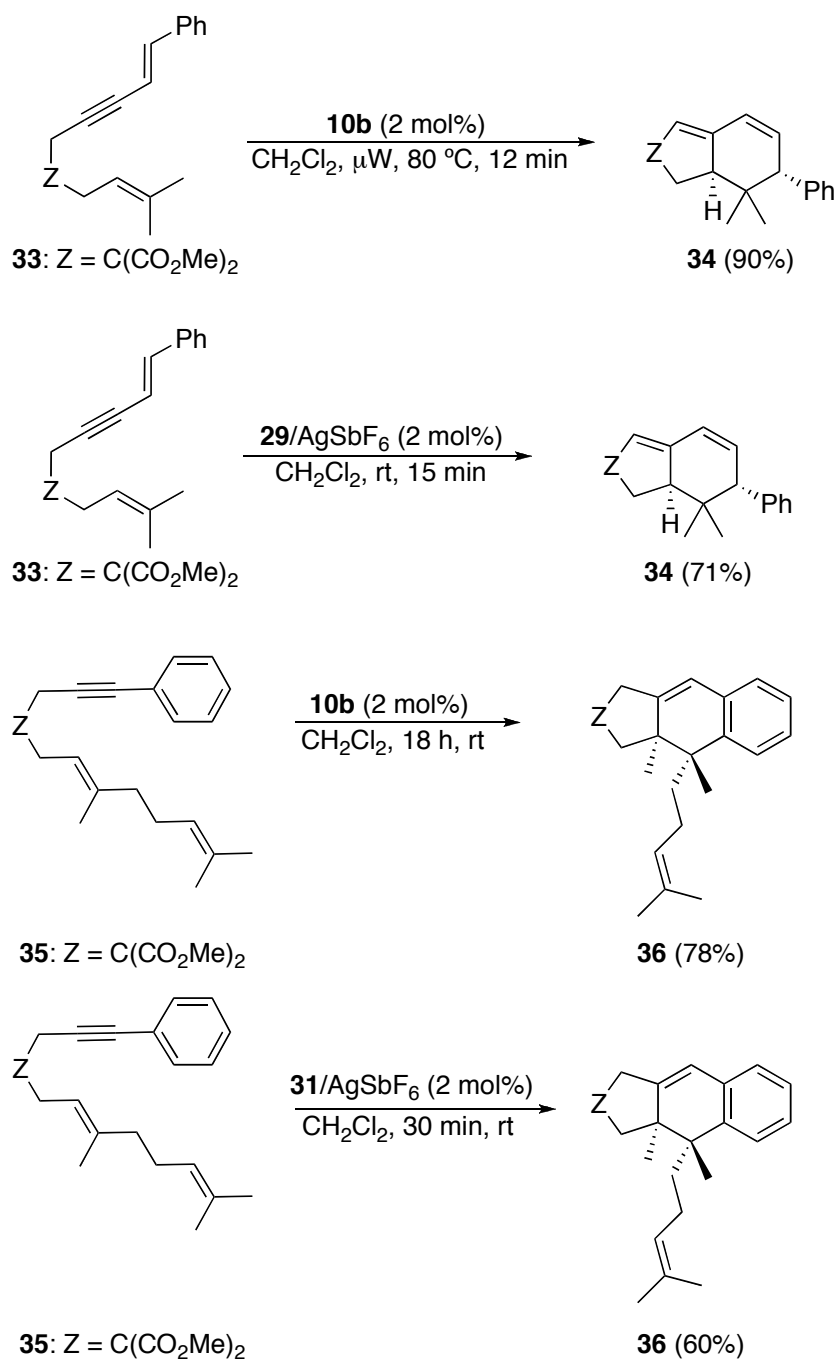
Using the novel catalyst **29** together with AgSbF<sub>6</sub> as chloride scavenger, both transformations can be accomplished in 5 min at 0 °C, albeit the isolated yields were lower: 59% for enyne **30a** and 16-26% for the phenyl-substituted enyne **30b** (Table 10, entries 4 and 5). The ratio of the formed cyclization products somehow resembles the one obtained with phosphine-based catalyst **10a**.

As expected, the high electrophilicity on the gold center has as a consequence an increased activity of the gold catalysts **29**. However, for the particular case of the gold-catalyzed skeletal rearrangement of 1,6-enynes, the use of this new catalyst **29** does not mean a significant improvement since this reaction already takes place smoothly using phosphine-containing gold catalysts. In addition, the higher activity displayed by **29** can lead to decomposition of starting material or unwanted side reactions, since the desired products were isolated in low yields.

Therefore, catalyst **29** seems better suited for sluggish reactions, in which longer reaction times or higher temperatures were needed. This is the case, for example, of gold(I)-catalyzed [4+2]-cyclization of enynes, where a remarkably decrease of reaction times were observed when catalyst **29** was employed. Some examples are shown in Scheme 13. Thus, cyclization of substituted enyne **33** needed microwave heating at 80°C to be completed using gold complex **10b**, while the same transformation can be accomplished at room temperature in 15 min using cationic phosphite-based catalyst **29**. In a similar way, reaction time for cyclization of enyne **35** was reduced from 18 h to 30 min with the use of catalyst **29**.<sup>78</sup>

---

78 Examples taken from: Nieto-Oberhuber, C.; Pérez-Galán, P.; Herrero-Gómez, E.; Lauterbach, T.; Rodríguez, C.; López, S.; Bour, C.; Rosellón, A.; Cárdenas, D. J.; Echavarren, A. M. *J. Am. Chem. Soc.* **2008**, *130*, 269-279.



Scheme 13

In conclusion, the use of  $\pi$ -acceptor ligands increases the electrophilicity on the gold center, enhancing the activity of the gold catalyst, as it has been found for catalysts **29**. This higher reactivity is an advantage for the less reactive substrates, for which longer reaction times and harder conditions were employed.

UNIVERSITAT ROVIRA I VIRGILI

GOLD(I)-CATALYZED CYCLIZATIONS OF 1,6- AND 1,7-ENYNES: NEW GOLD COMPLEXES AND CYCLOPROPANATION REACTIONS

Elena Herrero Gómez

ISBN: 978-84-692-5924-5/DL:T-1663-2009

## *Chapter 1. Conclusions*

UNIVERSITAT ROVIRA I VIRGILI

GOLD(I)-CATALYZED CYCLIZATIONS OF 1,6- AND 1,7-ENYNES: NEW GOLD COMPLEXES AND CYCLOPROPANATION REACTIONS

Elena Herrero Gómez

ISBN: 978-84-692-5924-5/DL:T-1663-2009

- An X-ray and computational study of a family of gold, silver, and copper complexes with biphenyl phosphines was performed. Silver and copper complexes had a significant interaction with the aromatic moiety, which was clearly reflected in the bending of the P-[M]-N angle. On the contrary, P-[Au]-N angle was close to 180°, which is the computed value for a complex lacking the second phenyl ring (Figure 25).

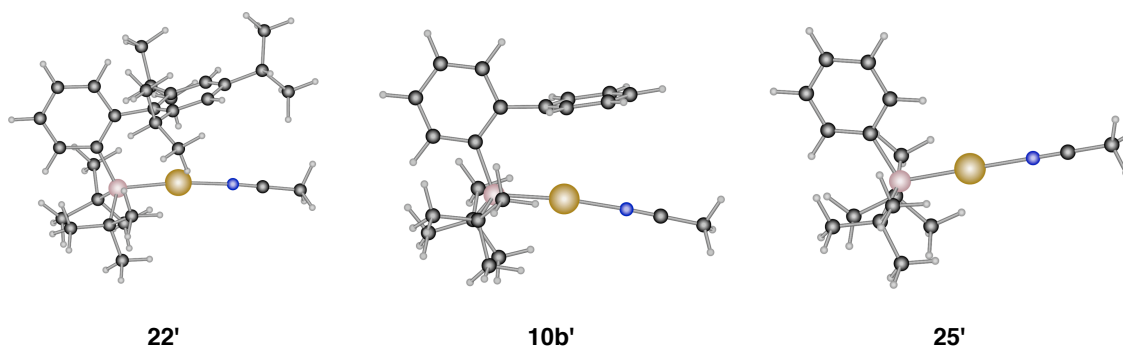


Figure 25. Computed structures of complexes **22'**, **10b'** and **25'**.

- A number of new gold complexes **28a-d** with simple arenes as ligands have been prepared and characterized (Figure 26). The X-ray characterization of such complexes enables to study the interactions between the gold center and the coordinated aromatic solvent. A marked difference in bond distances was found between the coordinated molecule and the covalently attached phenyl moiety. Therefore and in agreement with what was found in the previous computational study, gold does not have significant interactions with the covering arene of the biphenylphosphine.

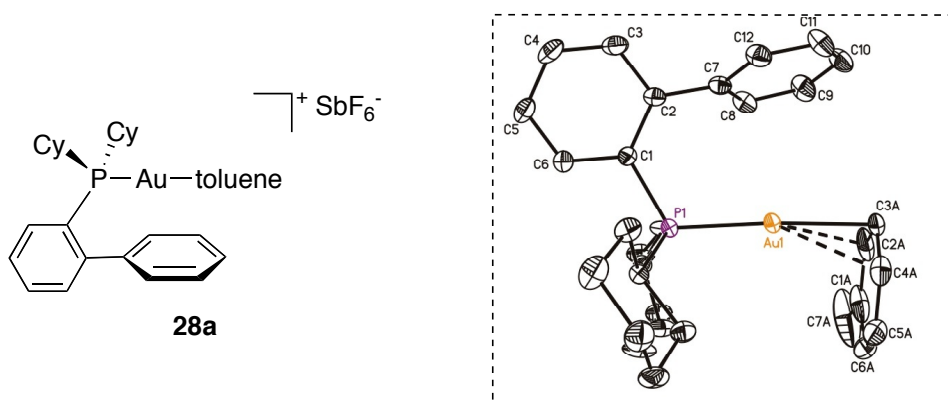


Figure 26. X-Ray structure of complex **28a**.

- This study indicates that the bulky phosphine isolates the gold center from the environment, thus preventing the formation of aggregates through aurophilic interactions. This has a positive effect in the catalytic properties of acetonitrile-containing cationic complexes **10a-b**. Complexes **28a-d** are also active catalysts for enyne cycloisomerizations, but no further efforts were put in studying their catalytic properties due to their instability and more difficult preparation.
- A novel gold complex with a phosphite ligand, Au(I)-tris(2,4-di-*tert*-butylphenyl)phosphite **29**, has been also described. Complex **29** was obtained as an air and moisture stable solid. In combination with AgSbF<sub>6</sub>, it has turned out to be the most active catalyst for enyne cycloisomerization and related reactions. In particular, it has been successfully applied to the gold-catalyzed [4+2]-cycloaddition of enynes.

UNIVERSITAT ROVIRA I VIRGILI

GOLD(I)-CATALYZED CYCLIZATIONS OF 1,6- AND 1,7-ENYNES: NEW GOLD COMPLEXES AND CYCLOPROPANATION REACTIONS

Elena Herrero Gómez

ISBN: 978-84-692-5924-5/DL:T-1663-2009

*Chapter 1. Experimental Section*

UNIVERSITAT ROVIRA I VIRGILI

GOLD(I)-CATALYZED CYCLIZATIONS OF 1,6- AND 1,7-ENYNES: NEW GOLD COMPLEXES AND CYCLOPROPANATION REACTIONS

Elena Herrero Gómez

ISBN: 978-84-692-5924-5/DL:T-1663-2009

**Experimental Section: Index**

	<b>Page</b>
<b>1. Computational Study of Group 11 Metal Complexes with Bulky, Biphenyl Phosphines</b>	<b>103</b>
1.1. Computational Details	103
1.2. Cartesian Coordinates ( $\text{\AA}$ ) and Absolute Energies (a.u.)	103
Complex 22'	104
Complex 20'	108
Complex 21'	112
Complex 10b'	116
Complex 23'	119
complex 24'	122
Complex 25'	125
Complex 26'	127
Complex 27'	129
<b>2. Cationic <math>\eta^1/\eta^2</math>-Gold(I) Complexes with Simple Arenes</b>	<b>131</b>
2.1. Crystallographic Data	131
X-Ray Structure of Complex 28a	132
X-Ray Structure of Complex 28b	139
X-Ray Structure of Complex 28c	145
X-Ray Structure of Complex 28d	152
<b>3. Gold Complexes with <math>\pi</math> Acceptors Ligands</b>	<b>162</b>
3.1. Tris(2,4-di-tert-butyl-phenyl)phosphite-gold(I) chloride 29	162

UNIVERSITAT ROVIRA I VIRGILI

GOLD(I)-CATALYZED CYCLIZATIONS OF 1,6- AND 1,7-ENYNES: NEW GOLD COMPLEXES AND CYCLOPROPANATION REACTIONS

Elena Herrero Gómez

ISBN: 978-84-692-5924-5/DL:T-1663-2009

# 1. Computational Study of Group 11 Metal Complexes with Bulky, Biphenyl Phosphines

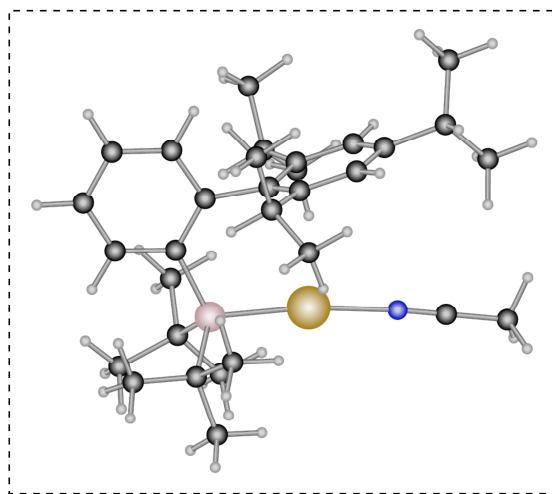
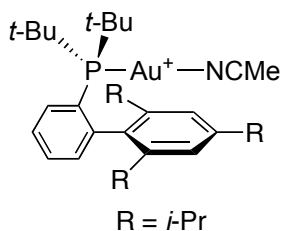
## 1.1. Computational Details

All calculations were performed with Gaussian03.<sup>79</sup> The method was B3LYP<sup>80</sup>. The inner electrons of Au, Ag, Cu were described by an effective core potential (SDD), and the associated double- $\zeta$  basis set was used for the outer electrons.<sup>81</sup> The 6-31G(d) basis set was used for H, C, N and P.<sup>82</sup> The starting phosphine conformation was taken from available X-ray structures. Optimizations of cationic species were performed. The nature of the stationary points as local minima was confirmed through frequency calculations. No solvation effects were considered in this chapter.

## 1.2. Cartesian Coordinates (in Å) and Absolute Energies (in a.u.)

- 
- 79 Frisch, M. J.; Trucks, G. W.; Schlegel, H. B.; Scuseria, G. E.; Robb, M. A.; Cheeseman, J. R.; Montgomery, Jr., J. A.; Vreven, T.; Kudin, K. N.; Burant, J. C.; Millam, J. M.; Iyengar, S. S.; Tomasi, J.; Barone, V.; Mennucci, B.; Cossi, M.; Scalmani, G.; Rega, N.; Petersson, G. A.; Nakatsuji, H.; Hada, M.; Ehara, M.; Toyota, K.; Fukuda, R.; Hasegawa, J.; Ishida, M.; Naka jima, T.; Honda, Y.; Kitao, O.; Nakai, H.; Klene, M.; Li, X.; Knox, J. E.; Hratchian, H. P.; Cross, J. B.; Bakken, V.; Adamo, C.; Jaramillo, J.; Gomperts, R.; Stratmann, R. E.; Yazyev, O.; Austin, A. J.; Cammi, R.; Pomelli, C.; Ochterski, J. W.; Ayala, P. Y.; Morokuma, K.; Voth, G. A.; Salvador, P.; Dannenberg, J. J.; Zakrzewski, V. G.; Dapprich, S.; Daniels, A. D.; Strain, M. C.; Farkas, O.; Malick, D. K.; Rabuck, A. D.; Raghavachari, K.; Foresman, J. B.; Ortiz, J. V.; Cui, Q.; Baboul, A. G.; Clifford, S.; Cioslowski, J.; Stefanov, B. B.; Liu, G.; Liashenko, A.; Piskorz, P.; Komaromi, I.; Martin, R. L.; Fox, D. J.; Keith, T.; Al-Laham, M. A.; Peng, C. Y.; Nanayakkara, A.; Challa-combe, M.; Gill, P. M. W.; Johnson, B.; Chen, W.; Wong, M. W.; Gonzalez, C.; and Pople, J. A.; "Gaussian 03, Revision C.02", Gaussian, Inc., Wallingford, CT, **2004**.
- 80 (a) Lee, C.; Parr, R. G.; Yang, W. *Phys. Rev.* **1988**, *37*, 785-789. (b) Becke, A. D. *J. Phys. Chem.* **1993**, *98*, 5648-5652. (c) Stephens, P. J.; Devlin, F. J.; Chabalowski, C. F.; Frisch, M. J. *J. Phys. Chem.* **1994**, *98*, 11623-11627.
- 81 (a) Hay, P. J.; Wadt, W. R. *J. Chem. Phys.* **1985**, *82*, 299-310. (b) Wadt, W. R.; Hay, P. J. *J. Chem. Phys.* **1985**, *82*, 284-298.
- 82 Francl, M. M.; Pietro, W. J.; Hehre, W. J.; Binkley, J. S.; Gordon, M. S.; Defrees, D. J.; Pople, J. A. *J. Chem. Phys.* **1982**, *77*, 3654-3665.

Cartesian coordinates (Å) of **22'** (E = -1388.13769984 a.u.).



Au	1.070233	-0.672410	-0.035739
P	-1.254498	-0.670908	0.030130
C	-1.779486	-1.447842	1.702422
C	-3.291390	-1.375068	1.996268
H	-3.901426	-1.869420	1.236650
H	-3.638632	-0.345331	2.111180
H	-3.478607	-1.888266	2.947123
C	-1.038263	-0.653220	2.800417
H	-1.320184	-1.059480	3.779272
H	-1.311293	0.407195	2.792161
H	0.049898	-0.733162	2.704954
C	-1.319517	-2.919551	1.741608
H	-0.255601	-3.029456	1.503741
H	-1.895747	-3.552037	1.059944
H	-1.474830	-3.308451	2.754992
C	-1.861615	-1.627621	-1.528525
C	-3.310600	-2.148762	-1.449764
H	-3.543753	-2.653297	-2.395147
H	-4.047794	-1.351943	-1.327884
H	-3.449016	-2.883564	-0.651763
C	-0.924853	-2.833936	-1.765593

H	-0.947737	-3.556849	-0.946340
H	0.113568	-2.521352	-1.915776
H	-1.252070	-3.354364	-2.673796
C	-1.986988	1.025391	-0.034380
C	-3.392602	1.121726	-0.104693
H	-3.996267	0.224328	-0.088797
C	-1.226412	2.222205	-0.054754
C	0.268129	2.337373	0.017773
C	1.016271	2.558798	-1.151183
H	0.517691	2.535016	-2.116473
C	2.382787	2.842070	-1.079653
H	2.940709	3.028510	-1.993186
C	0.920404	2.416262	1.260024
H	0.348491	2.286677	2.174466
C	-1.725931	-0.658632	-2.722902
H	-0.707290	-0.264936	-2.817646
H	-2.417072	0.185445	-2.653549
H	-1.953698	-1.206380	-3.645079
C	-4.045458	2.347459	-0.194168
H	-5.129526	2.379218	-0.246544
C	-1.908358	3.449050	-0.147665
H	-1.321528	4.362590	-0.161092
C	-3.296334	3.522160	-0.217325
H	-3.786169	4.488774	-0.288093
C	3.020036	2.917247	0.161269
H	4.075962	3.167117	0.218207
C	2.286623	2.700468	1.330518
H	-3.478607	-1.888266	2.947123
C	-1.038263	-0.653220	2.800417
H	-1.320184	-1.059480	3.779272
H	-1.311293	0.407195	2.792161
H	0.049898	-0.733162	2.704954
C	-1.319517	-2.919551	1.741608
H	-0.255601	-3.029456	1.503741

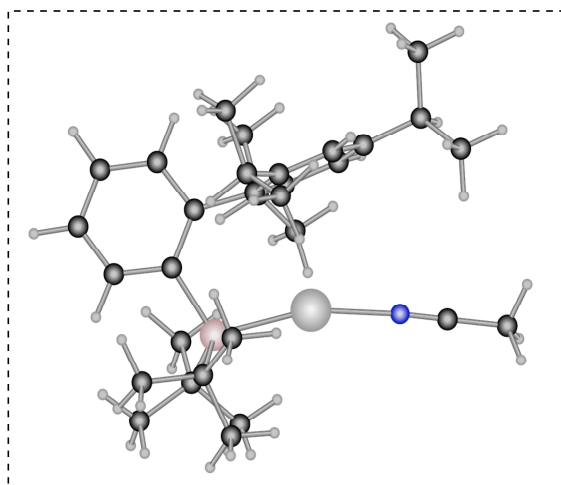
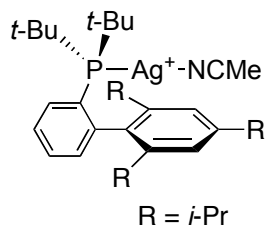
H	-1.895747	-3.552037	1.059944
H	-1.474830	-3.308451	2.754992
C	-1.861615	-1.627621	-1.528525
C	-3.310600	-2.148762	-1.449764
H	-3.543753	-2.653297	-2.395147
H	-4.047794	-1.351943	-1.327884
H	-3.449016	-2.883564	-0.651763
C	-0.924853	-2.833936	-1.765593
H	-0.947737	-3.556849	-0.946340
H	0.113568	-2.521352	-1.915776
H	-1.252070	-3.354364	-2.673796
C	-1.986988	1.025391	-0.034380
C	-3.392602	1.121726	-0.104693
H	-3.996267	0.224328	-0.088797
C	-1.226412	2.222205	-0.054754
C	0.268129	2.337373	0.017773
C	1.016271	2.558798	-1.151183
H	0.517691	2.535016	-2.116473
C	2.382787	2.842070	-1.079653
H	2.940709	3.028510	-1.993186
C	0.920404	2.416262	1.260024
H	0.348491	2.286677	2.174466
C	-1.725931	-0.658632	-2.722902
H	-0.707290	-0.264936	-2.817646
H	-2.417072	0.185445	-2.653549
H	-1.953698	-1.206380	-3.645079
C	-4.045458	2.347459	-0.194168
H	-5.129526	2.379218	-0.246544
C	-1.908358	3.449050	-0.147665
H	-1.321528	4.362590	-0.161092
C	-3.296334	3.522160	-0.217325
H	-3.786169	4.488774	-0.288093
C	3.020036	2.917247	0.161269
H	4.075962	3.167117	0.218207

C	2.286623	2.700468	1.330518
H	2.769233	2.777986	2.300927
N	3.151131	-0.886510	-0.089733
C	4.295331	-1.044511	-0.114621
C	5.736966	-1.247206	-0.145527
H	6.004086	-2.100878	0.485450
H	6.245941	-0.352566	0.226530
H	6.061333	-1.444698	-1.172153

---

---

Cartesian coordinates (Å) of **20'** (E = -1399.36572707 a.u.).



Ag	1.317169	-0.606404	-0.089866
P	-1.093243	-0.778097	0.015834
C	-1.549065	-1.518253	1.726173
C	-3.054075	-1.529605	2.057368
H	-3.644317	-2.110274	1.344597
H	-3.468219	-0.519841	2.114866
H	-3.188317	-1.991759	3.043137
C	-0.831579	-0.632864	2.769582
H	-1.066892	-1.004800	3.774210
H	-1.159581	0.410638	2.717216
H	0.258416	-0.658663	2.653938
C	-0.989337	-2.951973	1.814821
H	0.076420	-2.996717	1.560632
H	-1.528779	-3.650451	1.168422
H	-1.097501	-3.312424	2.844866
C	-1.693126	-1.824183	-1.483975
C	-3.082855	-2.473353	-1.332436
H	-3.316826	-3.012859	-2.258474
H	-3.881741	-1.743802	-1.180017
H	-3.116333	-3.203161	-0.518633
C	-0.655919	-2.944147	-1.726661

H	-0.573096	-3.634232	-0.882752
H	0.340945	-2.538594	-1.935797
H	-0.963067	-3.529730	-2.601889
C	-1.935018	0.867592	-0.066378
C	-3.343336	0.910762	-0.110109
H	-3.910273	-0.011278	-0.127189
C	-1.224589	2.095512	-0.048506
C	0.266825	2.251977	-0.056097
C	1.000322	2.113172	-1.250814
H	0.486010	1.816180	-2.160917
C	2.364514	2.422012	-1.291415
H	2.905710	2.337167	-2.229823
C	0.937659	2.701771	1.092845
H	0.380717	2.837590	2.015839
C	-1.694297	-0.886826	-2.710690
H	-0.720656	-0.404049	-2.858835
H	-2.455503	-0.105784	-2.636057
H	-1.904991	-1.479876	-3.608758
C	-4.045196	2.113138	-0.123964
H	-5.130383	2.104969	-0.161903
C	-1.953102	3.298478	-0.044716
H	-1.403558	4.235058	-0.028640
C	-3.344371	3.317082	-0.082522
H	-3.874338	4.264935	-0.086546
C	3.017790	2.868307	-0.139296
H	4.071803	3.128494	-0.175736
C	2.302541	3.001788	1.052706
H	-3.188317	-1.991759	3.043137
C	-0.831579	-0.632864	2.769582
H	-1.066892	-1.004800	3.774210
H	-1.159581	0.410638	2.717216
H	0.258416	-0.658663	2.653938
C	-0.989337	-2.951973	1.814821
H	0.076420	-2.996717	1.560632

H	-1.528779	-3.650451	1.168422
H	-1.097501	-3.312424	2.844866
C	-1.693126	-1.824183	-1.483975
C	-3.082855	-2.473353	-1.332436
H	-3.316826	-3.012859	-2.258474
H	-3.881741	-1.743802	-1.180017
H	-3.116333	-3.203161	-0.518633
C	-0.655919	-2.944147	-1.726661
H	-0.573096	-3.634232	-0.882752
H	0.340945	-2.538594	-1.935797
H	-0.963067	-3.529730	-2.601889
C	-1.935018	0.867592	-0.066378
C	-3.343336	0.910762	-0.110109
H	-3.910273	-0.011278	-0.127189
C	-1.224589	2.095512	-0.048506
C	0.266825	2.251977	-0.056097
C	1.000322	2.113172	-1.250814
H	0.486010	1.816180	-2.160917
C	2.364514	2.422012	-1.291415
H	2.905710	2.337167	-2.229823
C	0.937659	2.701771	1.092845
H	0.380717	2.837590	2.015839
C	-1.694297	-0.886826	-2.710690
H	-0.720656	-0.404049	-2.858835
H	-2.455503	-0.105784	-2.636057
H	-1.904991	-1.479876	-3.608758
C	-4.045196	2.113138	-0.123964
H	-5.130383	2.104969	-0.161903
C	-1.953102	3.298478	-0.044716
H	-1.403558	4.235058	-0.028640
C	-3.344371	3.317082	-0.082522
H	-3.874338	4.264935	-0.086546
C	3.017790	2.868307	-0.139296
H	4.071803	3.128494	-0.175736

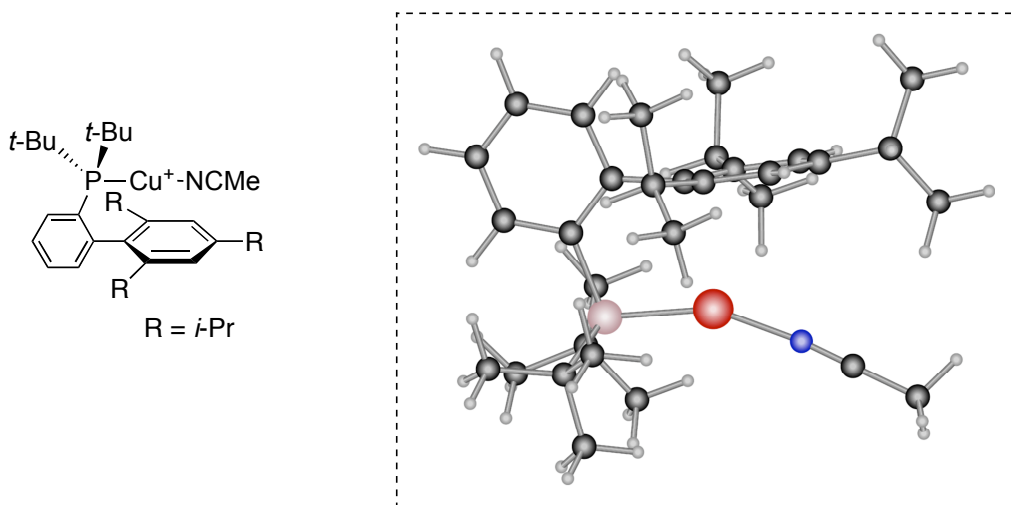
---

C	2.302541	3.001788	1.052706
H	2.799183	3.361391	1.949530
N	3.444424	-0.961648	-0.003062
C	4.573895	-1.198088	0.071336
C	5.996882	-1.496474	0.166218
H	6.184574	-2.135465	1.034841
H	6.565658	-0.567813	0.275132
H	6.328305	-2.015837	-0.738443

---

---

Cartesian coordinates (Å) of **21'** (E = -1449.72325137 a.u.).



Cu	1.252800	-0.616160	-0.102977
P	-0.972454	-0.756830	-0.008700
C	-1.454781	-1.514957	1.685384
C	-2.952435	-1.444749	2.039743
H	-3.588022	-1.965435	1.319519
H	-3.302575	-0.413600	2.133700
H	-3.101627	-1.927580	3.013449
C	-0.669824	-0.701712	2.739437
H	-0.902187	-1.092453	3.737654
H	-0.944064	0.358453	2.727188
H	0.414714	-0.780243	2.597370
C	-0.981080	-2.982133	1.729227
H	0.074730	-3.086420	1.452729
H	-1.574550	-3.630205	1.077582
H	-1.092792	-3.360635	2.752426
C	-1.637983	-1.731343	-1.524433
C	-3.064525	-2.293310	-1.375072
H	-3.337964	-2.803729	-2.306810
H	-3.812704	-1.513991	-1.208019
H	-3.141563	-3.029447	-0.570397

C	-0.665845	-2.902302	-1.793345
H	-0.625782	-3.616494	-0.966794
H	0.353126	-2.547707	-1.987591
H	-1.001719	-3.447416	-2.683986
C	-1.710476	0.935089	-0.041194
C	-3.108865	1.100281	-0.046061
H	-3.754004	0.230894	-0.077066
C	-0.891502	2.092588	-0.007814
C	0.606554	2.099697	-0.068809
C	1.284446	1.819887	-1.274350
H	0.712381	1.529900	-2.151541
C	2.666849	2.014269	-1.379573
H	3.162467	1.830020	-2.328793
C	1.358287	2.554927	1.028248
H	0.850279	2.792162	1.958833
C	-1.591730	-0.772455	-2.733344
H	-0.587613	-0.361542	-2.890672
H	-2.291876	0.060953	-2.630627
H	-1.861193	-1.330186	-3.638287
C	-3.698886	2.361138	-0.001660
H	-4.780851	2.452618	-0.010621
C	-1.506035	3.355335	0.058332
H	-0.875988	4.239564	0.085468
C	-2.891338	3.495832	0.061912
H	-3.334968	4.486113	0.104801
C	3.396966	2.474201	-0.281068
H	4.466006	2.645563	-0.368931
C	2.740453	2.734762	0.924035
H	-3.101627	-1.927580	3.013449
C	-0.669824	-0.701712	2.739437
H	-0.902187	-1.092453	3.737654
H	-0.944064	0.358453	2.727188
H	0.414714	-0.780243	2.597370
C	-0.981080	-2.982133	1.729227

H	0.074730	-3.086420	1.452729
H	-1.574550	-3.630205	1.077582
H	-1.092792	-3.360635	2.752426
C	-1.637983	-1.731343	-1.524433
C	-3.064525	-2.293310	-1.375072
H	-3.337964	-2.803729	-2.306810
H	-3.812704	-1.513991	-1.208019
H	-3.141563	-3.029447	-0.570397
C	-0.665845	-2.902302	-1.793345
H	-0.625782	-3.616494	-0.966794
H	0.353126	-2.547707	-1.987591
H	-1.001719	-3.447416	-2.683986
C	-1.710476	0.935089	-0.041194
C	-3.108865	1.100281	-0.046061
H	-3.754004	0.230894	-0.077066
C	-0.891502	2.092588	-0.007814
C	0.606554	2.099697	-0.068809
C	1.284446	1.819887	-1.274350
H	0.712381	1.529900	-2.151541
C	2.666849	2.014269	-1.379573
H	3.162467	1.830020	-2.328793
C	1.358287	2.554927	1.028248
H	0.850279	2.792162	1.958833
C	-1.591730	-0.772455	-2.733344
H	-0.587613	-0.361542	-2.890672
H	-2.291876	0.060953	-2.630627
H	-1.861193	-1.330186	-3.638287
C	-3.698886	2.361138	-0.001660
H	-4.780851	2.452618	-0.010621
C	-1.506035	3.355335	0.058332
H	-0.875988	4.239564	0.085468
C	-2.891338	3.495832	0.061912
H	-3.334968	4.486113	0.104801
C	3.396966	2.474201	-0.281068

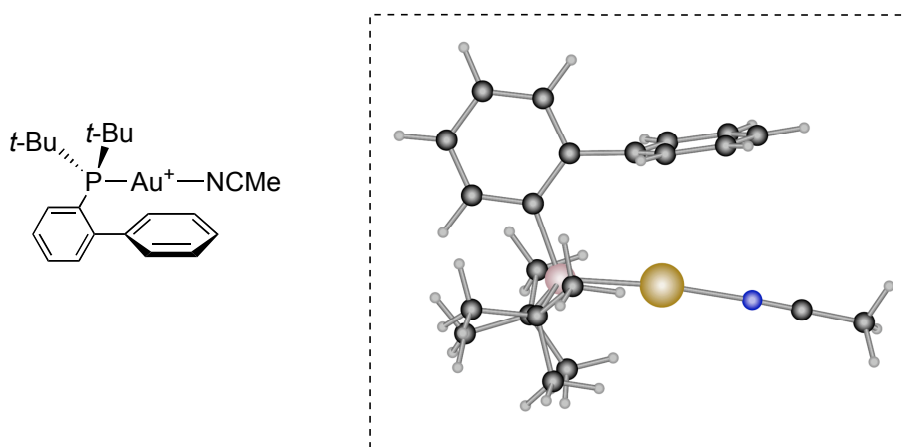
---

H	4.466006	2.645563	-0.368931
C	2.740453	2.734762	0.924035
H	3.298779	3.101932	1.780599
N	3.080858	-1.155729	0.038348
C	4.168770	-1.533641	0.145351
C	5.537578	-2.012383	0.279481
H	5.538804	-3.024608	0.696242
H	6.099541	-1.350358	0.945852
H	6.023196	-2.029057	-0.701443

---

---

Cartesian coordinates (Å) of **10b'** (E = -1741.95345663 a.u.).



Au	0.145177	-1.491624	-0.133804
P	2.126011	-0.285587	-0.022632
C	-0.804203	1.547090	0.083346
C	1.839183	1.530117	0.214405
C	0.565794	2.165263	0.262330
C	-1.540594	1.115703	1.221066
C	-1.456114	1.638588	-1.174688
C	0.540325	3.552464	0.509145
H	-0.427924	4.040663	0.557846
C	-0.791874	2.247695	-2.410512
H	0.286682	2.294585	-2.227640
C	-2.881190	0.743227	1.062755
H	-3.442014	0.435444	1.940839
C	2.936213	3.686283	0.640082
H	3.851820	4.252433	0.781709
C	1.692478	4.310317	0.695352
H	1.615787	5.377219	0.883482
C	-0.960785	1.159096	2.635818
H	0.121803	1.292393	2.554532
C	2.995830	2.316561	0.405500
H	3.972242	1.851207	0.372810
C	-3.536116	0.807112	-0.170746

C	-2.799421	1.250522	-1.269851
H	-3.303057	1.336662	-2.229094
C	-5.013710	0.464267	-0.312698
H	-5.293105	0.669337	-1.354685
C	-1.016864	1.421201	-3.691553
H	-0.752367	0.368032	-3.552016
H	-0.406652	1.821645	-4.509015
H	-2.060500	1.461882	-4.022011
C	-1.275148	3.697291	-2.635653
H	-2.356793	3.726165	-2.810171
H	-0.781099	4.132552	-3.511990
H	-1.057803	4.336585	-1.774552
C	-1.207774	-0.134118	3.435277
H	-0.691415	-0.086517	4.400963
H	-0.845400	-1.018860	2.897751
H	-2.271562	-0.287715	3.647313
C	-1.508515	2.376571	3.411183
H	-2.596562	2.312912	3.526699
H	-1.281617	3.315604	2.896104
H	-1.065306	2.424579	4.412557
C	3.145358	-0.932384	1.489424
C	2.908032	-2.454722	1.625371
H	3.473164	-2.817701	2.492558
H	3.246382	-3.019367	0.753324
H	1.852020	-2.688092	1.795529
C	4.665826	-0.686041	1.400100
H	4.929189	0.373134	1.347927
H	5.131406	-1.205478	0.559240
H	5.125319	-1.079912	2.314653
C	2.601334	-0.246012	2.757933
H	3.112344	-0.671930	3.629887
H	1.529963	-0.420693	2.888757
H	2.780246	0.832333	2.759258
C	3.054513	-0.539889	-1.687232

*Chapter 1. Experimental section*

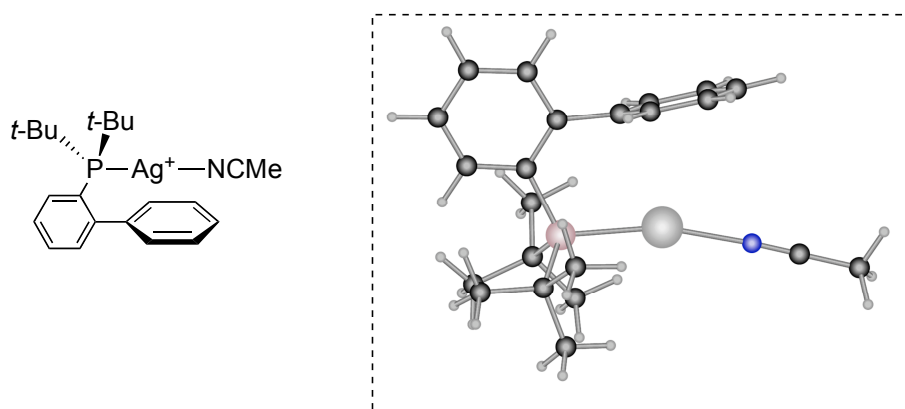
---

C	4.285597	0.369384	-1.874703
H	4.747145	0.121644	-2.838268
H	5.049376	0.231566	-1.106435
H	4.009740	1.426351	-1.910190
C	3.472509	-2.019757	-1.813099
H	2.626615	-2.701655	-1.671766
H	4.264037	-2.297389	-1.112632
H	3.862601	-2.184361	-2.824686
C	2.052285	-0.217469	-2.812332
H	1.707968	0.818551	-2.769456
H	1.177444	-0.874970	-2.784612
H	2.549885	-0.362037	-3.779062
C	-2.338757	-3.576589	-0.321485
C	-3.407665	-4.563028	-0.388174
H	-3.476790	-4.966027	-1.403603
H	-4.359274	-4.092819	-0.122014
H	-3.200548	-5.380974	0.309160
C	-5.288178	-1.029459	-0.053750
H	-5.016566	-1.311655	0.971271
H	-4.712805	-1.653377	-0.748886
H	-6.351196	-1.257033	-0.193206
C	-5.899273	1.350052	0.584620
H	-6.959370	1.139092	0.404570
H	-5.725840	2.412676	0.385272
H	-5.701708	1.171345	1.648138
N	-1.488522	-2.795987	-0.267079

---

---

Cartesian coordinates (Å) of **23'** (E = -1753.18166891 a.u.).




---

Ag	0.073463	1.540283	-0.080320
P	-2.108470	0.515037	-0.193078
C	-1.977938	-1.304938	0.131443
N	1.712476	2.946661	-0.157365
C	-3.175867	-2.043742	0.227253
H	-4.124924	-1.549867	0.060542
C	-3.191459	-3.400229	0.538128
H	-4.136605	-3.930974	0.602582
C	-1.986085	-4.057834	0.772402
H	-1.971938	-5.113433	1.027523
C	-0.791526	-3.349363	0.677219
H	0.146424	-3.864211	0.860414
C	-0.743314	-1.980300	0.351706
C	0.651948	-1.397320	0.272316
C	1.426477	-1.574509	-0.909478
C	2.767876	-1.171482	-0.908947
H	3.353642	-1.323632	-1.810413
C	3.390691	-0.623284	0.216230
C	2.623792	-0.487939	1.374507
H	3.101828	-0.102697	2.271663
C	1.276749	-0.877832	1.439858
C	0.889626	-2.295130	-2.148728

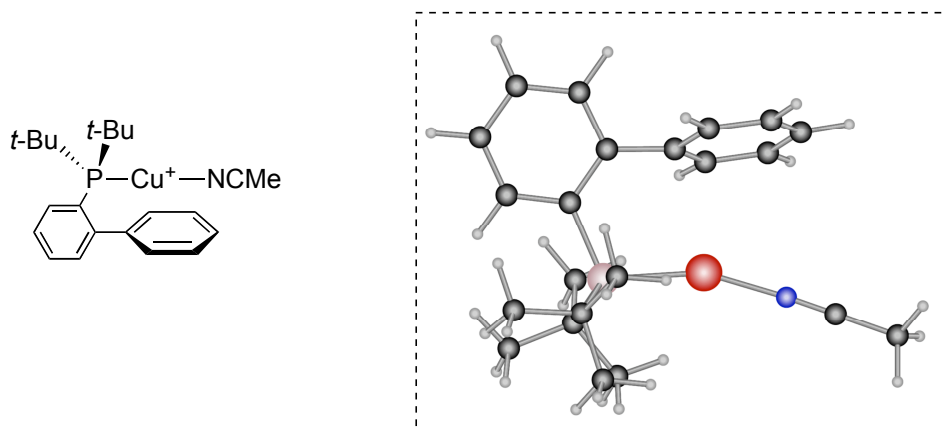
H	-0.203217	-2.314128	-2.083828
C	1.271194	-1.607939	-3.474327
H	1.025835	-0.541153	-3.472360
H	0.735911	-2.078966	-4.306248
H	2.341097	-1.704114	-3.689104
C	1.368254	-3.763716	-2.173513
H	2.462035	-3.816067	-2.222608
H	0.966311	-4.280355	-3.052580
H	1.045673	-4.312925	-1.284222
C	4.869586	-0.257146	0.213486
H	5.077325	0.250061	1.165748
C	0.577585	-0.851132	2.800027
H	-0.490832	-1.015198	2.634112
C	1.078091	-2.012968	3.685411
H	0.910904	-2.982637	3.205604
H	0.550525	-2.016253	4.646108
H	2.150865	-1.920172	3.889785
C	0.736592	0.488545	3.543313
H	1.776040	0.675115	3.834566
H	0.139693	0.485246	4.462299
H	0.407745	1.337801	2.930379
C	-2.810749	0.753980	-1.967384
C	-4.054823	-0.095437	-2.294874
H	-4.908990	0.124592	-1.651030
H	-3.841407	-1.166239	-2.239295
H	-4.360938	0.122358	-3.325517
C	-3.120337	2.248773	-2.191307
H	-3.354112	2.402948	-3.251776
H	-2.263462	2.888318	-1.948687
H	-3.983720	2.595278	-1.617536
C	-1.688006	0.343202	-2.939092
H	-1.415233	-0.708795	-2.826884
H	-0.786144	0.952031	-2.807036
H	-2.036099	0.486554	-3.969457

C	-3.280181	1.272450	1.145467
C	-2.945973	2.778487	1.259281
H	-3.126390	3.326961	0.331350
H	-1.903199	2.942957	1.554224
H	-3.581594	3.224275	2.034284
C	-4.788999	1.124777	0.863853
H	-5.113096	0.082177	0.815926
H	-5.100538	1.629481	-0.053502
H	-5.340067	1.590123	1.690375
C	-2.961202	0.607541	2.498674
H	-3.553042	1.101535	3.279002
H	-1.907861	0.717307	2.769684
H	-3.213028	-0.456175	2.510890
C	2.540760	3.752606	-0.198739
C	3.587279	4.765368	-0.246004
H	3.590004	5.340015	0.685523
H	3.409595	5.444794	-1.085506
H	4.562007	4.284364	-0.374354
C	5.752980	-1.520102	0.160185
H	5.526511	-2.197325	0.990359
H	5.598153	-2.071342	-0.774793
H	6.813696	-1.251221	0.218823
C	5.239747	0.715671	-0.921026
H	6.293971	1.005598	-0.847773
H	5.092042	0.262318	-1.907871
H	4.628929	1.625841	-0.880662

---

---

Cartesian coordinates (Å) of **24'** (E = -1803.53871789 a.u.).



---

Cu	0.012450	1.370715	-0.168327
P	-2.074029	0.578626	-0.081342
C	-1.921866	-1.236554	0.233658
N	1.367158	2.696437	-0.424972
C	-0.650313	-1.866700	0.333235
C	-0.616530	-3.236062	0.656533
H	0.350841	-3.720292	0.747860
C	-1.774079	-3.981966	0.864455
H	-1.701164	-5.036688	1.113178
C	-3.018735	-3.365432	0.752323
H	-3.933348	-3.929561	0.908554
C	-3.081583	-2.009154	0.444630
H	-4.057566	-1.544236	0.371104
C	0.705993	-1.221325	0.124535
C	1.426156	-0.691625	1.238115
C	2.764098	-0.307437	1.068519
H	3.307060	0.070976	1.929944
C	3.439668	-0.456202	-0.145505
C	2.724403	-0.991497	-1.218284
H	3.244703	-1.144134	-2.159936
C	1.386220	-1.395606	-1.115940
C	0.845381	-0.674227	2.653328

H	-0.232476	-0.839490	2.578808
C	1.421358	-1.840814	3.484955
H	2.507468	-1.747287	3.598081
H	1.214750	-2.807612	3.014946
H	0.977094	-1.850679	4.486765
C	1.066081	0.661841	3.387224
H	2.126012	0.845977	3.593671
H	0.547704	0.652661	4.352529
H	0.688827	1.514661	2.808833
C	4.919374	-0.122626	-0.286041
H	5.206468	-0.361466	-1.318639
C	5.785864	-0.992235	0.646223
H	5.573047	-0.784806	1.701573
H	6.849642	-0.792408	0.476302
H	5.608145	-2.058462	0.471313
C	5.207433	1.374184	-0.066453
H	4.649571	1.987324	-0.784395
H	6.274420	1.583776	-0.201142
H	4.931306	1.690733	0.947024
C	0.763605	-2.123636	-2.309141
H	-0.318563	-2.170229	-2.151947
C	1.273446	-3.580251	-2.385106
H	0.813141	-4.098754	-3.233834
H	1.036324	-4.144071	-1.478252
H	2.360349	-3.607245	-2.523492
C	1.019145	-1.419051	-3.656013
H	0.751001	-0.358487	-3.624524
H	0.427849	-1.896333	-4.445220
H	2.069823	-1.488787	-3.957816
C	-2.948570	0.821377	-1.776374
C	-4.226192	-0.016747	-1.971757
H	-5.004597	0.207375	-1.239805
H	-4.015851	-1.089245	-1.940900
H	-4.639102	0.205040	-2.963755

*Chapter 1. Experimental section*

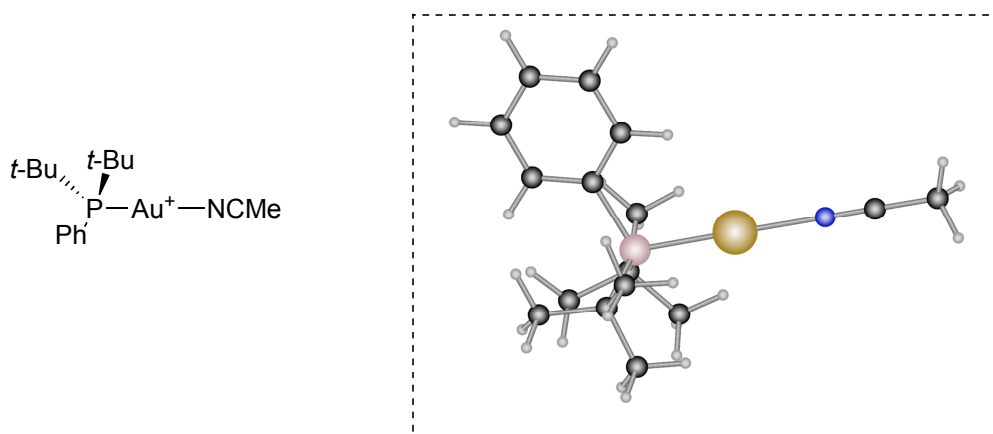
---

C	-3.261527	2.319075	-1.974231
H	-3.597443	2.473644	-3.006802
H	-2.377487	2.948298	-1.818779
H	-4.059185	2.676597	-1.318628
C	-1.931373	0.397372	-2.852415
H	-1.670616	-0.660584	-2.772229
H	-1.009479	0.987634	-2.800397
H	-2.371152	0.555126	-3.844967
C	-3.105836	1.353196	1.355536
C	-2.674526	0.690596	2.678439
H	-3.204477	1.181440	3.503807
H	-1.604269	0.808780	2.863896
H	-2.917852	-0.374839	2.711346
C	-4.635391	1.216326	1.217878
H	-5.102430	1.676765	2.097304
H	-4.967549	0.174781	1.192119
H	-5.032020	1.730052	0.339356
C	-2.741306	2.854324	1.431118
H	-3.019976	3.407648	0.530886
H	-1.669152	3.001443	1.602799
H	-3.277505	3.307065	2.274266
C	2.100972	3.578135	-0.574656
C	3.019657	4.692903	-0.760314
H	3.147725	4.894461	-1.828641
H	3.992678	4.448761	-0.323133
H	2.620435	5.588398	-0.273447

---

---

Cartesian coordinates (Å) of **25'** (E = -1157.09411903 a.u.).



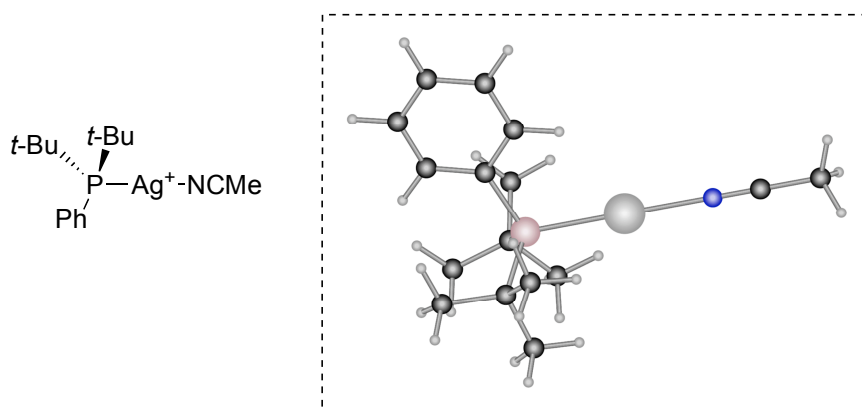
Au	1.357634	0.049959	0.006106
P	-0.908228	-0.496632	0.014570
C	-1.319672	-1.379440	1.658826
C	-2.833238	-1.573559	1.880434
H	-3.301345	-2.198614	1.116038
H	-3.364802	-0.619624	1.928980
H	-2.976379	-2.076574	2.844141
C	-0.773425	-0.469697	2.782596
H	-1.020015	-0.922000	3.750521
H	-1.220902	0.529406	2.760446
H	0.316018	-0.363195	2.733024
C	-0.600918	-2.741998	1.710955
H	0.472549	-2.654188	1.507868
H	-1.029755	-3.466683	1.012634
H	-0.711317	-3.158901	2.719069
C	-1.253509	-1.507243	-1.575584
C	-2.594767	-2.266478	-1.562168
H	-2.714008	-2.771097	-2.528334
H	-3.458170	-1.608140	-1.438053
H	-2.626972	-3.038466	-0.788700
C	-0.110090	-2.525478	-1.783909
H	-0.051231	-3.267734	-0.984161

H	0.865145	-2.033865	-1.869117
H	-0.291933	-3.065010	-2.720985
C	-1.907920	1.043905	-0.037119
C	-3.306227	1.022986	-0.201509
H	-3.838835	0.084980	-0.303212
C	-1.267229	2.288040	0.097225
C	-1.237895	-0.500633	-2.747262
H	-0.303198	0.071126	-2.786320
H	-2.069605	0.207112	-2.699517
H	-1.322640	-1.058554	-3.687301
C	-4.034418	2.211801	-0.234135
H	-5.111868	2.175778	-0.364821
C	-1.999781	3.475692	0.069348
H	-1.485660	4.426311	0.175846
C	-3.384116	3.440269	-0.098525
H	-3.954533	4.363929	-0.124158
N	3.397951	0.520800	-0.017176
C	4.524250	0.779187	-0.037286
C	5.942881	1.104233	-0.063249
H	6.502343	0.364379	0.518080
H	6.102799	2.097289	0.368709
H	6.304388	1.098513	-1.096517
H	-0.188949	2.331418	0.223304

---

---

Cartesian coordinates (Å) of **26'** (E = -1168.31802168 a.u.).



Ag	1.634821	0.050774	0.007566
P	-0.713731	-0.489839	0.014833
C	-1.153838	-1.369496	1.655913
C	-2.669166	-1.535044	1.885717
H	-3.150583	-2.152369	1.123158
H	-3.182404	-0.570776	1.931301
H	-2.821611	-2.032282	2.851294
C	-0.583186	-0.473095	2.778032
H	-0.832523	-0.917254	3.749114
H	-1.006866	0.536437	2.757057
H	0.509355	-0.391602	2.724763
C	-0.460345	-2.744842	1.706315
H	0.615341	-2.676251	1.503770
H	-0.899850	-3.460387	1.005269
H	-0.576839	-3.163865	2.712994
C	-1.085593	-1.499719	-1.570394
C	-2.421903	-2.266829	-1.549258
H	-2.548636	-2.773396	-2.513718
H	-3.285925	-1.610664	-1.416868
H	-2.446002	-3.037325	-0.773921
C	0.064551	-2.508397	-1.787575
H	0.143500	-3.243398	-0.982538

*Chapter 1. Experimental section*

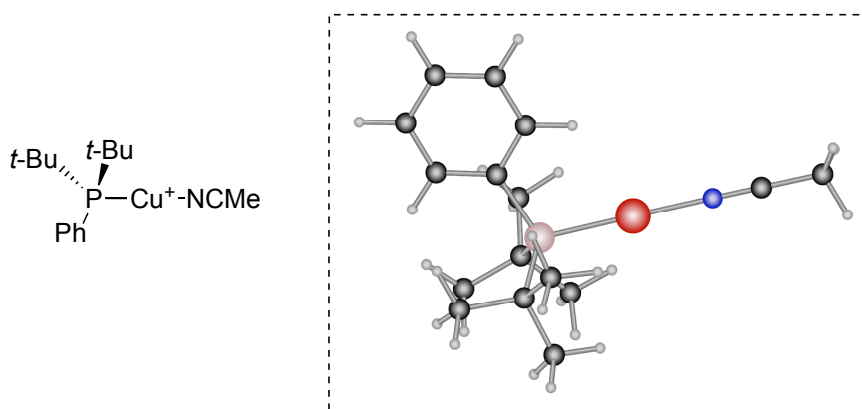
---

H	1.034301	-2.006421	-1.890459
H	-0.118569	-3.058231	-2.718496
C	-1.704715	1.058703	-0.036704
C	-3.101898	1.065978	-0.210807
H	-3.649906	0.137514	-0.320132
C	-1.044253	2.291334	0.106158
C	-1.083875	-0.495405	-2.743702
H	-0.154329	0.085430	-2.788831
H	-1.920146	0.206548	-2.692096
H	-1.167953	-1.053102	-3.684083
C	-3.807773	2.268315	-0.244317
H	-4.884780	2.253219	-0.383059
C	-1.752566	3.493673	0.078578
H	-1.221662	4.434244	0.192298
C	-3.136050	3.484289	-0.099173
H	-3.689135	4.418428	-0.125443
N	3.723295	0.514896	-0.016282
C	4.852537	0.763149	-0.035913
C	6.274525	1.075808	-0.060475
H	6.784763	0.542714	0.748017
H	6.419199	2.152746	0.071584
H	6.704143	0.770293	-1.019799
H	0.034710	2.316152	0.240334

---

---

Cartesian coordinates (Å) of **27'** (E = -1218.67348378 a.u.).



Cu	1.703197	0.125876	0.007922
P	-0.441677	-0.483919	0.014943
C	-0.830042	-1.383370	1.656494
C	-2.332065	-1.632230	1.893242
H	-2.780399	-2.279923	1.135613
H	-2.897973	-0.697910	1.934727
H	-2.453362	-2.131879	2.862004
C	-0.302765	-0.452393	2.772125
H	-0.515333	-0.908008	3.746650
H	-0.785593	0.530210	2.753623
H	0.782632	-0.306107	2.707322
C	-0.061551	-2.718600	1.708066
H	1.009544	-2.592074	1.508633
H	-0.459373	-3.456134	1.004900
H	-0.157671	-3.144690	2.713929
C	-0.755638	-1.513773	-1.568046
C	-2.044700	-2.356643	-1.550297
H	-2.138362	-2.873281	-2.513265
H	-2.945107	-1.749604	-1.424343
H	-2.029319	-3.124242	-0.771695
C	0.454935	-2.450760	-1.780650
H	0.570214	-3.186853	-0.980909

H	1.394259	-1.890816	-1.869185
H	0.315417	-3.002920	-2.717764
C	-1.514165	1.007697	-0.037569
C	-2.910167	0.944592	-0.207081
H	-3.411213	-0.010563	-0.314009
C	-0.914206	2.271615	0.099914
C	-0.808788	-0.511146	-2.741993
H	0.086050	0.122080	-2.785059
H	-1.683790	0.142017	-2.691956
H	-0.859118	-1.072445	-3.682609
C	-3.674817	2.110455	-0.239381
H	-4.750314	2.042191	-0.373753
C	-1.681329	3.437320	0.073505
H	-1.197673	4.403445	0.183548
C	-3.063480	3.358455	-0.098086
H	-3.662503	4.263883	-0.122668
N	3.533354	0.617419	-0.014280
C	4.652531	0.908611	-0.034355
C	6.060826	1.273664	-0.060237
H	6.666530	0.437269	0.303289
H	6.229630	2.145068	0.580583
H	6.361368	1.516800	-1.084506
H	0.162956	2.349969	0.229078

---

---

## 2. Cationic $\eta^1/\eta^2$ -Gold(I) Complexes with Simple Arenes.

### 2.1. Crystallographic Data.

Crystal structure determination was carried out using a Bruker-Nonius diffractometer equipped with a APPEX 2 4K CCD area detector, a FR591 rotating anode with  $\text{MoK}_\alpha$  radiation, Montel mirrors as monochromator and a Kryoflex low temperature device ( $T = 100 \text{ K}$ ). Fullsphere data collection omega and phi scans. Programs used: Data collection Apex2 V. 1.0-22 (Bruker-Nonius 2004), data reduction Saint + Version 6.22 (Bruker-Nonius 2001) and absorption correction SADABS V. 2.10 (2003). Crystal structure solution was achieved using direct methods as implemented in SHELXTL Version 6.10 (Sheldrick, Universität Göttingen (Germany), 2000) and visualized using XP program. Missing atoms were subsequently located from difference Fourier synthesis and added to the atom list. Least-squares refinement on F2 using all measured intensities was carried out using the program SHELXTL Version 6.10 (Sheldrick, Universität Göttingen (Germany), 2000). All non hydrogen atoms were refined including anisotropic displacement parameters.

Crystals of **30a-d** were obtained by evaporation of the solvent at room temperature, after heating a solution in an aromatic solvent (toluene or *p*-xylene) of **10a** or **10b**. Although the measured crystals are stable under atmosphere conditions, they were prepared under inert conditions immersed in perfluoropolyether as protecting oil for manipulation.

### X-Ray structure of complex **28a**.

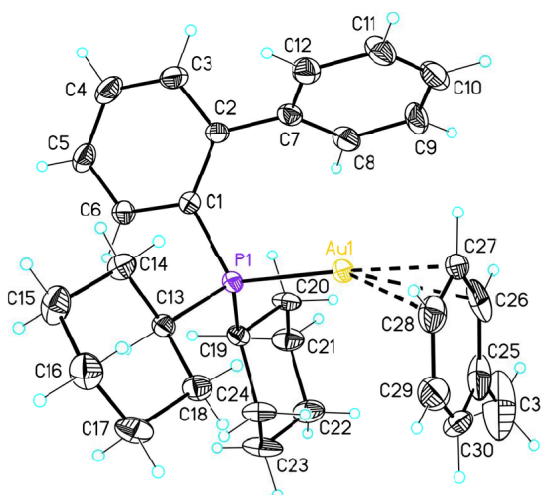


**Table 1.** Crystal data and structure refinement for **28a**.

Empirical formula	$C_{31}H_{39}AuF_6PSb$	
Formula weight	875.31	
Temperature	100(2) K	
Wavelength	0.71073 Å	
Crystal system	Monoclinic	
Space group	Cc	
Unit cell dimensions	$a = 10.5275(7)$ Å	$\alpha = 90^\circ$ .
	$b = 16.2109(11)$ Å	$\beta = 96.3960(10)^\circ$ .
	$c = 18.4159(15)$ Å	$\gamma = 90^\circ$ .
Volume	$3123.3(4)$ Å <sup>3</sup>	
Z	4	
Density (calculated)	1.861 Mg/m <sup>3</sup>	
Absorption coefficient	5.663 mm <sup>-1</sup>	
F(000)	1696	
Crystal size	0.10 x 0.04 x 0.01 mm <sup>3</sup>	
Theta range for data collection	3.36 to 35.13°.	
Index ranges	$-17 \leq h \leq 6, -26 \leq k \leq 26, -29 \leq l \leq 29$	
Reflections collected	23427	
Independent reflections	9026 [R(int) = 0.0656]	
Completeness to theta = 35.13°	98.9 %	

Absorption correction	None
Refinement method	Full-matrix least-squares on F <sup>2</sup>
Data / restraints / parameters	9026 / 2 / 362
Goodness-of-fit on F <sup>2</sup>	0.958
Final R indices [I>2sigma(I)]	R1 = 0.0364, wR2 = 0.0794
R indices (all data)	R1 = 0.0481, wR2 = 0.0823
Absolute structure parameter	0.011(4)
Largest diff. peak and hole	2.311 and -1.480 e.Å <sup>-3</sup>

**Table 2.** Bond lengths [Å] and angles [°] for **28a**.

Au(1)-P(1)	2.2459(13)	C(3)-C(2)-C(1)	117.5(5)
Au(1)-C(27)	2.263(5)	C(3)-C(2)-C(7)	117.8(5)
Au(1)-C(26)	2.535(6)	C(1)-C(2)-C(7)	124.5(5)
Au(1)-C(28)	2.689(6)	C(4)-C(3)-C(2)	122.3(5)
P(1)-C(1)	1.812(5)	C(3)-C(4)-C(5)	119.7(5)
P(1)-C(19)	1.837(5)	C(6)-C(5)-C(4)	119.1(5)
P(1)-C(13)	1.851(5)	C(5)-C(6)-C(1)	122.0(5)
C(1)-C(6)	1.395(8)	C(12)-C(7)-C(8)	118.1(5)
C(1)-C(2)	1.423(8)	C(12)-C(7)-C(2)	122.1(5)
C(2)-C(3)	1.398(8)	C(8)-C(7)-C(2)	119.8(5)
C(2)-C(7)	1.463(10)	C(9)-C(8)-C(7)	120.0(5)
C(3)-C(4)	1.389(9)	C(10)-C(9)-C(8)	120.4(6)
C(4)-C(5)	1.395(9)	C(9)-C(10)-C(11)	120.1(6)
C(5)-C(6)	1.382(7)	C(10)-C(11)-C(12)	120.6(6)
C(7)-C(12)	1.392(9)	C(7)-C(12)-C(11)	120.9(5)
C(7)-C(8)	1.416(6)	C(18)-C(13)-C(14)	108.9(4)
C(8)-C(9)	1.414(11)	C(18)-C(13)-P(1)	112.7(3)
C(9)-C(10)	1.366(10)	C(14)-C(13)-P(1)	111.6(3)
C(10)-C(11)	1.385(8)	C(15)-C(14)-C(13)	110.0(5)
C(11)-C(12)	1.394(9)	C(16)-C(15)-C(14)	111.2(5)
C(13)-C(18)	1.527(7)	C(15)-C(16)-C(17)	110.5(5)
C(13)-C(14)	1.539(7)	C(18)-C(17)-C(16)	111.1(5)

*Chapter 1. Experimental section*

---

C(14)-C(15)	1.533(7)	C(13)-C(18)-C(17)	111.3(4)
C(15)-C(16)	1.520(8)	C(20)-C(19)-C(24)	110.6(4)
C(16)-C(17)	1.533(8)	C(20)-C(19)-P(1)	109.7(3)
C(17)-C(18)	1.527(7)	C(24)-C(19)-P(1)	113.0(3)
C(19)-C(20)	1.532(7)	C(19)-C(20)-C(21)	111.3(4)
C(19)-C(24)	1.540(7)	C(20)-C(21)-C(22)	109.2(5)
C(20)-C(21)	1.536(7)	C(23)-C(22)-C(21)	110.6(5)
C(21)-C(22)	1.543(8)	C(22)-C(23)-C(24)	111.8(5)
C(22)-C(23)	1.522(8)	C(23)-C(24)-C(19)	110.0(4)
C(23)-C(24)	1.527(8)	C(26)-C(25)-C(30)	117.7(5)
C(25)-C(26)	1.400(11)	C(26)-C(25)-C(31)	118.5(9)
C(25)-C(30)	1.405(11)	C(30)-C(25)-C(31)	123.8(9)
C(25)-C(31)	1.497(9)	C(25)-C(26)-C(27)	120.8(6)
C(26)-C(27)	1.406(9)	C(25)-C(26)-Au(1)	102.8(4)
C(27)-C(28)	1.409(9)	C(27)-C(26)-Au(1)	62.6(3)
C(28)-C(29)	1.354(9)	C(26)-C(27)-C(28)	118.7(5)
C(29)-C(30)	1.362(10)	C(26)-C(27)-Au(1)	83.9(4)
Sb(1)-F(4)	1.861(4)	C(28)-C(27)-Au(1)	91.1(4)
Sb(1)-F(1)	1.868(4)	C(29)-C(28)-C(27)	120.1(5)
Sb(1)-F(3)	1.871(4)	C(29)-C(28)-Au(1)	102.2(4)
Sb(1)-F(6)	1.877(4)	C(27)-C(28)-Au(1)	57.3(3)
Sb(1)-F(5)	1.879(4)	C(28)-C(29)-C(30)	121.4(6)
Sb(1)-F(2)	1.881(5)	C(29)-C(30)-C(25)	121.3(6)
P(1)-Au(1)-C(27)	174.64(16)	F(4)-Sb(1)-F(1)	179.5(2)
P(1)-Au(1)-C(26)	148.87(16)	F(4)-Sb(1)-F(3)	89.3(2)
C(27)-Au(1)-C(26)	33.5(2)	F(1)-Sb(1)-F(3)	91.00(19)
P(1)-Au(1)-C(28)	143.04(13)	F(4)-Sb(1)-F(6)	90.0(2)
C(27)-Au(1)-C(28)	31.6(2)	F(1)-Sb(1)-F(6)	89.67(19)
C(26)-Au(1)-C(28)	55.14(18)	F(3)-Sb(1)-F(6)	179.33(19)
C(1)-P(1)-C(19)	103.4(2)	F(4)-Sb(1)-F(5)	90.1(2)
C(1)-P(1)-C(13)	104.3(2)	F(1)-Sb(1)-F(5)	90.3(2)
C(19)-P(1)-C(13)	108.3(2)	F(3)-Sb(1)-F(5)	89.9(2)
C(1)-P(1)-Au(1)	117.74(18)	F(6)-Sb(1)-F(5)	90.1(2)

---

C(19)-P(1)-Au(1)	111.18(17)	F(4)-Sb(1)-F(2)	90.8(3)
C(13)-P(1)-Au(1)	111.20(17)	F(1)-Sb(1)-F(2)	88.8(2)
C(6)-C(1)-C(2)	119.4(5)	F(3)-Sb(1)-F(2)	90.23(19)
C(6)-C(1)-P(1)	115.6(4)	F(6)-Sb(1)-F(2)	89.82(19)
C(2)-C(1)-P(1)	124.8(4)	F(5)-Sb(1)-F(2)	179.1(2)

---

---

**Table 3.** Torsion angles [°] for **28a**.

C(27)-Au(1)-P(1)-C(1)	130.1(16)
C(26)-Au(1)-P(1)-C(1)	-118.0(3)
C(28)-Au(1)-P(1)-C(1)	130.8(3)
C(27)-Au(1)-P(1)-C(19)	-110.8(16)
C(26)-Au(1)-P(1)-C(19)	1.0(4)
C(28)-Au(1)-P(1)-C(19)	-110.2(3)
C(27)-Au(1)-P(1)-C(13)	10.0(16)
C(26)-Au(1)-P(1)-C(13)	121.8(3)
C(28)-Au(1)-P(1)-C(13)	10.6(3)
C(19)-P(1)-C(1)-C(6)	59.7(4)
C(13)-P(1)-C(1)-C(6)	-53.5(4)
Au(1)-P(1)-C(1)-C(6)	-177.2(3)
C(19)-P(1)-C(1)-C(2)	-125.2(4)
C(13)-P(1)-C(1)-C(2)	121.6(4)
Au(1)-P(1)-C(1)-C(2)	-2.2(5)
C(6)-C(1)-C(2)-C(3)	2.2(7)
P(1)-C(1)-C(2)-C(3)	-172.7(4)
C(6)-C(1)-C(2)-C(7)	-173.4(5)
P(1)-C(1)-C(2)-C(7)	11.8(7)
C(1)-C(2)-C(3)-C(4)	-1.4(8)
C(7)-C(2)-C(3)-C(4)	174.4(5)
C(2)-C(3)-C(4)-C(5)	-0.2(8)
C(3)-C(4)-C(5)-C(6)	1.0(8)
C(4)-C(5)-C(6)-C(1)	-0.1(8)
C(2)-C(1)-C(6)-C(5)	-1.4(7)
P(1)-C(1)-C(6)-C(5)	173.9(4)
C(3)-C(2)-C(7)-C(12)	66.7(8)
C(1)-C(2)-C(7)-C(12)	-117.8(6)
C(3)-C(2)-C(7)-C(8)	-112.0(7)
C(1)-C(2)-C(7)-C(8)	63.5(9)

C(12)-C(7)-C(8)-C(9)	-2.8(10)
C(2)-C(7)-C(8)-C(9)	175.9(5)
C(7)-C(8)-C(9)-C(10)	2.7(10)
C(8)-C(9)-C(10)-C(11)	-1.0(10)
C(9)-C(10)-C(11)-C(12)	-0.5(9)
C(8)-C(7)-C(12)-C(11)	1.4(9)
C(2)-C(7)-C(12)-C(11)	-177.3(6)
C(10)-C(11)-C(12)-C(7)	0.3(9)
C(1)-P(1)-C(13)-C(18)	-163.4(4)
C(19)-P(1)-C(13)-C(18)	86.9(4)
Au(1)-P(1)-C(13)-C(18)	-35.5(4)
C(1)-P(1)-C(13)-C(14)	-40.6(4)
C(19)-P(1)-C(13)-C(14)	-150.2(4)
Au(1)-P(1)-C(13)-C(14)	87.3(4)
C(18)-C(13)-C(14)-C(15)	-59.0(6)
P(1)-C(13)-C(14)-C(15)	176.0(4)
C(13)-C(14)-C(15)-C(16)	58.7(7)
C(14)-C(15)-C(16)-C(17)	-56.1(7)
C(15)-C(16)-C(17)-C(18)	54.8(7)
C(14)-C(13)-C(18)-C(17)	58.6(6)
P(1)-C(13)-C(18)-C(17)	-177.1(4)
C(16)-C(17)-C(18)-C(13)	-56.9(6)
C(1)-P(1)-C(19)-C(20)	67.6(4)
C(13)-P(1)-C(19)-C(20)	177.8(3)
Au(1)-P(1)-C(19)-C(20)	-59.7(4)
C(1)-P(1)-C(19)-C(24)	-168.5(4)
C(13)-P(1)-C(19)-C(24)	-58.2(4)
Au(1)-P(1)-C(19)-C(24)	64.3(4)
C(24)-C(19)-C(20)-C(21)	57.6(6)
P(1)-C(19)-C(20)-C(21)	-177.0(4)
C(19)-C(20)-C(21)-C(22)	-57.7(7)
C(20)-C(21)-C(22)-C(23)	57.3(7)
C(21)-C(22)-C(23)-C(24)	-57.9(8)

C(22)-C(23)-C(24)-C(19)	56.7(7)
C(20)-C(19)-C(24)-C(23)	-55.9(7)
P(1)-C(19)-C(24)-C(23)	-179.4(4)
C(30)-C(25)-C(26)-C(27)	-0.8(9)
C(31)-C(25)-C(26)-C(27)	177.6(6)
C(30)-C(25)-C(26)-Au(1)	-66.3(6)
C(31)-C(25)-C(26)-Au(1)	112.0(6)
P(1)-Au(1)-C(26)-C(25)	-52.7(6)
C(27)-Au(1)-C(26)-C(25)	118.2(6)
C(28)-Au(1)-C(26)-C(25)	84.2(5)
P(1)-Au(1)-C(26)-C(27)	-171.0(3)
C(28)-Au(1)-C(26)-C(27)	-34.1(3)
C(25)-C(26)-C(27)-C(28)	-1.0(9)
Au(1)-C(26)-C(27)-C(28)	87.9(5)
C(25)-C(26)-C(27)-Au(1)	-89.0(6)
P(1)-Au(1)-C(27)-C(26)	119.5(16)
C(28)-Au(1)-C(27)-C(26)	118.7(5)
P(1)-Au(1)-C(27)-C(28)	0.8(19)
C(26)-Au(1)-C(27)-C(28)	-118.7(5)
C(26)-C(27)-C(28)-C(29)	1.6(9)
Au(1)-C(27)-C(28)-C(29)	85.3(6)
C(26)-C(27)-C(28)-Au(1)	-83.7(5)
P(1)-Au(1)-C(28)-C(29)	62.0(5)
C(27)-Au(1)-C(28)-C(29)	-118.1(5)
C(26)-Au(1)-C(28)-C(29)	-82.0(4)
P(1)-Au(1)-C(28)-C(27)	-179.9(3)
C(26)-Au(1)-C(28)-C(27)	36.1(4)
C(27)-C(28)-C(29)-C(30)	-0.3(10)
Au(1)-C(28)-C(29)-C(30)	58.8(7)
C(28)-C(29)-C(30)-C(25)	-1.6(10)
C(26)-C(25)-C(30)-C(29)	2.1(10)
C(31)-C(25)-C(30)-C(29)	-176.1(7)

---

**X-ray structure of complex 28b.**

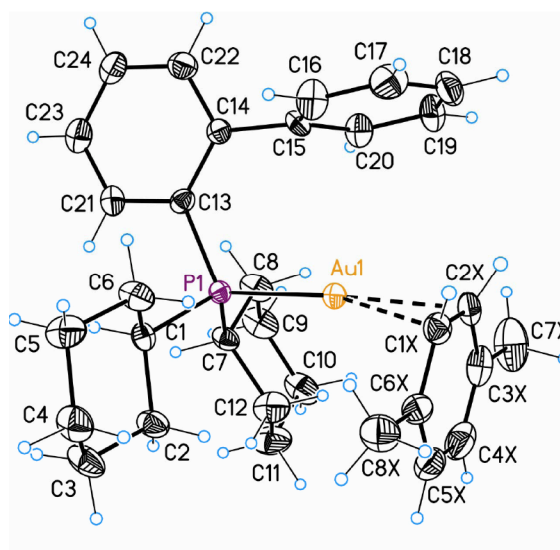


Table 1. Crystal data and structure refinement for **28b**.

Empirical formula	$C_{32}H_{41}AuF_6PSb$	
Formula weight	889.33	
Temperature	100(2) K	
Wavelength	0.71073 Å	
Crystal system	Orthorhombic	
Space group	<i>Pbca</i>	
Unit cell dimensions	$a = 17.749(3)$ Å	$\alpha = 90^\circ$ .
	$b = 14.9500(18)$ Å	$\beta = 90^\circ$ .
	$c = 24.056(3)$ Å	$\gamma = 90^\circ$ .
Volume	$6383.1(15)$ Å <sup>3</sup>	
Z	8	
Density (calculated)	1.851 Mg/m <sup>3</sup>	
Absorption coefficient	5.544 mm <sup>-1</sup>	
F(000)	3456	
Crystal size	0.10 x 0.05 x 0.01 mm <sup>3</sup>	
Theta range for data collection	2.67 to 36.60°.	
Index ranges	$29 \leq h \leq 28$ , $-24 \leq k \leq 19$ , $-36 \leq l \leq 40$	
Reflections collected	110052	
Independent reflections	15691 [R(int) = 0.1264]	

Completeness to theta = 36.60°	99.4 %
Absorption correction	SADABS (Bruker-Nonius)
Max. and min. transmission	0.9466 and 0.6071
Refinement method	Full-matrix least-squares on F <sup>2</sup>
Data / restraints / parameters	15691 / 0 / 372
Goodness-of-fit on F <sup>2</sup>	1.028
Final R indices [I>2sigma(I)]	R1 = 0.0745, wR2 = 0.1666
R indices (all data)	R1 = 0.1378, wR2 = 0.2028
Largest diff. peak and hole	7.795 and -2.590 e.Å <sup>-3</sup>

**Table 2.** Bond lengths [Å] and angles [°] for **28b**.

Au(1)-P(1)	2.2384(17)	C(7)-P(1)-Au(1)	110.4(2)
Au(1)-C(2X)	2.334(7)	C(3)-C(2)-C(1)	110.8(6)
Au(1)-C(1X)	2.339(7)	C(3X)-C(2X)-C(1X)	120.5(7)
C(1)-C(2)	1.520(10)	C(3X)-C(2X)-Au(1)	99.5(5)
C(1)-C(6)	1.522(9)	C(1X)-C(2X)-Au(1)	72.5(4)
C(1)-P(1)	1.837(6)	C(2)-C(3)-C(4)	112.4(7)
C(1X)-C(6X)	1.407(11)	C(4X)-C(3X)-C(2X)	117.7(8)
C(1X)-C(2X)	1.422(11)	C(4X)-C(3X)-C(7X)	122.1(9)
P(1)-C(13)	1.813(7)	C(2X)-C(3X)-C(7X)	120.2(9)
P(1)-C(7)	1.846(7)	C(5)-C(4)-C(3)	111.3(7)
C(2)-C(3)	1.516(10)	C(3X)-C(4X)-C(5X)	121.7(8)
C(2X)-C(3X)	1.409(12)	C(4)-C(5)-C(6)	111.5(7)
C(3)-C(4)	1.525(12)	C(6X)-C(5X)-C(4X)	121.3(8)
C(3X)-C(4X)	1.388(14)	C(1)-C(6)-C(5)	110.8(6)
C(3X)-C(7X)	1.512(12)	C(5X)-C(6X)-C(1X)	118.1(7)
C(4)-C(5)	1.517(13)	C(5X)-C(6X)-C(8X)	121.6(8)
C(4X)-C(5X)	1.408(13)	C(1X)-C(6X)-C(8X)	120.3(8)
C(5)-C(6)	1.534(11)	C(12)-C(7)-C(8)	109.8(6)
C(5X)-C(6X)	1.381(12)	C(12)-C(7)-P(1)	112.0(5)
C(6X)-C(8X)	1.500(11)	C(8)-C(7)-P(1)	110.2(5)
C(7)-C(12)	1.516(12)	C(9)-C(8)-C(7)	111.2(6)

C(7)-C(8)	1.530(9)	C(10)-C(9)-C(8)	112.0(8)
C(8)-C(9)	1.527(11)	C(9)-C(10)-C(11)	109.4(7)
C(9)-C(10)	1.505(14)	C(10)-C(11)-C(12)	110.3(7)
C(10)-C(11)	1.534(12)	C(7)-C(12)-C(11)	109.8(7)
C(11)-C(12)	1.543(12)	C(14)-C(13)-C(21)	118.6(6)
C(13)-C(14)	1.410(9)	C(14)-C(13)-P(1)	125.1(5)
C(13)-C(21)	1.413(10)	C(21)-C(13)-P(1)	116.3(5)
C(14)-C(22)	1.380(10)	C(22)-C(14)-C(13)	119.0(6)
C(14)-C(15)	1.499(9)	C(22)-C(14)-C(15)	117.2(6)
C(15)-C(16)	1.380(10)	C(13)-C(14)-C(15)	123.8(6)
C(15)-C(20)	1.393(9)	C(16)-C(15)-C(20)	118.2(7)
C(16)-C(17)	1.388(12)	C(16)-C(15)-C(14)	121.3(6)
C(17)-C(18)	1.402(13)	C(20)-C(15)-C(14)	120.0(6)
C(18)-C(19)	1.364(12)	C(15)-C(16)-C(17)	122.5(8)
C(19)-C(20)	1.390(11)	C(16)-C(17)-C(18)	118.1(8)
C(21)-C(23)	1.376(11)	C(19)-C(18)-C(17)	120.2(7)
C(22)-C(24)	1.392(11)	C(18)-C(19)-C(20)	120.9(7)
C(23)-C(24)	1.386(12)	C(19)-C(20)-C(15)	120.0(7)
Sb(1S)-F(2S)	1.862(5)	C(23)-C(21)-C(13)	121.4(7)
Sb(1S)-F(1S)	1.865(5)	C(14)-C(22)-C(24)	121.7(7)
Sb(1S)-F(3S)	1.867(5)	C(21)-C(23)-C(24)	119.5(7)
Sb(1S)-F(5S)	1.869(5)	C(23)-C(24)-C(22)	119.8(7)
Sb(1S)-F(6S)	1.873(5)	F(2S)-Sb(1S)-F(1S)	90.7(3)
Sb(1S)-F(4S)	1.880(5)	F(2S)-Sb(1S)-F(3S)	90.0(3)
P(1)-Au(1)-C(2X)	160.38(19)	F(1S)-Sb(1S)-F(3S)	90.3(3)
P(1)-Au(1)-C(1X)	160.35(19)	F(2S)-Sb(1S)-F(5S)	178.2(3)
C(2X)-Au(1)-C(1X)	35.4(3)	F(1S)-Sb(1S)-F(5S)	90.9(3)
C(2)-C(1)-C(6)	111.8(6)	F(3S)-Sb(1S)-F(5S)	90.8(3)
C(2)-C(1)-P(1)	113.4(5)	F(2S)-Sb(1S)-F(6S)	90.2(3)
C(6)-C(1)-P(1)	109.2(5)	F(1S)-Sb(1S)-F(6S)	89.7(2)
C(6X)-C(1X)-C(2X)	120.7(7)	F(3S)-Sb(1S)-F(6S)	179.8(3)
C(6X)-C(1X)-Au(1)	100.7(5)	F(5S)-Sb(1S)-F(6S)	89.0(2)
C(2X)-C(1X)-Au(1)	72.1(4)	F(2S)-Sb(1S)-F(4S)	89.1(3)

C(13)-P(1)-C(1)	103.9(3)	F(1S)-Sb(1S)-F(4S)	179.0(3)
C(13)-P(1)-C(7)	104.5(3)	F(3S)-Sb(1S)-F(4S)	90.7(3)
C(1)-P(1)-C(7)	109.6(3)	F(5S)-Sb(1S)-F(4S)	89.2(3)
C(13)-P(1)-Au(1)	116.9(2)	F(6S)-Sb(1S)-F(4S)	89.3(2)
C(1)-P(1)-Au(1)	111.2(2)		

**Table 3.** Torsion angles [°] for **28b**.

P(1)-Au(1)-C(1X)-C(6X)	34.5(9)
C(2X)-Au(1)-C(1X)-C(6X)	-119.0(7)
P(1)-Au(1)-C(1X)-C(2X)	153.6(5)
C(2)-C(1)-P(1)-C(13)	165.4(5)
C(6)-C(1)-P(1)-C(13)	-69.3(6)
C(2)-C(1)-P(1)-C(7)	54.2(6)
C(6)-C(1)-P(1)-C(7)	179.5(5)
C(2)-C(1)-P(1)-Au(1)	-68.2(5)
C(6)-C(1)-P(1)-Au(1)	57.1(6)
C(2X)-Au(1)-P(1)-C(13)	-100.9(6)
C(1X)-Au(1)-P(1)-C(13)	129.3(6)
C(2X)-Au(1)-P(1)-C(1)	140.2(6)
C(1X)-Au(1)-P(1)-C(1)	10.4(7)
C(2X)-Au(1)-P(1)-C(7)	18.3(6)
C(1X)-Au(1)-P(1)-C(7)	-111.5(6)
C(6)-C(1)-C(2)-C(3)	55.3(9)
P(1)-C(1)-C(2)-C(3)	179.2(6)
C(6X)-C(1X)-C(2X)-C(3X)	1.0(11)
Au(1)-C(1X)-C(2X)-C(3X)	-90.9(7)
C(6X)-C(1X)-C(2X)-Au(1)	91.9(7)
P(1)-Au(1)-C(2X)-C(3X)	-34.4(9)
C(1X)-Au(1)-C(2X)-C(3X)	119.1(7)
P(1)-Au(1)-C(2X)-C(1X)	-153.5(5)
C(1)-C(2)-C(3)-C(4)	-54.4(10)
C(1X)-C(2X)-C(3X)-C(4X)	-0.7(11)

Au(1)-C(2X)-C(3X)-C(4X)	-76.0(8)
C(1X)-C(2X)-C(3X)-C(7X)	-179.3(8)
Au(1)-C(2X)-C(3X)-C(7X)	105.4(8)
C(2)-C(3)-C(4)-C(5)	54.2(11)
C(2X)-C(3X)-C(4X)-C(5X)	0.0(12)
C(7X)-C(3X)-C(4X)-C(5X)	178.5(9)
C(3)-C(4)-C(5)-C(6)	-54.2(10)
C(3X)-C(4X)-C(5X)-C(6X)	0.5(13)
C(2)-C(1)-C(6)-C(5)	-55.8(9)
P(1)-C(1)-C(6)-C(5)	178.0(6)
C(4)-C(5)-C(6)-C(1)	55.2(10)
C(4X)-C(5X)-C(6X)-C(1X)	-0.2(12)
C(4X)-C(5X)-C(6X)-C(8X)	178.8(8)
C(2X)-C(1X)-C(6X)-C(5X)	-0.5(11)
Au(1)-C(1X)-C(6X)-C(5X)	74.9(7)
C(2X)-C(1X)-C(6X)-C(8X)	-179.6(7)
Au(1)-C(1X)-C(6X)-C(8X)	-104.2(7)
C(13)-P(1)-C(7)-C(12)	166.4(5)
C(1)-P(1)-C(7)-C(12)	-82.8(6)
Au(1)-P(1)-C(7)-C(12)	39.9(6)
C(13)-P(1)-C(7)-C(8)	43.8(6)
C(1)-P(1)-C(7)-C(8)	154.6(5)
Au(1)-P(1)-C(7)-C(8)	-82.7(6)
C(12)-C(7)-C(8)-C(9)	56.4(9)
P(1)-C(7)-C(8)-C(9)	-179.7(6)
C(7)-C(8)-C(9)-C(10)	-56.2(10)
C(8)-C(9)-C(10)-C(11)	56.5(10)
C(9)-C(10)-C(11)-C(12)	-58.2(11)
C(8)-C(7)-C(12)-C(11)	-58.3(9)
P(1)-C(7)-C(12)-C(11)	178.8(6)
C(10)-C(11)-C(12)-C(7)	59.9(11)
C(1)-P(1)-C(13)-C(14)	125.0(6)
C(7)-P(1)-C(13)-C(14)	-120.1(6)

Au(1)-P(1)-C(13)-C(14)	2.2(6)
C(1)-P(1)-C(13)-C(21)	-55.2(6)
C(7)-P(1)-C(13)-C(21)	59.7(6)
Au(1)-P(1)-C(13)-C(21)	-178.0(4)
C(21)-C(13)-C(14)-C(22)	2.5(9)
P(1)-C(13)-C(14)-C(22)	-177.8(5)
C(21)-C(13)-C(14)-C(15)	-176.2(6)
P(1)-C(13)-C(14)-C(15)	3.5(9)
C(22)-C(14)-C(15)-C(16)	78.8(9)
C(13)-C(14)-C(15)-C(16)	-102.5(9)
C(22)-C(14)-C(15)-C(20)	-93.6(8)
C(13)-C(14)-C(15)-C(20)	85.1(9)
C(20)-C(15)-C(16)-C(17)	0.6(13)
C(14)-C(15)-C(16)-C(17)	-172.0(8)
C(15)-C(16)-C(17)-C(18)	0.9(14)
C(16)-C(17)-C(18)-C(19)	-1.6(14)
C(17)-C(18)-C(19)-C(20)	0.7(14)
C(18)-C(19)-C(20)-C(15)	0.9(13)
C(16)-C(15)-C(20)-C(19)	-1.5(12)
C(14)-C(15)-C(20)-C(19)	171.1(7)
C(14)-C(13)-C(21)-C(23)	-2.2(10)
P(1)-C(13)-C(21)-C(23)	178.0(6)
C(13)-C(14)-C(22)-C(24)	-1.4(11)
C(15)-C(14)-C(22)-C(24)	177.3(7)
C(13)-C(21)-C(23)-C(24)	0.8(11)
C(21)-C(23)-C(24)-C(22)	0.3(11)
C(14)-C(22)-C(24)-C(23)	0.0(12)

---

**X-ray structure of complex 28c.**

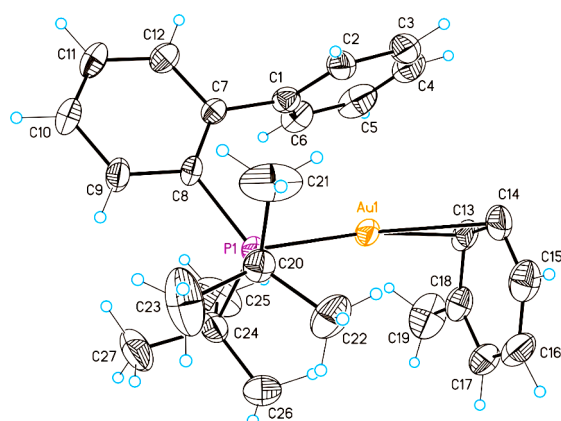


**Table 1.** Crystal data and structure refinement for **28c**.

Empirical formula	$C_{27}H_{35}AuF_6PSb$	
Formula weight	823.24	
Temperature	100(2) K	
Wavelength	0.71073 Å	
Crystal system	Monoclinic	
Space group	P2(1)/n	
Unit cell dimensions	$a = 10.0342(12)$ Å	$\alpha = 90^\circ$ .
	$b = 25.189(3)$ Å	$\beta = 95.413(4)^\circ$ .
	$c = 11.8275(14)$ Å	$\gamma = 90^\circ$ .
Volume	$2976.1(6)$ Å <sup>3</sup>	
Z	4	
Density (calculated)	$1.837$ Mg/m <sup>3</sup>	
Absorption coefficient	$5.937$ mm <sup>-1</sup>	
F(000)	1584	
Crystal size	$0.10 \times 0.10 \times 0.01$ mm <sup>3</sup>	
Theta range for data collection	2.60 to $37.13^\circ$ .	
Index ranges	$-16 \leq h \leq 12$ , $-42 \leq k \leq 40$ , $-19 \leq l \leq 19$	
Reflections collected	55182	
Independent reflections	14113 [R(int) = 0.0509]	
Completeness to theta = $37.13^\circ$	92.6 %	
Absorption correction	SADABS (Bruker-Nonius)	
Max. and min. transmission	0.9430 and 0.5882	

Refinement method	Full-matrix least-squares on F <sup>2</sup>
Data / restraints / parameters	14113 / 35 / 351
Goodness-of-fit on F <sup>2</sup>	1.022
Final R indices [I>2sigma(I)]	R1 = 0.0546, wR2 = 0.1752
R indices (all data)	R1 = 0.1040, wR2 = 0.2146
Largest diff. peak and hole	3.350 and -1.696 e.Å <sup>-3</sup>

**Table 2.** Bond lengths [Å] and angles [°] for **28c**.

Au(1)-P(1)	2.2643(10)	C(10)-C(11)-C(12)	117.8(8)
Au(1)-C(2A)	2.299(5)	C(7)-C(12)-C(11)	122.5(6)
Au(1)-C(3A)	2.423(5)	C(16)-C(13)-C(15)	109.8(8)
P(1)-C(1)	1.840(4)	C(16)-C(13)-C(14)	108.3(6)
P(1)-C(13)	1.877(5)	C(15)-C(13)-C(14)	105.9(8)
P(1)-C(17)	1.888(5)	C(16)-C(13)-P(1)	109.8(4)
C(1)-C(6)	1.396(6)	C(15)-C(13)-P(1)	116.5(4)
C(1)-C(2)	1.405(7)	C(14)-C(13)-P(1)	106.1(5)
C(1A)-C(6A)	1.356(11)	C(19)-C(17)-C(18)	109.6(8)
C(1A)-C(2A)	1.416(10)	C(19)-C(17)-C(20)	108.9(7)
C(1A)-C(7A)	1.490(10)	C(18)-C(17)-C(20)	110.5(7)
C(2A)-C(3A)	1.416(9)	C(19)-C(17)-P(1)	109.5(4)
C(3A)-C(4A)	1.344(12)	C(18)-C(17)-P(1)	115.0(4)
C(4A)-C(5A)	1.359(12)	C(20)-C(17)-P(1)	103.0(5)
C(5A)-C(6A)	1.358(10)	F(3')-Sb(1)-F(1)	119.5(10)
C(2)-C(3)	1.393(6)	F(3')-Sb(1)-F(2')	92.9(11)
C(2)-C(7)	1.484(7)	F(1)-Sb(1)-F(2')	145.2(10)
C(3)-C(4)	1.372(8)	F(3')-Sb(1)-F(4)	64.5(10)
C(4)-C(5)	1.355(10)	F(1)-Sb(1)-F(4)	93.2(6)
C(5)-C(6)	1.415(8)	F(2')-Sb(1)-F(4)	89.8(9)
C(7)-C(12)	1.394(8)	F(3')-Sb(1)-F(2)	62.1(10)
C(7)-C(8)	1.411(7)	F(1)-Sb(1)-F(2)	178.2(7)
C(8)-C(9)	1.380(11)	F(2')-Sb(1)-F(2)	33.5(9)
C(9)-C(10)	1.385(15)	F(4)-Sb(1)-F(2)	88.2(8)

C(10)-C(11)	1.319(14)	F(3')-Sb(1)-F(3)	39.8(8)
C(11)-C(12)	1.403(9)	F(1)-Sb(1)-F(3)	90.8(7)
C(13)-C(16)	1.496(8)	F(2')-Sb(1)-F(3)	123.8(10)
C(13)-C(15)	1.515(10)	F(4)-Sb(1)-F(3)	91.2(6)
C(13)-C(14)	1.536(10)	F(2)-Sb(1)-F(3)	90.4(7)
C(17)-C(19)	1.468(10)	F(3')-Sb(1)-F(5)	137.3(10)
C(17)-C(18)	1.515(9)	F(1)-Sb(1)-F(5)	96.5(8)
C(17)-C(20)	1.553(10)	F(2')Sb(1)F(5)	48.7(9)
Sb(1)-F(3')	1.756(19)	F(4)-Sb(1)-F(5)	93.5(5)
Sb(1)-F(1)	1.763(11)	F(2)-Sb(1)-F(5)	82.3(6)
Sb(1)-F(2')	1.800(19)	F(3)-Sb(1)-F(5)	171.1(7)
Sb(1)-F(4)	1.821(6)	F(3')-Sb(1)-F(1')	97.7(11)
Sb(1)-F(2)	1.824(10)	F(1)-Sb(1)-F(1')	22.9(9)
Sb(1)-F(3)	1.826(7)	F(2')-Sb(1)-F(1')	168.0(12)
Sb(1)-F(5)	1.827(6)	F(4)-Sb(1)-F(1')	89.6(10)
Sb(1)-F(1')	1.84(2)	F(2)-Sb(1)-F(1')	158.4(10)
Sb(1)-F(6)	1.848(7)	F(3)-Sb(1)-F(1')	68.2(10)
Sb(1)-F(6')	1.91(2)	F(5)-Sb(1)-F(1')	119.4(10)
Sb(1)-F(4')	1.95(2)	F(3')-Sb(1)-F(6)	116.8(10)
Sb(1)-F(5')	1.98(2)	F(1)-Sb(1)-F(6)	87.3(7)
P(1)-Au(1)-C(2A)	164.94(18)	F(2')-Sb(1)-F(6)	88.7(10)
P(1)-Au(1)-C(3A)	157.22(19)	F(4)-Sb(1)-F(6)	178.1(6)
C(2A)-Au(1)-C(3A)	34.8(2)	F(2)-Sb(1)-F(6)	91.2(8)
C(1)-P(1)-C(13)	107.5(2)	F(3)-Sb(1)-F(6)	90.6(5)
C(1)-P(1)-C(17)	106.3(2)	F(5)-Sb(1)-F(6)	84.7(5)
C(13)-P(1)-C(17)	115.0(3)	F(1')-Sb(1)-F(6)	91.5(10)
C(1)-P(1)-Au(1)	113.89(15)	F(3')-Sb(1)-F(6')	114.9(13)
C(13)-P(1)-Au(1)	107.40(16)	F(1)-Sb(1)-F(6')	84.2(11)
C(17)-P(1)-Au(1)	106.83(16)	F(2')-Sb(1)-F(6')	93.6(11)
C(6)-C(1)-C(2)	120.2(4)	F(4)-Sb(1)-F(6')	176.6(10)
C(6)-C(1)-P(1)	117.0(4)	F(2)-Sb(1)-F(6')	94.4(12)
C(2)-C(1)-P(1)	122.8(3)	F(3)-Sb(1)-F(6')	86.7(10)
C(6A)-C(1A)-C(2A)	119.2(6)	F(5)-Sb(1)-F(6')	89.0(10)

*Chapter 1. Experimental section*

C(6A)-C(1A)-C(7A)	119.8(8)	F(1')-Sb(1)-F(6')	87.1(11)
C(2A)-C(1A)-C(7A)	121.0(8)	F(6)-Sb(1)-F(6')	5.1(12)
C(3A)-C(2A)-C(1A)	119.5(6)	F(3')-Sb(1)-F(4')	89.1(11)
C(3A)-C(2A)-Au(1)	77.4(3)	F(1)-Sb(1)-F(4')	80.2(11)
C(1A)-C(2A)-Au(1)	100.1(4)	F(2')-Sb(1)-F(4')	88.9(11)
C(4A)-C(3A)-C(2A)	118.7(7)	F(4)-Sb(1)-F(4')	24.6(8)
C(4A)-C(3A)-Au(1)	103.9(5)	F(2)-Sb(1)-F(4')	100.8(12)
C(2A)-C(3A)-Au(1)	67.8(3)	F(3)-Sb(1)-F(4')	111.9(9)
C(3A)-C(4A)-C(5A)	120.4(7)	F(5)-Sb(1)-F(4')	74.5(8)
C(6A)-C(5A)-C(4A)	122.8(7)	F(1')-Sb(1)-F(4')	85.7(11)
C(1A)-C(6A)-C(5A)	119.4(7)	F(6)-Sb(1)-F(4')	154.1(9)
C(3)-C(2)-C(1)	118.5(4)	F(6')-Sb(1)-F(4')	155.7(12)
C(3)-C(2)-C(7)	115.3(5)	F(3')-Sb(1)-F(5')	163.8(11)
C(1)-C(2)-C(7)	126.2(4)	F(1)-Sb(1)-F(5')	60.2(9)
C(4)-C(3)-C(2)	121.3(6)	F(2')-Sb(1)-F(5')	85.1(10)
C(5)-C(4)-C(3)	120.7(5)	F(4)-Sb(1)-F(5')	99.4(9)
C(4)-C(5)-C(6)	120.5(5)	F(2)-Sb(1)-F(5')	118.4(9)
C(1)-C(6)-C(5)	118.9(6)	F(3)-Sb(1)-F(5')	149.4(9)
C(12)-C(7)-C(8)	117.6(5)	F(5)-Sb(1)-F(5')	36.6(8)
C(12)-C(7)-C(2)	121.6(4)	F(1')-Sb(1)-F(5')	83.2(10)
C(8)-C(7)-C(2)	120.4(5)	F(6)-Sb(1)-F(5')	79.3(10)
C(9)-C(8)-C(7)	118.7(7)	F(6')-Sb(1)-F(5')	81.3(11)
C(8)-C(9)-C(10)	120.8(7)	F(4')-Sb(1)-F(5')	74.8(10)
C(11)-C(10)-C(9)	122.5(7)		

---

Symmetry transformations used to generate equivalent atoms.

**Table 3.** Torsion angles [ $^{\circ}$ ] for **28c**.

C(2A)-Au(1)-P(1)-C(1)	-105.4(6)
C(3A)-Au(1)-P(1)-C(1)	121.4(5)
C(2A)-Au(1)-P(1)-C(13)	135.7(6)
C(3A)-Au(1)-P(1)-C(13)	2.5(5)
C(2A)-Au(1)-P(1)-C(17)	11.7(7)
C(3A)-Au(1)-P(1)-C(17)	-121.5(5)
C(13)-P(1)-C(1)-C(6)	-57.8(4)
C(17)-P(1)-C(1)-C(6)	65.9(4)
Au(1)-P(1)-C(1)-C(6)	-176.7(3)
C(13)-P(1)-C(1)-C(2)	123.8(4)
C(17)-P(1)-C(1)-C(2)	-112.5(4)
Au(1)-P(1)-C(1)-C(2)	4.9(4)
C(6A)-C(1A)-C(2A)-C(3A)	0.0(8)
C(7A)-C(1A)-C(2A)-C(3A)	-179.3(6)
C(6A)-C(1A)-C(2A)-Au(1)	-81.1(6)
C(7A)-C(1A)-C(2A)-Au(1)	99.5(7)
P(1)-Au(1)-C(2A)-C(3A)	-150.3(5)
P(1)-Au(1)-C(2A)-C(1A)	-32.1(9)
C(3A)-Au(1)-C(2A)-C(1A)	118.2(6)
C(1A)-C(2A)-C(3A)-C(4A)	-0.4(8)
Au(1)-C(2A)-C(3A)-C(4A)	94.2(5)
C(1A)-C(2A)-C(3A)-Au(1)	-94.6(5)
P(1)-Au(1)-C(3A)-C(4A)	44.9(8)
C(2A)-Au(1)-C(3A)-C(4A)	-115.7(7)
P(1)-Au(1)-C(3A)-C(2A)	160.6(4)
C(2A)-C(3A)-C(4A)-C(5A)	1.8(10)
Au(1)-C(3A)-C(4A)-C(5A)	73.9(7)
C(3A)-C(4A)-C(5A)-C(6A)	-2.8(11)
C(2A)-C(1A)-C(6A)-C(5A)	-1.0(10)
C(7A)-C(1A)-C(6A)-C(5A)	178.4(7)
C(4A)-C(5A)-C(6A)-C(1A)	2.4(11)

C(6)-C(1)-C(2)-C(3)	-0.2(6)
P(1)-C(1)-C(2)-C(3)	178.1(3)
C(6)-C(1)-C(2)-C(7)	178.2(4)
P(1)-C(1)-C(2)-C(7)	-3.5(6)
C(1)-C(2)-C(3)-C(4)	-0.2(7)
C(7)-C(2)-C(3)-C(4)	-178.8(4)
C(2)-C(3)-C(4)-C(5)	0.7(8)
C(3)-C(4)-C(5)-C(6)	-0.7(9)
C(2)C(1)C(6)C(5)	0.2(7)
P(1)-C(1)-C(6)-C(5)	-178.2(4)
C(4)-C(5)-C(6)-C(1)	0.2(8)
C(3)-C(2)-C(7)-C(12)	92.5(6)
C(1)-C(2)-C(7)-C(12)	-85.9(7)
C(3)-C(2)-C(7)-C(8)	-80.4(6)
C(1)-C(2)-C(7)-C(8)	101.2(6)
C(12)-C(7)-C(8)-C(9)	1.9(10)
C(2)-C(7)-C(8)-C(9)	175.0(6)
C(7)-C(8)-C(9)-C(10)	-3.1(12)
C(8)-C(9)-C(10)-C(11)	3.1(14)
C(9)-C(10)-C(11)-C(12)	-1.6(14)
C(8)-C(7)-C(12)-C(11)	-0.6(10)
C(2)-C(7)-C(12)-C(11)	-173.6(6)
C(10)-C(11)-C(12)-C(7)	0.4(12)
C(1)-P(1)-C(13)-C(16)	-162.2(5)
C(17)-P(1)-C(13)-C(16)	79.6(6)
Au(1)-P(1)-C(13)-C(16)	-39.2(6)
C(1)-P(1)-C(13)-C(15)	72.2(8)
C(17)-P(1)-C(13)-C(15)	-46.0(8)
Au(1)-P(1)-C(13)-C(15)	-164.8(8)
C(1)-P(1)-C(13)-C(14)	-45.4(6)
C(17)-P(1)-C(13)-C(14)	-163.6(5)
Au(1)-P(1)-C(13)-C(14)	77.6(6)
C(1)-P(1)-C(17)-C(19)	176.3(6)

C(13)-P(1)-C(17)-C(19)	-64.8(6)
Au(1)-P(1)-C(17)-C(19)	54.3(6)
C(1)-P(1)-C(17)-C(18)	-59.8(7)
C(13)-P(1)-C(17)-C(18)	59.2(7)
Au(1)-P(1)-C(17)-C(18)	178.3(6)
C(1)-P(1)-C(17)-C(20)	60.5(5)
C(13)-P(1)-C(17)-C(20)	179.5(5)
Au(1)-P(1)-C(17)-C(20)	61.4(5)

---

Symmetry transformations used to generate equivalent atoms.

### X-ray structure of complex **28d**.

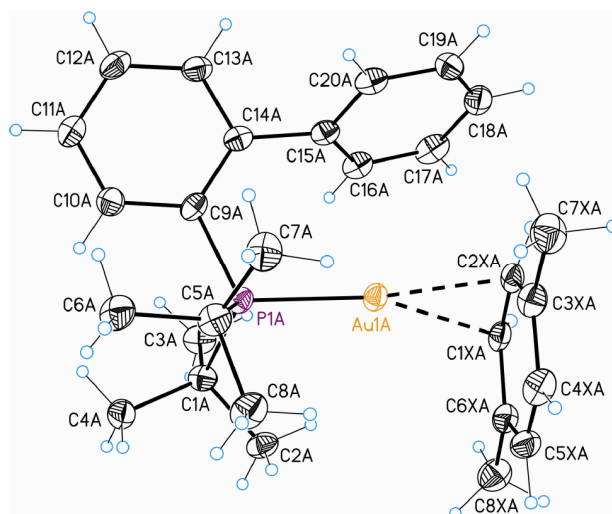


**Table 1.** Crystal data and structure refinement for **28d**.

Empirical formula	$C_{60}H_{79} Au_2F_{12}P_2Sb_2$	
Formula weight	1727.60	
Temperature	100(2) K	
Wavelength	0.71073 Å	
Crystal system	Monoclinic	
Space group	$P2_1c$	
Unit cell dimensions	$a = 25.471(7)$ Å	$\alpha = 90^\circ$ .
	$b = 13.423(2)$ Å	$\beta = 92.598(9)^\circ$ .
	$c = 18.588(3)$ Å	$\gamma = 90^\circ$ .
Volume	$6349(2)$ Å <sup>3</sup>	
Z	4	
Density (calculated)	1.803 Mg/m <sup>3</sup>	
Absorption coefficient	5.571 mm <sup>-1</sup>	
F(000)	3348	
Crystal size	0.10 x 0.05 x 0.01 mm <sup>3</sup>	
Theta range for data collection	2.43 to 35.86°.	
Index ranges	$-39 \leq h \leq 41, -22 \leq k \leq 10, -30 \leq l \leq 27$	
Reflections collected	108860	
Independent reflections	29337 [R(int) = 0.0969]	

Completeness to theta = 35.86°	98.5 %
Absorption correction	SADABS (Bruker-Nonius)
Max. and min. transmission	0.9464 and 0.6058
Refinement method	Full-matrix least-squares on F <sup>2</sup>
Data / restraints / parameters	29337 / 0 / 720
Goodness-of-fit on F <sup>2</sup>	0.933
Final R indices [ <i>I</i> > 2σ( <i>I</i> )]	R1 = 0.0468, wR2 = 0.0878
R indices (all data)	R1 = 0.1072, wR2 = 0.1040
Largest diff. peak and hole	2.749 and -2.349 e.Å <sup>-3</sup>

**Table 2.** Bond lengths [Å] and angles [°] for **28d**.

Au(1A)-P(1A)	2.2656(11)	C(6A)-C(5A)-P(1A)	114.9(3)
Au(1A)-C(2XA)	2.303(4)	C(8A)-C(5A)-P(1A)	109.0(3)
Au(1A)-C(1XA)	2.360(4)	C(6XA)-C(5XA)-C(4XA)	122.2(4)
P(1A)-C(9A)	1.838(4)	C(5XA)-C(6XA)-C(1XA)	117.6(4)
P(1A)-C(5A)	1.881(5)	C(5XA)-C(6XA)-C(8XA)	121.7(4)
P(1A)-C(1A)	1.896(4)	C(1XA)-C(6XA)-C(8XA)	120.5(4)
C(1A)-C(3A)	1.534(6)	C(10A)-C(9A)-C(14A)	118.5(3)
C(1A)-C(4A)	1.540(6)	C(10A)-C(9A)-P(1A)	118.5(3)
C(1A)-C(2A)	1.550(5)	C(14A)-C(9A)-P(1A)	122.9(3)
C(1XA)-C(6XA)	1.425(6)	C(11A)-C(10A)-C(9A)	122.1(4)
C(1XA)-C(2XA)	1.431(6)	C(12A)-C(11A)-C(10A)	119.5(4)
C(2XA)-C(3XA)	1.402(6)	C(11A)-C(12A)-C(13A)	119.7(4)
C(3XA)-C(4XA)	1.396(6)	C(12A)-C(13A)-C(14A)	121.9(4)
C(3XA)-C(7XA)	1.503(6)	C(13A)-C(14A)-C(9A)	118.2(4)
C(4XA)-C(5XA)	1.397(6)	C(13A)-C(14A)-C(15A)	114.5(3)
C(5A)-C(7A)	1.529(6)	C(9A)-C(14A)-C(15A)	127.3(3)
C(5A)-C(6A)	1.539(6)	C(16A)-C(15A)-C(20A)	119.0(4)
C(5A)-C(8A)	1.550(6)	C(16A)-C(15A)-C(14A)	120.8(4)
C(5XA)-C(6XA)	1.391(7)	C(20A)-C(15A)-C(14A)	119.5(4)
C(6XA)-C(8XA)	1.505(6)	C(15A)-C(16A)-C(17A)	120.1(4)
C(9A)-C(10A)	1.402(6)	C(18A)-C(17A)-C(16A)	120.0(4)

C(9A)-C(14A)	1.424(6)	C(19A)-C(18A)-C(17A)	119.4(4)
C(10A)-C(11A)	1.399(5)	C(18A)-C(19A)-C(20A)	121.4(4)
C(11A)-C(12A)	1.381(6)	C(19A)-C(20A)-C(15A)	120.0(4)
C(12A)-C(13A)	1.395(6)	P(1B)-Au(1B)-C(1XB)	161.91(10)
C(13A)-C(14A)	1.413(5)	P(1B)-Au(1B)-C(2XB)	159.62(11)
C(14A)-C(15A)	1.500(6)	C(1XB)-Au(1B)-C(2XB)	35.28(14)
C(15A)-C(16A)	1.392(6)	C(9B)-P(1B)-C(5B)	105.87(17)
C(15A)-C(20A)	1.411(6)	C(9B)-P(1B)-C(1B)	108.09(19)
C(16A)-C(17A)	1.410(6)	C(5B)-P(1B)-C(1B)	115.06(19)
C(17A)-C(18A)	1.395(6)	C(9B)-P(1B)-Au(1B)	113.26(12)
C(18A)-C(19A)	1.377(7)	C(5B)-P(1B)-Au(1B)	107.92(14)
C(19A)-C(20A)	1.381(6)	C(1B)-P(1B)-Au(1B)	106.82(12)
Au(1B)-P(1B)	2.2636(10)	C(3B)-C(1B)-C(4B)	110.6(4)
Au(1B)-C(1XB)	2.314(4)	C(3B)-C(1B)-C(2B)	107.1(4)
Au(1B)-C(2XB)	2.375(4)	C(4B)-C(1B)-C(2B)	107.7(4)
P(1B)-C(9B)	1.837(4)	C(3B)-C(1B)-P(1B)	117.0(3)
P(1B)-C(5B)	1.876(4)	C(4B)-C(1B)-P(1B)	105.3(3)
P(1B)-C(1B)	1.883(4)	C(2B)-C(1B)-P(1B)	108.9(3)
C(1B)-C(3B)	1.524(6)	C(2XB)-C(1XB)-C(6XB)	119.7(4)
C(1B)-C(4B)	1.535(6)	C(2XB)-C(1XB)-Au(1B)	74.7(2)
C(1B)-C(2B)	1.551(6)	C(6XB)-C(1XB)-Au(1B)	98.7(2)
C(1XB)-C(2XB)	1.422(6)	C(3XB)-C(2XB)-C(1XB)	120.8(4)
C(1XB)-C(6XB)	1.431(6)	C(3XB)-C(2XB)-Au(1B)	102.2(3)
C(2XB)-C(3XB)	1.410(6)	C(1XB)-C(2XB)-Au(1B)	70.0(2)
C(3XB)-C(4XB)	1.392(6)	C(4XB)-C(3XB)-C(2XB)	118.1(4)
C(3XB)-C(7XB)	1.520(6)	C(4XB)-C(3XB)-C(7XB)	122.0(4)
C(4XB)-C(5XB)	1.395(6)	C(2XB)-C(3XB)-C(7XB)	119.8(4)
C(5B)-C(7B)	1.538(7)	C(3XB)-C(4XB)-C(5XB)	121.9(4)
C(5B)-C(6B)	1.540(6)	C(7B)-C(5B)-C(6B)	108.3(4)
C(5B)-C(8B)	1.542(6)	C(7B)-C(5B)-C(8B)	108.7(4)
C(5XB)-C(6XB)	1.394(6)	C(6B)-C(5B)-C(8B)	109.5(4)
C(6XB)-C(8XB)	1.517(6)	C(7B)-C(5B)-P(1B)	106.0(3)
C(9B)-C(14B)	1.407(5)	C(6B)-C(5B)-P(1B)	113.8(3)

C(9B)-C(10B)	1.410(5)	C(8B)-C(5B)-P(1B)	110.3(3)
C(10B)-C(11B)	1.397(5)	C(6XB)-C(5XB)-C(4XB)	121.3(4)
C(10B)-C(15B)	1.511(6)	C(5XB)-C(6XB)-C(1XB)	118.2(4)
C(11B)-C(12B)	1.374(6)	C(5XB)-C(6XB)-C(8XB)	122.1(4)
C(12B)-C(13B)	1.380(6)	C(1XB)-C(6XB)-C(8XB)	119.7(4)
C(13B)-C(14B)	1.388(6)	C(14B)-C(9B)-C(10B)	118.1(3)
C(15B)-C(16B)	1.379(7)	C(14B)-C(9B)-P(1B)	118.5(3)
C(15B)-C(20B)	1.396(8)	C(10B)-C(9B)-P(1B)	123.4(3)
C(16B)-C(17B)	1.420(8)	C(11B)-C(10B)-C(9B)	119.2(3)
C(17B)-C(18B)	1.394(11)	C(11B)-C(10B)-C(15B)	114.8(4)
C(18B)-C(19B)	1.336(11)	C(9B)-C(10B)-C(15B)	126.0(3)
C(19B)-C(20B)	1.394(8)	C(12B)-C(11B)-C(10B)	121.6(4)
Sb(1A)-F(5A)	1.861(4)	C(11B)-C(12B)-C(13B)	119.9(4)
Sb(1A)-F(4A)	1.864(3)	C(12B)-C(13B)-C(14B)	119.8(4)
Sb(1A)-F(6A)	1.866(3)	C(13B)-C(14B)-C(9B)	121.4(4)
Sb(1A)-F(1A)	1.868(3)	C(16B)-C(15B)-C(20B)	119.0(5)
Sb(1A)-F(2A)	1.878(4)	C(16B)-C(15B)-C(10B)	119.8(5)
Sb(1A)-F(3A)	1.884(3)	C(20B)-C(15B)-C(10B)	120.5(4)
Sb(1B)-F(4B)	1.876(3)	C(15B)-C(16B)-C(17B)	120.2(7)
Sb(1B)-F(5B)	1.879(3)	C(18B)-C(17B)-C(16B)	118.8(6)
Sb(1B)-F(6B)	1.879(3)	C(19B)-C(18B)-C(17B)	120.8(6)
Sb(1B)-F(1B)	1.880(2)	C(18B)-C(19B)-C(20B)	121.0(7)
Sb(1B)-F(2B)	1.884(3)	C(19B)-C(20B)-C(15B)	120.1(6)
Sb(1B)-F(3B)	1.889(3)	F(5A)-Sb(1A)-F(4A)	90.7(2)
C(1S)-C(2S)	1.519(9)	F(5A)-Sb(1A)-F(6A)	90.9(2)
C(2S)-C(4S)#1	1.386(9)	F(4A)-Sb(1A)-F(6A)	91.34(15)
C(2S)-C(3S)	1.401(8)	F(5A)-Sb(1A)-F(1A)	91.4(2)
C(3S)-C(4S)	1.394(9)	F(4A)-Sb(1A)-F(1A)	177.8(2)
C(4S)-C(2S)#1	1.386(9)	F(6A)-Sb(1A)-F(1A)	88.92(15)
P(1A)-Au(1A)-C(2XA)	163.75(11)	F(5A)-Sb(1A)-F(2A)	177.7(2)
P(1A)-Au(1A)-C(1XA)	158.93(10)	F(4A)-Sb(1A)-F(2A)	90.3(2)
C(2XA)-Au(1A)-C(1XA)	35.72(14)	F(6A)-Sb(1A)-F(2A)	91.05(19)
C(9A)-P(1A)-C(5A)	106.02(19)	F(1A)-Sb(1A)-F(2A)	87.54(18)

*Chapter 1. Experimental section*

---

C(9A)-P(1A)-C(1A)	108.71(18)	F(5A)-Sb(1A)-F(3A)	90.15(18)
C(5A)-P(1A)-C(1A)	114.05(19)	F(4A)-Sb(1A)-F(3A)	88.78(14)
C(9A)-P(1A)-Au(1A)	112.89(14)	F(6A)-Sb(1A)-F(3A)	178.90(18)
C(5A)-P(1A)-Au(1A)	107.04(14)	F(1A)-Sb(1A)-F(3A)	90.92(14)
C(1A)-P(1A)-Au(1A)	108.23(13)	F(2A)-Sb(1A)-F(3A)	87.85(15)
C(3A)-C(1A)-C(4A)	109.3(4)	F(4B)-Sb(1B)-F(5B)	90.03(15)
C(3A)-C(1A)-C(2A)	108.9(4)	F(4B)-Sb(1B)-F(6B)	90.30(12)
C(4A)-C(1A)-C(2A)	108.0(3)	F(5B)-Sb(1B)-F(6B)	90.80(15)
C(3A)-C(1A)-P(1A)	106.8(3)	F(4B)-Sb(1B)-F(1B)	179.38(13)
C(4A)-C(1A)-P(1A)	115.4(3)	F(5B)-Sb(1B)-F(1B)	89.99(13)
C(2A)-C(1A)-P(1A)	108.3(3)	F(6B)-Sb(1B)-F(1B)	89.08(12)
C(6XA)-C(1XA)-C(2XA)	119.8(4)	F(4B)-Sb(1B)-F(2B)	89.71(13)
C(6XA)-C(1XA)-Au(1A)	103.9(3)	F(5B)-Sb(1B)-F(2B)	90.50(13)
C(2XA)-C(1XA)-Au(1A)	70.0(2)	F(6B)-Sb(1B)-F(2B)	178.70(14)
C(3XA)-C(2XA)-C(1XA)	121.0(4)	F(1B)-Sb(1B)-F(2B)	90.90(12)
C(3XA)-C(2XA)-Au(1A)	102.6(3)	F(4B)-Sb(1B)-F(3B)	90.32(14)
C(1XA)-C(2XA)-Au(1A)	74.3(2)	F(5B)-Sb(1B)-F(3B)	179.65(14)
C(4XA)-C(3XA)-C(2XA)	118.1(4)	F(6B)-Sb(1B)-F(3B)	89.15(14)
C(4XA)-C(3XA)-C(7XA)	120.5(4)	F(1B)-Sb(1B)-F(3B)	89.66(11)
C(2XA)-C(3XA)-C(7XA)	121.4(4)	F(2B)-Sb(1B)-F(3B)	89.55(13)
C(3XA)-C(4XA)-C(5XA)	121.2(4)	C(4S)#1-C(2S)-C(3S)	118.3(6)
C(7A)-C(5A)-C(6A)	108.0(4)	C(4S)#1-C(2S)-C(1S)	120.7(6)
C(7A)-C(5A)-C(8A)	107.9(4)	C(3S)-C(2S)-C(1S)	120.9(7)
C(6A)-C(5A)-C(8A)	109.7(4)	C(4S)-C(3S)-C(2S)	119.9(7)
C(7A)-C(5A)-P(1A)	107.0(3)	C(2S)#1-C(4S)-C(3S)	121.8(5)

---

Symmetry transformations used to generate equivalent atoms: #1 -x+1,-y+2,-z

**Table 3.** Torsion angles [°] for **28d**.

C(2XA)-Au(1A)-P(1A)-C(9A)	82.4(4)
C(1XA)-Au(1A)-P(1A)-C(9A)	-131.0(3)
C(2XA)-Au(1A)-P(1A)-C(5A)	-33.8(4)
C(1XA)-Au(1A)-P(1A)-C(5A)	112.7(3)
C(2XA)-Au(1A)-P(1A)-C(1A)	-157.2(4)
C(1XA)-Au(1A)-P(1A)-C(1A)	-10.6(3)
C(9A)-P(1A)-C(1A)-C(3A)	40.3(3)
C(5A)-P(1A)-C(1A)-C(3A)	158.3(3)
Au(1A)-P(1A)-C(1A)-C(3A)	-82.7(3)
C(9A)-P(1A)-C(1A)-C(4A)	-81.4(3)
C(5A)-P(1A)-C(1A)-C(4A)	36.6(4)
Au(1A)-P(1A)-C(1A)-C(4A)	155.6(3)
C(9A)-P(1A)-C(1A)-C(2A)	157.4(3)
C(5A)-P(1A)-C(1A)-C(2A)	-84.5(3)
Au(1A)-P(1A)-C(1A)-C(2A)	34.5(3)
P(1A)-Au(1A)-C(1XA)-C(6XA)	-47.7(5)
C(2XA)-Au(1A)-C(1XA)-C(6XA)	117.0(4)
P(1A)-Au(1A)-C(1XA)-C(2XA)	-164.7(2)
C(6XA)-C(1XA)-C(2XA)-C(3XA)	0.6(6)
Au(1A)-C(1XA)-C(2XA)-C(3XA)	95.5(4)
C(6XA)-C(1XA)-C(2XA)-Au(1A)	-94.9(3)
P(1A)-Au(1A)-C(2XA)-C(3XA)	41.1(5)
C(1XA)-Au(1A)-C(2XA)-C(3XA)	-119.1(4)
P(1A)-Au(1A)-C(2XA)-C(1XA)	160.2(3)
C(1XA)-C(2XA)-C(3XA)-C(4XA)	0.4(6)
Au(1A)-C(2XA)-C(3XA)-C(4XA)	79.5(4)
C(1XA)-C(2XA)-C(3XA)-C(7XA)	179.5(4)
Au(1A)-C(2XA)-C(3XA)-C(7XA)	-101.3(4)
C(2XA)-C(3XA)-C(4XA)-C(5XA)	-0.6(6)
C(7XA)-C(3XA)-C(4XA)-C(5XA)	-179.7(4)

C(9A)-P(1A)-C(5A)-C(7A)	-68.3(3)
C(1A)-P(1A)-C(5A)-C(7A)	172.1(3)
Au(1A)-P(1A)-C(5A)-C(7A)	52.5(3)
C(9A)-P(1A)-C(5A)-C(6A)	51.7(3)
C(1A)-P(1A)-C(5A)-C(6A)	-67.9(3)
Au(1A)-P(1A)-C(5A)-C(6A)	172.4(3)
C(9A)-P(1A)-C(5A)-C(8A)	175.3(3)
C(1A)-P(1A)-C(5A)-C(8A)	55.7(4)
Au(1A)-P(1A)-C(5A)-C(8A)	-64.0(3)
C(3XA)-C(4XA)-C(5XA)-C(6XA)	-0.2(7)
C(4XA)-C(5XA)-C(6XA)-C(1XA)	1.2(6)
C(4XA)-C(5XA)-C(6XA)-C(8XA)	178.3(4)
C(2XA)-C(1XA)-C(6XA)-C(5XA)	-1.4(6)
Au(1A)-C(1XA)-C(6XA)-C(5XA)	-76.0(4)
C(2XA)-C(1XA)-C(6XA)-C(8XA)	-178.5(4)
Au(1A)-C(1XA)-C(6XA)-C(8XA)	106.9(4)
C(5A)-P(1A)-C(9A)-C(10A)	-65.9(4)
C(1A)-P(1A)-C(9A)-C(10A)	57.1(4)
Au(1A)-P(1A)-C(9A)-C(10A)	177.2(3)
C(5A)-P(1A)-C(9A)-C(14A)	110.1(4)
C(1A)-P(1A)-C(9A)-C(14A)	-126.9(4)
Au(1A)-P(1A)-C(9A)-C(14A)	-6.8(4)
C(14A)-C(9A)-C(10A)-C(11A)	-2.0(7)
P(1A)-C(9A)-C(10A)-C(11A)	174.2(4)
C(9A)-C(10A)-C(11A)-C(12A)	-0.9(7)
C(10A)-C(11A)-C(12A)-C(13A)	2.8(7)
C(2XA)-C(3XA)-C(4XA)-C(5XA)	-0.6(6)
C(7XA)-C(3XA)-C(4XA)-C(5XA)	-179.7(4)
C(9A)-P(1A)-C(5A)-C(7A)	-68.3(3)
C(1A)-P(1A)-C(5A)-C(7A)	172.1(3)
Au(1A)-P(1A)-C(5A)-C(7A)	52.5(3)
C(9A)-P(1A)-C(5A)-C(6A)	51.7(3)
C(1A)-P(1A)-C(5A)-C(6A)	-67.9(3)

Au(1A)-P(1A)-C(5A)-C(6A)	172.4(3)
C(9A)-P(1A)-C(5A)-C(8A)	175.3(3)
C(1A)-P(1A)-C(5A)-C(8A)	55.7(4)
Au(1A)-P(1A)-C(5A)-C(8A)	-64.0(3)
C(3XA)-C(4XA)-C(5XA)-C(6XA)	-0.2(7)
C(4XA)-C(5XA)-C(6XA)-C(1XA)	1.2(6)
C(4XA)-C(5XA)-C(6XA)-C(8XA)	178.3(4)
C(2XA)-C(1XA)-C(6XA)-C(5XA)	-1.4(6)
Au(1A)-C(1XA)-C(6XA)-C(5XA)	-76.0(4)
C(2XA)-C(1XA)-C(6XA)-C(8XA)	-178.5(4)
Au(1A)-C(1XA)-C(6XA)-C(8XA)	106.9(4)
C(5A)-P(1A)-C(9A)-C(10A)	-65.9(4)
C(1A)-P(1A)-C(9A)-C(10A)	57.1(4)
Au(1A)-P(1A)-C(9A)-C(10A)	177.2(3)
C(5A)-P(1A)-C(9A)-C(14A)	110.1(4)
C(1A)-P(1A)-C(9A)-C(14A)	-126.9(4)
Au(1A)-P(1A)-C(9A)-C(14A)	-6.8(4)
C(14A)-C(9A)-C(10A)-C(11A)	-2.0(7)
P(1A)-C(9A)-C(10A)-C(11A)	174.2(4)
C(9A)-C(10A)-C(11A)-C(12A)	-0.9(7)
C(10A)-C(11A)-C(12A)-C(13A)	2.8(7)
Au(1B)-C(2XB)-C(3XB)-C(7XB)	-105.8(4)
C(2XB)-C(3XB)-C(4XB)-C(5XB)	-1.6(6)
C(7XB)-C(3XB)-C(4XB)-C(5XB)	178.5(4)
C(9B)-P(1B)-C(5B)-C(7B)	67.0(3)
C(1B)-P(1B)-C(5B)-C(7B)	-173.7(3)
Au(1B)-P(1B)-C(5B)-C(7B)	-54.5(3)
C(9B)-P(1B)-C(5B)-C(6B)	-51.9(4)
C(1B)-P(1B)-C(5B)-C(6B)	67.4(4)
Au(1B)-P(1B)-C(5B)-C(6B)	-173.5(3)
C(9B)-P(1B)-C(5B)-C(8B)	-175.5(3)
C(1B)-P(1B)-C(5B)-C(8B)	-56.2(4)
Au(1B)-P(1B)-C(5B)-C(8B)	63.0(3)

C(3XB)-C(4XB)-C(5XB)-C(6XB)	1.0(6)
C(4XB)-C(5XB)-C(6XB)-C(1XB)	0.7(6)
C(4XB)-C(5XB)-C(6XB)-C(8XB)	178.6(4)
C(2XB)-C(1XB)-C(6XB)-C(5XB)	-1.8(5)
Au(1B)-C(1XB)-C(6XB)-C(5XB)	-79.1(4)
C(2XB)-C(1XB)-C(6XB)-C(8XB)	-179.8(4)
Au(1B)-C(1XB)-C(6XB)-C(8XB)	102.9(4)
C(5B)-P(1B)-C(9B)-C(14B)	70.1(4)
C(1B)-P(1B)-C(9B)-C(14B)	-53.7(3)
Au(1B)-P(1B)-C(9B)-C(14B)	-171.9(3)
C(5B)-P(1B)-C(9B)-C(10B)	-108.4(3)
C(1B)-P(1B)-C(9B)-C(10B)	127.8(3)
Au(1B)-P(1B)-C(9B)-C(10B)	9.6(4)
C(14B)-C(9B)-C(10B)-C(11B)	-2.6(6)
P(1B)-C(9B)-C(10B)-C(11B)	175.9(3)
C(14B)-C(9B)-C(10B)-C(15B)	175.2(4)
P(1B)-C(9B)-C(10B)-C(15B)	-6.3(6)
C(9B)-C(10B)-C(11B)-C(12B)	3.1(6)
C(15B)-C(10B)-C(11B)-C(12B)	-174.9(4)
C(10B)-C(11B)-C(12B)-C(13B)	-1.2(7)
C(11B)-C(12B)-C(13B)-C(14B)	-1.3(7)
C(12B)-C(13B)-C(14B)-C(9B)	1.7(6)
C(10B)-C(9B)-C(14B)-C(13B)	0.2(6)
P(1B)-C(9B)-C(14B)-C(13B)	-178.3(3)
C(11B)-C(10B)-C(15B)-C(16B)	88.7(5)
C(9B)-C(10B)-C(15B)-C(16B)	-89.2(5)
C(11B)-C(10B)-C(15B)-C(20B)	-81.8(5)
C(9B)-C(10B)-C(15B)-C(20B)	100.3(5)
C(20B)-C(15B)-C(16B)-C(17B)	-0.5(7)
C(10B)-C(15B)-C(16B)-C(17B)	-171.1(4)
C(15B)-C(16B)-C(17B)-C(18B)	-0.9(7)
C(16B)-C(17B)-C(18B)-C(19B)	1.9(8)
C(17B)-C(18B)-C(19B)-C(20B)	-1.5(9)

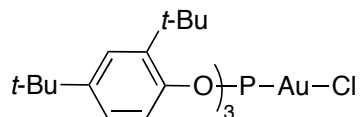
C(18B)-C(19B)-C(20B)-C(15B)	0.1(8)
C(16B)-C(15B)-C(20B)-C(19B)	0.9(7)
C(10B)-C(15B)-C(20B)-C(19B)	171.5(4)
C(4S)#1-C(2S)-C(3S)-C(4S)	-1.5(9)
C(1S)-C(2S)-C(3S)-C(4S)	-179.6(6)
C(2S)-C(3S)-C(4S)-C(2S)#1	1.5(9)

---

---

### 3. Gold Complexes with $\pi$ Acceptors Ligands

#### Tris(2,4-di-*tert*-butyl-phenyl) phosphite gold(I)chloride (29)



Sodium tetrachloroaurate dihydrate (1.38 mmol) was dissolved in water, and the orange solution was cooled in ice. To this solution 2,2'-thiodiethanol (3.77 mmol) was slowly added with stirring. A solution of the phosphite ligand (1.25 mmol) in pentane was added dropwise to give a white solid. The solid was filtered off, washed with pentane, and dried in vacuo. Yield: 94%.  $^1\text{H}$  NMR (400 MHz,  $\text{CDCl}_3$ )  $\delta$  7.43-7.40 (m, 6H), 7.13 (dd,  $J = 8.6, 2.5$  Hz, 3H), 1.44 (s, 27 H), 1.29 (s, 27H).  $^{31}\text{P}$  NMR (161.98 MHz,  $\text{CDCl}_3$ )  $\delta$  103.78.  $^{13}\text{C}$  NMR (100 MHz,  $\text{CDCl}_3$ )  $\delta$  148.30 (C), 147.42 ( $^2J(^{13}\text{C}-^{31}\text{P}) = 5.9$  Hz, C), 139.28 ( $^3J(^{13}\text{C}-^{31}\text{P}) = 6.9$  Hz, C), 125.54 (CH), 124.34 (CH), 119.35 ( $^3J(^{13}\text{C}-^{31}\text{P}) = 8.8$  Hz, CH), 35.27 (C), 34.84 (C), 31.56 ( $\text{CH}_3$ ), 30.72 ( $\text{CH}_3$ ); HRMS-ESI calcd for  $\text{C}_{42}\text{H}_{63}\text{AuClNaO}_3\text{P}$   $[\text{M}+\text{Na}]^+$ : 901.3767. Found: 901.3752.

UNIVERSITAT ROVIRA I VIRGILI

GOLD(I)-CATALYZED CYCLIZATIONS OF 1,6- AND 1,7-ENYNES: NEW GOLD COMPLEXES AND CYCLOPROPANATION REACTIONS

Elena Herrero Gómez

ISBN: 978-84-692-5924-5/DL:T-1663-2009

## *Chapter 2. Introduction*

UNIVERSITAT ROVIRA I VIRGILI

GOLD(I)-CATALYZED CYCLIZATIONS OF 1,6- AND 1,7-ENYNES: NEW GOLD COMPLEXES AND CYCLOPROPANATION REACTIONS

Elena Herrero Gómez

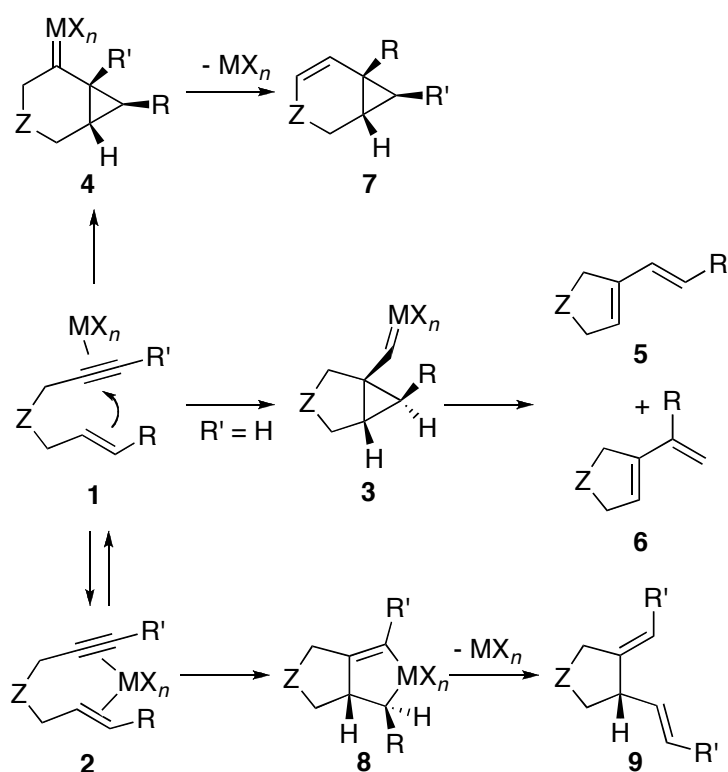
ISBN: 978-84-692-5924-5/DL:T-1663-2009

The search for more efficient processes that can be applied in the synthesis of complex molecules is the driving force of the research in organic chemistry methodology. In this direction, transition metal-catalyzed cyclization of enynes has attracted much attention since it provides an easy, straightforward access to carbo- and heterocyclic derivatives. This transformation can be achieved with a number of transition metals as catalysts,<sup>1,2,3,4,5,6,7,8</sup> and the variety of cyclic structures that can be

- 
- 1 (a) Trost, B. M.; Gelling, O. J. *Tetrahedron Lett.* **1993**, *34*, 8233-8236. (b) Trost, B. M.; Lautens, M.; Chan, C.; Jebratnam, D. J.; Mueller, T. *J. Am. Chem. Soc.* **1991**, *113*, 636-644. (c) Trost, B. M.; Hipskind, P. A.; Chung, J. Y. L.; Chan, C. *Angew. Chem., Int. Ed. Engl.* **1989**, *28*, 1502-1504. (d) Trost, B. M.; Lautens, M. *J. Am. Chem. Soc.* **1985**, *107*, 1781-1783.
  - 2 (a) Trost, B. M.; Doherty, G. A. *J. Am. Chem. Soc.* **2000**, *122*, 3801-3810. (b) Trost, B. M.; Yanai, M.; Hoogsteed, K. *J. Am. Chem. Soc.* **1993**, *115*, 5294-5295. (c) Trost, B. M.; Trost, M. K. *Tetrahedron Lett.* **1991**, *32*, 3647-3650. (d) Trost, B. M.; Tanoury, G. J. *J. Am. Chem. Soc.* **1988**, *110*, 1636-1638.
  - 3 (a) Nakai, H.; Chatani, N. *Chem. Lett.* **2007**, 1494-1495. (b) Miyanoana, Y.; Chatani, N. *Org. Lett.* **2006**, *8*, 2155-2158. (c) Miyanoana, Y.; Inoue, H.; Chatani, N. *J. Org. Chem.* **2004**, *69*, 8541-8543. (d) Chatani, N.; Inoue, H.; Kotsuma, T.; Murai, S. *J. Am. Chem. Soc.* **2002**, *124*, 10294-10295. (e) Chatani, N.; Inoue, H.; Morimoto, T.; Muto, T.; Murai, S. *J. Org. Chem.* **2001**, *66*, 4433-4436. (f) Chatani, N.; Kataoka, K.; Murai, S.; Furukawa, N.; Seki, Y. *J. Am. Chem. Soc.* **1998**, *120*, 9104-9105. (g) Chatani, N.; Furukawa, N.; Sakurai, H.; Murai, S. *Organometallics* **1996**, *15*, 901-903. (h) Chatani, N.; Morimoto, T.; Muto, T.; Murai, S. *J. Am. Chem. Soc.* **1994**, *116*, 6049-6050.

obtained starting from rather simple structures is remarkable. Two major pathways are reported in metal-catalyzed reactions of enynes, which proceed through coordination complexes **1** or **2** (Scheme 1).<sup>9,10,11,12,13,14,15</sup>

- 
- 4 (a) Fürstner, A.; Stelzer, F.; Szillat, H. *J. Am. Chem. Soc.* **2001**, *123*, 11863-11869. (b) Fürstner, A.; Szillat H.; Stelzer, F. *J. Am. Chem. Soc.* **2000**, *122*, 6785-6786. (c) Fürstner, A.; Szillat, H. F.; Gabor, B.; Mynott, R. *J. Am. Chem. Soc.* **1998**, *120*, 8305-8314
- 5 Oi, S.; Tsukamoto, I.; Miyano, S.; Inoue, Y. *Organometallics* **2001**, *20*, 3704-3709
- 6 Oh, C. H.; Bang, S. Y.; Rhim, C. Y. *Bull. Korean Chem. Soc.* **2003**, *24*, 887-888.
- 7 Bajracharya, G. B.; Nakamura, I.; Yamamoto, Y. *J. Org. Chem.* **2005**, *70*, 892-897.
- 8 Kim, S. M.; Lee, S. I.; Chung, Y. K. *Org. Lett.* **2006**, *8*, 5425-5427.
- 9 (a) Ma, S.; Yu, S.; Gu, Z. *Angew. Chem. Int. Ed.* **2006**, *45*, 200-203. (b) Bruneau, C. *Angew. Chem. Int. Ed.* **2005**, *44*, 2328-2334 (c) Hoffmann-Röder, A.; Krause, N. *Org. Biomol. Chem.* **2005**, *3*, 387-391. (d) Lloyd-Jones, G. C. *Org. Biomol. Chem.* **2003**, *1*, 215-236. (e) Diver, S. T.; Giessert, A. J. *Chem. Rev.* **2004**, *104*, 1317-1382. (f) Aubert, C.; Buisine, O.; Malacria, M. *Chem. Rev.* **2002**, *102*, 813-834.
- 10 (a) Hashmi, A. S. K. *Chem. Rev.* **2007**, *107*, 3180-3211. (b) Hashmi, A. S. K.; Hutchings, G. J. *Angew. Chem. Int. Ed.* **2006**, *45*, 7896-7936.
- 11 (a) Jiménez-Núñez, E.; Echavarren, A. M. *Chem. Rev.* **2008**, *108*, 3326-3350. (b) Jiménez-Núñez, E.; Echavarren, A. M. *Chem. Commun.* **2007**, 333-346. (c) Echavarren, A. M.; Nevado, C. *Chem. Soc. Rev.* **2004**, *33*, 431-436. (d) Echavarren, A. M.; Méndez, M.; Muñoz, M. P.; Nevado, C.; Martín-Matute, B.; Nieto-Oberhuber, C.; Cárdenas, D. J. *Pure Appl. Chem.* **2004**, *76*, 453-463.
- 12 Zhang, L.; Sun J.; Kozmin, S. A. *Adv. Synth. Catal.* **2006**, *348*, 2271-2296.
- 13 Fürstner, A.; Davies, P. W. *Angew. Chem. Int. Ed.* **2007**, *46*, 3410-3449.
- 14 Gorin, D. J.; Toste, F. D. *Nature* **2007**, *446*, 395-403.
- 15 Michelet, V.; Toullec, P. Y.; Genêt, J. P. *Angew. Chem. Int. Ed.* **2008**, *47*, 4268-4315.



Scheme 1

Complex **1** is formed upon selective coordination of the metal to the alkyne moiety. This activation of the alkyne moiety promotes a nucleophilic attack from the alkene, giving rise to cyclopropyl metal carbene intermediates of type **3** by an *exo-dig* cyclization or **4** by an *endo-dig* process.<sup>16</sup> In the absence of nucleophiles, intermediates **3** usually evolve by skeletal rearrangement to afford dienes **5** and/or **6**, whereas intermediates **4** lead to bicyclic compounds **7**.<sup>17,18,19</sup> The involvement of such cyclopropylcarbene intermediates was first sustained in reactions catalyzed by Pd(II), in which the initially formed cyclopropyl palladium carbenes undergo a [4+2] cycloaddition with the double bond of the conjugate enyne.<sup>20</sup>

- 16 Nieto-Oberhuber, C.; López, S.; Jiménez-Núñez, E.; Echavarren, A. M. *Chem. Eur. J.* **2006**, *12*, 5916-5923.
- 17 Blum, J.; Beer-Kraft, H.; Badrieh, Y. *J. Org. Chem.* **1995**, *60*, 5567-5569.
- 18 Borodkin, V. S.; Shpiro, N. A.; Azov, V. A.; Kochetkov, N. K. *Tetrahedron Lett.* **1996**, *37*, 1489-1492.
- 19 Nevado, C.; Ferrer, C.; Echavarren, A. M. *Org. Lett.* **2004**, *6*, 3191-3194.
- 20 (a) Trost, B. M.; Hashmi, A. S. K.; Ball, R. G. *Adv. Synth. Catal.* **2001**, *343*, 490-494. (b) Trost, B. M.; Hashmi, A. S. K. *J. Am. Chem. Soc.* **1994**, *116*, 2183-2184. (c) Trost, B. M.; Hashmi, A. S. K. *Angew. Chem. Int. Ed. Engl.* **1993**, *32*, 1085-1087.

Alternatively, an Alder-ene cycloisomerization process can take place by simultaneous coordination of the metal fragment to the alkyne and the alkene, giving rise to complex **2**. Oxidative cyclometallation yields **8**<sup>11</sup> that undergoes  $\beta$ -hydrogen elimination and reductive elimination to furnish diene **9**.<sup>9,10,11,13</sup> The Alder-ene cyclization was initially developed using Pd(II) salts or complexes as catalysts<sup>1,2,21,22</sup> but it can also be successfully performed using many other metal complexes. Thus, similar results were obtained using catalysts such as [CpRu(cod)Cl],<sup>23</sup> [CpRu(CH<sub>3</sub>CN)<sub>3</sub>]PF<sub>6</sub>,<sup>24,25</sup> Rh(I) complexes,<sup>26</sup> [CpCo(CO)<sub>2</sub>],<sup>27,28</sup> [Cp<sub>2</sub>Ti(CO)<sub>2</sub>]<sup>29</sup> or Pt(II) in non-nucleophilic solvents.<sup>30</sup> Certain Fe(0)-ate complexes are also good catalysts for a variety of Alder-ene, [4+2], [5+2], and [2+2+2] cycloaddition and cycloisomerization reactions of polyunsaturated substrates.<sup>31</sup> Enantioselective versions have been also achieved using Pd(OCOCF<sub>3</sub>)<sub>2</sub> in combination with chiral bidentate phosphines such as (*R*)-BINAP<sup>32</sup> as well as with Rh(I)/Me-DuPhos.<sup>33</sup>

- 
- 21 Trost, B. M.; Dumas, J.; Villa, M. *J. Am. Chem. Soc.* **1992**, *114*, 9836-9845.
- 22 Harada, K.; Tono, Y.; Kato, H.; Fukuyama, Y. *Tetrahedron Lett.* **2002**, *43*, 3829-3832.
- 23 Trost, B. M.; Indolese, A.; Müller, T. J. J.; Treptow, B. *Angew. Chem. Int. Ed.* **1995**, *34*, 615-623.
- 24 Trost, B. M.; Toste, F. D. *J. Am. Chem. Soc.* **2000**, *122*, 714-715.
- 25 See also: Le Paih, J.; Cuervo-Rodríguez, D.; Dérien, S.; Dixneuf, P. H. *Synlett* **2000**, 95-97.
- 26 Cao, P.; Wang, B.; Zhang, X. *J. Am. Chem. Soc.* **2000**, *122*, 6490-6491.
- 27 Llerena, D.; Aubert, C.; Malacria, M. *Tetrahedron Lett.* **1996**, *37*, 3517-3525.
- 28 Buisine, O.; Aubert, C.; Malacria, M. *Chem. Eur. J.* **2001**, *7*, 7353-7356.
- 29 Sturla, S. J.; Kablaoui, N. M.; Buchwald, S. L. *J. Am. Chem. Soc.* **1999**, *121*, 1976-1977.
- 30 (a) Nevado, C.; Charruault, L.; Michelet, V.; Nieto-Oberhuber, C.; Muñoz, M. P.; Méndez, M.; Rager, M. N.; Genêt, J.-P.; Echavarren, A. M. *Eur. J. Org. Chem.* **2003**, 706-713. (b) Muñoz, M. P.; Méndez, M.; Nevado, C.; Cárdenas, D. J.; Echavarren, A. M. *Synthesis* **2003**, 2898-2902. (c) Nevado, C.; Cárdenas, D. J.; Echavarren, A. M. *Chem. Eur. J.* **2003**, *9*, 2627-2635. (d) Méndez, M.; Muñoz, M. P.; Nevado, C.; Cárdenas, D. J.; Echavarren, A. M. *J. Am. Chem. Soc.* **2001**, *123*, 10511-10520. (e) Méndez, M.; Muñoz, M. P.; Echavarren, A. M. *J. Am. Chem. Soc.* **2000**, *122*, 11549-11550.
- 31 Fürstner, A.; Majima, K.; Martín, R.; Krause, H.; Katting, E.; Goddard, R.; Lehmann, C. W. *J. Am. Chem. Soc.* **2008**, *130*, 1992-2004.
- 32 Hatano, M.; Terada, M.; Mikami, K. *Angew. Chem. Int. Ed.* **2001**, *40*, 249-253.
- 33 Cao, P.; Zhang, X. *Angew. Chem. Int. Ed.* **2000**, *39*, 4104-4106.

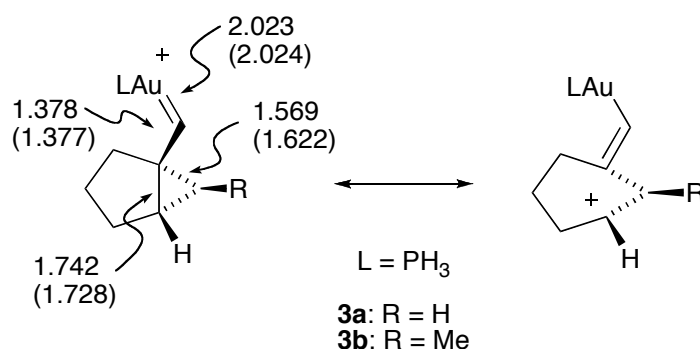
## 1. Gold(I)-Catalyzed Cycloisomerization of Enynes

Although some transition metal-based catalysts can react *via* both routes depicted in Scheme 1, depending on the ligands and coordinating solvents, the Alder-ene cycloisomerization does not occur for gold(I).<sup>34,35</sup> This selectivity is caused by two main reasons: first, the fragment  $[\text{Au}(\text{L})]^+$ , having only one vacant site, cannot coordinate simultaneously to the alkene and the alkyne, and second, oxidative addition processes are not facile for gold catalysts.<sup>14</sup> Therefore, cyclizations involving this noble metal proceed exclusively through complexes of type **3** or **4** (Scheme 1).

Consequently, gold(I) complexes act as an electrophilic  $\pi$  acid, in a similar way as  $\text{H}^{+36}$  or  $\text{Hg}^{2+}$ .<sup>37</sup> The comparison is obviously very simplistic,<sup>38</sup> since electrophilic metals are by far better catalysts for this transformation.<sup>39</sup> A higher affinity for the substrate is found in this large, polarizable (“soft” by Pearson’s definition)<sup>40</sup> metal moiety together with the advantage of a kinetically labile carbon-metal bond.<sup>13</sup> On the other hand, toxicity issues related with the use of  $\text{Hg}(\text{II})$  salts are overcome. Gold(I) complexes usually surpass the reactivity shown by  $\text{Pt}(\text{II})$  and other electrophilic metal salts and complexes for the activation of enynes, a result that has been attributed to relativistic effects.<sup>14</sup>

- 
- 34 Nieto-Oberhuber, C.; Muñoz, M. P.; Buñuel, E.; Nevado, C.; Cárdenas, D. J.; Echavarren, A. M. *Angew. Chem. Int. Ed.* **2004**, *43*, 2402-2406.
- 35 Nieto-Oberhuber, C.; Muñoz, M. P.; López, S.; Jiménez-Núñez, E.; Nevado, C.; Herrero-Gómez, E.; Raducan, M.; Echavarren, A. M. *Chem. Eur. J.* **2006**, *12*, 1677-1693.
- 36 Recent advances in the field of Brønsted acid catalysis: Rosenfeld, D. C.; Shekhar, S.; Takemiya, A.; Utsunomiya, M.; Hartwig, J. F. *Org. Lett.* **2006**, *8*, 4179-4182.
- 37 Larock, R. C. *Solvomercuration/Demercuration Reactions in Organic Synthesis*, Springer, Berlin, 1986.
- 38 Hoffmann, R. *Angew. Chem., Int. Ed. Engl.* **1982**, *21*, 711-724.
- 39 Overview of the older literature on the activation of  $\pi$  systems with a range of traditional electrophiles: Freeman, F. *Chem. Rev.* **1975**, *75*, 439-490.
- 40 (a) Pearson, R. G. *J. Chem. Educ.* **1987**, *64*, 561-567. (b) Pearson, R. G. *J. Am. Chem. Soc.* **1963**, *85*, 3533-3539.

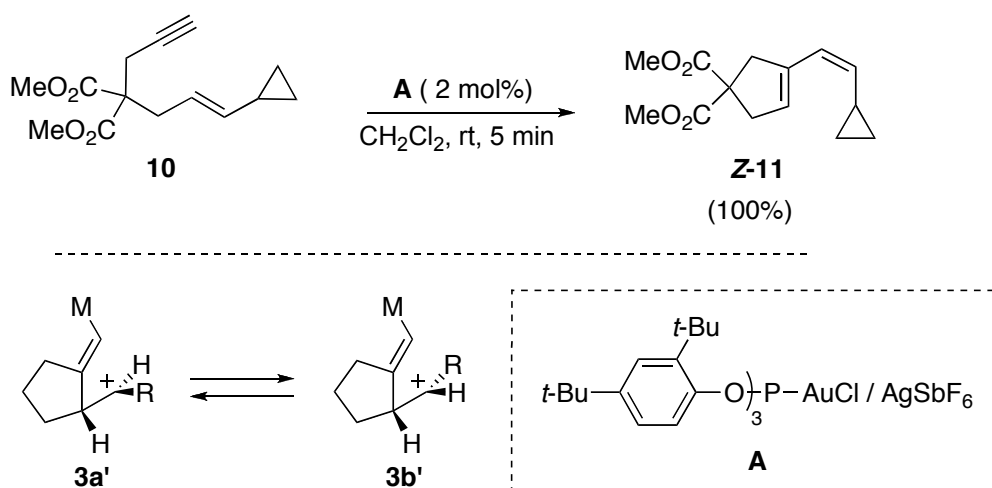
Another important feature of gold catalysts is their ability to stabilize carbene intermediates,<sup>41</sup> since backbonding to the carbene ligand has been shown to be significant.<sup>13,14</sup> For this reason, intermediates **3** and **4** (Scheme 1) are conveniently drawn as cyclopropyl gold carbenes, although it is important to bear in mind that they are highly distorted structures. DFT calculations<sup>42</sup> of cyclopropyl gold carbene **3** show a rather short C-C bond between the carbene and the cyclopropane, which is consistent with a substantial double bond character (Scheme 2).<sup>43,44</sup>



**Scheme 2**

Therefore, structures of **3a-b** can be envisioned as delocalized cyclopropylmethyl/cyclobutyl/homoallyl carbocations stabilized by gold (Scheme 3).<sup>43,45</sup> The recent finding that *trans*-1,6-enynes bearing electron-donating groups at the alkene, such as **10**, give rise to *cis*-dienes **11** in a non-stereospecific reaction further supports this multifaceted character (Scheme 3).<sup>46</sup>

- 41 (a) Heinemann, C.; Hertwig, R. H.; Wesendrup, R.; Knoch, W.; Schwarz, H. *J. Am. Chem. Soc.* **1995**, *117*, 495-500. (b) Irikura, K. K.; Goddard, W. A. *J. Am. Chem. Soc.* **1994**, *116*, 8733-8740.
- 42 Calculated bond distances (Å) for **3a-b** (values in parentheses are for **3b**). DFT calculations at the B3LYP/6-31G(d) (C,H,P), LANL2DZ (Au) level.
- 43 Cabello, N.; Jiménez-Núñez, E.; Buñuel, E.; Cárdenas, D. J.; Echavarren, A. M. *Eur. J. Org. Chem.* **2007**, 4217-4223.
- 44 Nieto-Oberhuber, C.; López, S.; Muñoz, M. P.; Cárdenas, D. J.; Buñuel, E.; Nevado, C.; Echavarren, A. M. *Angew. Chem. Int. Ed.* **2005**, *44*, 6146-6148.
- 45 Casanova, J.; Kent, D. R.; Goddard, W. A.; Roberts, J. D. *Proc. Nat. Acad. Sci.* **2003**, *100*, 15-19.
- 46 Jiménez-Núñez, E.; Claverie, C. K.; Bour, C.; Cárdenas, D. J.; Echavarren, A. M. *Angew. Chem. Int. Ed.* **2008**, *47*, 7892-7895.



Scheme 3

However, none of the carbene intermediates involved in the reaction of enynes has been spectroscopically characterized.<sup>47</sup> Experimental evidence of their existence has been achieved by trapping of the carbene intermediates with alkenes giving rise to cyclopropanation reactions (*see Section 2*) as well as by formation of the corresponding aldehydes when the gold(I)-catalyzed cyclization is carried out in the presence of a mild oxidant such as  $\text{Ph}_2\text{SO}$ .<sup>48</sup> Interestingly, a gold carbene has been generated recently in the gas phase showing the reactivity expected for a metal carbene.<sup>49</sup>

### 1.1. Gold(I)-Catalyzed Cycloisomerization of 1,6-Enynes

1,6-Enynes have been historically the most important substrates in the development of metal-catalyzed cycloisomerization reactions, and in the investigation of the mechanistic aspects of this chemistry.<sup>9d,11a,12,16,50</sup> In the absence of external

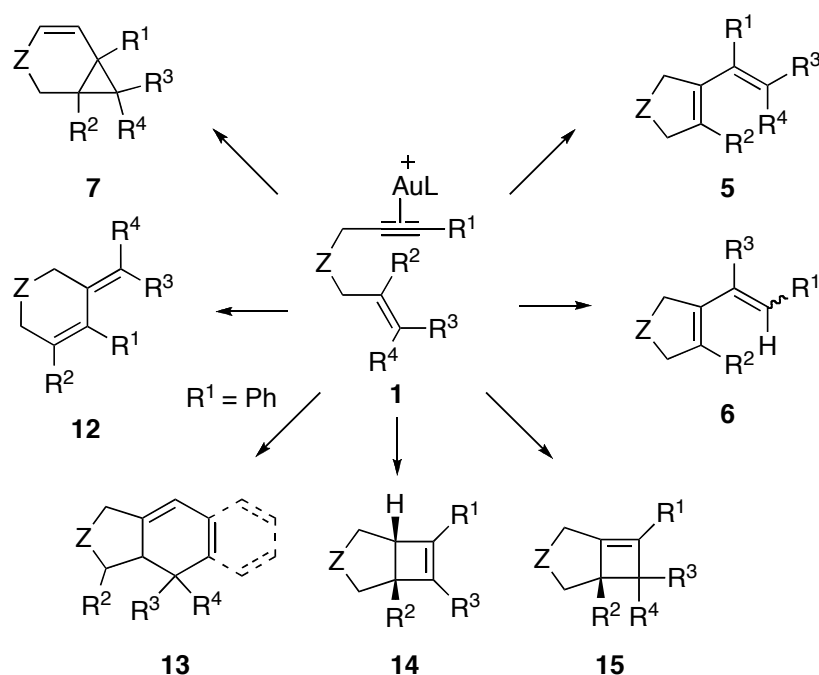
47 Anti cyclopropyl iron and ruthenium carbenes have been characterized spectroscopically at low temperatures: Brookhart, M.; Studabaker, W. B.; Husk, G. R. *Organometallics* **1987**, *6*, 1141-1145.

48 Witham, C. A.; Mauleón, P.; Shapiro, N. D.; Sherry, B. D.; Toste, F. D. *J. Am. Chem. Soc.* **2007**, *129*, 5838-5839.

49 (a) Fedorov, A.; Chen, P. *Organometallics* **2009**, *28*, 1278-1281. (b) Fedorov, A.; Moret, M.-E.; Chen, P. *J. Am. Chem. Soc.* **2008**, *130*, 8880-8881.

50 Reviews: (a) Bruneau, C. *Angew. Chem. Int. Ed.* **2005**, *44*, 2328-2334. (b) Añorbe, L.; Domínguez, G.; Pérez-Castells, J. *Chem. Eur. J.* **2004**, *10*, 4938-4943. (c) Echavarren, A. M.;

nucleophiles, a variety of products can be obtained in the gold(I)-catalyzed cycloisomerization (Scheme 4). Nevertheless, this structural diversity can also be viewed as a drawback since it can lead to a high degree of unpredictability. Consequently, a deep understanding of the reaction mechanism is needed in order to develop a reliable methodology.



Scheme 4

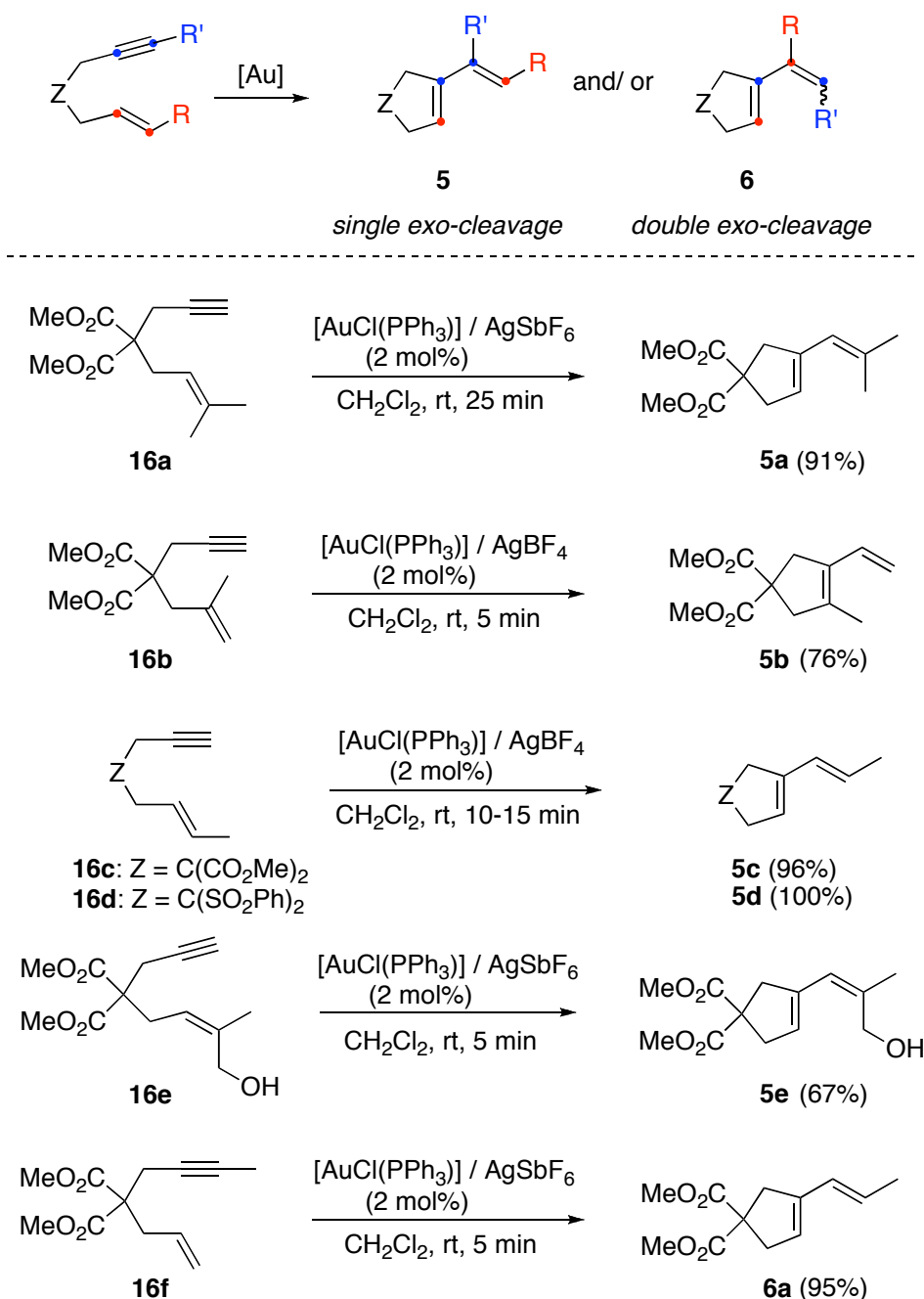
As explained in the previous section, the reaction starts with an initial coordination of the metal to the alkyne. Then, the alkene attacks in an *anti* fashion forming either *exo*- or *endo*-cyclopropyl gold carbenes **3** or **4** by *5-exo-dig* or *6-endo-dig* pathways, respectively (Scheme 5). Dienes **5**, **6** and **12** are formed by skeletal rearrangement of cyclopropyl carbene **3**. The mechanistic details behind the formation of these rather simple products will be explained in more detail in the following sections. If the alkyne is substituted with an aromatic ring, then tricyclic structures **13** are formed by a formal [4+2] cycloaddition.<sup>51</sup> Formation of cyclobutenes **14** or **15** has

Nevado, C. *Chem. Soc. Rev.* **2004**, *33*, 431-436. (d) Echavarren, A. M.; Méndez, M.; Muñoz, M. P.; Nevado, C.; Martín-Matute, B.; Nieto-Oberhuber, C.; Cárdenas, D. J. *Pure Appl. Chem.* **2004**, *76*, 453-463. (e) Aubert, C.; Buisine, O.; Malacria, M. *Chem. Rev.* **2002**, *102*, 813-834. (f) Diver, S. T.; Giessert, A. *J. Chem. Res.* **2004**, *104*, 1317-1382.

51 Nieto-Oberhuber, C.; López S.; Echavarren, A. M. *J. Am. Chem. Soc.* **2005**, *127*, 6178-6179.



cleavage rearrangements, in which only the alkene is cleaved. In certain cases, the skeletal rearrangement implies the cleavage of both the alkyne and the alkene, furnishing dienes **6**.<sup>44</sup> This is the case of enyne **16f**, with a methyl substituent in the alkyne, that reacts to yield exclusively diene **6a**. Despite the simplicity of the products, finding a mechanism to explain such a complex rearrangement has been a challenge.



Scheme 6

Formation of products of single cleavage in metal-catalyzed reaction of enynes had been proposed to take place by conrotatory ring opening of intermediate cyclobutenes. However, experimental and theoretical calculations did not support that proposal.<sup>44</sup> Thus, a detailed study of the rearrangement of enyne **16a** to give diene **5a** allowed the determination of the activation parameters. This reaction proceeds with low enthalpies of activation ( $\Delta H^\ddagger = 6.2$  and  $3.7$  kcal mol<sup>-1</sup> for [Au((2-di-*tert*-butylphosphino)biphenyl)(NCMe)] **B** and [Au((di-cyclohexylphosphino)biphenyl)(NCMe)] **C**, respectively) and negative entropies of activation ( $\Delta S^\ddagger = -50.3$  and  $-60.6$  cal mol<sup>-1</sup> K<sup>-1</sup> for **B** and **C**, respectively). These results establish a very low activation energy for the hypothetical conrotatory opening of a cyclobutene, which should be a fast process at temperatures as low as  $-63$  °C. This is not consistent with theoretical data for the ring opening of cyclobutenes related to bicyclo[3.2.0]hept-5-ene.

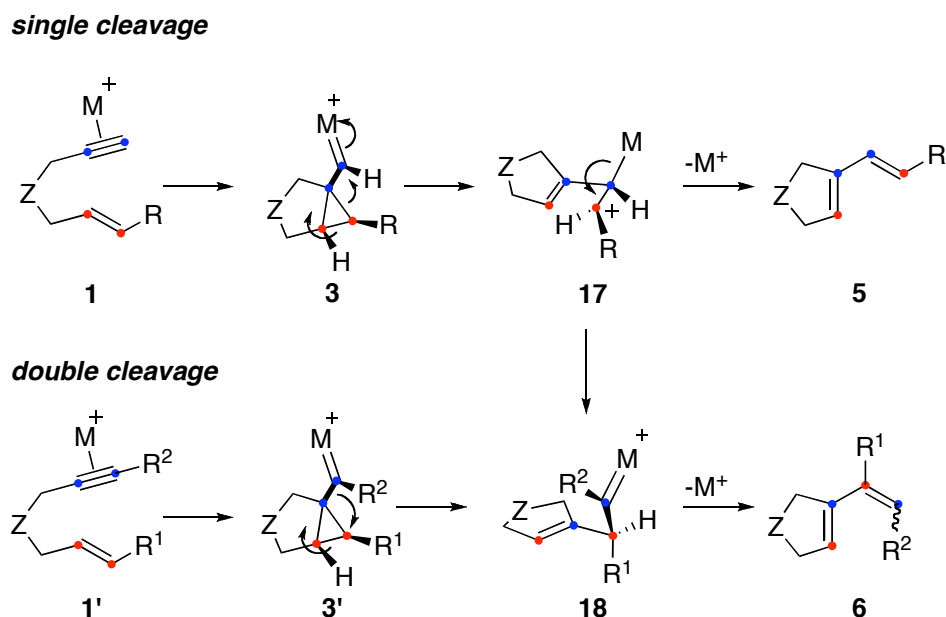
Overall, the mechanism for the skeletal rearrangement is consistent with the evolution of the initial *anti*-cyclopropyl gold carbenes **3**, formed in the *5-exo-dig* cyclization, to give carbocation **17**, which then undergoes metal-elimination to give dienes **5** (single cleavage) (Scheme 7). For the double cleavage rearrangement, intermediates **3'** can suffer a diatropic rearrangement<sup>57,58</sup> to give new carbenes **18**, which lose a  $\alpha$ -hydrogen and then undergo protodemetalation to form dienes **6** (double cleavage). Intermediates **18** can also be formed by a carbocationic 1,2-shift of the cyclic alkenyl group in **17**.<sup>44</sup> The double *exo*-cleavage skeletal rearrangement often leads to dienes **6** with predominant *Z* configuration (Scheme 7).<sup>59</sup>

---

57 (a) Reetz, M. T. *Angew. Chem., Int. Ed. Engl.* **1972**, *11*, 129-130. (b) Reetz, M. T. *Angew. Chem. Int. Ed. Engl.* **1972**, *11*, 130-131.

58 Nouri, D. H.; Tantillo, D. J. *J. Org. Chem.* **2006**, *71*, 3686-3695.

59 Ota, K.; Chatani, N. *Chem. Commun.* **2008**, 2906-2907.



Scheme 7

Gold(I) catalysts allow performing the skeletal rearrangement under the mildest conditions (Scheme 6).<sup>11b,34,35</sup> Formation of **5a** from **16a** can be carried out even at  $-40$  to  $-60^{\circ}\text{C}$  using catalyst **B** or **C**.<sup>44</sup> Similar transformations have been carried out with other gold(I) catalysts.<sup>60,61,62</sup>

### 1.1.2. Endocyclic Rearrangement of 1,6-Enynes

*Endo*-cyclizations to give products of type **12** were first observed using gold(I) as catalyst (Scheme 8).<sup>34,35,43</sup> Only a few additional examples of this type of rearrangement have been reported from simple 1,6-enynes using  $\text{FeCl}_3$ ,<sup>35</sup>  $\text{InCl}_3$ ,<sup>3b</sup> or  $\text{Ru(II)}$ <sup>63</sup> as catalyst. Endocyclic rearrangements have also been observed in the reaction of *cis*-4,6-dien-1-yl-3-ol derivatives with gold or platinum catalysts.<sup>64</sup>

60 Mézailles, N.; Ricard, L.; Gagosz, F. *Org. Lett.* **2005**, *7*, 4133-4136.

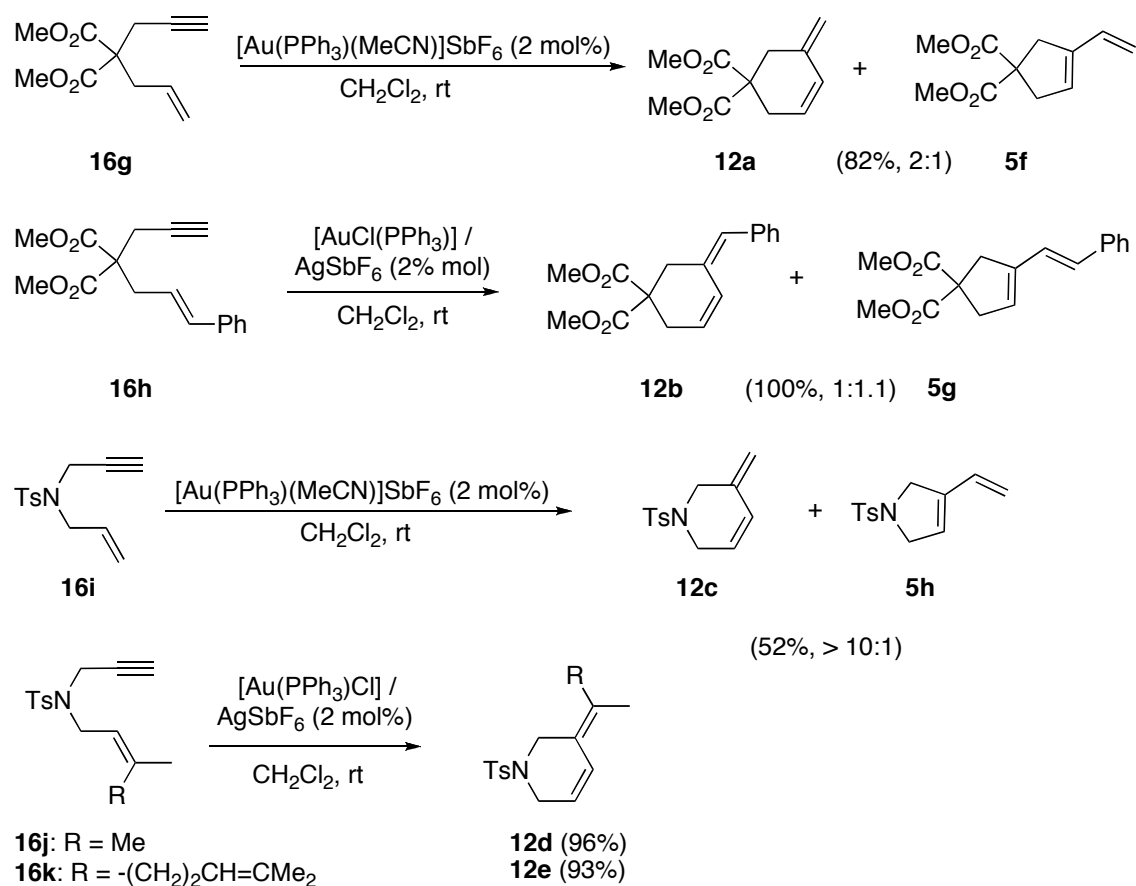
61 Ricard, L.; Gagosz, F. *Organometallics* **2007**, *26*, 4704-4707.

62 Freytag, M.; Ito, S.; Yoshifuji, M. *Chem. Asian J.* **2006**, *1*, 693-700.

63 Faller, J. W.; Fontaine, P. P. *J. Organomet. Chem.* **2006**, *691*, 1912-1918.

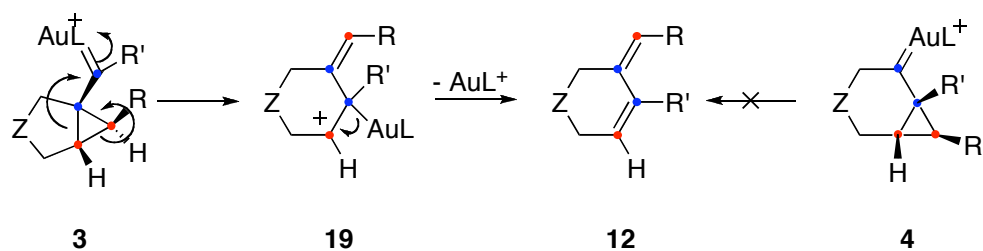
64 (a) Tang, J.-M.; Bhunia, S.; Sohel, S. M. A.; Lin, M.-Y.; Liao, H. Y.; Datta, S.; Das, A. Liu, R.-S. *J. Am. Chem. Soc.* **2007**, *129*, 15677-15683. (b) Lin, M.-Y.; Das, A.; Liu, R.-S. *J. Am. Chem. Soc.* **2006**, *128*, 9340-9341.

As shown in the reactions of **16h** and **16k**, this endocyclic rearrangement is stereospecific. Labeling experiments are consistent with an intramolecular process in which the terminal carbon of the alkene is attached to C-2 of the alkyne.<sup>43</sup>



Scheme 8

The formation of the six-membered ring led to the initial conclusion that products **12** were formed by the rearrangement of carbene **4**. However, DFT calculations for the gold(I)-catalyzed process support a mechanism in which cyclopropyl gold(I) carbene **3** rearranges with ring opening to give cation **19** in a moderately endothermic process with an activation energy of only 9.6 kcal mol<sup>-1</sup> (Scheme 9). Metal loss from **19** gives products **12**. Consequently, the mechanism of this endocyclic rearrangement is just a variation of the single cleavage rearrangement of **3** to give **5** via intermediate **17** (see Scheme 7).

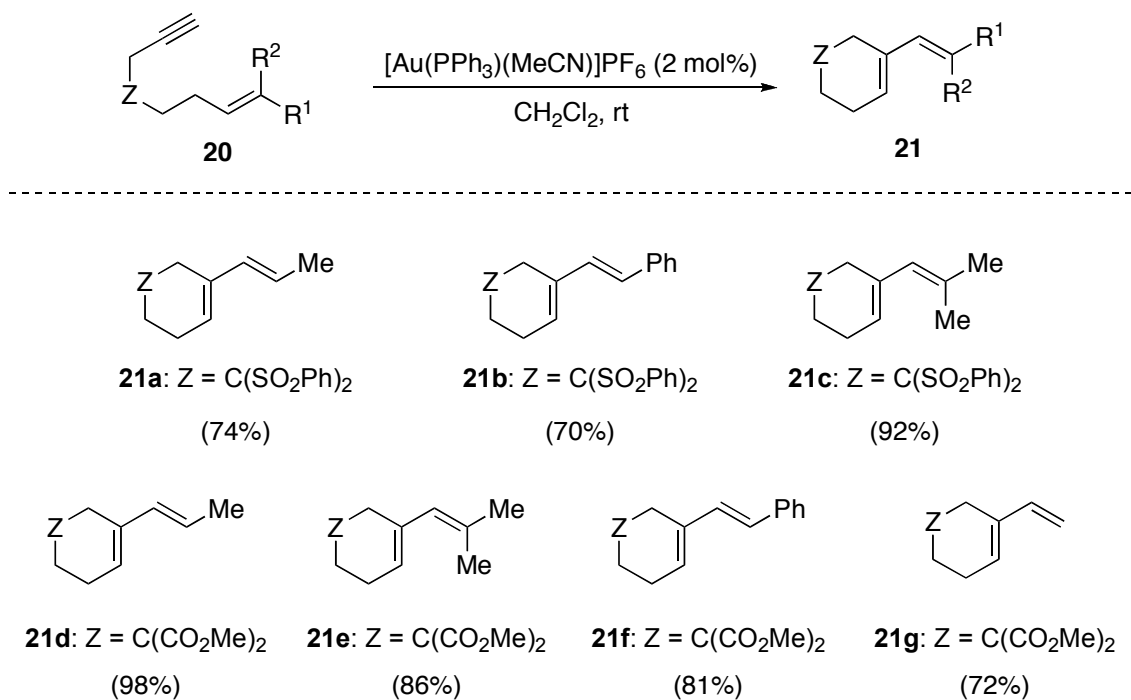


Scheme 9

## 1.2. Gold(I)-Catalyzed Cycloisomerization of 1,7-Enynes

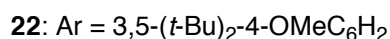
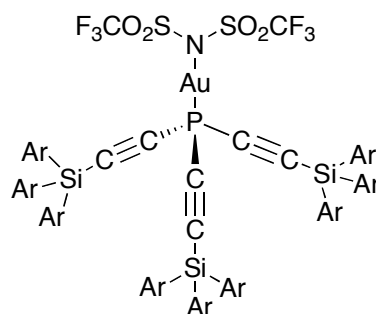
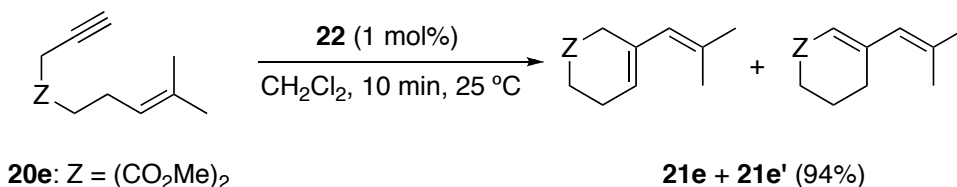
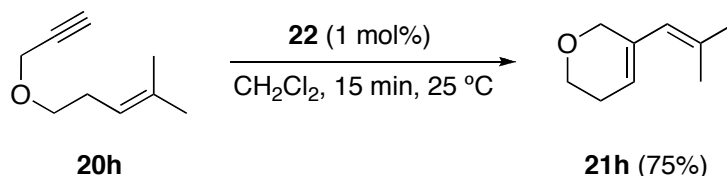
Although relatively less studied, 1,7-enynes also react with gold catalysts in skeletal rearrangements as well as in hydroxy and alkoxy cyclizations. Only a few examples of skeletal rearrangement of 1,7-enynes have been reported by using other metal catalysts such as  $[\text{RuCl}(\text{CO})_2]_2$ ,<sup>3h</sup>  $\text{PtCl}_2$ ,<sup>3c,g</sup>  $[\text{IrCl}(\text{CO})_3]_n$ ,<sup>3e</sup>  $\text{GaCl}_3$ ,<sup>3d,65,66</sup> and  $\text{InCl}_3$ .<sup>3b</sup> Gold(I) complexes are again the best catalyst to effect this skeletal rearrangement.<sup>67,68</sup> Thus, a variety of enynes of general structure **20**, differently substituted at the alkene, react at room temperature with cationic catalyst  $[\text{Au}(\text{PPh}_3)(\text{MeCN})]\text{PF}_6$  to provide dienes **21** in good yields at room temperature (Scheme 10).<sup>68</sup> In high contrast with the structural diversity provided by 1,6-enynes, for the 1,7-counterparts only single cleavage dienes were obtained in all cases studied.

- 
- 65 Simmons, E. M.; Sarpong, R. *Org. Lett.* **2006**, *8*, 2883-2886.  
66 Simmons, E. M.; Yen, J. R.; Sarpong, R. *Org. Lett.* **2007**, *9*, 2705-2708.  
67 Ochida, A.; Ito, H.; Sawamura, M. *J. Am. Chem. Soc.* **2006**, *128*, 16486-16487.  
68 Cabello, N.; Rodríguez, C.; Echavarren, A. M. *Synlett* **2007**, 1753-1758.



**Scheme 10**

The gold-catalyzed cyclization of related enynes was successfully accomplished using triethynylphosphine gold complex **22** (Scheme 11).<sup>67</sup> The use of this sterically hindered catalyst **22** is believed to enhance the formation of larger rings, since the cavity in the ligand places the nucleophilic center closer to the activated alkyne, thus favoring the ring closing process.



Scheme 11

### 1.3. Gold(I)-Catalyzed Cycloisomerization of 1,*n*-Enynes

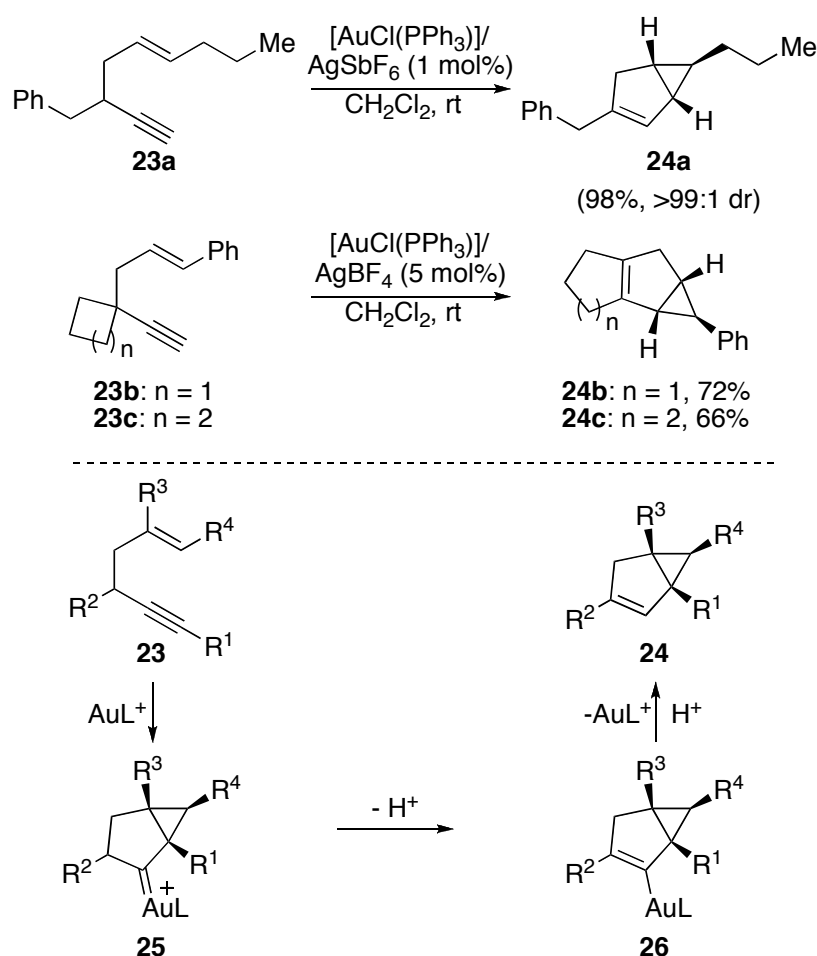
Although the study of 1,5-, 1,8- and 1,9-enynes is beyond the scope of this Doctoral Thesis, for the sake of completeness, the most important cycloisomerization reactions of these substrates will also be reviewed.

#### 1.3.1. Gold(I)-Catalyzed Cycloisomerization of 1,5-Enynes

The first examples of cyclization of 1,5-enynes with gold were actually reported in the context of a new synthesis of pyridines by cyclization of propargyl enamines catalyzed by NaAuCl<sub>4</sub>·2H<sub>2</sub>O.<sup>69</sup> However, the significant breakthrough in this area was made simultaneously by three groups which independently reported in 2004 that the

69 Abbiati, G.; Arcadi, A.; Bianchi, G.; Di Giuseppe, S.; Marinelli, F.; Rossi, E. *J. Org. Chem.* **2003**, *68*, 6959-6966.

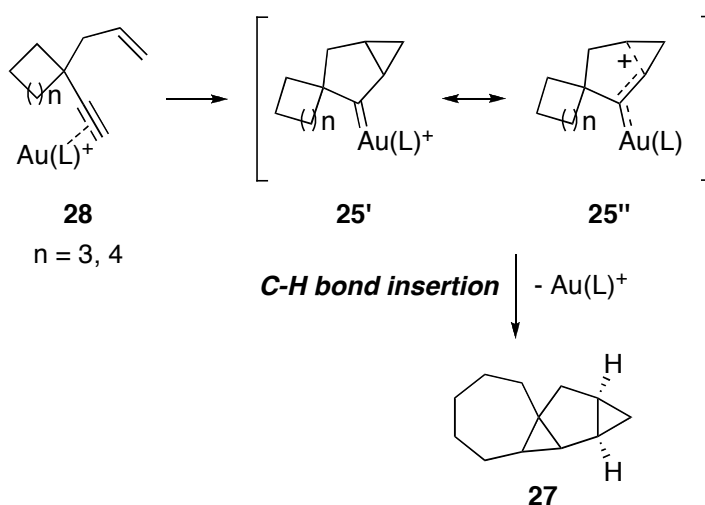
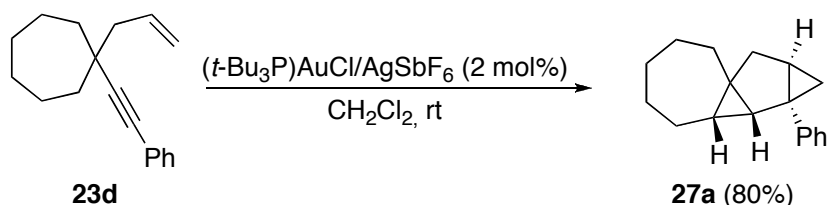
gold- or platinum-catalyzed cyclization of 1,5-enynes gave bicyclo[3.1.0]hexanes.<sup>70,71,72</sup> Thus, for example, simple enynes **23** afford derivatives **24** under mild conditions (Scheme 12).<sup>71</sup> Substrates **23b-c** react with concomitant ring expansion to form tricyclic derivatives **24b-c**. This reaction of 1,5-enynes presumably proceeds by formation of cyclopropyl gold carbene **25**, which evolves by proton loss to form alkenyl-gold complex **26**, followed by protonolysis to form bicyclo[3.1.0]hexanes **24**. In the case of **23b-c**, intermediates of type **25** undergo ring expansion.



Scheme 12

- 70 Mamane, V.; Gress, T.; Krause, H.; Fürstner, A. *J. Am. Chem. Soc.* **2004**, *126*, 8654-8655.  
71 Luzung, M. R.; Markham, J. P.; Toste, F. D. *J. Am. Chem. Soc.* **2004**, *126*, 10858-10859.  
72 Harrak, Y.; Blaszykowski, C.; Bernard, M.; Cariou, K.; Mainetti, E.; Mouriès, V.; Dhimane, A.-L.; Fensterbank, L.; Malacria, M. *J. Am. Chem. Soc.* **2004**, *126*, 8656-8657.

Interestingly, when a more flexible ring is present in substrates of type **23** ( $n = 3, 4$ ) the gold(I)-catalyzed cycloisomerization is followed by C-H bond insertion, allowing the formation of tetracyclododecane derivatives **27** (Scheme 13).<sup>73</sup>

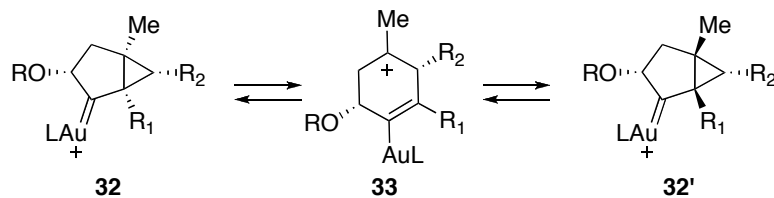
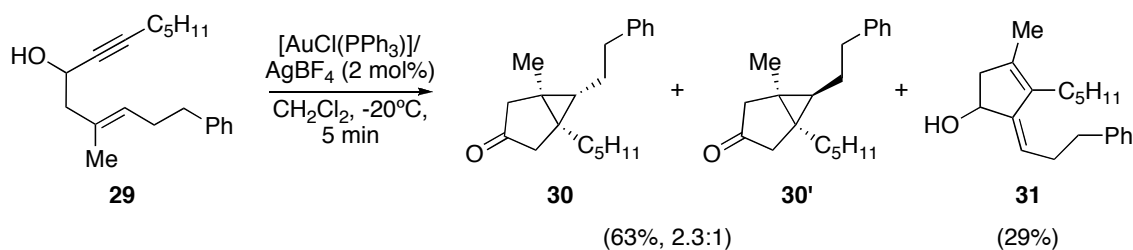


**Scheme 13**

Similarly, enynes **29** gave bicyclo[3.1.0]hexanes **30** (Scheme 14).<sup>60,74</sup> In this case, products of skeletal rearrangement such as **30** were also obtained. Although the presence of an additional stereogenic center in **29** leads to mixtures of diastereomers, formation of **30'** as a minor product in the cycloisomerization of substrates **29** is noteworthy since this product correspond to that expected from the Z isomer of **29**. This lack of stereospecificity was explained by the equilibrium between two rapidly interconverting six-membered ring cations.<sup>74</sup>

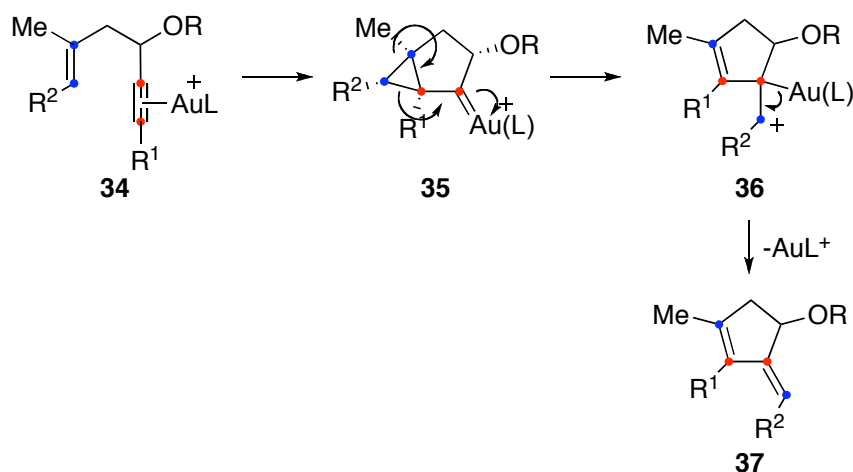
73 Horino, Y.; Yamamoto, T.; Ueda, K.; Kuroda, S.; Toste, F. D. *J. Am. Chem. Soc.* **2009**, *131*, 2809-2811.

74 Gagosz, F. *Org. Lett.* **2005**, *7*, 4129-4132.



Scheme 14

Products of type **37** had been obtained from 1,5-enynes, which can be rationalized by a skeletal rearrangement (Scheme 15). Thus, upon complexation of gold(I) to the alkyne in **34**, an *endo*-cyclization could occur to form cyclopropyl gold carbene **35**, which might suffer a skeletal rearrangement *via* **36** to give **37**. This is an example of a single cleavage rearrangement occurring in 1,5-enynes.

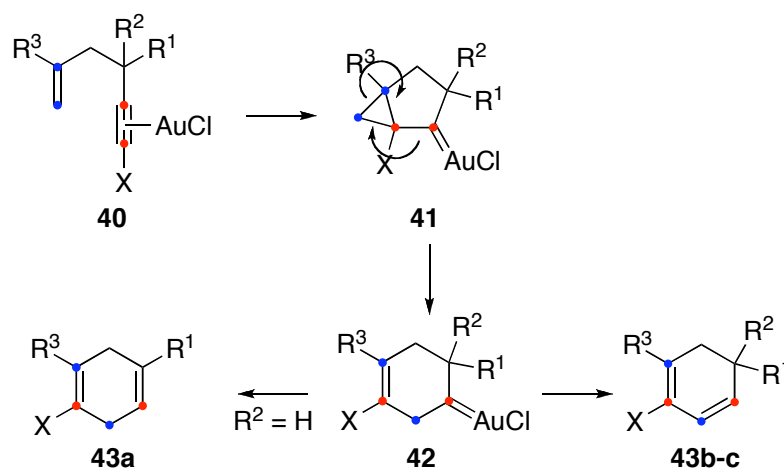
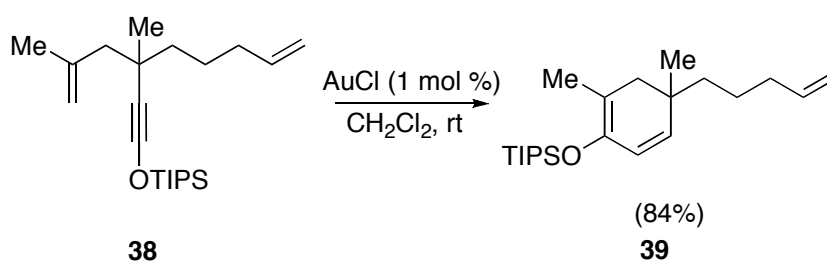


Scheme 15

Siloxy 1,5-enynes like **38** react with  $\text{AuCl}$  as catalyst to give cyclohexadienes **39** (Scheme 16).<sup>75</sup> The analogous reaction of 1,5-enynes in which the OTIPS group has been replaced by an alkyl or aryl group is better performed with less electrophilic

75 (a) Zhang, L.; Kozmin, S. A. *J. Am. Chem. Soc.* **2004**, *126*, 11806-11807. (b) Sun, J.; Conley, M. P.; Zhang, L.; Kozmin, S. A. *J. Am. Chem. Soc.* **2006**, *128*, 9705-9710.

PtCl<sub>2</sub>.<sup>75b</sup> This mechanistically intriguing transformation probably involves a double cleavage rearrangement of 1,5-enynes (Scheme 16). Thus, complex **40** (X = OTIPS) forms gold carbene **41**, which then undergoes ring expansion in a diotropic rearrangement to give **42** by a process reminiscent of that found for **3'** in the double cleavage rearrangement of 1,6-enynes (Scheme 7). Proton loss and demetalation then affords either 1,4-cyclohexadienes **43a** or **43b-c**. Similar transformations have been found with other 1,5-enynes.<sup>74</sup>



**Scheme 16**

### 1.3.2. Gold(I)-Catalyzed Cycloisomerization of 1,8- and 1,9-Enynes

The cyclization of substrates such as **44a-b** gives tricyclic derivatives **45a-b** with high stereoselectivity by an endocyclic pathway (Scheme 17).<sup>76</sup> In the cyclization of this type of substrates, better yields were usually obtained with PtCl<sub>2</sub> or AuCl<sub>3</sub> as catalyst. Remarkably, the cyclization of **44b** is an example of a cyclization of a 1,8-

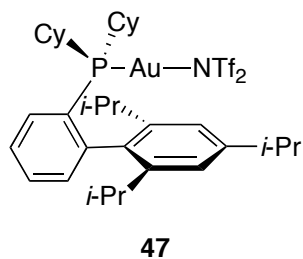
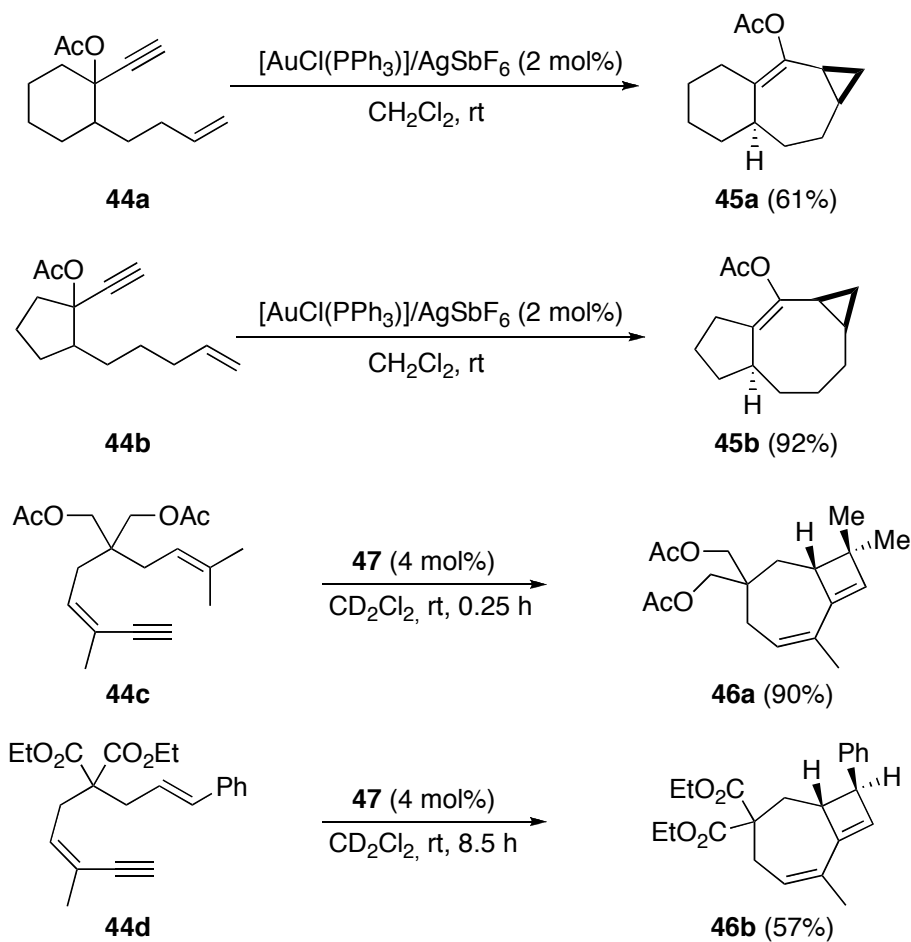
76 Moreau, X.; Goddard, J.-P.; Bernard, M.; Lemièrre, G.; López-Romero, J. M.; Mainetti, E.; Marion, N.; Mouriès, V.; Thorimbert, S.; Fensterbank, L.; Malacria, M. *Adv. Synth. Catal.* **2008**, *350*, 43-48.

enyne, although mechanistically this transformation could be interpreted as an intramolecular cyclopropanation of the terminal alkene by the gold carbene formed in a 1,2-acyl migration. This type of cyclization has been applied for the synthesis of an allolcolchicinoid.<sup>77</sup> Recently, gold catalyzed cyclization of substituted 1,8-enynes **44c-d** was achieved, yielding cyclobutenes **46a-b** as isolable intermediates. These intermediates can also evolve in the reaction medium to give isomerization or fragmentation products.<sup>78</sup>

---

77 Boyer, F. D.; Le Goff, X.; Hanna, I. *J. Org. Chem.* **2008**, *73*, 5163-5166.

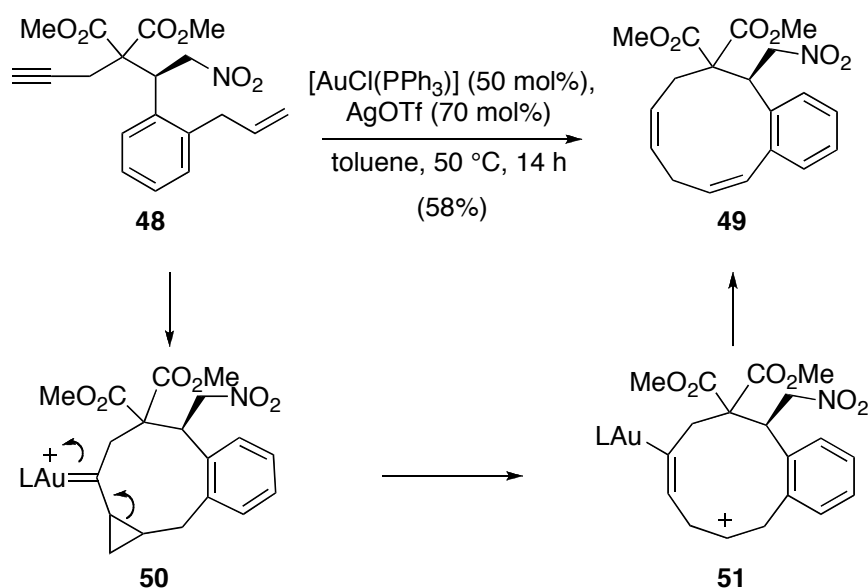
78 Odabachiana, Y.; Gagosz, F. *Adv. Synth. Catal.* **2009**, *351*, 379-386.



Scheme 17

In addition, a remarkable cyclization of the 1,9-enyne **48** to form the 10-membered ring **49** has been reported using 50 mol% of gold(I) complex with triphenylphosphine (Scheme 18).<sup>79</sup> This reaction presumably occurs via intermediates **50** and **51** and demonstrates that formation of large rings from 1,*n*-enynes ( $n \geq 7$ ) by using gold-chemistry is possible.

79 Comer, E.; Rohan, E.; Deng, L.; Porco, J. A. *Org. Lett.* **2007**, *9*, 2123-2126.



Scheme 18

## 2. Gold(I)-Catalyzed Cyclopropanations

The ability of gold species to form carbene intermediates has been exploited to achieve efficient cyclopropanation reactions. Previous to our work on the gold(I)-catalyzed intermolecular cyclopropanation, there were only three reported examples of gold(I) catalyzed cyclopropanation.<sup>34,80,81,82</sup> The increase in the number of publications dedicated to this field in recent years highlights the interest in developing such reaction.

1,3-*Bis*(diisopropylphenyl)imidazol-2-ylidene gold complex **55** in combination with sodium tetrakis(3,5-bis(trifluoromethyl)phenyl)borate ( $\text{NaBAR}'_4$ ) has been successfully applied to carbene transfer reactions from ethyl diazoacetate to yield cyclopropanes **52** (Scheme 19).<sup>80</sup> Although this reaction has been described with other transition metals of groups 8-11, this was the first example of such reactivity in gold-based complexes. The results showed that catalyst **55** was very chemoselective, since no ethyl diazoacetate coupling products were detected. Interestingly, gold catalyst **55**

80 Fructos, M. F.; Belderrain, T. R.; de Frémont, P.; Scott, N. M.; Nolan, S. P.; Díaz-Requejo, M. M.; Pérez, P. J. *Angew. Chem. Int. Ed.* **2005**, *44*, 5284-5288.

81 Johansson, M. J.; Gorin, D. J.; Staben, S. T.; Toste, F. D. *J. Am. Chem. Soc.* **2005**, *127*, 18002-18003.

82 Nieto-Oberhuber, C.; López, S.; Muñoz, M. P.; Jiménez-Núñez, E.; Buñuel, E.; Cárdenas, D. J.; Echavarren, A. M. *Chem. Eur. J.* **2006**, *12*, 1694-1702.

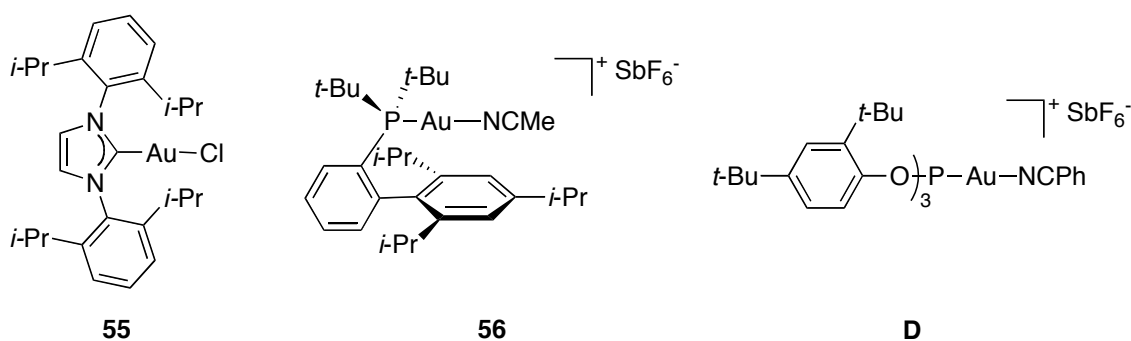
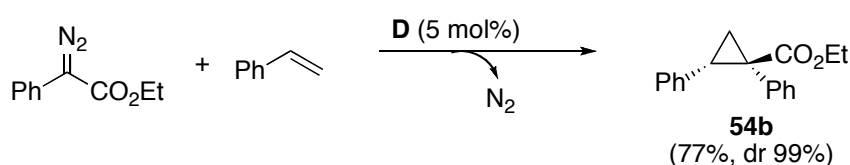
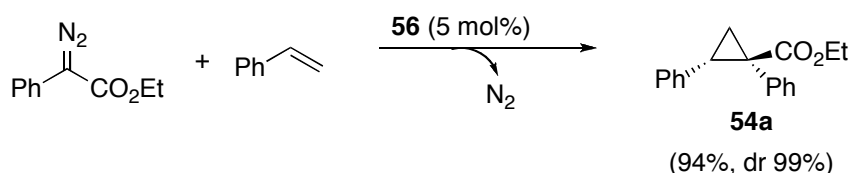
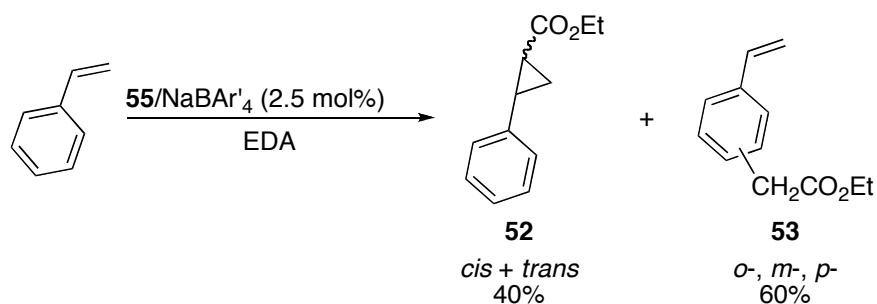
promotes a novel insertion reaction of the carbene moieties into the C-H bonds of simple aromatic compounds furnishing products **53**.

Broader studies on this carbene transfer reaction were carried out with a variety of gold catalysts bearing biphenyl phosphine, *N*-heterocyclic carbenes and a phosphite as ligands (Scheme 19).<sup>83</sup> High conversions and complete diastereoselectivity towards the *trans*-isomer were achieved, and the choice of a new carbene source, phenyldiazoacetate, turned out to be a key factor for obtaining the best results. The use of ionic liquids as solvents for similar transformations employing NaAuCl<sub>4</sub> or KAuCN<sub>2</sub> as catalyst has emerged as a strategy for recovering the catalysts *via* the formation of gold(0) nanoparticles.<sup>84</sup>

---

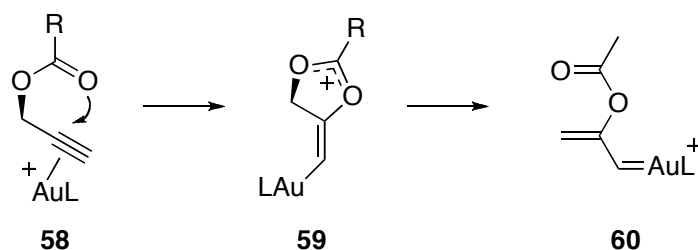
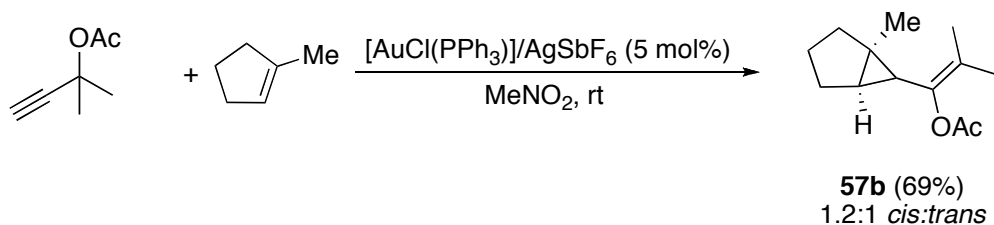
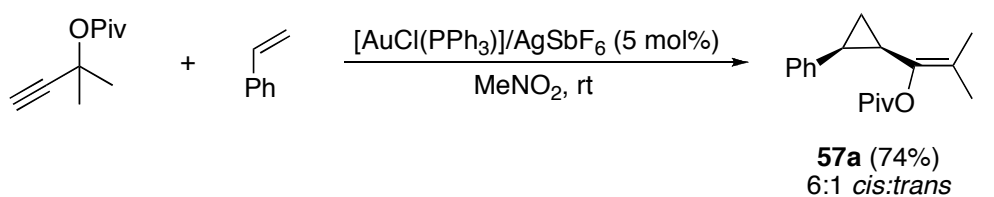
83 Prieto, A.; Fructos, M. R.; Díaz-Requejo, M. M.; Pérez, P. J.; Pérez-Galán, P.; Delpont, N.; Echavarren, A. M. *Tetrahedron* **2009**, *65*, 1790-1793.

84 Corma, A.; Domínguez, I.; Ródenas, T.; Sabater, M. J. *J. Catal.* **2008**, *259*, 26-59.



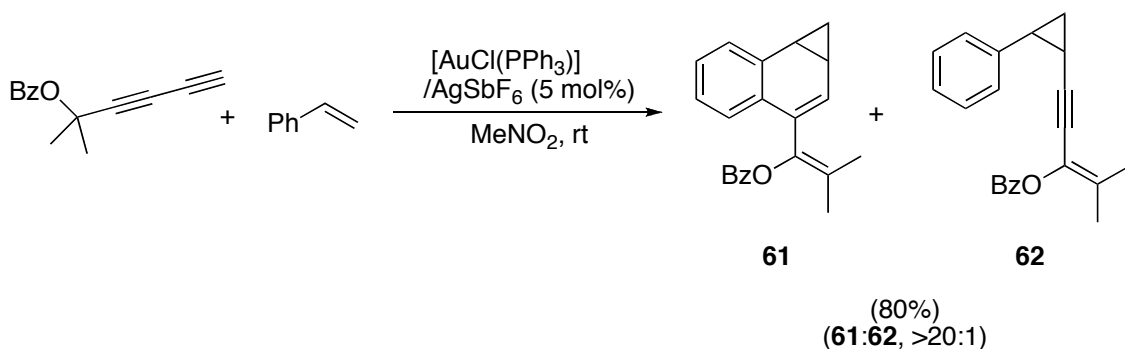
Scheme 19

In the context of alkyne activation, cyclopropanation of olefins with propargyl acetates was developed using the cationic species derived from  $[\text{AuCl}(\text{PPh}_3)]$ .<sup>81</sup> Gold(I) vinyl carbene species **60** are formed by the gold(I)-catalyzed rearrangement of propargylic esters, which are able to cyclopropanate olefins in a stereoselective manner furnishing derivatives **57** (Scheme 20). In addition, an enantioselective cyclopropanation is achieved by using chiral DTBM-SEGPHOS-gold(I) complex (60–85% *ee*), which is remarkable due to the few examples of gold(I)-catalyzed enantioselective transformations (see Introduction of Chapter 1, Section 3.3).



Scheme 20

An extension of this methodology using diynes containing a propargylic ester together with vinyl arenes provides access to functionalized benzenorcaradienes **61** in a catalyzed tandem cyclopropanation/hydroarylation reaction (Scheme 21).<sup>85</sup>



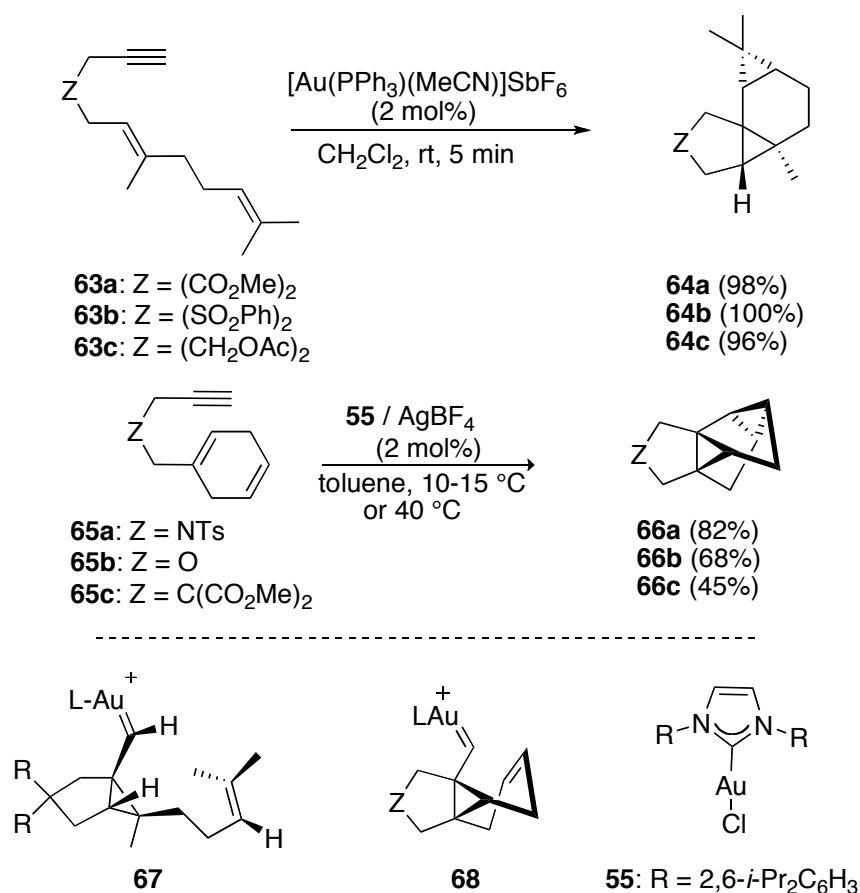
Scheme 21

The formation of biscyclopropanated derivatives in the gold(I)-catalyzed cycloisomerization of enynes would not only be synthetically interesting, but it would also provide experimental support for the involvement of cyclopropylgold(I) carbenes

85 Gorin, D. J.; Dub, P.; Toste, F. D. *J. Am. Chem. Soc.* **2006**, *128*, 14480-14481.

in the mentioned reaction. Evidence for the existence of cyclopropyl metal carbenes as intermediates was previously obtained in the Ru(II)<sup>3f</sup> and Pt(II)<sup>72,86,87</sup>-catalyzed reaction of enynes bearing additional double bonds at the alkenyl chain. When dienynes were submitted to gold catalysis, tetracycles containing two cyclopropanes **64** were furnished in good yields and at room temperature.<sup>82</sup> Similarly, enynes bearing a cyclohexadiene group like **65** yielded tetracyclo[3.3.0.0<sup>2,8</sup>.0<sup>4,6</sup>]octane derivatives **66** when treated with *N*-heterocyclic carbene gold(I) complexes<sup>88</sup> (Scheme 22). In these reactions, the intermediate cyclopropyl metal carbenes, such as **67** and **68**, were trapped intramolecularly by the terminal double bond.

- 
- 86 (a) Blaszykowski, C.; Harrak, Y.; Brancour, C.; Nakama, K.; Dhimane, A.-L.; Fensterbank, L.; Malacria, M. *Synthesis* **2007**, 2037-2049. (b) Marco-Contelles, J.; Arroyo, N.; Anjum, S.; Mainetti, E.; Marion, N.; Cariou, K.; Lemièrre, G.; Mouriès, V.; Fensterbank, L.; Malacria, M. *Eur. J. Org. Chem.* **2006**, 4618-4633. (c) Blaszykowski, C.; Harrak, Y.; Gonçalves, M.-H.; Cloarec, J.-M.; Dhimane, A.-L.; Fensterbank, L.; Malacria, M. *Org. Lett.* **2004**, *6*, 3771-3774. (d) Mainetti, E.; Mouriès, V.; Fensterbank, L.; Malacria, M.; Marco-Contelles, J. *Angew. Chem. Int. Ed.* **2002**, *41*, 2132-2135.
- 87 Peppers, B. P.; Divers, S. T. *J. Am. Chem. Soc.* **2004**, *126*, 9524-9525.
- 88 Kim, S. M.; Park, J. H.; Choi, S. Y.; Chung, Y. K. *Angew. Chem. Int. Ed.* **2007**, *46*, 6172-6175.

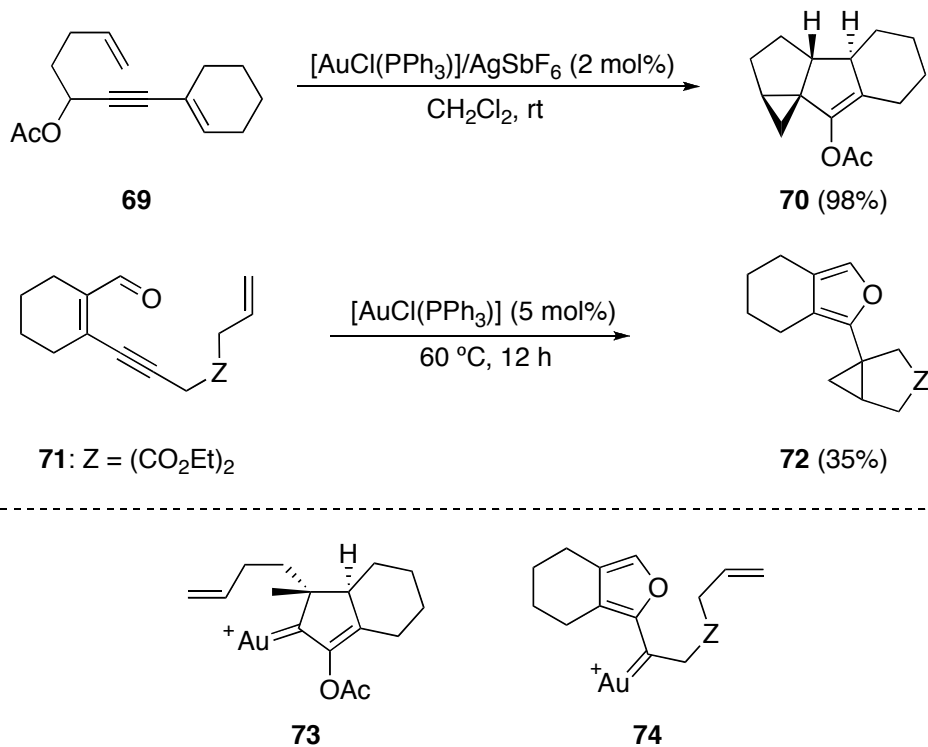


Scheme 22

Intramolecular cyclopropanations of gold carbenes formed in the reaction with propargylic acetates **69** or vinyl allenes have also been applied to the synthesis of polycyclic structures **70**.<sup>89</sup> In this case, the steps involved in the formation of the final product are a 3,3-rearrangement, a metalla-Nazarov reaction and finally the cyclopropanation of gold carbene **73** generated *in situ*. Finally, the synthesis of 2-(bicyclo[3.1.0]hexan-1-yl)furan derivatives compounds **72** can also be accomplished from 2-alkynyl-1-cycloalkencarbaldehydes **71** *via* intermediate **74** (Scheme 23).<sup>90</sup>

89 Lemière, G.; Gandon, V.; Cariou, K.; Fukuyama, T.; Dhimana, A.-L.; Fensterbank, L.; Malacria, M. *Org. Lett.* **2007**, *9*, 2207-2209.

90 Oh, C. H.; Lee, S. J.; Lee, J. H.; Na, Y. J. *Chem. Commun.* **2008**, 5794-5796.



Scheme 23

UNIVERSITAT ROVIRA I VIRGILI

GOLD(I)-CATALYZED CYCLIZATIONS OF 1,6- AND 1,7-ENYNES: NEW GOLD COMPLEXES AND CYCLOPROPANATION REACTIONS

Elena Herrero Gómez

ISBN: 978-84-692-5924-5/DL:T-1663-2009

## *Chapter 2. Objectives*

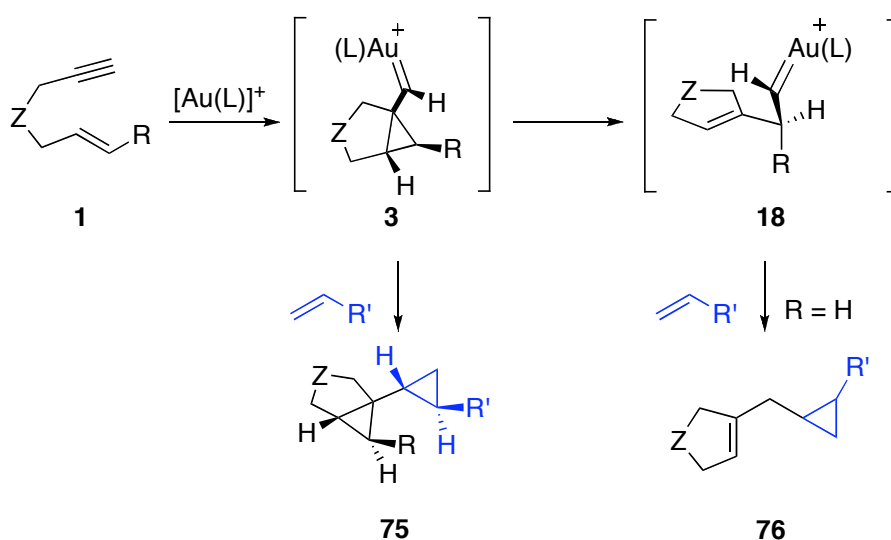
UNIVERSITAT ROVIRA I VIRGILI

GOLD(I)-CATALYZED CYCLIZATIONS OF 1,6- AND 1,7-ENYNES: NEW GOLD COMPLEXES AND CYCLOPROPANATION REACTIONS

Elena Herrero Gómez

ISBN: 978-84-692-5924-5/DL:T-1663-2009

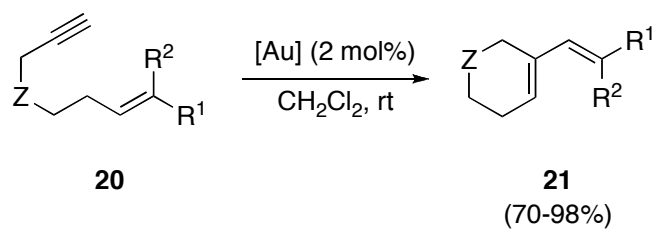
One of the main interests of our research group is the development of new synthetic methodologies based on the gold(I)-catalyzed cyclization of enynes as well as understanding the mechanistic aspects of these transformations. In this context, the intermolecular trapping of gold(I) carbenes **3** and **18**, intermediates proposed by DFT calculations, was our first objective. Taking advantage of the standard reactivity of metal carbenes, we intended an intermolecular trapping of these carbene intermediates using olefins to obtain the corresponding cyclopropanes **75** and **76**, respectively (Scheme 24).



Scheme 24

This reaction would be of interest also as a method for an easy access to complex bicyclopropanated derivatives in a stereoselective manner.

On the other hand, previous studies carried out in our research group showed a significantly different reactivity between 1,6- and 1,7-enynes in the gold(I)-catalyzed cycloisomerization. With the aim of understanding the high selectivity of 1,7-enynes for the formation of single cleavage products in the skeletal rearrangement (Scheme 25), a computational analysis of the reaction was carried out. We also decided to study new cascade reactions with substituted 1,7-enynes.

**Scheme 25**

*Chapter 2. Results and discussion*

UNIVERSITAT ROVIRA I VIRGILI

GOLD(I)-CATALYZED CYCLIZATIONS OF 1,6- AND 1,7-ENYNES: NEW GOLD COMPLEXES AND CYCLOPROPANATION REACTIONS

Elena Herrero Gómez

ISBN: 978-84-692-5924-5/DL:T-1663-2009

## 1. Gold(I)-Catalyzed Intermolecular Cyclopropanation<sup>91,92</sup>

### 1.1. Gold(I)-Catalyzed Intermolecular Cyclopropanation of 1,6-enynes

Enyne **16h** was selected for this study since it has been successfully used before in gold(I)-catalyzed cyclization of enynes.<sup>35</sup> To avoid competition with the intramolecular reaction, which is obviously more favored, the external alkene was added in excess to the reaction mixture. A 5:1 ratio of the external alkene to the enyne proved to be optimal to obtain the desired cyclopropanated products. Additionally, the reactions were started at low temperature (-60 to -40 °C), although to achieve complete conversion it was necessary to warm the reaction mixtures slowly (16 h) up to room temperature. Dichloromethane was the solvent of choice because of the excellent solubility of both gold(I) catalysts and enynes, of its non-coordinating character and because it allows to decrease reaction temperature to the stated values. Gold(I)-catalyzed cycloisomerization of enynes has been extensively performed in this solvent.<sup>34,35</sup>

In the developed experimental conditions, a screening of gold catalysts was also performed (Figure 1). Our experience in the gold-catalyzed reactions of enynes tells us that the reactivity of the catalytic system can be efficiently tuned by the use of different ligands in the gold center. Electrophilicity in the gold center, which it is related with higher activity of the corresponding catalysts, varies according to the different electron withdrawing power of the ligands. Usually the reactions were carried out with 5 mol% of the gold catalysts, but smaller amounts such as 2 mol% also work uneventfully.

---

91 Taken from: López, S.; Herrero-Gómez, E.; Pérez-Galán, P.; Nieto-Oberhuber, C.; Echavarren, A. *M. Angew. Chem. Int. Ed.* **2006**, *45*, 6029-6032.

92 Part of this work has been done in collaboration with Dr. Salomé López, Cristina Nieto-Oberhuber and Daniel T. Hog (may-july 2008).

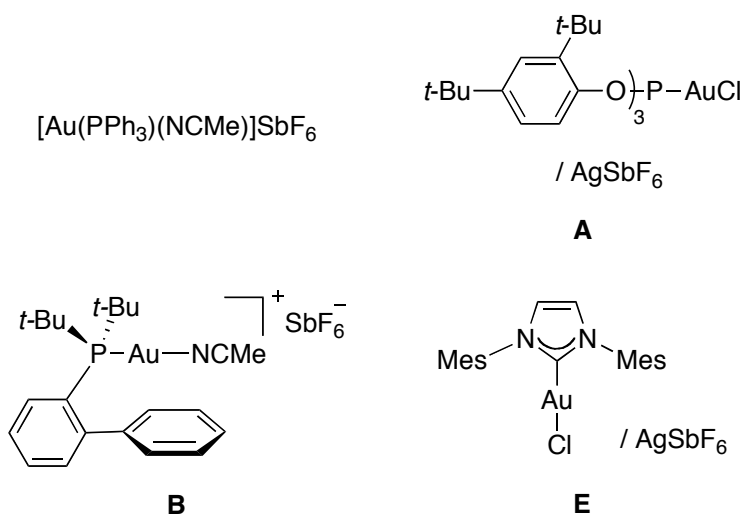
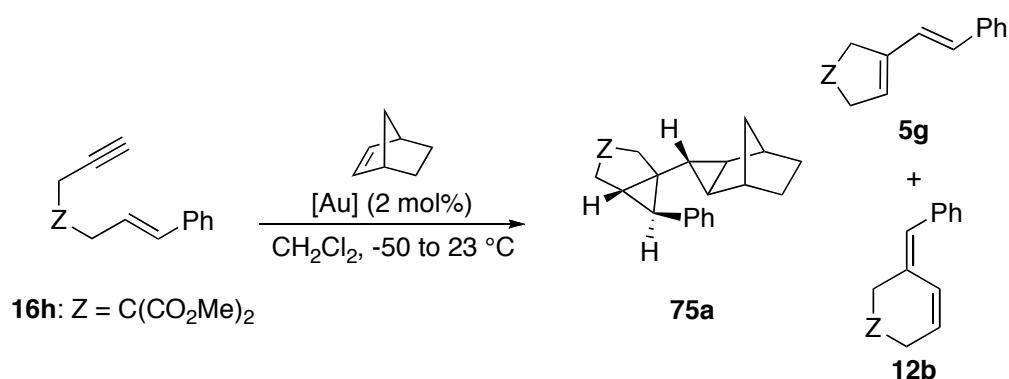


Figure 1

The cyclization occurred as usual in the absence of external olefin under the new reaction conditions using  $[\text{Au}(\text{PPh}_3)(\text{NCMe})]\text{SbF}_6$  (Scheme 26, Table 1, entry 1). When norbornene was added, biscyclopropanated product **75a** was observed in all cases. The formation of product **75a** is the result of an intermolecular trapping of the cyclopropylgoldcarbene **3**, proposed as a key intermediate for gold catalyzed cyclizations of enynes.<sup>43,44,45</sup> The ratios of desired product vs. usual cycloisomerization varied in great extent depending on the gold catalysts employed. Cationic derivative of the triphenylphosphinegold complex provided desired product **75a** in moderate yield (Table 1, entry 2). As could be expected, more active catalysts such as **A** and **B**, which give rise to very fast reactions, were not suitable for trapping the intermediates, and favored the intramolecular reaction that leads to **5g** and **12b** (Table 1, entries 4 and 5). On the contrary, simple AuCl and NHC-derivative **E** gave **75a** in excellent yields (Table 1, entries 3 and 6).



**Scheme 26**

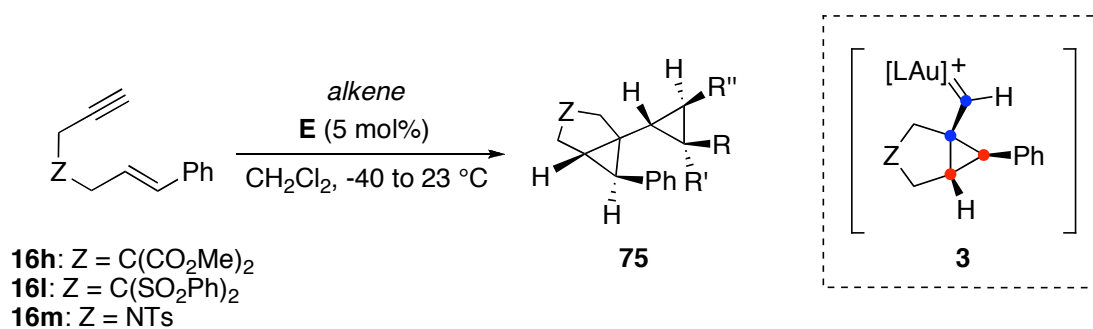
**Table 1.** Screening of gold catalysts for the intermolecular cyclopropanation reaction.

entry <sup>[a]</sup>	[Au]	norbornene (equiv)	<b>75a</b> (yield, %) <sup>[b]</sup>	<b>5g + 12b</b> (yield, %; ratio) <sup>[b]</sup>
1	[Au(PPh <sub>3</sub> )(NCMe)]SbF <sub>6</sub>	-	-	99 (1:1.4)
2	[Au(PPh <sub>3</sub> )(NCMe)]SbF <sub>6</sub>	5	66	29 (1:1.2)
3	<b>E</b>	5	93	3 (>10:1)
4	<b>B</b>	5	34	62 (1.1:1)
5	<b>A</b>	5	40	52 (1:1.6)
6	AuCl	5	94	0 <sup>[c]</sup>

[a] Reactions carried out by slow warming from -50 to 23°C over *ca.* 15 h using 5 equiv of norbornene. [b] Yields and ratios determined by GC for reactions with *ca.* 100% conversion. [c] *ca.* 2% of other uncharacterized products.

Although AuCl gave the best results in this preliminary work with enyne **16h**, the results were not satisfactory with other substrates. Using catalyst **E**, good yields and selectivities were observed.

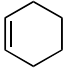
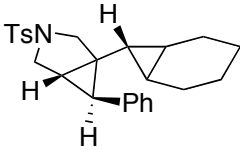
The scope of this transformation was examined by using enynes **16h-m**, in which the substitution pattern in the alkene is maintained (Scheme 27, Table 2). Simple, disubstituted olefins like norbornene and cyclohexene were employed under the optimized reaction conditions. Olefins with electron withdrawing substituents, such as allyl bromide, did not react to give the cyclopropanation products in this reaction.



Scheme 27

Table 2. Gold(I)-catalyzed intermolecular biscyclopropanation of 1,6-enynes.

entry	alkene	enyne	Product	yield (%) <sup>[b]</sup>
1		<b>16h</b>		67
2 <sup>[c]</sup>		<b>16l</b>		31
3 <sup>[c]</sup>		<b>16m</b>		73
4		<b>16h</b>		77
5		<b>16l</b>		53

entry	alkene	enyne	Product	yield (%) <sup>[b]</sup>
6		<b>16m</b>	 <b>75f</b>	75

[a] Reactions carried out by slow warming from -540 to 23 °C over *ca.* 15 h with 5 equiv of olefin and 5 mol% of catalyst **E**. [b] Isolated yields are the average of at least two reactions. [c] Reaction time = 40 h.

Enynes **16h** and **16m** gave rise to high yields and only one diastereoisomer (Table 2, entries 1, 3, 4, and 6). Reaction of substrate **16l** with norbornene and cyclohexene proceeded more sluggishly to furnish tetracycles **75b** and **75e** (Table 2, entries 2 and 5). In this case, the yields were lower than found with substrates **16h** and **16m**, which can be attributed to a difficult purification of the corresponding products. In addition, hydroxycyclization products, resulting from the gold catalyzed addition of water to the enyne, were observed as minor byproducts.<sup>35</sup> This unwanted side reaction was easily avoided by the use of activated molecular sieves.

The relative configurations follow those assigned in the intramolecular processes and were assigned based on <sup>1</sup>H-NOESY experiments. They were also confirmed by means of X-ray structure analysis of derivatives **75c** and **75f** (Figure 2).

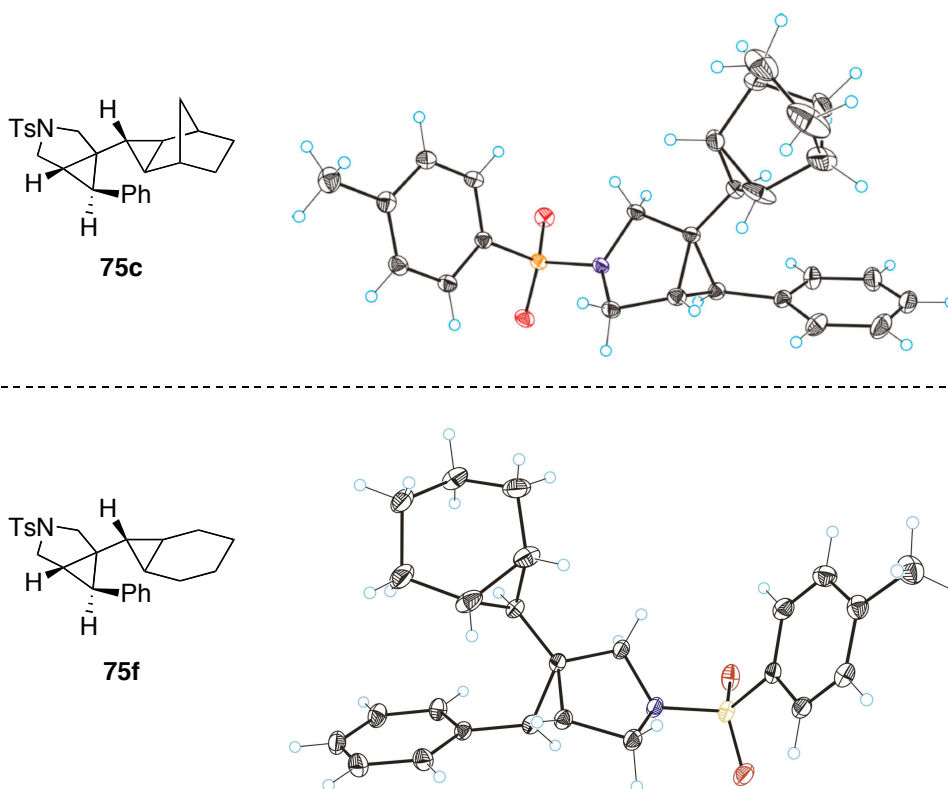
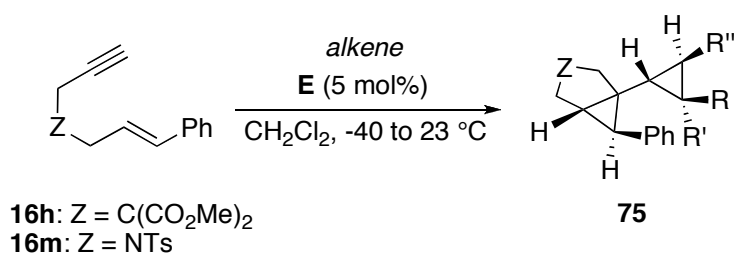


Figure 2. X-Ray structures of **75c** and **75f**.

Reaction of enynes **16h** and **16m** with non symmetrical alkenes also led to bicyclopropanated compounds under gold(I) catalysis (Table 3). Compound **16h** reacted with 4-methylpenta-1,3-diene to give **75i** in 60% yield (Table 3, entry 1). The reaction proceeds with excellent regioselectivity, since no product derived from the attack on the more substituted double bond was detected. Highly reactive olefins such as styrene also reacted cleanly to afford derivatives **75g** and **75h** (Table 3, entries 2 and 3). Styrene reacted with more active gold(I) catalysts to give polystyrene.<sup>93</sup> In the reaction of **16m** with styrene (Table 3, entry 3), bicyclopropane **75h** was obtained as a 10:1 mixture of diastereoisomers, while **75g** was obtained as a single diastereomer (Table 3, entry 2). Reaction of **16h** with 2-methylprop-1-ene was performed using AuCl as catalyst, giving **75j** in 52% yield as a 3.7:1 mixture of diastereomers (Table 3, entry 4).

93 Gold-promoted styrene polymerization has been reported in: Urbano, J.; Hormigo, A. J.; de Frémont, P.; Nolan, S. P.; Díaz-Requejo, M. M.; Pérez, P. J. *Chem. Commun.* **2008**, 759-761.



**Scheme 28**

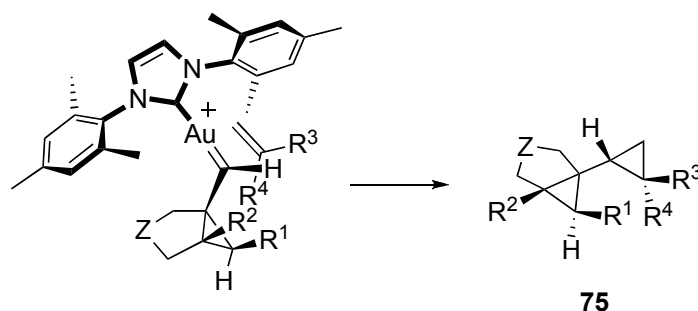
**Table 3.** Gold(I)-catalyzed cyclopropanation with non symmetrical olefins.

entry <sup>[a]</sup>	alkene	enyne	Product	yield (%) <sup>[b]</sup>
1 <sup>[c]</sup>		<b>16h</b>		60 (5:1)
2		<b>16h</b>		76
14 <sup>[c]</sup>		<b>16m</b>		68 (10:1)
15 <sup>[d]</sup>		<b>16h</b>		52 (3.7:1)

[a] Reactions carried out by slow warming from -40 to 23 °C over *ca.* 15 h with 5 equiv of olefin and 5 mol% of catalyst **E**. [b] Isolated yields are the average of at least two reactions. Diastereomeric ratios are reported in brackets. [c] Only the major isomer is shown. [d] Reaction carried out with AuCl (2 mol%).

A high selectivity was observed in all these transformations (Table 3, entries 1-4). This fact can be explained by the bulkiness of the ligand in the gold center, that only allows for the approach of the incoming olefin reagent in which the substituents are far

away from the ligand (Scheme 29). This is a plausible explanation for the observed products **75g-75j**.



**Scheme 29**

Poor-quality crystals of **75g** were obtained by crystallization from CH<sub>2</sub>Cl<sub>2</sub> (Figure 3). The X-ray structure of the compound, although not completely resolved, was useful to confirm the structure proposed by NMR studies.

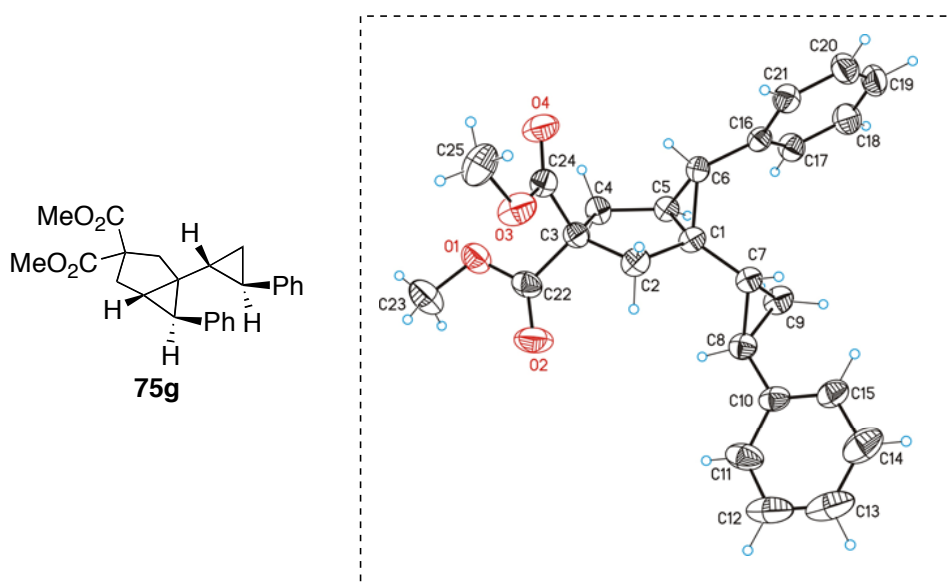
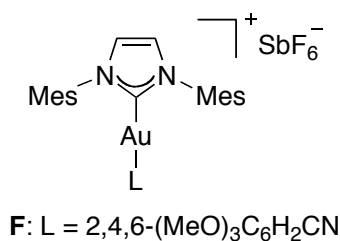
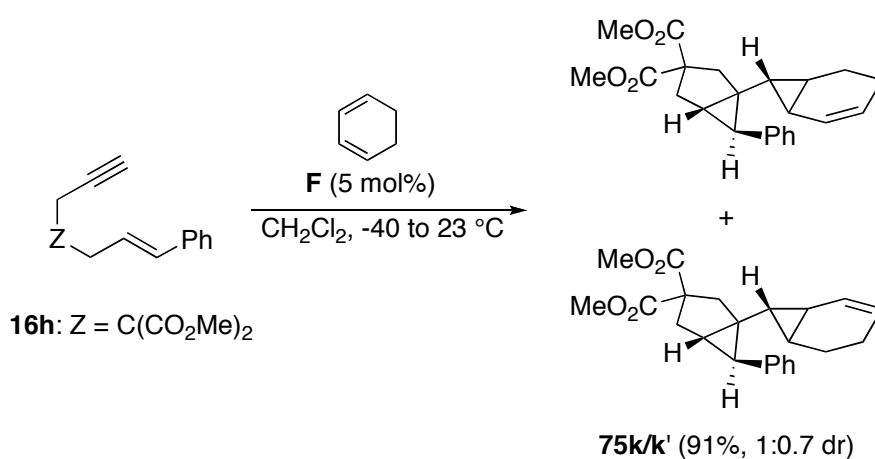


**Figure 3.** Preliminary X-ray structure of compound **75g**.

A less selective transformation was achieved when the reaction was performed with 1,3-cyclohexadiene (Scheme 30). Using the optimized reaction conditions, a mixture of, at least, two diastereoisomers **75k/75k'** in a 1:0.7 ratio was obtained. In this reaction, newly developed cationic catalyst **F** was employed. The use of cationic gold catalysts considerably simplifies experimental procedures and avoids unwanted side reactions.



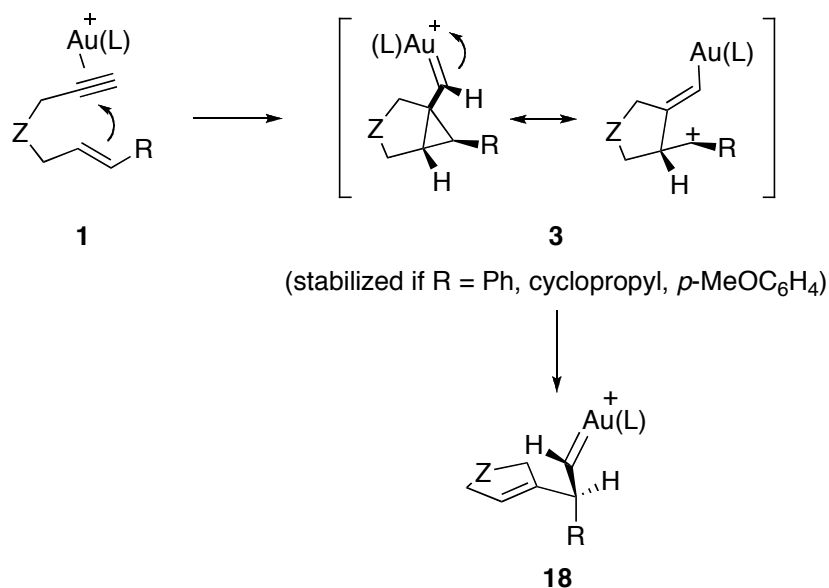
Scheme 30

1,6-Enynes with a different substitution pattern in the alkene were also tested (Scheme 31). Enyne **16g** and methyl-substituted enyne **16n** reacted with olefins, although the use of more active gold(I) catalysts, such as phosphite-based catalytic system **A**, was needed. Unexpectedly, no bicyclopropanated derivatives **75** were isolated in these cases. The cyclopropanation of the gold carbene led for these substrates to the formation of cyclopentenyl derivatives **76**.



of the existence of rearranged carbene type **18** has been achieved by the attack of carbon nucleophiles.<sup>94</sup>

The trapping of different species depending on the substitution of the alkene moiety confirms the calculated low energy barrier for the isomerization of these intermediates. It also indicates that these cyclopropylcarbene intermediates are very distorted structures. The presence of substituents that stabilize the positive charge in different position of the cyclopropane ring seems to be the determining factor for the isolation of different trapped products (Scheme 32).



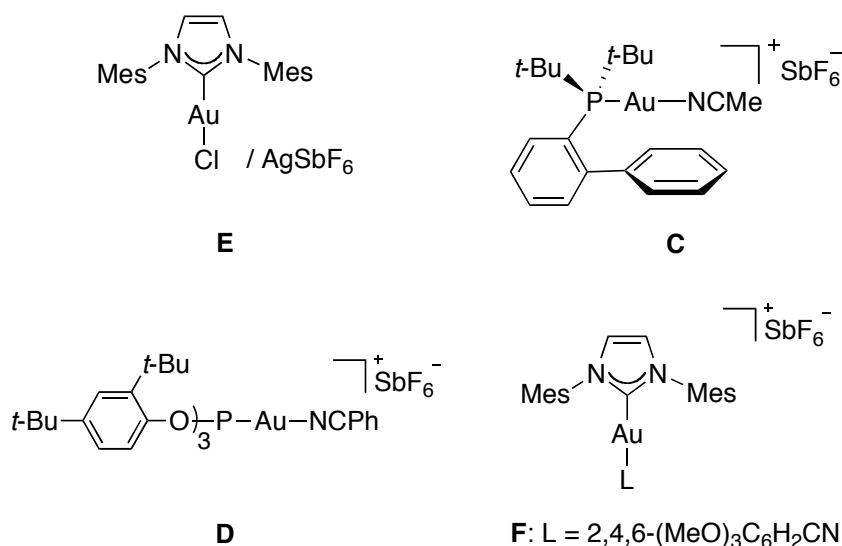
Scheme 32

## 1.2. Gold(I)-Catalyzed Intermolecular Cyclopropanation of 1,7-Enynes

With the aim to broaden the scope of this transformation, gold(I)-catalyzed cyclopropanation of simple 1,7-enynes was also attempted. 1,7-Enynes are known to react smoothly upon mixing with gold(I) catalysts to yield exclusively single cleavage rearrangement products, although longer reaction times compared to their 1,6-counterparts are needed in certain cases. The trapping of the gold carbene intermediate with these substrates would be also of interest in the context of the study of the mechanism of the gold(I)-catalyzed cycloisomerization of such enynes.

94 Amijs, C. H. M.; López-Carrillo, V.; Raducan, M.; Pérez-Galán, P.; Ferrer, C.; Echavarren, A. *M. J. Org. Chem.* **2008**, *73*, 7721–7730.

Firstly, we tried the optimized reaction conditions developed for 1,6-enynes. In addition, some of the recently developed cationic complexes **D** and **F** (Scheme 33) were also tested. The use of cationic gold catalysts avoided the use of silver salts, which simplifies experimental procedures and avoids unwanted side reactions. Cationic derivatives of complexes **D** and **F** were found to be stable only when using electron-rich nitrile ligands.<sup>94</sup>



Scheme 34

Substrates **20e-g** were selected due to their known reactivity towards gold catalysis (Figure 4).<sup>68</sup>

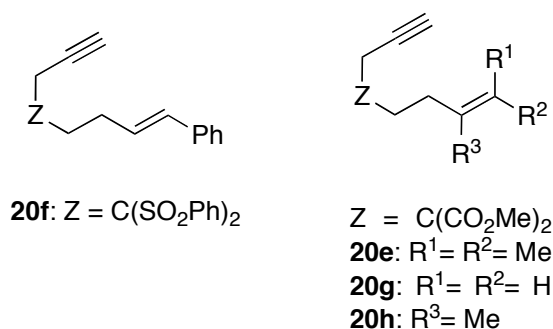
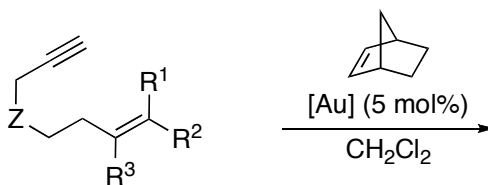


Figure 4. 1,7-Enynes tested in the gold(I)-catalyzed intermolecular cyclopropanation.





**20e:** Z = C(CO<sub>2</sub>Me)<sub>2</sub>; R<sup>1</sup> = R<sup>2</sup> = Me

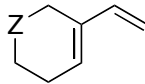
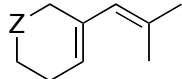
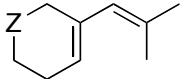
**20g:** Z = C(CO<sub>2</sub>Me)<sub>2</sub>; R<sup>1</sup> = R<sup>2</sup> = H

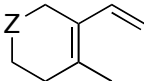
**20h:** Z = C(CO<sub>2</sub>Me)<sub>2</sub>; R<sup>3</sup> = Me

**20f:** Z = C(SO<sub>2</sub>Ph)<sub>2</sub>; R<sup>2</sup> = Ph

### Scheme 35

**Table 4.** Gold(I)-catalyzed cyclopropanation of 1,7-enynes.

entry	enyne	[Au]	Reaction Conditions	Product <sup>[a]</sup>
1	<b>20g</b>	<b>E</b>	-40 °C to rt 16 h	s.m.
2	<b>20g</b>	<b>B</b>	-40 °C to rt 16 h	s.m.
3	<b>20g</b>	<b>D</b>	-40 °C to rt 16 h	s.m. +  <b>21g:</b> Z = C(CO <sub>2</sub> Me) <sub>2</sub> ratio = 1:0.3
4	<b>20g</b>	<b>E</b>	0 °C to rt. 15 h	s.m.
5	<b>20e</b>	<b>E</b>	-40 °C to rt. 16 h	s.m. +  <b>21c:</b> Z = C(CO <sub>2</sub> Me) <sub>2</sub> ratio = 1:0.2
6	<b>20e</b>	<b>B</b>	0 °C to rt 15 h	 <b>21c:</b> Z = C(CO <sub>2</sub> Me) <sub>2</sub>
7	<b>20h</b>	<b>F</b>	-40 °C to rt. 16 h	s.m.

entry	enyne	[Au]	Reaction Conditions	Product <sup>[a]</sup>
8	<b>20h</b>	<b>F</b>	rt 38 h	s.m. +  <b>21h</b> : Z = C(CO <sub>2</sub> Me) <sub>2</sub> ratio = 1:0.4
9	<b>20h</b>	<b>B</b>	rt 30 h	s.m.
10	<b>20f</b>	<b>F</b>	-40 °C to rt 16 h	s.m.

[a] Products and ratios determined by <sup>1</sup>H NMR.

Increasing the electrophilicity on the gold center by using catalysts **B** or **G** in the reaction of enyne **20g** (Table 4, entries 2 and 3) was not successful, and only a small amount of the cyclized enyne **21g** was detected when more active catalysts **D** was employed (Table 4, entry 3). For enyne **20e**, the use of phosphine-based catalyst **B** at the same temperature only yielded cycloisomerization product **21c** (Table 4, entry 6). Reactions at room temperature of enyne **20h** with catalysts **F** and **B** did not proceed (Table 4, entries 8 and 9), and only traces of cyclized product were observed in the first case. Although in certain cases <sup>1</sup>H NMR spectra of reaction mixture could indicate the formation of traces of the desired tricyclic derivatives, the efforts to obtain them in significant yield were not successful. The trapping of the carbene intermediates responsible for the gold(I)-catalyzed cyclization of 1,7-enynes has not been achieved yet.

### 1.3. Insights in the Mechanism of the Gold(I)-Catalyzed Cyclopropanation of Olefins.

The mechanism of the gold catalyzed cyclopropanation was also investigated. Two possibilities were considered for this reaction: either the cyclopropanation occurs through a concerted or a stepwise mechanism, the latter involving cationic species.

According to DFT calculations on the related intramolecular cyclopropanation reaction catalyzed by gold, this process should be concerted.<sup>82</sup> In order to have an insight into this mechanism, the intermolecular cyclopropanation reaction was carried out using non-conjugated polyolefins, such as 1,5-cyclooctadiene or squalene (Figure 5).

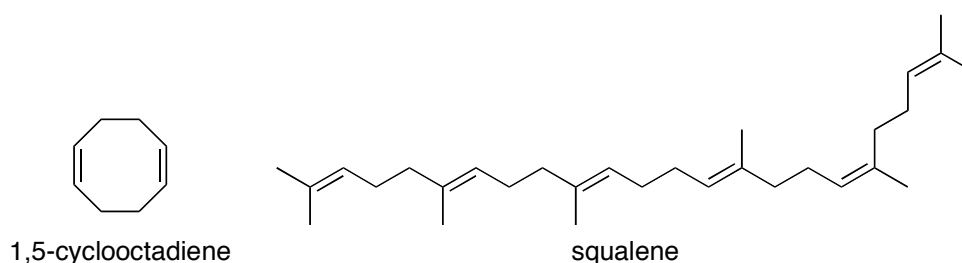
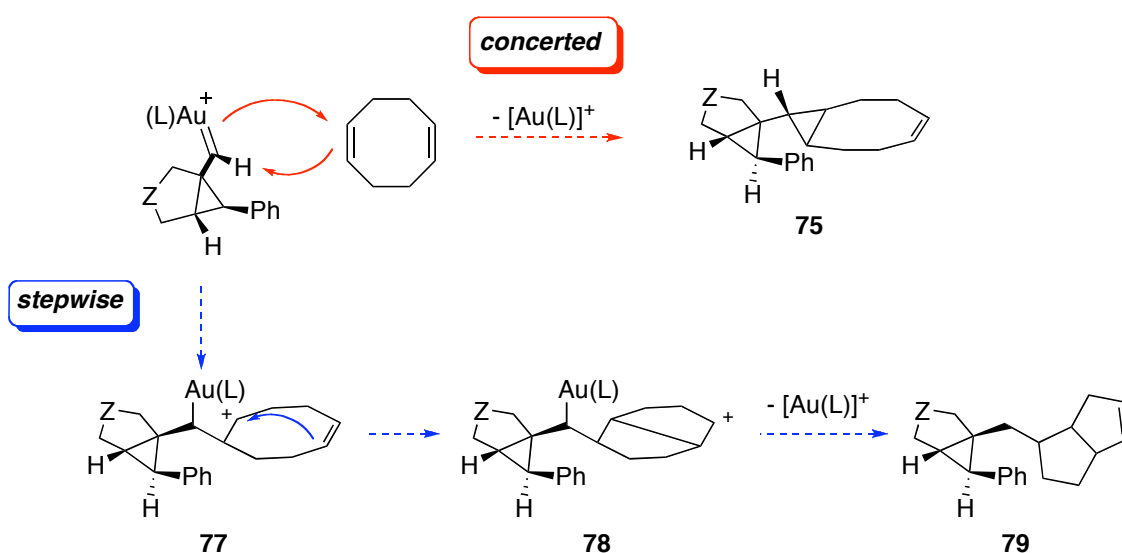


Figure 5

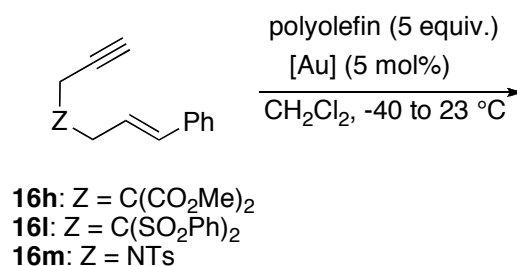
We envisioned that the additional double bond would remain as a spectator in a purely concerted mechanism, while if any cationic species were generated during the reaction, such as **78**, then a subsequent attack from the remaining alkene was likely to happen, providing new polycyclic structures. Both reaction pathways are depicted in Scheme 36 for 1,5-cyclooctadiene.



Scheme 36

Enynes **16h**, **16l**, **16m** reacted uneventfully with 1,5-cyclooctadiene (Scheme 37) under standard reaction conditions (Table 5, entries 1-3), furnishing bicyclopentanated derivatives **75k-m** as single diastereoisomers. Higher yields were

obtained in the reaction of enynes **16h** and **16m**, 77% and 87% respectively (Table 5, entries 1 and 3), than in the reaction with enyne **16l** (Table 5, entry 2). According to our experience, lower yields are usually obtained with enyne **16l**. Reaction of **16h** with squalene only led to a complex mixture of undefined products (Table 5, entry 4).



Scheme 37

Table 5. Gold(I)-catalyzed cyclopropanation with 1,5-cyclooctadiene and squalene.

entry	alkene	enyne	catalyst	Product	yield (%) <sup>[a]</sup>
1	1,5-COD	<b>16h</b>	<b>E</b>	 <b>75k</b>	72
2	1,5-COD	<b>16l</b>	<b>E</b>	 <b>75l</b>	55
3	1,5-COD	<b>16m</b>	<b>F</b>	 <b>75m</b>	87
4	squalene	<b>16h</b>	<b>E</b>	Complex mixture	

[a] Yields are the average of two reactions.

The structure of **75l** was confirmed by X-ray crystallography (Figure 6).

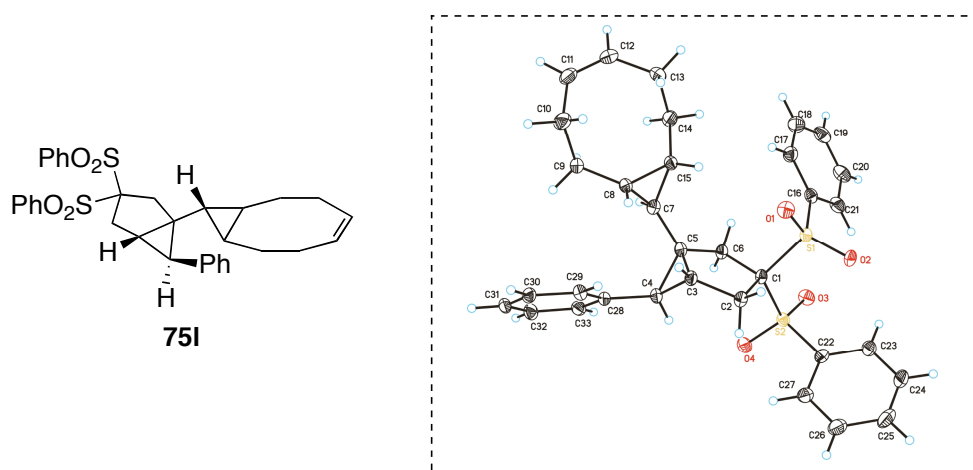


Figure 6. X-ray structure of **75l**.

The isolation of only bicyclopropanated products **75l-n** suggests that the gold-catalyzed cyclopropanation proceeds in a concerted fashion. Thus, presumably cationic species such as **77** (Scheme 36) are not taking part in this transformation. However, although this experimental evidence supports the concerted pathway, the second possibility cannot be completely excluded. Additional experimental work would be needed to further confirm this mechanistic proposal.

#### 1.4. Exploratory Studies Towards the Synthesis of Myliol Sesquiterpenes.

The intermolecular trapping of the cyclopropylgold carbene intermediates involved in the gold(I)-catalyzed cyclization of 1,6-enynes provided an experimental insight in the intermediates involved in this complex rearrangement. In addition, it provides an easy access to bicyclopropanated structures. Thus, we envisioned that this transformation would also be of interest in the context of natural product synthesis. More precisely, a family of natural occurring sesquiterpenes possesses the same tricyclic motif as the one found in our cyclopropanation reaction products. Two members of this family, myliol and dihydromyliolone A, are shown in Figure 7.

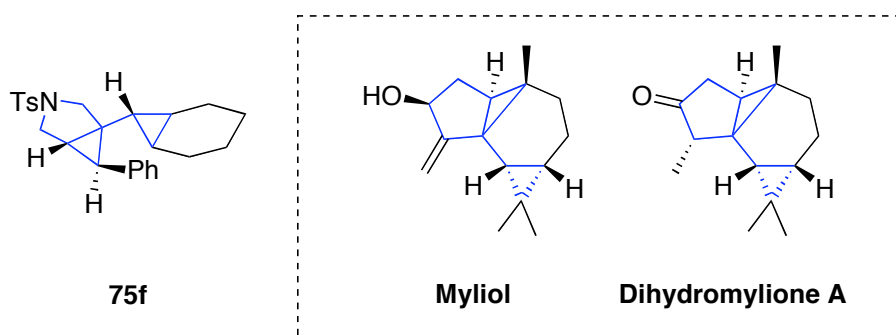
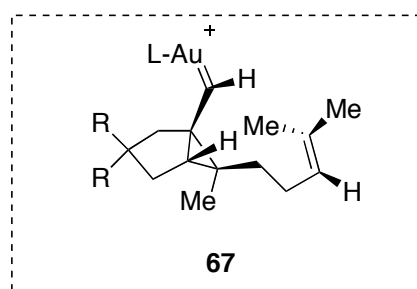
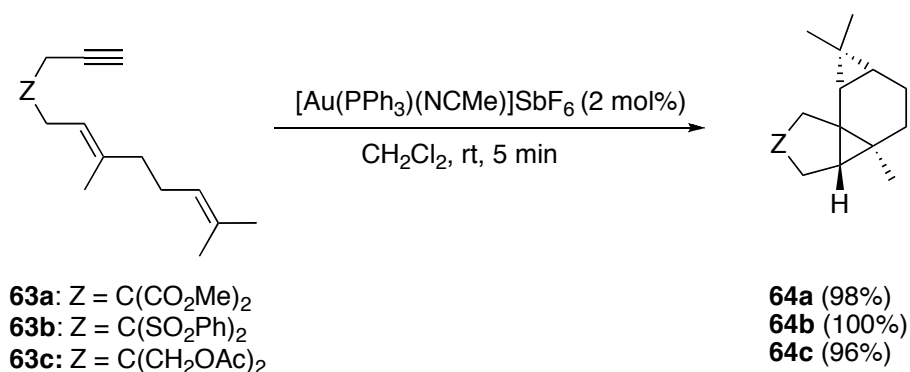


Figure 7

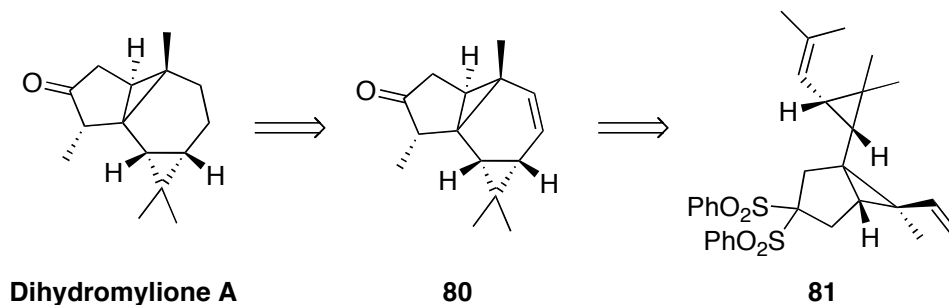
Previous studies carried out in our group on the gold(I)-catalyzed intramolecular cyclopropanation of dienynes also provided similar structures (Scheme 38).<sup>82</sup> However, the relative configuration in the cyclopropane ring is opposite to the one found in the family of myliol. An intermolecular version of this transformation would presumably allow for changing the outcome of the reaction, by changing the substitution in the alkene or the nature of the gold catalysts.



Scheme 38

Thus, our synthetic proposal for the approach to the synthesis of the myliol family is based on a ring closing metathesis that would provide the six membered ring starting from the bicyclopropanated derivatives (Scheme 39). For this reason, two

double bonds are required in the corresponding positions as in structure **81**. The carbonyl group can be obtained from **80** by cleavage of one of the sulfone groups with Al/Hg<sup>96</sup> followed by oxidation with MoOPh.<sup>97</sup>



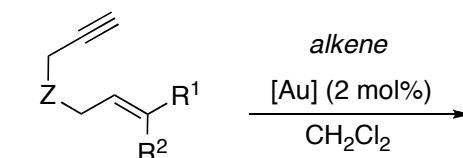
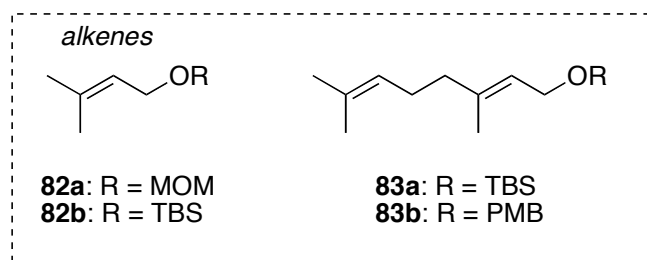
**Scheme 39**

Our first objective was to investigate the feasibility of the cyclopropanation reaction using olefins bearing additional double bonds or their synthetic equivalents. Protected alcohols derived from 3-methylbut-2-en-1-ol **82a-b** and geraniol **83a-b** were tested in a model system (Scheme 40, Table 6).

---

96 Herve du Penhoat, C.; Julia, M. *Tetrahedron* **1986**, *42*, 4807-4816.

97 (a) Little, R. D.; Myong, S. O. *Tetrahedron Lett.* **1980**, *21*, 3339-3342. (b) Vedejs, E.; Engler, D. A.; Telschow, J. E. *J. Org. Chem.* **1978**, *43*, 188-196.



Z = C(CO<sub>2</sub>Me)<sub>2</sub>  
**16a:** R<sup>1</sup> = R<sup>2</sup> = Me  
**16h:** R<sup>1</sup> = Ph

**Scheme 40**

**Table 6.** Gold-catalyzed cyclopropanation with protected alcohols **82a-b** and **83a-b**.

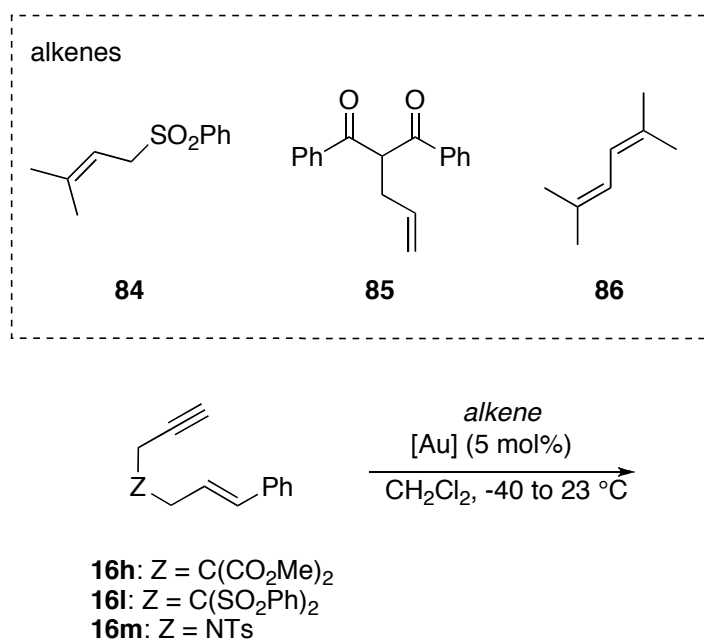
entry	enyne	alkene	[Au]	Reaction conditions	product
1	<b>16a</b>	<b>82a</b>	<b>B</b>	rt, 16 h	s.m.
2	<b>16h</b>	<b>82a</b>	<b>B</b>	0 °C to rt, 16 h 50 °C, 16 h	s.m. s.m. + rearr.
3	<b>16h</b>	<b>82b</b>	<b>B</b>	0 °C to 15 °C, 16 h carbene cat	s.m.
4 <sup>[a]</sup>	<b>16h</b>	<b>83a</b>	<b>E</b>	-40 °C to rt, 16 h carbene cat	Complex mixture
5 <sup>[a]</sup>	<b>16h</b>	<b>83b</b>	<b>E</b>	-40 °C to rt, 16 h	Complex mixture

[a] 5 mol% of catalyst was used.

Unfortunately, no bicyclopromated products were observed in any case (Table 6, entries 1-5). The lack of reactivity when using **82a-b** can be caused by the bulkiness of the protecting groups, that can be blocking the reaction center, or by the oxophilicity

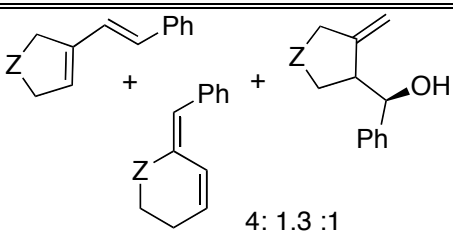
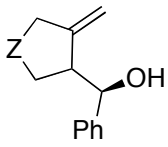
of gold, *i.e.* its tendency to coordinate to oxygen. Protected alcohols with a longer chain, such as derivatives from geraniol **83a-b**, gave complex mixtures (Table 5, entries 4-5).

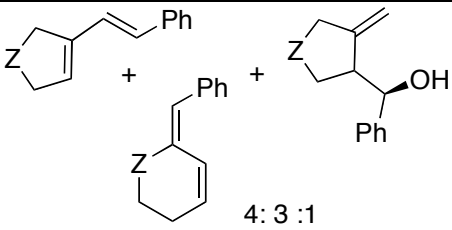
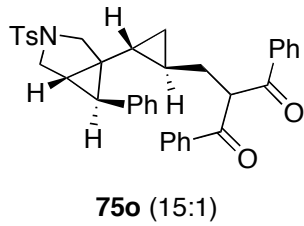
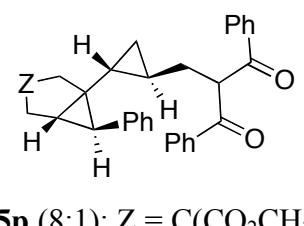
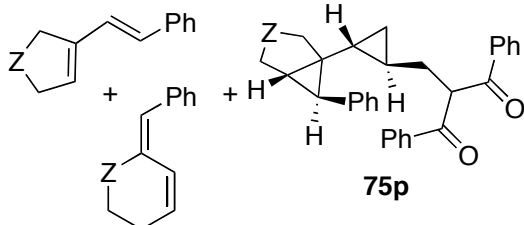
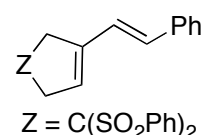
In the search for the suitable olefin, we tested in our model system three new olefins: allylic sulfone **84**, dicarbonyl compound **85** and 2,5-dimethylhexa-2,4-diene **86** (Scheme 41, Table 7).

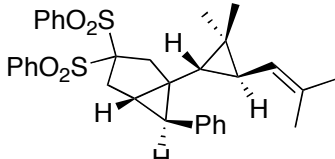


Scheme 41

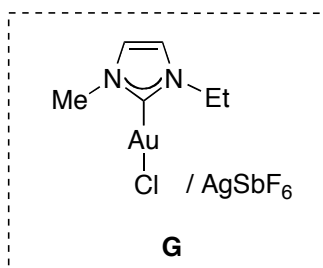
Table 7. Gold-catalyzed cyclopropanation with **84**, **85**, and **86**.

entry	enyne	alkene	[Au]	Products	yield (%)
1	<b>16h</b>	<b>84</b>	<b>E</b>	 <p style="text-align: center;">4: 1.3 :1</p>	-
2	<b>16h</b>	<b>84</b>	<b>E</b>		-

entry	enyne	alkene	[Au]	Products	yield (%)
3	16h	84	B	 <p>4: 3 :1</p>	-
4 <sup>[a]</sup>	16m	85	B	 <p>75o (15:1)</p>	61 <sup>[b]</sup>
5 <sup>[a]</sup>	16h	85	F	 <p>75p (8:1); Z = C(CO<sub>2</sub>CH<sub>3</sub>)<sub>2</sub></p>	14
6 <sup>[a]</sup>	16h	85	B	 <p>75p</p> <p>1.0: 1.3 :0.01</p>	-
7 <sup>[a]</sup>	16l	85	F	No conversion	-
8 <sup>[a]</sup>	16l	85	E	 <p>Z = C(SO<sub>2</sub>Ph)<sub>2</sub></p>	-
9	16h	86	F	Complex mixture	-
10	16h	86	G	Complex mixture	-

entry	enyne	alkene	[Au]	Products	yield (%)
11	<b>16l</b>	<b>86</b>	<b>F</b>	 <b>75q</b>	59

[a] Carried out with activated molecular sieves. [b] Yield is the average of two reactions.



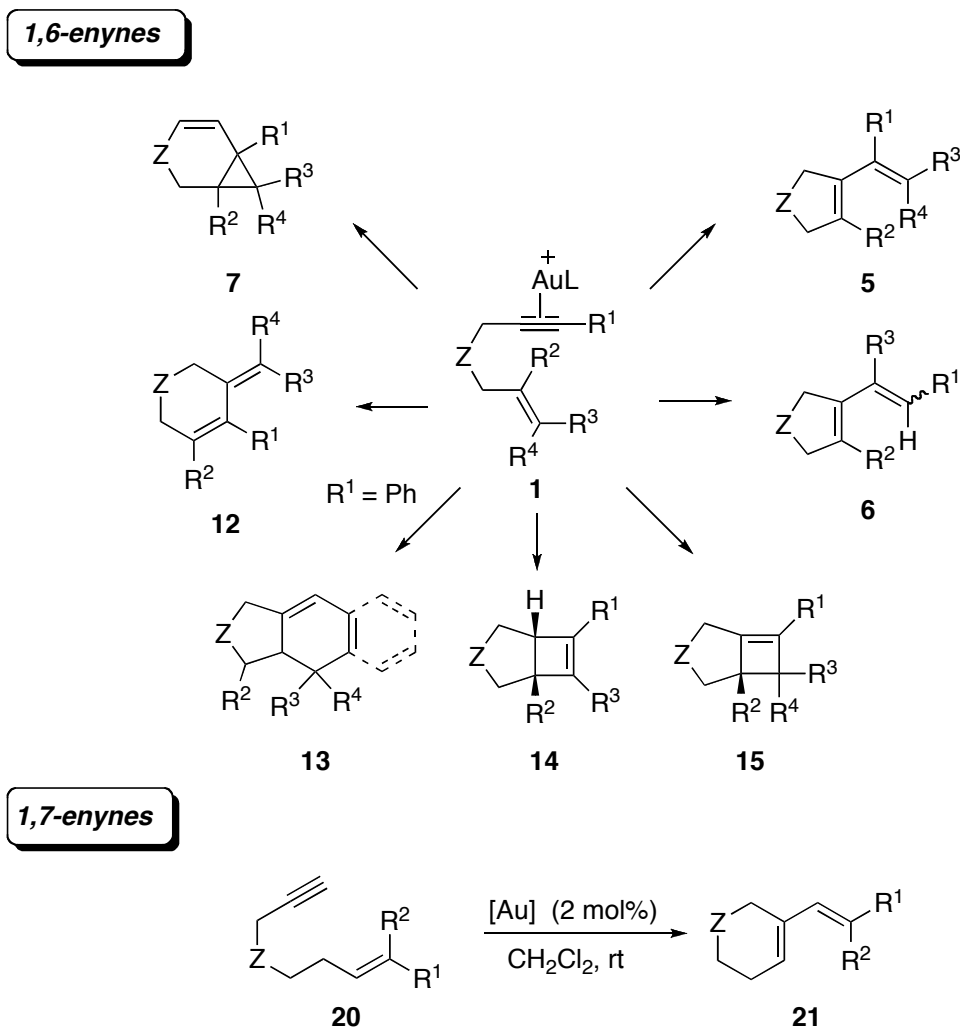
Unfortunately, only cycloisomerization products were obtained in the reaction with allylic sulfone **84** (Table 7, entries 1-3). Dicarboxyl compound **85** in combination with enyne **16m** provided bicyclopropanated product **75p** in good yield as a 15:1 mixture of diastereoisomers (Table 7, entry 4). On the contrary, only low yield of product **75p** was isolated in the reaction with enyne **16h** (Table 7, entry 5) and no reaction was observed with **16l** (Table 7, entry 7). Attempts to perform these reactions with a more active catalyst, such as **B**, only provided cycloisomerization dienes (Table 7, entries 6 and 8). The use of diene **86** did not lead to satisfactory results in the reaction with enyne **16h**, a complex mixture of products was detected using catalyst **F** (Table 7, entry 9), and the use of a less sterically hindered NHC-based catalyst **G**<sup>94</sup> did not increase the selectivity of the transformation (Table 7, entry 10). Interestingly, bicyclopropanated product **75q** was obtained in 59% yield with enyne **16l** (Table 7, entry 11). The relative configuration of **75q** was tentatively assigned based on NMR data. This entry represents a promising result for further developing this synthetic route. Future work will be focused on its application to real systems suitable for the synthesis of the myliol sesquiterpenes.

## 2. Computational Study of the Gold(I)-Catalyzed Cyclization of 1,7-Enynes<sup>98</sup>

As mentioned in the introduction of this chapter, the gold(I)-catalyzed cyclization of 1,7-enynes was studied in our group as a straightforward extension of the investigations on gold-catalyzed cyclization of 1,6-enynes. In contrast to the high structural diversity obtained when employing 1,6-enynes, for the 1,7-counterparts a complete selectivity in the cyclization reaction was observed (Scheme 42).<sup>68</sup> Remarkably, only single cleavage dienes from the *exo* pathway were obtained under the same experimental conditions developed for 1,6-enynes. Since no obvious reason could be envisioned to explain this different behavior, we decided to carry out a computational study of this transformation.

---

98 This work has been done in collaboration with Dr. Ataulpa A. C. Braga.

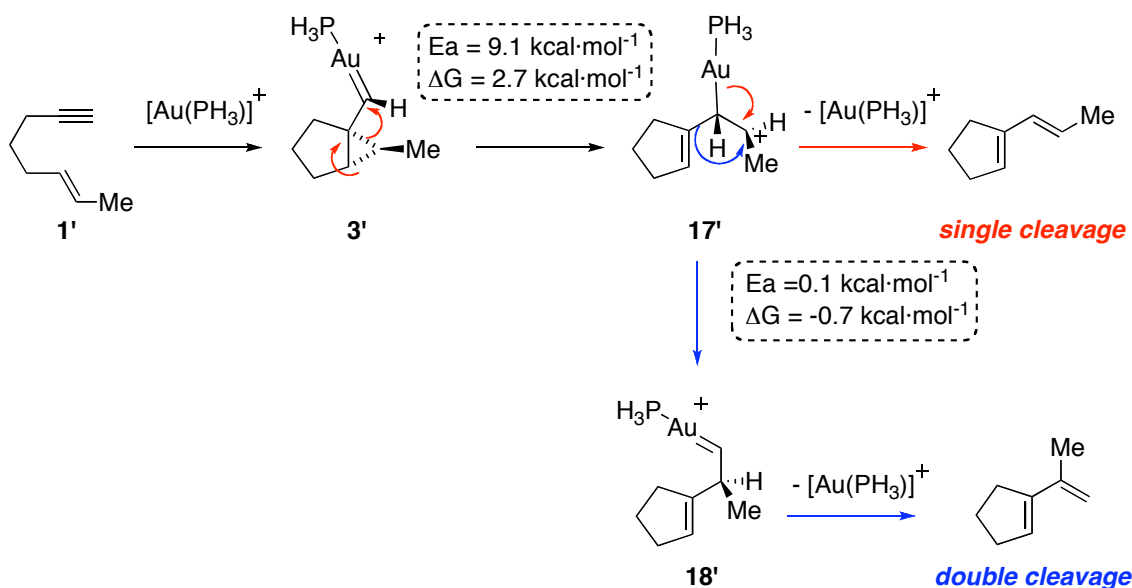


**Scheme 42**

DFT was again the method of choice. With the aim of having comparable results to the computational work already developed in the gold(I)-catalyzed cyclization of 1,6-enynes, hybrid functional B3LYP was used, and the basis sets were 6-31G(d) (C, P, N, H) and LAN2DZ (Au). Simplified models of the molecules were also chosen based on previous studies on gold-catalyzed reactions of enynes.<sup>44</sup>  $\text{PH}_3$  was selected as an initial model to replace bulky phosphines. More realistic models were considered in the later stages of our work.

The previous section of the chapter highlighted the important role of gold carbenes in the gold-catalyzed cyclization of 1,6-enynes (Scheme 43).<sup>44</sup> Formation of cyclopropylcarbene **3** occurs after the nucleophilic attack of the alkene to the alkyne. Migration of electron pairs (Scheme 43, red arrows) gives as a consequence the formation of cationic species **17'**, which is the precursor for the single cleavage products. This diene **5** is formed by proton loss and protodemetalation. In certain cases, a different reaction pathway can be accessed from intermediate **17'**. By a migration of

the cyclopentenyl group (Scheme 43, blue arrows) the rearranged carbene **18'** is yielded. This carbene is the key intermediate in the formation of double cleavage dienes. DFT calculations showed that the transformation of **17'** to **18'** occurs with a very low activation barrier ( $E_a = 0.1 \text{ kcal}\cdot\text{mol}^{-1}$ ), which explains why different substitution in the starting enyne give rise to differently rearranged product. Rearranged carbene **18'** is also accessible directly from **3'** in one step.

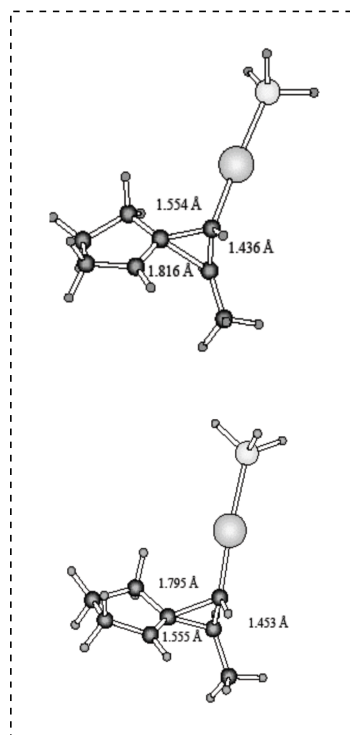
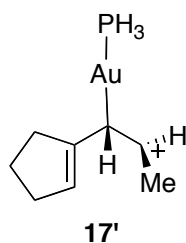


Scheme 43

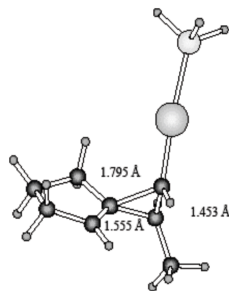
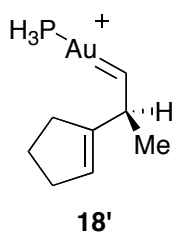
In principle, the same reactivity should be expected for 1,7-enynes, *i.e.*, an activation of the alkyne moiety by gold that promotes a nucleophilic attack from the alkene. The subsequent formation of a cyclopropylgold(I) carbene intermediate was expected to happen in the same way, and the shape of main intermediates was envisioned to be quite similar. As a first approach to the problem, we decided to have a closer look to the intermediates **17'** and **18'** and calculate the corresponding structures for 1,7-enynes.

In the case of 1,6-enynes, the available structures of **17'** and **18'** are shown in Scheme 44.<sup>44</sup> Indeed, they are very similar structures, in which one can draw an imaginary cyclopropane ring including the two closer-to-the-cyclopentenyl group carbon atoms. Thus, the difference between **17'** and **18'** is in the bond length within this imaginary three membered ring, the longest length corresponding to the bond that it is going to be broken to yield the product.

*single cleavage*



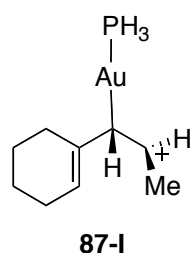
*double cleavage*



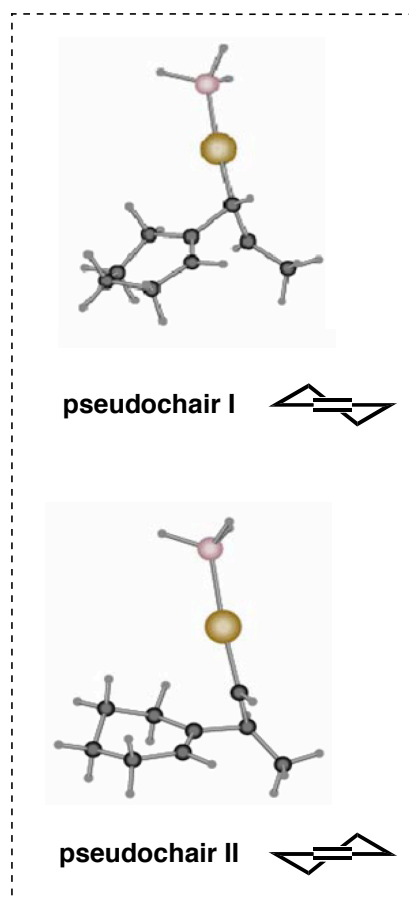
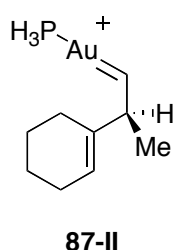
**Scheme 44**

The computed structures for 1,7-enynes **87-I** and **87-II** clearly resemble **17'** and **18'** (Scheme 45). The bond distances in the imaginary cyclopropane rings anticipate the kind of product that it is going to be formed. In addition, there is another remarkable feature that differentiates **87-I** from **87-II**, a different conformation in the six-membered ring. Due to the higher conformational flexibility of a six-membered ring compared with the five-membered ring formed in the reaction with 1,6-enynes, two different pseudochair conformations are obtained in 1,7-enynes reaction intermediates.

single cleavage



double cleavage

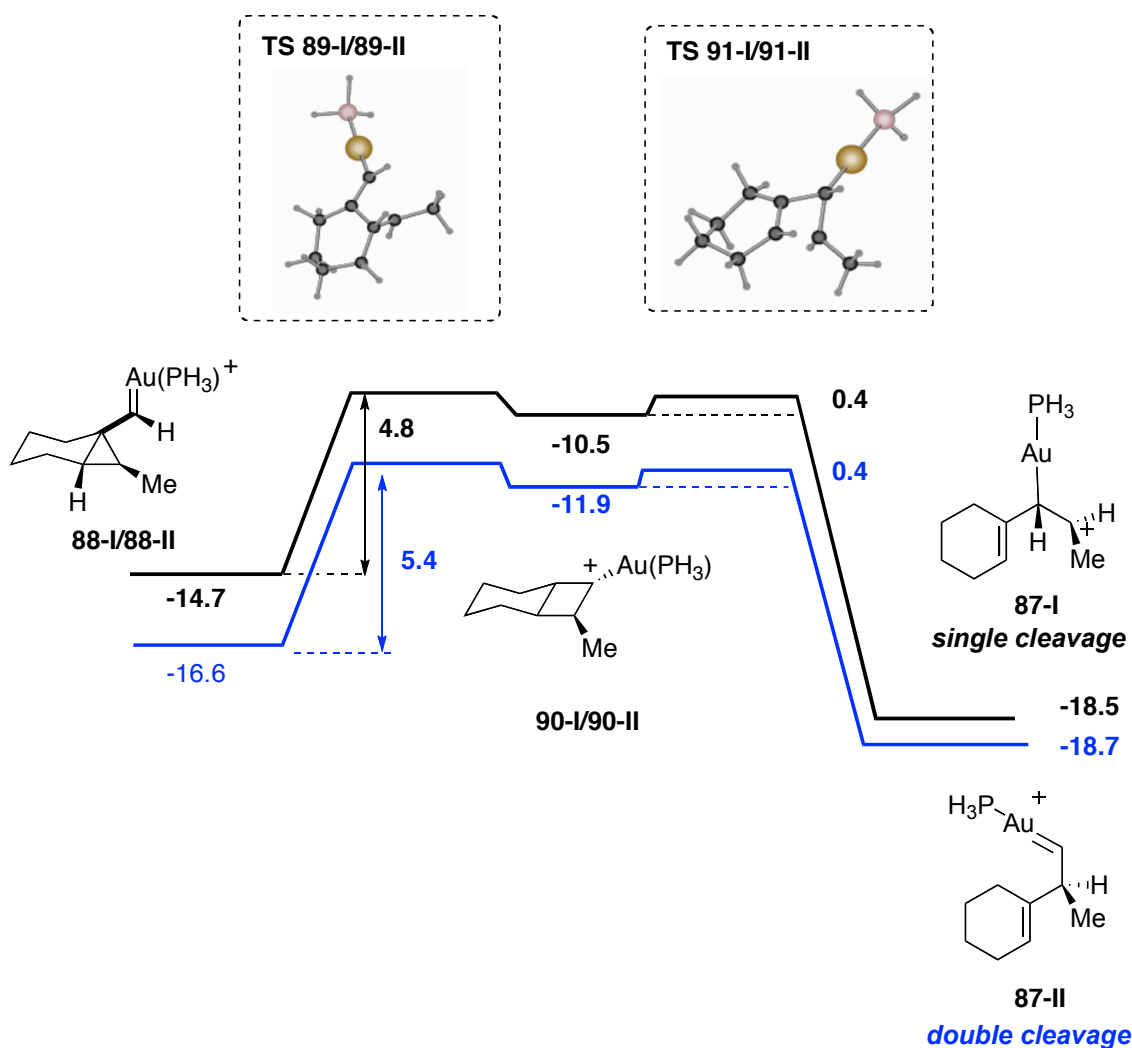


Scheme 45

The finding of this different conformation in the key intermediates of the reaction could indicate that the ring conformation is the discriminating factor in this transformation. In order to study its effect on the outcome of the reaction, the reaction coordinate was calculated for both pseudochairs **I** and **II** separately.

The reaction profile was found to be very similar between the two conformations and to that already known for 1,6-enynes (Scheme 46). Stable cyclopropylgold(I) carbene intermediates **88-I** and **88-II** are formed in the first step. From them, the reaction evolves *via* **TS<sub>89-I</sub>** or **TS<sub>89-II</sub>** through cyclobutane type intermediates **90-I/90-II**. This is a difference with respect to 1,6-enynes, since cyclobutene intermediates were only found in the special case of the formation of cyclopropylcarbene intermediate **3''** in a *syn* fashion.<sup>99</sup> **TS<sub>91-I</sub>** or **TS<sub>91-II</sub>** is reached in an almost flat energy surface, leading to the formation of the already mentioned key intermediates **87-I** and **87-II**.

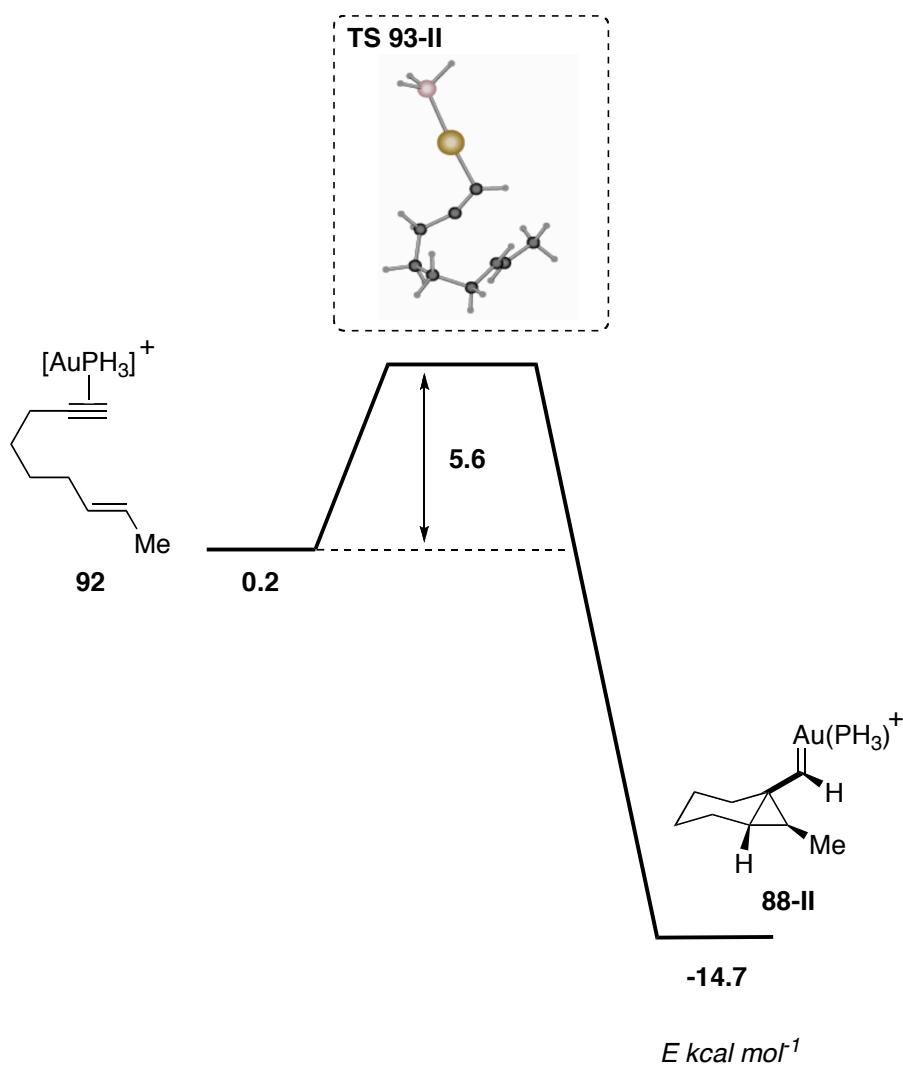
99 Nieto-Oberhuber, C.; López, S.; Jiménez-Núñez, E.; Echavarren, A. M. *Chem. Eur. J.* **2006**, *12*, 5916-5923.



Scheme 46

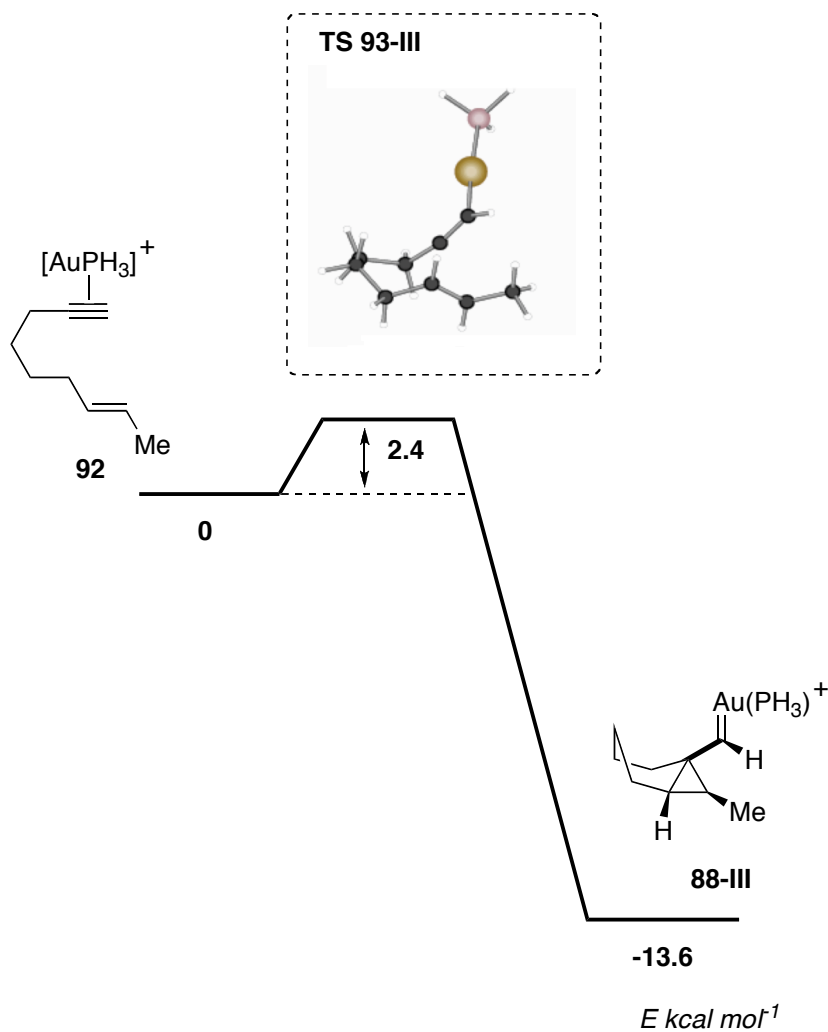
These results established that while the activation energy for each step is very similar between the two conformations, all intermediates are lower in energy for the pathway involving pseudochair **II**, which corresponds with the formation of double cleavage products.

The formation of cyclopropyl intermediate **88-I** and **88-II** from the starting enyne **92** was also computed (Scheme 47). For the case of the double cleavage pathway, this step proceeds through **TS<sub>93-II</sub>** with a energetic barrier of 5.6 kcal. Intriguingly, the corresponding transition state leading to the single cleavage pathway **TS<sub>93-I</sub>** could not be located.



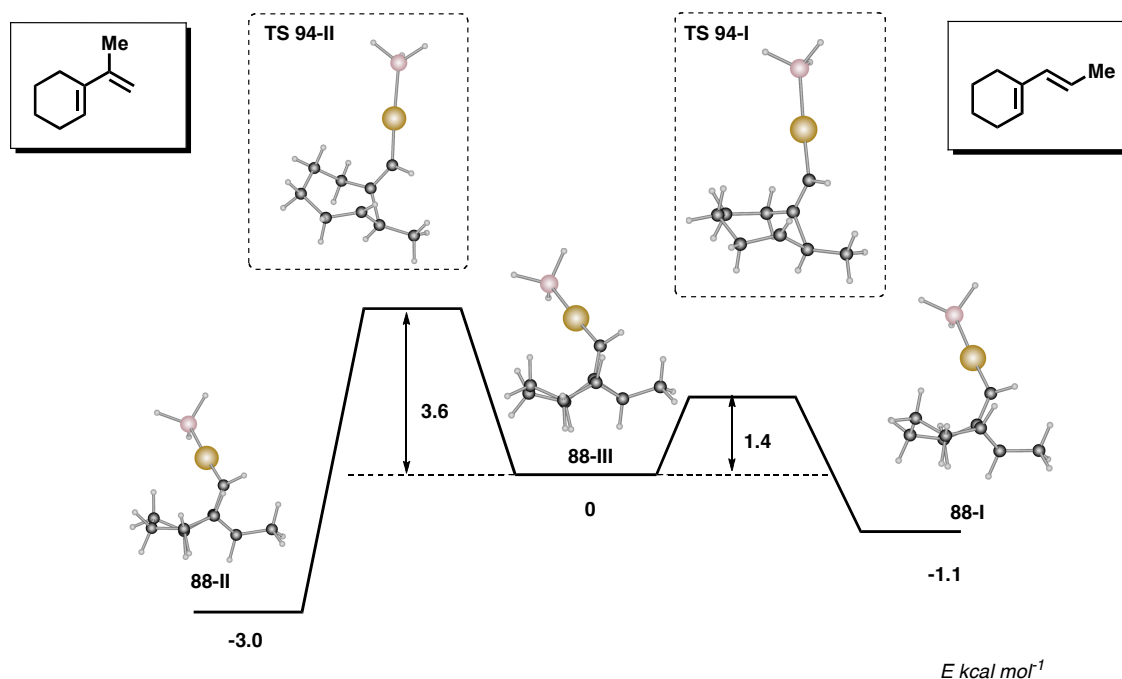
Scheme 47

Further exploration of the reactivity of starting enyne **92** showed the existence of a low energy path leading to an additional conformation of **88**, labeled as **88-III** (Scheme 48). **88-III** has a boat conformation in the cyclohexene ring.



Scheme 48

Indeed, formation of intermediate **88-III** in such boat conformation was found to have the lowest energy barrier for this step, less than the formation of the pseudochair derivative **88-II**. Then, cyclization of 1,7-enynes presumably proceeds through a boat-type cyclopropylgoldcarbene from which both pseudo-chairs corresponding to single-, and double cleavage pathway can be produced. The equilibrium between the six-membered ring conformations for intermediate **88** was then investigated (Scheme 49).



Scheme 49

Our results indicate that both reaction pathways can be accessed from this common intermediate, being the lowest energy barrier the one found for the formation of **88-I**, which gives access to single cleavage dienes. The difference between the two activation energies is roughly 2 kcal·mol<sup>-1</sup>, which corresponds to a ratio of 60:1 favoring single cleavage products for the case of a reaction performed at room temperature. This is consistent with the high selectivity towards single products found experimentally.

In order to get more accurate values for this energetic barrier, QM/MM calculations were performed for this equilibrium using real systems. In such systems, steric effects can also play an important role. More precisely, in structure **88-II** the bulky tether of the enyne (usually malonate, sulfone or tosylamide group) is pointing towards the bulky substituent of the phosphine ligand present in the gold catalyst. Intuitively, this steric hindrance would increase the activation energy for the formation of double cleavage products and thus reinforce the tendency already found in the simple model calculations. For this purpose, ONIOM calculations of **88** in all three conformations were performed for a real system, containing enyne **20d** and biphenyl-based gold catalyst **B**. The conformation of the bulky substituent in the phosphine was taken from available X-ray structure. The malonate tether in the enyne as well as the bulky ligand on the gold catalysts were calculated using molecular mechanics (UFF)

while the rest of the system was computed in quantum mechanics level (ONIOM (B3LYP/6-31G, LAND2Z:UFF). Surprisingly, ONIOM calculations of our real system did not provide any meaningful results. Conformational problems on the bad description of certain steric repulsions by UFF may be the origin of this poor result, which was not further explored.

The question that arises after the DFT study is whether it is possible to modify this selectivity in the gold(I)-catalyzed cyclization of 1,7-enynes. As a summary, the calculations showed that the conformational diversity of intermediates in the initial stage of the skeletal rearrangement process was the key factor for the selective formation of single cleavage products. In addition, this selectivity is only determined by a small energy difference (2 kcal·mol<sup>-1</sup> aprox.). It would be interesting to perform the cyclization with enynes that have some structural constrains to avoid the flexibility of the formed six-membered ring and also to perform the reaction at a higher temperature.

Enynes **20h**, **20g-d<sub>1</sub>** and **95** were selected for the experimental study to add more information to the DFT results (Figure 8). Enyne **20h** was chosen to evaluate if the different substitution in the alkene would favor the formation of the diene through a rearranged carbene species. Studies on the intermolecular trapping with olefins in the cyclization of enyne **20h** have been reported in the previous section.

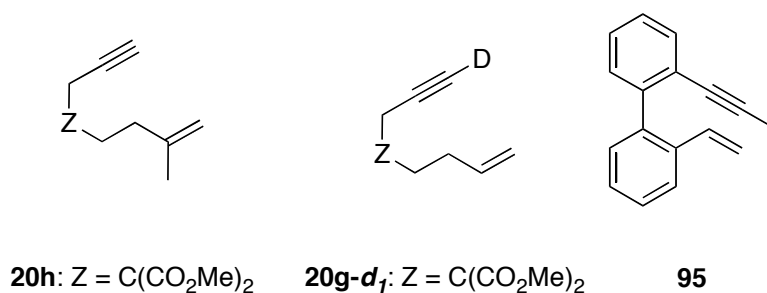
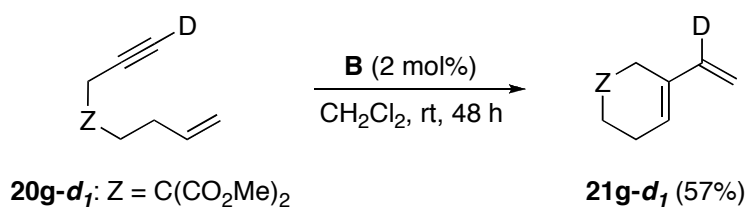


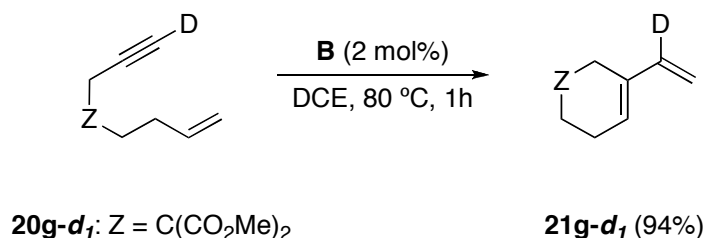
Figure 8. Selected 1,7-enynes **20h**, **20g-d<sub>1</sub>** and **95**.

The purpose of using deuterated enyne **20g-d<sub>1</sub>** was to examine the influence of performing the reaction at higher temperature. Gold(I)-catalyzed cyclization of **20g-d<sub>1</sub>**, at room temperature has been already reported (Scheme 50).<sup>68</sup> Using gold catalyst **B**, single cleavage product **21g-d<sub>1</sub>** was obtained in 57% yield.



Scheme 50

When the reaction was carried out at 80 °C in 1,2-dichloroethane, the reaction time was drastically decreased from 48 h to 1 h, but no change was observed in the outcome of the reaction. Only single cleavage cyclization product **21g-d<sub>1</sub>** was furnished in 94% yield, together with traces of the non-deuterated diene (Scheme 51).

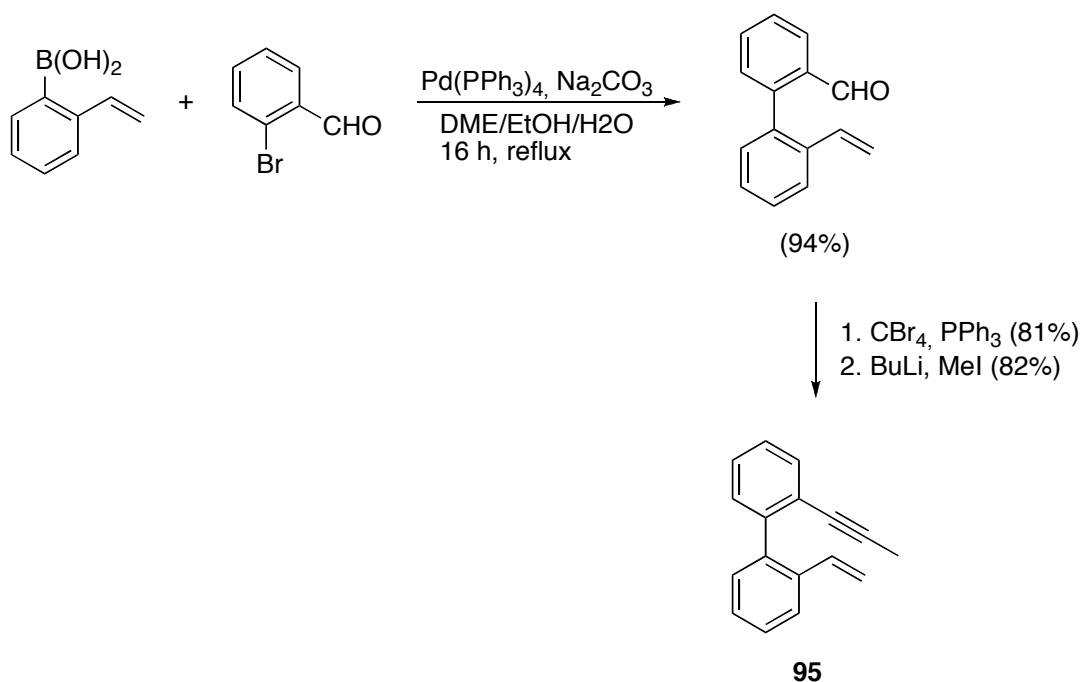


Scheme 51

This experimental result suggests that the energy difference between the barrier to access to the single and double cleavage products is higher than calculated by DFT, since product distribution remained unchanged.

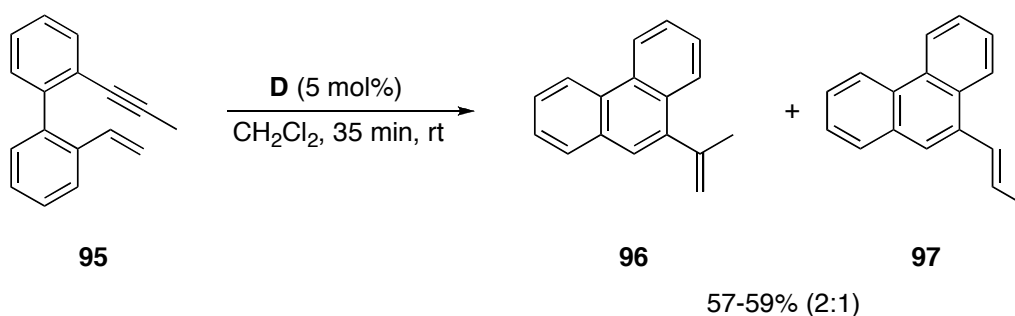
Finally, the effect of the six membered ring conformation was evaluated. The choice of an enyne with a lower conformational freedom conformation such as **95**, would show experimentally the real influence of the conformational flexibility. Enyne **95** was prepared by Suzuki coupling between 2-vinylphenylboronic acid and 2-bromobenzaldehyde, followed by a Corey-Fuchs reaction on the aldehyde to yield the methyl-substituted alkyne (Scheme 52). The use of enyne **95** and related substrates have been reported in the context of metathesis of enynes.<sup>100</sup>

100 Katz, T. J.; Sivavec, T. M. *J. Am. Chem. Soc.* **1985**, *107*, 737-738.



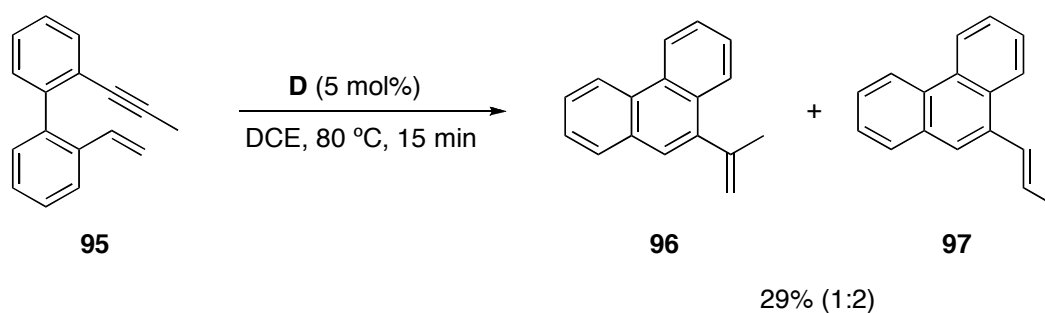
Scheme 52

Reaction of **95** proceeded sluggishly with catalyst **B**. When cationic complex **D** was employed, complete conversion was observed after 35 min at room temperature (Scheme 53). Interesting enough, phenanthrenes **96** and **97** were obtained in a 2:1 ratio. These products correspond to the single- and double cleavage pathway, respectively.



Scheme 53

When the reaction was performed at 80 °C, the ratio between **96** and **97** was reversed, albeit with a decrease in yield (Scheme 54). The low yield observed in these transformations could be related with the presence of a very reactive styrene moiety in starting enyne **95**. However, the use of BHT as polymerization inhibitor did not lead to a significant improvement.

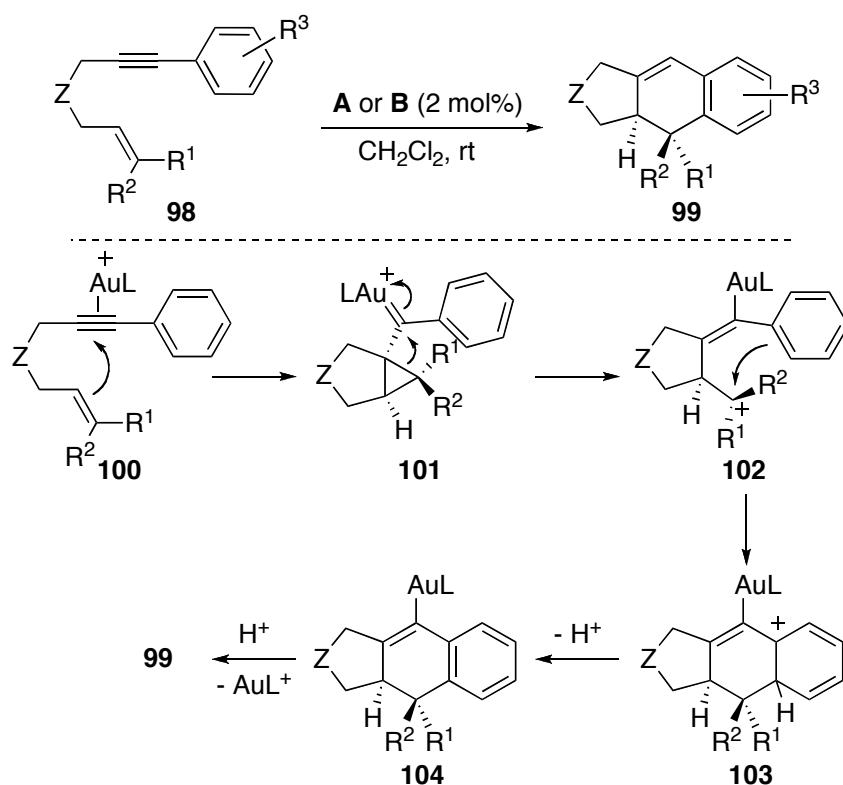


**Scheme 54**

This set of experiments supported our computational results on the gold(I)-catalyzed cyclization of 1,7-enynes. The relevance of the conformation in the six-membered ring in the outcome of the transformation is highlighted by the experiments carried out with enyne **95**. Enyne **95**, having a rather rigid backbone, allows for the formation of both single and double cleavage products, being the first time that the latter is observed in gold-catalyzed cyclization of 1,7-enynes.

### 3. Gold(I)-Catalyzed [4+2]-Cycloadditions of 1,7-Enynes<sup>101</sup>

We were also interested in exploring the synthetic possibilities of 1,7-enynes. For this reason, and as part of the ongoing studies in our research group on the development of new cascade reactions, we decided to explore the performance of substituted 1,7-enynes in the gold(I)-catalyzed [4+2]-cycloaddition. This reaction was originally developed for 1,6-enynes substituted with an additional insaturation (typically, an aromatic ring) in the alkyne (Scheme 55).<sup>51</sup> This reaction consists of a gold catalyzed cyclization that yields intermediate **101**, which evolves to form intermediate **102** that undergoes a formal [4+2]-cycloaddition similar to a Nazarov cyclization, to furnish tricyclic structures such as **99**.<sup>51</sup>



Scheme 55

101 Taken from: Nieto-Oberhuber, C.; Pérez-Galán, P.; Herrero-Gómez, E.; Lauterbach, T.; Rodríguez, C.; López, S.; Bour, C.; Rosellón, A.; Cárdenas, D. J.; Echavarren, A. M. *J. Am. Chem. Soc.* **2008**, *130*, 269-279.

Phenyl-substituted enynes **105a-f** were prepared by Sonogashira coupling of the corresponding enynes unsubstituted at the alkyne with phenyl iodide (Figure 9). Enyne **105f** was synthesized by reduction of the malonate tether of **105a** using  $\text{LiAlH}_4$ . Standard procedures were employed for the protection of the alcohols to give derivatives **105e-f**.

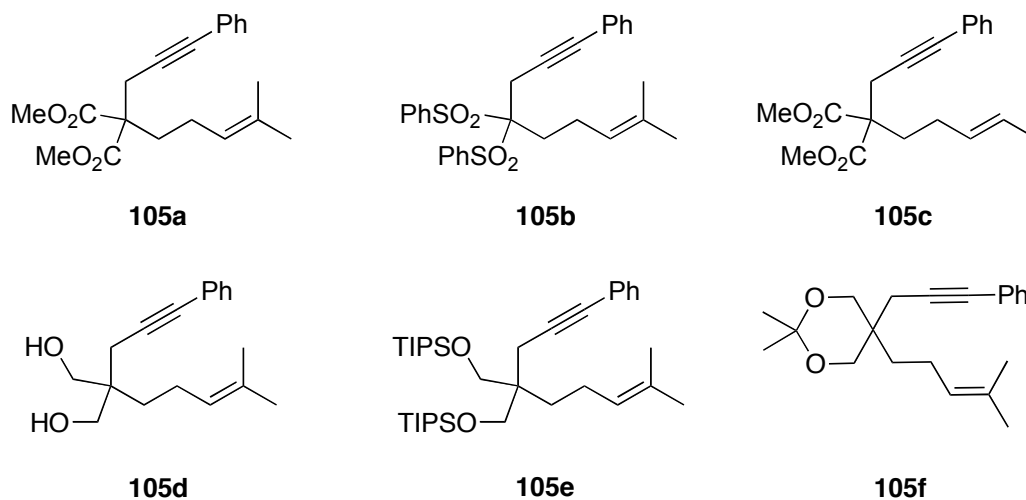
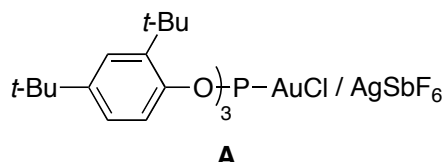
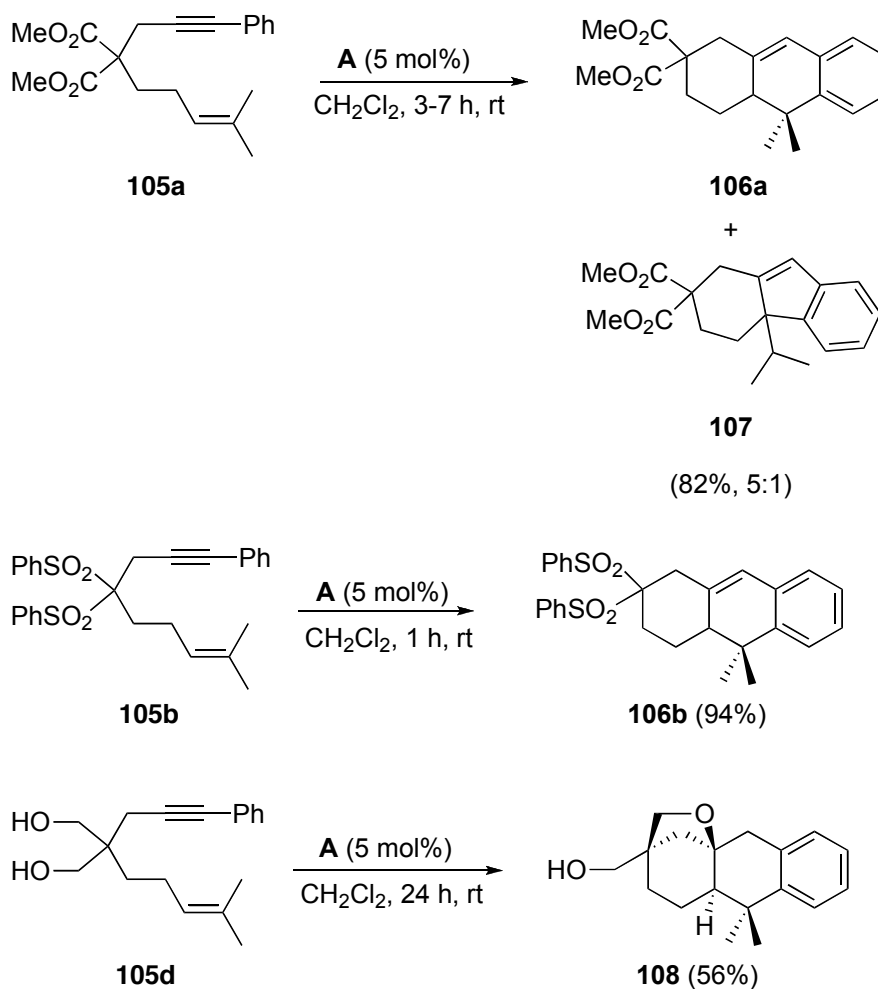


Figure 9. Alkyne-substituted 1,7-enynes **105a-f**.

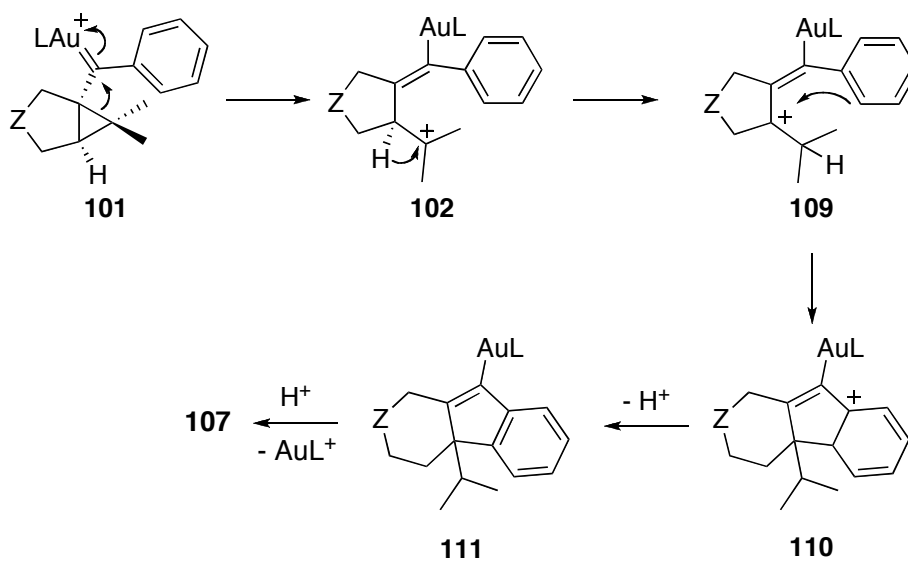
A formal [4+2] cycloaddition reaction was successfully accomplished using enynes **105a-b,d** (Scheme 56), whereas enynes **105c,e-f** only led to single cleavage products or unreacted starting material.



Scheme 56

Cyclization of **105a** afforded the expected tricyclic **106a** along with fluorene derivative **107** as a minor product. Formation of **107** occurs through migration of the positive charge in the corresponding intermediate **102** (Scheme 57), with the subsequent attack of the phenyl ring to the carbon belonging to the five membered ring. Compounds **106a** and **107** were separated by means of semi-preparative HPLC to perform a complete NMR characterization. Reaction of **105b** proceeded uneventfully to provide **106b** in good yield. Unprotected diol **105d** furnished **108**, in which one of the primary alcohols has been added to the alkene in a subsequent reaction that could be catalyzed by gold(I) or  $\text{H}^+$ . The relative configuration of **108** was assigned on the basis of NOESY experiments. Thus, gold(I)-catalyzed [4+2]-cycloaddition can be

satisfactorily extended to substituted 1,7-enynes. These reactions also represent additional examples of the good performance of newly developed catalytic system **A** in cyclization reactions of enynes.



Scheme 57

UNIVERSITAT ROVIRA I VIRGILI

GOLD(I)-CATALYZED CYCLIZATIONS OF 1,6- AND 1,7-ENYNES: NEW GOLD COMPLEXES AND CYCLOPROPANATION REACTIONS

Elena Herrero Gómez

ISBN: 978-84-692-5924-5/DL:T-1663-2009

## *Chapter 2. Conclusions*

UNIVERSITAT ROVIRA I VIRGILI

GOLD(I)-CATALYZED CYCLIZATIONS OF 1,6- AND 1,7-ENYNES: NEW GOLD COMPLEXES AND CYCLOPROPANATION REACTIONS

Elena Herrero Gómez

ISBN: 978-84-692-5924-5/DL:T-1663-2009

- We have developed a novel methodology based on the intermolecular trapping by olefins of the gold(I)-carbene species involved in the gold(I)-catalyzed cyclization of 1,6-enynes. Biscyclopropanated derivatives **75** and alkenylcyclopropane products **76** have been obtained in good yields and selectivities. These experiments support the involvement of carbenic species **3** and **18** in the gold-catalyzed cyclization of 1,6-enynes. Especially relevant was the isolation of derivatives **76**, since it represented the first experimental evidence of the participation of rearranged carbene **18** in such reaction.
- The selective isolation of products type **75** in the reaction with 1,5-cyclooctadiene strongly supports a concerted mechanism for the gold(I)-catalyzed cyclopropanation reaction.
- We have also carried out a DFT study on the gold catalyzed cyclization of 1,7-enynes and have proposed that the observed selectivity towards single cleavage products is due to the conformational diversity of the six-membered ring in the intermediates. In the case of 1,7-enynes the reaction pathway is splitted in two, depending on the pseudochair conformation of the six-membered ring, being the lowest energy barrier the one that give access to the experimentally observed single cleavage derivatives. Additional experiments were carried out to confirm this hypothesis. Using conformationally less flexible 1,7-enynes, we have observed the first example of a double cleavage rearrangement in these systems.
- Substituted 1,7-enynes were also employed as substrates for the formal [4+2] cycloaddition catalyzed by gold in order to broaden the scope of this transformation. Moreover, we have found that the newly developed complex **A** is an excellent precatalyst for this reaction.

UNIVERSITAT ROVIRA I VIRGILI

GOLD(I)-CATALYZED CYCLIZATIONS OF 1,6- AND 1,7-ENYNES: NEW GOLD COMPLEXES AND CYCLOPROPANATION REACTIONS

Elena Herrero Gómez

ISBN: 978-84-692-5924-5/DL:T-1663-2009

*Chapter 2. Experimental section*

UNIVERSITAT ROVIRA I VIRGILI

GOLD(I)-CATALYZED CYCLIZATIONS OF 1,6- AND 1,7-ENYNES: NEW GOLD COMPLEXES AND CYCLOPROPANATION REACTIONS

Elena Herrero Gómez

ISBN: 978-84-692-5924-5/DL:T-1663-2009

## **Experimental Section: Index**

	<b>Page</b>
<b>1. General Methods</b>	253
<b>2. Catalysts</b>	253
<i>Synthesis of tris(2,4-di-tert-butyl-phenyl) phosphite gold(I)chloride (A)</i>	253
<b>3. Gold-Catalyzed Intermolecular Cyclopropanation Reaction</b>	254
3.1 <i>Procedures for the Synthesis of Starting Materials</i>	254
<i>(E)-tert-Butyl(3,7dimethylocta-2,6-dienyloxy)dimethylsilane (83a)</i>	254
<i>(E)-1-(4-Methoxybenzyloxy)-3,7-dimethylocta-2,6-diene (83b)</i>	255
<i>(3-Methylbut-2-enylsulfonyl)benzene (84)</i>	255
<i>2-Allyl-1,3-diphenylpropane-1,3-dione (85)</i>	256
3.2 <i>General Procedure for the Intermolecular Cyclopropanation Reaction</i>	257
<i>Biscyclopropane 75a</i>	257
<i>Biscyclopropane 75b</i>	258
<i>Biscyclopropane 75c</i>	258
<i>Biscyclopropane 75d</i>	259
<i>Biscyclopropane 75e</i>	259
<i>Biscyclopropane 75f</i>	260
<i>Biscyclopropane 75g</i>	260
<i>Biscyclopropane 75h/75h'</i>	262
<i>Biscyclopropane 75i/75i'</i>	262
<i>Biscyclopropanes 75j/75j'</i>	263
<i>Biscyclopropanes 75k/75k'</i>	263
<i>Cyclopropanes 76a/76a'</i>	264
<i>Cyclopropanes 76b/76b'</i>	265
<i>Cyclopropanes 76c/76c'</i>	265
<i>Biscyclopropane 75k</i>	266
<i>Biscyclopropane 75l</i>	266
<i>Biscyclopropane 75m</i>	267
<i>Biscyclopropane 75o</i>	267
<i>Biscyclopropane 75p</i>	268
<i>Biscyclopropane 75q</i>	268

<b>4. Gold(I)-Catalyzed Cyclization of 1,7-Enynes</b>	270
4.1. Computational Details	272
4.2. Cartesian Coordinates (in Å) and Absolute Energies (in a.u.)	271
<b>Compound 88-I</b>	272
<b>TS89-I</b>	273
<b>Compound 90-I</b>	274
<b>TS91-I</b>	275
<b>Compound 87-I</b>	276
<b>Compound 88-II</b>	277
<b>TS89-II</b>	278
<b>Compound 90-II</b>	279
<b>TS91-II</b>	280
<b>Compound 87-II</b>	281
<b>Compound 92</b>	283
<b>TS93-II</b>	284
<b>TS93-III</b>	286
<b>Compound 88-III</b>	287
<b>TS94-II</b>	288
<b>TS94-I</b>	290
4.3. Procedures for the Synthesis of Starting Enynes	291
Dimethyl 2-(3-methylpent-3-enyl)-2-(prop-2-ynyl)malonate ( <b>20h</b> )	291
Dimethyl 2-(but-3-enyl)-2-(prop-2-ynyl)malonate ( <b>20g</b> )	291
2-(But-3-enyl)-2-(3-deuterioprop-2-ynyl)malonic acid dimethyl ester ( <b>20g-d<sub>1</sub></b> )	291
Synthesis of 2-(Prop-1-ynyl)-2'-vinylbiphenyl ( <b>95</b> )	292
2-(2,2-Dibromovinyl)-2'-vinylbiphenyl	292
2-(Prop-1-ynyl)-2'-vinylbiphenyl ( <b>95</b> )	293
4.4. Procedure for the Gold(I)-Catalyzed Cyclization of Enyne <b>20h</b>	293
Dimethyl 4-methyl-3-vinylcyclohex-3-ene-1,1-dicarboxylate ( <b>21h</b> )	293
4.5. Procedure for the Gold(I)-Catalyzed Cyclization of Enyne <b>20g-d<sub>1</sub></b>	294
D-dimethyl 3-vinylcyclohex-3-ene-1,1-dicarboxylate ( <b>21g-d<sub>1</sub></b> )	294
4.6. Procedure for the Gold(I)-Catalyzed Cyclization of Enyne <b>95</b>	294
9-(prop-1-en-2-yl)phenantrene ( <b>96</b> )	294

<i>E</i> -9-(prop-1-enyl)phenantrene ( <b>97</b> )	295
<b>5. Gold(I)-Catalyzed [4+2] Cycloaddition of Substituted 1,7-Enynes</b>	295
5.1. Procedures for the Synthesis of Starting Enynes	295
Dimethyl 2-(4-methylpent-3-enyl)-2-(prop-2-ynyl)malonate ( <b>20e</b> )	295
4,4-Bis(phenylsulfonyl)-8,8-dimethyl-7-hepten-1-yne ( <b>20c</b> )	296
( <i>E</i> )-dimethyl-2-(pent-3-enyl)-2-(prop-2-ynyl)malonate ( <b>20d</b> )	296
5.2. General procedure for the Sonogashira coupling	297
Dimethyl 2-(4-methylpent-3-enyl)-2-(3-phenylprop-2-ynyl)malonate ( <b>105a</b> )	297
4,4-Bis(phenylsulfonyl)-8,8-dimethyl-7-hepten-1-yne ( <b>105b</b> )	297
( <i>E</i> )-dimethyl 2-(pent-3-enyl)-2-(3-phenylprop-2-ynyl)malonate ( <b>105c</b> )	298
2-(4-methylpent-3-enyl)-2-(3-phenylprop-2-ynyl)propane-1,3-diol ( <b>105d</b> )	298
3,3,9,9-tetraisopropyl-2,10-dimethyl-6-(4-methylpent-3-enyl)-6-(3-phenylprop-2-ynyl)-4,8-dioxa-3,9-disilaundecane ( <b>105e</b> )	299
2,2-dimethyl-5-(4-methylpent-3-enyl)-5-(3-phenylprop-2-ynyl)-1,3-dioxane ( <b>105f</b> )	299
5.3. General Procedure for the [4+2] Cycloaddition of Substituted 1,7-Enynes	300
Dimethyl 10,10-dimethyl-3,4,4a,10-tetrahydroanthracene-2,2(1 <i>H</i> )-dicarboxylate ( <b>106a</b> )	300
Dimethyl 4a-isopropyl-4,4a-dihydro-1 <i>H</i> -fluorene-2,2(3 <i>H</i> )-dicarboxylate ( <b>107</b> )	301
2,2-Bis(phenylsulfonyl)-10,10-dimethyl-1,2,3,4,4a,10-hexahydroanthracene ( <b>106b</b> )	301
Cyclization product <b>108</b>	302
<b>6. Crystallographic Data</b>	303
Biscyclopropane <b>75c</b>	303
Biscyclopropane <b>75f</b>	311
Biscyclopropane <b>75l</b>	317

UNIVERSITAT ROVIRA I VIRGILI

GOLD(I)-CATALYZED CYCLIZATIONS OF 1,6- AND 1,7-ENYNES: NEW GOLD COMPLEXES AND CYCLOPROPANATION REACTIONS

Elena Herrero Gómez

ISBN: 978-84-692-5924-5/DL:T-1663-2009

## 1. General Methods

All reactions were carried out under inert atmosphere of N<sub>2</sub> or Ar. Solvents were dried using a Solvent Purification System (SPS) or using standard procedures,<sup>102</sup> except for dimethylformamide that was purchased anhydrous and packaged under nitrogen (Aldrich).

Analytical thin layer chromatography was carried out using TLC-aluminium sheets with 0.2 mm of silica gel (Merk GF<sub>234</sub>). Flash chromatography purifications were carried out using flash grade silica gel (SDS Chromatogel 60 ACC, 40-60 μm).

NMR spectra were recorded at 23°C (except otherwise stated) on the following spectrometers: Bruker Avance 400 Ultrashield (400 MHz for <sup>1</sup>H, and 100 MHz for <sup>13</sup>C) and Bruker Avance 500 Ultrashield (500 MHz for <sup>1</sup>H, and 125 MHz for <sup>13</sup>C) at the *Institut Català d'Investigació Química (ICIQ)*. Mass spectra were recorded on a Waters LCT Premier (ESI) and Waters GCT (EI, CI) spectrometers at the ICIQ. Melting points were determined using a Büchi melting point apparatus.

## 2. Catalysts

The following complexes and salts are commercially available and were used as received: NaAuCl<sub>4</sub> (Johnson Matthey PLC), [AuCl(PPh<sub>3</sub>)] (Stream), PdCl<sub>2</sub> (Alfa Aesar), CuI (Fluka), and AgSbF<sub>6</sub> (Aldrich). Complexes PdCl<sub>2</sub>(PPh<sub>3</sub>)<sub>2</sub>,<sup>103</sup> Pd(PPh<sub>3</sub>)<sub>4</sub>,<sup>104</sup> [Au(PPh<sub>3</sub>)(NCMe)]SbF<sub>6</sub>,<sup>35</sup> **B**,<sup>82</sup> **E**,<sup>51</sup> **F**,<sup>94</sup> **G**,<sup>94</sup> and **H**<sup>94</sup> were prepared following the described procedures.

### Synthesis of tris(2,4-di-tert-butyl-phenyl) phosphite gold(I)chloride (**A**).

Sodium tetrachloroaurate dihydrate (1.38 mmol) was dissolved in water, and the orange solution was cooled to 0 °C. To this solution 2,2'-thiodiethanol (3.77 mmol) was slowly added with stirring. Then, a solution of the phosphite ligand (1.25 mmol) in

---

102 (a) Burfield, D. R.; Smithers, R. H. *J. Org. Chem.* **1978**, *43*, 3966-3968. (b) Burfield, D. R.; Lee, K.-H.; Smithers, R. H. *J. Org. Chem.* **1977**, *42*, 3060-3065. (c) Perrin, D. D.; Armarego, S. L. F.; Perrin, D. R. *Purification of Laboratory Chemicals*; Pergamon: New York, 1980.

103 Heck, R. F. *Palladium Reagents in Organic Synthesis*; Academic Press: London, 1985.

104 Tellier, F.; Sauvetre, R.; Normant, J. F. *J. Organomet. Chem.* **1985**, *292*, 19-28

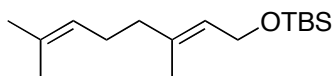
pentane was added dropwise to give a white solid. The solid was filtered off, washed with pentane, and dried *in vacuo*. Yield = 94%.  $^1\text{H}$  NMR (400 MHz,  $\text{CDCl}_3$ )  $\delta$  7.43-7.40 (m, 6H), 7.13 (dd,  $J = 8.6, 2.5$  Hz, 3H), 1.44 (s, 27 H), 1.29 (s, 27H).  $^{31}\text{P}$  NMR (161.98 MHz,  $\text{CDCl}_3$ )  $\delta$  103.78.  $^{13}\text{C}$  NMR (100 MHz,  $\text{CDCl}_3$ )  $\delta$  148.30 (C), 147.42 ( $^2J_{\text{C-P}} = 5.9$  Hz, C), 139.28 ( $^3J_{\text{C-P}} = 6.9$  Hz, C), 125.54 (CH), 124.34 (CH), 119.35 ( $^3J(^{13}\text{C}-^{31}\text{P}) = 8.8$  Hz, CH), 35.27 (C), 34.84 (C), 31.56 ( $\text{CH}_3$ ), 30.72 ( $\text{CH}_3$ ). HRMS-ESI calcd for  $\text{C}_{42}\text{H}_{63}\text{AuClNaO}_3\text{P}$   $[\text{M}+\text{Na}]^+$ : 901.3767. Found: 901.3752.

### 3. Gold-catalyzed Intermolecular Cyclopropanation Reaction

#### 3.1. Procedures for the synthesis of starting materials

The starting enynes were synthesized following literature procedures: **16a**,<sup>105</sup> **16g**,<sup>106</sup> **16h**,<sup>107</sup> **16l**,<sup>108</sup> **16m**<sup>109</sup> and **16n**.<sup>110</sup>

#### (*E*)-*tert*-Butyl(3,7dimethylocta-2,6-dienyloxy)dimethylsilane (**83a**)<sup>111</sup>

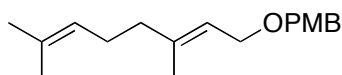


1.30 g of imidazole (19.06 mmol, 3.0 equiv) were added to a stirred solution of 1.43 g of TBSCl (9.53 mmol, 1.5 equiv) in 7 mL of  $\text{CH}_2\text{Cl}_2$ . After stirring for an additional 1 h, 1.12 mL of Geraniol (6.35 mmol, 1.0 equiv) were added dropwise and the reaction mixture was stirred for 16 h at rt. The reaction was quenched with water. Extractive work-up ( $\text{CH}_2\text{Cl}_2$ , brine) and flash chromatography (hexane:EtOAc, 19:1) yielded 433 mg of the desired product (1.61 mmol) as a colorless oil. Yield = 25%. 550

- 
- 105 Trost, B. M.; Braslau, R. *Tetrahedron Lett.* **1988**, *29*, 1231-1234.  
106 Trost, B. M.; Tanoury, G. J. *J. Am. Chem. Soc.* **1987**, *109*, 4753-4755.  
107 Chatani, N.; Morimoto, T.; Muto, T.; Murai, S. *J. Am. Chem. Soc.* **1994**, *116*, 6049-6050.  
108 M<sup>a</sup> Paz Muñoz Herranz, Doctoral Thesis, 2004, UAM.  
109 Nevado, C.; Charruault, L.; Michelet, V.; Nieto-Oberhuber, C.; Muñoz, M. P.; Méndez, M.; Rager, M.-N.; Genêt, J. P.; Echavarren, A.M. *Eur. J. Org. Chem.* **2003**, 706-713.  
110 Trost, B. M.; Tanoury, G. J. *J. Am. Chem. Soc.* **1998**, *110*, 1636-1638.  
111 (a) Lu, X.; Cseh, S.; Byun, H.-S.; Tigyi, G.; Bittman, R. *J. Org. Chem.* **2003**, *68*, 7046-7050. (b) Voelkert, M.; Uwai, K.; Tebbe, A.; Popkirova, B.; Wagner, M.; Kuehlmann, J.; Waldmann, H. *J. Am. Chem. Soc.* **2003**, *125*, 12749-12758.

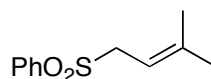
mg of geraniol (3.57 mmol, 55%) were also recovered.  $^1\text{H}$  NMR ( $\text{CDCl}_3$ , 400 MHz)  $\delta$  5.31 (t,  $J = 6.3$  Hz, 1H), 5.10 (t,  $J = 6.7$  Hz, 1H), 4.19 (d,  $J = 6.5$  Hz, 2H), 2.12-1.97 (m, 4H), 1.68 (s, 3H), 1.62 (s, 3H), 1.60 (s, 3H), 0.91 (s, 9H), 0.07 (s, 6H).

**(E)-1-(4-Methoxybenzyloxy)-3,7-dimethylocta-2,6-diene (83b)**<sup>112</sup>



260 mg of NaH (60% in mineral oil, 6.5 mmol, 1.0 equiv) were suspended in 10 mL of DMF. The, 1.12 mL of geraniol (6.5 mmol, 1.0 equiv) were added dropwise and the mixture was stirred for 1 h at rt. Afterwards, the solution was cooled down to 0 °C, and 240 mg of TBAI (0.65 mmol, 1.0 equiv) were added in one portion, followed by dropwise addition of 0.9 mL of PMBCl (6.5 mmol, 1.0 equiv). After stirring for 1 h at 0 °C, the mixture was allowed to warm up to rt and was stirred for additional 20 h. The reaction was quenched with water. Extractive work-up (EtOAc, 10% HCl) and flash chromatography (hexane:EtOAc, 49:1) yielded 1.74 g of the product as a colorless oil (99%). Yield : 97%.  $^1\text{H}$  NMR ( $\text{CDCl}_3$ , 400 MHz)  $\delta$  7.29-7.25 (m, 2H), 6.90-6.85 (m, 2H), 5.39 (t,  $J = 6.8$  Hz, 1H), 5.10 (t,  $J = 6.7$  Hz, 1H), 4.43 (s, 2H), 4.00 (d,  $J = 6.8$  Hz, 2H), 3.80 (s, 3H), 2.14-2.01 (m, 4H), 1.68 (s, 3H), 1.64 (s, 3H), 1.60 (s, 3H).

**(3-Methylbut-2-enylsulfonyl)benzene (84)**<sup>113</sup>



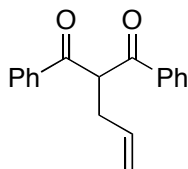
2.0 g of 3,3-dimethylallyl bromide (12.08 mmol 1.0 equiv) were dissolved in 25 mL of DMF and 1.98 g of benzenesulfonic acid sodium salt (12.08 mmol, 1.0 equiv) were added. The resulting yellow reaction mixture was stirred at rt for 24 h and quenched by adding  $\text{H}_2\text{O}$  at 0 °C. After extractive work-up (EtOAc, 10% HCl) and flash chromatography (hexane:EtOAc, 4:1) 1.891 g of the desired product were obtained (8.99 mmol). Yield = 75%. White solid; mp 54-55 °C.  $^1\text{H}$  NMR ( $\text{CDCl}_3$ , 400 MHz)  $\delta$  7.88-7.83 (m, 2H), 7.66-7.60 (m, 1H), 7.57-7.49 (m, 2H), 5.21-5.14 (m, 1H), 3.78 (d,  $J = 8.0$  Hz, 2H), 1.71 (s, 3H), 1.31 (s, 3H);  $^{13}\text{C}$  NMR ( $\text{CDCl}_3$ , 100 MHz)  $\delta$  143.1 (C),

112 Kanada, R. M.; Itoh, D.; Nagai, M.; Nijima, J.; Asai, N.; Mizui, Y.; Abe, S.; Kotake, Y. *Angew. Chem. Int. Ed.* **2007**, *46*, 4350-4355.

113 Chow, S. Y.; Williams, H. J.; Huang, Q.; Nanda, S.; Scott, A. I. *J. Org. Chem.* **2005**, *70*, 9997-10003.

138.90 (C), 133.68 (CH), 129.14 (CH), 128.65 (CH), 110.60 (CH), 56.38 (CH<sub>2</sub>), 26.00 (CH<sub>3</sub>), 17.90 (CH<sub>3</sub>). HRMS-ESI calcd for C<sub>11</sub>H<sub>14</sub>NaO<sub>2</sub>S [M+Na]<sup>+</sup>: 233.0612. Found 233.0609.

### 2-Allyl-1,3-diphenylpropane-1,3-dione (85)<sup>114</sup>



Procedure 1: 190 mg of tetrakis(triphenylphosphine)palladium (0.14 mmol, 0.02 equiv) and 0.015 mL of AcOH (0.27 mmol, 0.4 equiv) were added to a mixture of 1.50 g of dibenzoylmethane (6.69 mmol, 1.0 equiv) and 0.68 mL of allyl alcohol (10.03 mmol, 1.5 equiv). The system was heated up to 80 °C. The solids became a liquid solution, which was stirred for 2 h at this temperature. The reaction mixture was cooled down slowly to rt and stirred for 12 h while it became solid again. After dissolving in EtOAc and extraction with H<sub>2</sub>O the crude was purified by flash chromatography (hexane:EtOAc, 10:1) to yield 1.21 g of the desired product (4.56 mmol) as yellow solid. Yield = 68%.

Procedure 2: 720 mg of NaH (60% in mineral oil, 17.93 mmol, 1.0 equiv) were suspended in 24 mL of DMF. Afterwards, a solution of 4.00 g dibenzoylmethane (17.93 mmol, 1.0 equiv) in 11 mL of DMF was added at 0 °C, followed by slow addition of 1.56 mL allyl bromide (17.93 mmol, 1.0 equiv). The reaction mixture was allowed to warm up to rt and stirred for additional 24 h. The reaction was quenched with H<sub>2</sub>O and the crude was purified by extractive work-up (EtOAc, 10% HCl) and flash chromatography (hexane:EtOAc, 10:1) to yield 2.43 g (9.19 mmol) as slightly yellow solid. Yield = 52%. <sup>1</sup>H NMR (CDCl<sub>3</sub>, 400 MHz) δ 7.98-7.93 (m, 4H), 7.60-7.54 (m, 2H), 7.49-7.42 (m, 4H), 5.88 (ddt, *J* = 17.0, 10.2 Hz, 6.8 Hz, 1H), 5.29 (t, *J* = 6.8 Hz, 1H), 5.11 (dq, *J* = 17.0, 1.6, 1.6 Hz, 1H), 5.03 (dd, *J* = 10.2, 1.7 Hz, 1H), 2.90-2.85 (m, 2H).

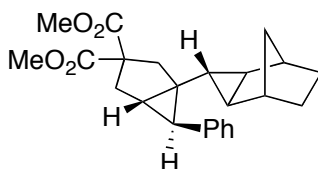
---

114 (a) Patil, N. T.; Yamamoto, Y. *Tetrahedron Lett.* **2004**, 3101-3103. (b) Hwu, J. R.; Chen, C. N.; Shiao, S.-S. *J. Org. Chem.* **1995**, 60, 856-862.

### 3.2 General procedure for the intermolecular cyclopropanation reaction with olefins:

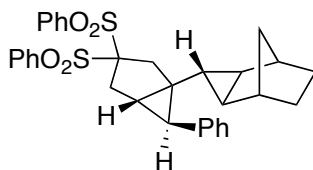
A solution of the corresponding enyne (0.15-0.50 mmol) in dry  $\text{CH}_2\text{Cl}_2$  (1 mL) was added to a mixture of gold(I) complex (5 mol%) and alkene (5 equiv) in dry  $\text{CH}_2\text{Cl}_2$  (1 mL) at  $-60^\circ\text{C}/-40^\circ\text{C}$  (Haake EK 90 immersion cooler). After stirring 1 h at the stated temperature, the mixture was then slowly warmed up in the cooling bath by turning the immersion cooler off until the mixture reached room temperature (*ca.* 15 h). The resulting mixture was purified by flash chromatography (hexanes/EtOAc) to give the corresponding cyclopropane adducts. If needed, solids were additionally purified by trituration in pentane.

#### Biscyclopropane 75a (Table 2, entry 1)



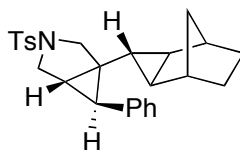
Colorless oil.  $^1\text{H}$  NMR (400 MHz,  $\text{CDCl}_3$ )  $\delta$  7.25-7.19 (m, 2H), 7.17-7.09 (m, 3H), 3.73 (s, 3H), 3.71 (s, 3H), 2.72 (d,  $J = 14.0$  Hz, 1H), 2.62-2.58 (m, 2H), 2.40 (d,  $J = 14.0$  Hz, 1H), 2.15-2.10 (m, 1H), 1.76-1.73 (m, 1H), 1.71 (d,  $J = 4.1$  Hz, 1H), 1.56 (dt,  $J = 4.1, 1.5$  Hz, 1H), 1.29 (dtt,  $J = 26.0, 10.7, 3.5$  Hz, 2H), 1.18-1.01 (m, 2H), 0.67 (d,  $J = 10.4$  Hz, 1H), 0.59 (t,  $J = 2.9$  Hz, 1H), 0.54 (dd,  $J = 7.2, 2.9$  Hz, 1H), 0.42 (d,  $J = 10.5$  Hz, 1H), 0.26 (dd,  $J = 7.2, 2.6$  Hz, 1H).  $^{13}\text{C}$  NMR (100 MHz,  $\text{CDCl}_3$ )  $\delta$  173.44 (C), 172.83 (C), 138.93 (C), 129.33 (CH), 127.86 (CH), 125.71 (CH), 60.48 (C), 53.14 ( $\text{CH}_3$ ), 53.03 ( $\text{CH}_3$ ), 42.25 ( $\text{CH}_2$ ), 37.31 ( $\text{CH}_2$ ), 36.11 (C), 36.05 (CH), 35.79 (CH), 32.57 (CH), 29.71 ( $\text{CH}_2$ ), 29.62 ( $\text{CH}_2$ ), 28.51 ( $\text{CH}_2$ ), 28.06 (CH), 23.98 (CH), 21.95 (CH), 13.85 (CH). HRMS-ESI calcd for  $\text{C}_{24}\text{H}_{28}\text{NaO}_4$   $[\text{M}+\text{Na}]^+$ : 403.1885. Found: 403.1877. The structure of **75a** was confirmed by COSY, HMQC, HMBC, and NOESY experiments.

### Biscyclopropane 75b (Table 2, entry 2)



White Solid, dec. at 177 °C.  $^1\text{H}$  NMR (400 MHz,  $\text{CDCl}_3$ )  $\delta$  8.18-8.12 (m, 2H), 8.09-8.03 (m, 2H), 7.77-7.69 (m, 2H), 7.67-7.58 (m, 4H), 7.27-7.20 (m, 2H), 7.18-7.07 (m, 3H), 3.14 (dd,  $J = 16.1, 6.3$  Hz, 1H), 2.93 (part A, AB system,  $J = 16.3$  Hz, 1H), 2.89 (part B, AB system,  $J = 16.3$  Hz, 1H), 2.72 (d,  $J = 16.1$ , 1H), 2.22 (d,  $J = 4.3$  Hz, 1H), 2.11-2.08 (m, 1H), 1.80-1.75 (m, 1H), 1.74-1.71 (m, 1H), 1.36-1.20 (m, 2H), 1.19-1.10 (m, 1H), 1.09-1.00 (m, 1H), 0.71 (dd,  $J = 7.3, 2.9$  Hz, 1H), 0.68-0.60 (m, 1H), 0.53 (t,  $J = 2.8$  Hz, 1H), 0.43 (d,  $J = 10.5$  Hz, 1H), 0.27 (dd,  $J = 7.3, 2.1$  Hz, 1H).  $^{13}\text{C}$  NMR (100 MHz,  $\text{CDCl}_3$ )  $\delta$  138.14 (C), 137.09 (C), 136.41 (C), 134.80 (CH), 134.76 (CH), 132.07 (CH), 131.65 (CH), 129.02 (CH), 128.93 (CH), 128.90 (CH), 127.95 (CH), 125.93 (CH), 97.52 (C), 42.01 ( $\text{CH}_2$ ), 39.24 (C), 36.77 ( $\text{CH}_2$ ), 36.14 (CH), 36.04 (CH), 35.81 (CH), 29.94 (CH), 29.61 ( $\text{CH}_2$ ), 29.46 ( $\text{CH}_2$ ), 28.48 ( $\text{CH}_2$ ), 24.58 (CH), 21.59 (CH), 14.16 (CH). HRMS-ESI calcd for  $\text{C}_{32}\text{H}_{32}\text{NaO}_2\text{S}$   $[\text{M}+\text{Na}]^+$ : 567.1640. Found: 567.1664. The structure of **75b** was confirmed by COSY, HMQC, HMBC, and NOESY experiments.

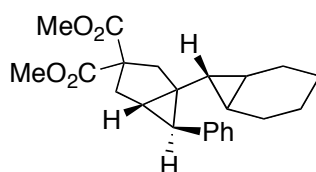
### Biscyclopropane 75c (Table 2, entry 3)



White solid, mp 143-145 °C.  $^1\text{H}$  NMR (400 MHz,  $\text{CDCl}_3$ )  $\delta$  7.71 (d,  $J = 8.2$  Hz, 2H), 7.34 (d,  $J = 8.2$  Hz, 2H), 7.27-7.21 (m, 2H), 7.19-7.07 (m, 3H), 3.62 (d,  $J = 9.2$  Hz, 1H), 3.57 (d,  $J = 9.4$  Hz, 1H), 3.13 (dd,  $J = 9.2, 3.8$  Hz, 1H), 3.03 (d,  $J = 9.4$  Hz, 1H), 2.45 (s, 3H), 2.08 (bs, 1H), 2.04 (d,  $J = 4.1$  Hz, 1H), 1.76 (bs, 1H), 1.59 (t,  $J = 4.0$  Hz, 1H), 1.35-1.18 (m, 2H), 1.11-0.98 (m, 2H), 0.62 (d,  $J = 10.7$  Hz, 1H), 0.54 (t,  $J = 2.8$  Hz, 1H), 0.43 (d,  $J = 10.7$  Hz, 1H), 0.35 (dd,  $J = 7.2, 2.7$  Hz, 1H), 0.20 (dd,  $J = 7.3, 1.8$  Hz, 1H).  $^{13}\text{C}$  NMR (100 MHz,  $\text{CDCl}_3$ )  $\delta$  143.63 (C), 137.60 (C), 134.13 (C), 129.86 (CH), 129.11 (CH), 128.06 (CH), 127.70 (CH), 126.10 (CH), 54.25 ( $\text{CH}_2$ ), 50.68 ( $\text{CH}_2$ ),

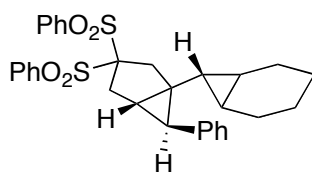
35.94 (CH), 35.68 (CH), 34.23 (C), 30.14 (CH), 29.55 (CH<sub>2</sub>), 29.45 (CH<sub>2</sub>), 28.34 (CH<sub>2</sub>), 25.98 (CH), 23.60 (CH), 21.86 (CH), 21.75 (CH<sub>3</sub>), 11.50 (CH). Anal calcd for (C<sub>26</sub>H<sub>29</sub>NO<sub>2</sub>S)<sub>2</sub>·H<sub>2</sub>O: C, 72.86; H, 7.06; N, 3.27; S, 7.48; found C, 73.19; H, 6.88; N, 3.24; S, 7.43. HRMS-IQ calcd for C<sub>26</sub>H<sub>30</sub>NO<sub>2</sub>S [M+H]<sup>+</sup>: 420.1997. Found 420.2004. The structure of **75c** was confirmed by COSY, HMQC, HMBC, and NOESY experiments.

#### Biscyclopropane **75d** (Table 2, entry 4)



Colorless oil. <sup>1</sup>H NMR (400 MHz, CDCl<sub>3</sub>) δ 7.26-7.20 (m, 2H), 7.15-7.08 (m, 3H), 3.73 (m, 3H), 3.71 (s, 3H), 2.78 (d, *J* = 13.9 Hz, 1H), 2.58 (d, *J* = 3.0 Hz, 2H), 2.42 (d, *J* = 13.9 Hz, 1H), 1.78 (d, *J* = 3.9 Hz, 1H), 1.80-1.70 (m, 1H), 1.56 (q, *J* = 3.3 Hz, 1H), 1.50-1.41 (m, 1H), 1.33 (sext, *J* = 6.7 Hz, 1H), 1.12-0.78 (m, 4H), 0.71-0.60 (m, 2H), 0.37-0.30 (m, 2H). <sup>13</sup>C NMR (100 MHz, CDCl<sub>3</sub>) δ 173.43 (C), 172.81 (C), 139.09 (C), 129.28 (CH), 127.95 (CH), 125.62 (CH), 60.74 (C), 53.12 (CH<sub>3</sub>), 53.02 (CH<sub>3</sub>), 42.41 (CH<sub>2</sub>), 38.37 (C), 37.22 (CH<sub>2</sub>), 32.88 (CH), 26.88 (CH), 24.11 (CH), 23.68 (CH<sub>2</sub>), 22.80 (CH<sub>2</sub>), 21.59 (CH<sub>2</sub>), 21.36 (CH<sub>2</sub>), 18.70 (CH), 16.39 (CH). HRMS-ESI calcd for C<sub>23</sub>H<sub>28</sub>NaO<sub>4</sub> [M+Na]<sup>+</sup>: 391.1885. Found: 391.1875. The structure of **75d** was confirmed by COSY, HMQC, HMBC, and NOESY experiments.

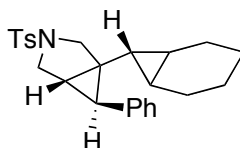
#### Biscyclopropane **75e** (Table 2, entry 5)



White Solid, dec. at 179 °C. <sup>1</sup>H NMR (400 MHz, CDCl<sub>3</sub>) δ 8.14 (dd, *J* = 8.3, 4.5 Hz, 2H), 8.07 (dd, *J* = 8.3, 4.5 Hz, 2H), 7.77-7.70 (m, 2H), 7.66-7.58 (m, 4H), 7.28-7.22 (m, 2H), 7.16-7.05 (m, 3H), 3.13 (dd, *J* = 16.1, 6.4 Hz, 1H), 3.02 (*J* = 16.1 Hz, 1H), 2.89 (*J* = 16.1 Hz, 1H), 2.67 (d, *J* = 16.1, 1H), 2.26 (d, *J* = 4.2 Hz, 1H), 1.86-1.76 (m, 2H), 1.52-1.43 (m, 1H), 1.40-1.30 (m, 1H), 1.15-0.78 (m, 5H), 0.66-0.57 (m, 1H), 0.43-0.35 (m, 1H), 0.31 (t, *J* = 5.0 Hz, 1H). <sup>13</sup>C NMR (100 MHz, CDCl<sub>3</sub>) δ 138.27 (C),

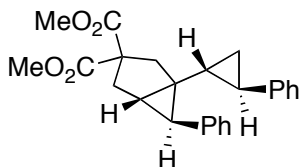
137.06 (C), 136.26 (C), 134.79 (CH), 134.75 (CH), 132.08 (CH), 131.69 (CH), 128.96 (CH), 128.91 (CH), 128.85 (CH), 128.09 (CH), 125.88 (CH), 97.66 (C), 42.19(CH<sub>2</sub>), 41.61 (C), 36.67 (CH<sub>2</sub>), 36.56 (CH), 29.04 (CH), 24.45 (CH), 23.68 (CH<sub>2</sub>), 22.69 (CH<sub>2</sub>), 21.51 (CH<sub>2</sub>), 21.31 (CH<sub>2</sub>), 19.46 (CH), 16.21 (CH). Anal calcd for (C<sub>31</sub>H<sub>32</sub>O<sub>4</sub>S<sub>2</sub>)·H<sub>2</sub>O: C, 67.61; H, 6.22; S, 11.64; found: C, 67.62; H, 5.82; S, 11.46. HRMS-ESI calcd for C<sub>31</sub>H<sub>32</sub>NaO<sub>4</sub>S<sub>2</sub> [M+Na]<sup>+</sup>: 555.1640. Found: 555.1626. The structure of **75e** was confirmed by COSY, HMQC, HMBC, and NOESY experiments.

### Biscyclopropane **75f** (Table 2, entry 6)



White Solid, mp 88-90 °C. <sup>1</sup>H NMR (400 MHz, CDCl<sub>3</sub>) δ 7.71 (d, *J* = 8.2 Hz, 2H), 7.34 (d, *J* = 8.2 Hz, 2H), 7.27-7.22 (m, 2H), 7.17-7.12 (m, 1H), 7.07 (d, *J* = 7.3 Hz, 2H), 3.63 (d, *J* = 9.2 Hz, 1H), 3.61 (d, *J* = 9.3 Hz, 1H), 3.14 (dd, *J* = 9.3, 3.9 Hz, 1H), 3.09 (d, *J* = 9.3 Hz, 1H), 2.44 (s, 3H), 2.06 (d, *J* = 3.9 Hz, 1H), 1.68 (sext, *J* = 6.9 Hz, 1H), 1.60 (t, *J* = 4.0 Hz, 1H), 1.42-1.31 (m, 2H), 1.10-0.78 (m, 4H), 0.76-0.67 (m, 1H), 0.49 (q, *J* = 7.1 Hz, 1H), 0.35-0.27 (m, 2H). <sup>13</sup>C NMR (100 MHz, CDCl<sub>3</sub>) δ 143.61 (C), 137.76 (C), 134.30 (C), 129.83 (CH), 129.07 (CH), 128.15 (CH), 127.66 (CH), 126.04 (CH), 54.41 (CH<sub>2</sub>), 50.71 (CH<sub>2</sub>), 36.56 (C), 30.44 (CH), 25.08 (CH), 23.43 (CH<sub>2</sub>), 22.66 (CH<sub>2</sub>), 21.74 (CH<sub>3</sub>), 21.46 (CH), 21.38 (CH<sub>2</sub>), 21.22 (CH<sub>2</sub>), 18.36 (CH), 16.49 (CH). Anal calcd for (C<sub>25</sub>H<sub>29</sub>NO<sub>2</sub>)<sub>2</sub>·H<sub>2</sub>O: C, 72.08; H, 7.26; N, 3.36; S, 7.70; Found: C, 72.25; H, 7.39; N, 3.25; S, 7.27. HRMS-ESI calcd for C<sub>25</sub>H<sub>29</sub>NaNO<sub>2</sub>S [M+Na]<sup>+</sup>: 430.1817. Found: 430.1828.

### Biscyclopropane **75g** (Table 3, entry 2)



White Solid; mp 125-127 °C. <sup>1</sup>H NMR (400 MHz, CDCl<sub>3</sub>) δ 7.24-7.06 (m, 8H), 6.92-6.87 (m, 2H), 3.75 (s, 3H), 3.74 (s, 3H), 2.84 (d, *J* = 14.1, 1H), 2.69 (part A, AB system d, *J* = 13.9, 5.0 Hz, 1H), 2.64 (part B, AB system, *J* = 13.9 Hz, 1H), 2.54 (d, *J* = 14.0 Hz, 1H), 1.88 (d, *J* = 4.2 Hz, 1H), 1.72 (t, *J* = 4.2 Hz, 1H), 1.68 (dt, *J* = 8.8, 5.4 Hz,

1H), 1.05 (dt,  $J = 8.7, 5.4$  Hz, 1H), 0.59 (ddt,  $J = 19.5, 8.6, 5.4$  Hz, 2H).  $^{13}\text{C}$  NMR (100 MHz,  $\text{CDCl}_3$ )  $\delta$  173.28 (C), 172.74 (C), 143.22 (C), 138.50 (C), 129.37 (CH), 128.29 (CH), 128.11 (CH), 126.02 (CH), 125.97 (CH), 125.49 (CH), 61.04 (C), 53.23 ( $\text{CH}_3$ ), 53.11 ( $\text{CH}_3$ ), 42.47 ( $\text{CH}_2$ ), 37.98 (C), 37.34 ( $\text{CH}_2$ ), 33.57 (CH), 27.34 (CH), 23.73 (CH), 22.21 (CH), 16.56 ( $\text{CH}_2$ ). Anal calcd for  $\text{C}_{25}\text{H}_{26}\text{O}_4$ : C, 76.90; H, 6.83; found: C, 76.74; H, 6.83. HRMS-ESI calcd for  $\text{C}_{25}\text{H}_{26}\text{NaO}_4$   $[\text{M}+\text{Na}]^+$ : 413.1729. Found: 413.1716. The structure of **75g** was confirmed by COSY, HMQC, HMBC, and NOESY experiments.

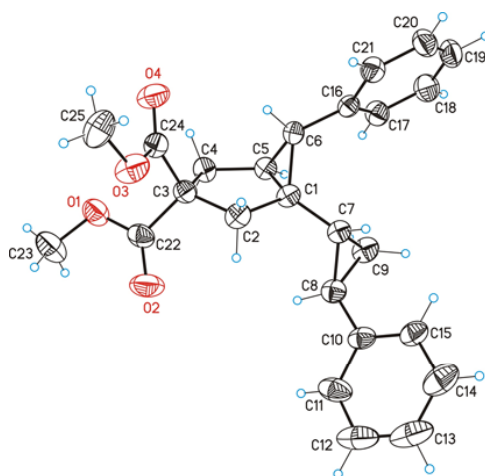
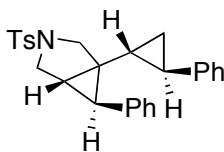


Figure 10. Ortep-Plot (30 %) of structure **75g**.

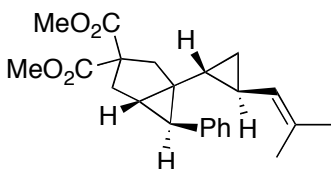
**X-ray Structure determination of 75g:** Poor-quality crystals of **75g** were obtained by crystallization from  $\text{CH}_2\text{Cl}_2$ . An initial structure with two independent molecules could be solved in the monoclinic space group  $P2_1/c$  reaching a R1 factor of 0.192. Considering a  $\beta$ -angle of  $91.28^\circ$  a twin matrix (1 0 0 0 -1 0 0 0 -1) for monoclinic cells with a beta angle close to  $90^\circ$ , which may emulate an orthorhombic cell was applied. In this case the R1 factor reduced to 0.1696 (BASF: 0.2062). A second structure solution could be obtained in the orthorhombic space group  $Pbca$ . In this case a R1 factor of 0.1884 could be reached. Not better result could be obtained with the selected crystal but the data were considered good enough to prove the relative stereochemistry of the molecule.

### Biscyclopropane **75h/75h'** (Table 3, entry 3)



White solid, mixture of isomers (**75h/75h'** = 10:1); mp 178-179°C. The following signals are the corresponding to the major isomer, only few signals of the minor isomer have been assigned. <sup>1</sup>H NMR (400 MHz, CDCl<sub>3</sub>) δ 7.73 (d, *J* = 8.3 Hz, 2H), 7.36 (d, *J* = 8.3 Hz, 2H), 7.28-7.04 (m, 8H), 6.76 (d, *J* = 7.4 Hz, 2H), 3.70 (t, *J* = 10.0 Hz, 2H), 3.23 (dd, *J* = 9.4, 4.1 Hz, 1H), 3.17 (d, *J* = 9.4 Hz, 1H), 2.46 (s, 3H), 2.19 (d, *J* = 4.3 Hz, 1H), 1.73 (t, *J* = 4.2 Hz, 1H), 1.50-1.43 (m, 1H), 1.50-1.43 (m, 1H), 1.03-0.94 (m, 1H), 0.68-0.51 (m, 2H). Significant signals for the minor isomer: 2.23 (d, *J* = 3.6 Hz, 1H), 1.55 (d, *J* = 1.5 Hz, 2H), 1.41-1.35 (m, 1H), 0.88-0.79 (m, 1H). <sup>13</sup>C NMR (100 MHz, CDCl<sub>3</sub>), δ 143.79 (C), 142.28 (C), 137.14 (C), 133.90 (C), 129.88 (CH), 129.12 (CH), 128.38 (CH), 128.32 (CH), 127.76 (CH), 126.34 (CH), 125.85 (CH), 125.81 (CH), 54.61 (CH<sub>2</sub>), 50.74 (CH<sub>2</sub>), 36.08 (CH<sub>2</sub>), 30.68 (C), 25.25 (CH), 22.29 (CH), 21.77 (CH), 21.32 (CH<sub>3</sub>), 16.00 (CH<sub>2</sub>). Anal. calcd for (C<sub>33</sub>H<sub>34</sub>O<sub>2</sub>)<sub>2</sub>·H<sub>2</sub>O: C, 73.94; H, 6.43; N, 3.19; S, 7.31; found: C, 73.75; H, 6.13; N, 3.17; S, 7.18. HRMS-ESI calcd for C<sub>27</sub>H<sub>27</sub>N O<sub>2</sub>NaS [M+Na]<sup>+</sup>: 452.1660. Found 452.1670.

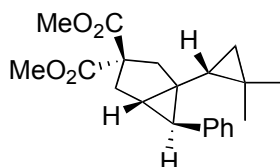
### Biscyclopropane **75i/75i'** (Table 3, entry 1)



Colorless oil, mixture of isomers (**75i/75i'** = 5:1). The following signals are the corresponding to the major isomer, only few signals of the minor isomer have been assigned. <sup>1</sup>H NMR (400 MHz, CDCl<sub>3</sub>) δ 7.24-7.10 (m, 5H), 4.41 (dq, *J* = 9.1, 1.3 Hz, 1H), 3.74 (s, 3H), 3.72 (s, 3H), 2.79 (d, *J* = 14.1 Hz, 1H), 2.64-2.61 (m, 2H), 2.47 (d, *J* = 14.1 Hz, 1H), 1.81 (d, *J* = 4.1 Hz, 1H), 1.68 (d, *J* = 1.0 Hz, 3H), 1.64-1.58 (m, 1H), 1.60 (d, *J* = 1.0 Hz, 3H), 1.23 (ddd, *J* = 13.9, 8.8, 4.6 Hz, 1H), 0.65 (dt, *J* = 8.6, 5.0 Hz, 1H), 0.39 (dt, *J* = 8.5, 5.2 Hz, 1H), 0.15 (dt, *J* = 8.6, 5.1 Hz, 1H). Significant signals for the minor isomer: 7.24-7.10 (m, 5H), 4.15 (d, *J* = 9.2 Hz, 1H), 1.49 (d, *J* = 1.0 Hz, 3H), 1.42 (d, *J* = 1.0 Hz, 3H). <sup>13</sup>C NMR (100 MHz, CDCl<sub>3</sub>), δ 173.37 (C), 172.82 (C), 138.73 (C), 130.51 (C), 129.37 (CH), 127.99 (CH), 127.82 (CH), 125.85 (CH), 60.98

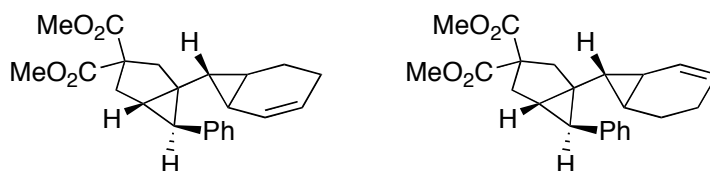
(C), 50.16 (CH<sub>3</sub>), 53.07 (CH<sub>3</sub>), 42.59 (CH<sub>2</sub>), 37.77 (C), 37.38 (CH<sub>2</sub>), 33.42 (CH), 27.71 (CH), 25.66 (CH<sub>3</sub>), 21.02 (CH), 18.28 (CH<sub>3</sub>), 17.10 (CH), 15.19 (CH<sub>2</sub>). HRMS-ESI calcd for C<sub>23</sub>H<sub>28</sub>NaO<sub>4</sub> [M+Na]<sup>+</sup>: 391.1885. Found: 391.1895. The structure of **75i** was confirmed by COSY, HMQC, HMBC, and NOESY experiments.

### Biscyclopropanes **75j/75j'** (Table 3, entry 4)



Mixture of diastereoisomers (**75j/75j'** = 3.3:1). <sup>1</sup>H NMR (400 MHz, CDCl<sub>3</sub>) δ major isomer, δ 7.27-7.10 (m, 5H), 3.71 (s, 6H), 2.83 (d, *J* = 13.8 Hz, 1H), 2.76-2.64 (m, 2H), 2.48 (d, *J* = 14.2 Hz, 1H), 1.73-1.68 (m, 2H), 0.99 (s, 3H), 0.85 (s, 3H), 0.68 (dd, *J* = 8.8, 5.6 Hz, 1H), 0.02 (dd, *J* = 8.8, 4.8 Hz, 1H), 0.24 (t, *J* = 5.1 Hz, 1H). Significant signals for minor isomer: δ 3.75 (s, 6H), 1.07 (s, 3H), 0.79 (s, 3H), 0.36 (dd, *J* = 9.3, 5.9 Hz, 1H), 0.27 (dd, *J* = 9.3, 4.4 Hz, 1H), 0.15 (dd, *J* = 5.9, 4.4 Hz, 1H). Signals for major isomer <sup>13</sup>C NMR (100 MHz, CDCl<sub>3</sub>) δ 173.40 (C), 172.53 (C), 139.00 (C), 129.05 (CH), 127.65 (CH), 125.45 (CH), 60.23 (C), 52.95 (CH<sub>3</sub>), 43.17 (CH<sub>2</sub>), 39.34 (C), 36.59 (CH<sub>2</sub>), 31.05 (CH), 28.87 (CH), 27.09 (CH<sub>3</sub>), 25.12 (CH), 20.47 (CH<sub>3</sub>), 19.95 (CH<sub>2</sub>), 15.50 (C). Significant signals for minor isomer: δ 138.72 (C), 128.15 (CH), 127.70 (CH), 125.48 (CH), 52.90 (CH<sub>3</sub>), 39.27 (C), 37.35 (CH<sub>2</sub>), 36.42 (CH<sub>2</sub>), 32.55 (CH), 30.08 (CH), 26.61 (CH<sub>3</sub>), 23.58 (CH), 21.56 (CH<sub>3</sub>), 18.26 (CH<sub>2</sub>). HRMS-ESI calcd for C<sub>21</sub>H<sub>27</sub>O<sub>4</sub> [M+H]<sup>+</sup>: 343.1909. Found: 343.1901. The structure of **75j** was confirmed by COSY, HMQC, HMBC, and NOESY experiments.

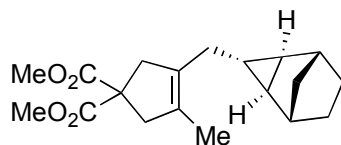
### Biscyclopropanes **75k/75k'**



Colorless oil, mixture of at least two diastereoisomers (**75k/75k'** = 1:0.7). Each diastereoisomer was assigned based in the chemical shift of the olefin protons. Due to extensive overlapping the assignment of <sup>1</sup>H is tentative (The structure was studied by COSY, HSQC, HMBC, and NOESY experiments). <sup>1</sup>H NMR (400 MHz, CDCl<sub>3</sub>) 7.28-

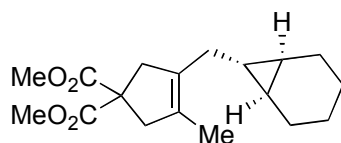
7.20 (m, 2H major, 2H minor), 7.17-7.09 (m, 3H major, 3H minor), 6.00-5.93 (m, 1H major), 5.50-5.41 (m, 1H minor), 5.31-5.24 (m, 1H major), 5.24-5.17 (m, 1H minor), 3.75-3.71 (m, 6H major, 6H minor), 2.83 (d,  $J = 13.8$  Hz, 1H major), 2.72 (d,  $J = 13.9$  Hz, 1H minor), 2.66-2.57 (m, 2H major, 2H minor), 2.48 (d,  $J = 13.9$  Hz, 1H major), 2.39 (d,  $J = 13.8$  Hz, 1H minor), 1.87-1.59 (m, 4H major, 3H minor), 1.53-1.32 (m, 2H major, 1H minor), 1.16-1.04 (m, 2H minor), 1.04-0.86 (m, 1H major, 2H minor), 0.84-0.73 (m, 1H major, 1H minor), 0.72-0.64 (m, 1H major).  $^{13}\text{C}$  NMR (100 MHz,  $\text{CDCl}_3$ )  $\delta$  173.33 (C), 172.71 (C), 138.74 (C), 138.69 (C), 129.27 (CH), 129.17 (CH), 128.09 (CH), 127.83 (CH), 127.79 (CH), 127.60 (CH), 125.67 (CH), 122.92 (CH), 122.43 (CH), 60.69 (C), 60.64 (C), 52.99 ( $\text{CH}_3$ ), 52.89 ( $\text{CH}_3$ ), 42.45 ( $\text{CH}_2$ ), 41.31 ( $\text{CH}_2$ ), 37.04 ( $\text{CH}_2$ ), 36.96 ( $\text{CH}_2$ ), 32.60 (CH), 27.56 (CH), 26.58 (CH), 24.61 (CH), 24.38 (CH), 22.86 (CH), 20.81 ( $\text{CH}_2$ ), 20.79 ( $\text{CH}_2$ ), 20.03 (CH), 18.04 ( $\text{CH}_2$ ), 17.65 (CH), 17.20 ( $\text{CH}_2$ ), 16.47 (CH). HRMS-ESI calcd for  $\text{C}_{23}\text{H}_{26}\text{O}_4\text{Na}$   $[\text{M}+\text{Na}]^+$ : 389.1729. Found: 389.1720.

### Cyclopropanes **76a/76a'** (Scheme 31)



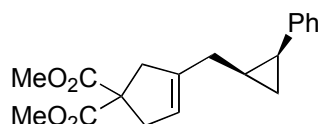
Colorless oil, mixture of two isomers (*anti/syn* = 2.9:1).  $^1\text{H}$  NMR (400 MHz,  $\text{CDCl}_3$ )  $\delta$  3.73 (s, 6H), 3.06 (bs, 2H minor), 3.01 (bs, 2H major), 2.93 (bs, 2H), 2.36 (bs, 2H minor), 2.27-2.21 (m, 2H), 1.78 (d,  $J = 7.1$  Hz, 2H major), 1.61-1.55 (m, 3H), 1.46-1.35 (m, 2H), 1.27-1.15 (m, 2H), 1.15-1.08 (m, 1H minor), 0.92 (d,  $J = 10.4$  Hz, 1H major), 0.71 (d,  $J = 7.8$  Hz, 2H minor), 0.67-0.60 (m, 2H major, 1H minor), 0.58 (d,  $J = 10.4$  Hz, 1H major), 0.45 (d,  $J = 2.2$  Hz, 2H major), 0.41 (quint,  $J = 7.6$  Hz, 1H minor).  $^{13}\text{C}$  NMR (100 MHz,  $\text{CDCl}_3$ )  $\delta$  173.26 (C minor), 173.23 (C major), 133.36 (C minor), 132.66 (C major), 128.00 (C major), 127.49 (C minor), 57.58 (C major), 57.51 (C minor), 52.90 ( $\text{CH}_3$ ), 45.98 ( $\text{CH}_2$ ), 44.17 ( $\text{CH}_2$  major), 43.92 ( $\text{CH}_2$  minor), 36.37 (CH minor), 36.07 (CH major), 31.03 ( $\text{CH}_2$  minor), 30.51 ( $\text{CH}_2$  minor), 30.40 ( $\text{CH}_2$  major), 29.83 ( $\text{CH}_2$  major), 28.79 ( $\text{CH}_2$  major), 25.46 ( $\text{CH}_2$  minor), 23.19 (CH major), 21.77 (CH minor), 13.53 ( $\text{CH}_3$  minor), 13.46 ( $\text{CH}_3$  major), 12.80 (CH major). HRMS-ESI calcd for  $\text{C}_{19}\text{H}_{26}\text{O}_4\text{Na}$   $[\text{M}+\text{Na}]^+$ : 341.1729. Found: 341.1731. The structure of **76a** was confirmed by COSY, HMQC, HMBC, and NOESY experiments.

### Cyclopropanes **76b/76b'** (Scheme 31)



Colorless oil, mixture of two isomers (*anti/syn* = 2.3:1). <sup>1</sup>H NMR (400 MHz, CDCl<sub>3</sub>) δ 3.72 (s, 6H), 3.05 (bs, 2H minor), 3.02 (bs, 2H major), 2.93 (bs, 2H), 2.02 (d, *J* = 7.1 Hz, 2H minor), 1.89 (d, *J* = 6.8 Hz, 2H major), 1.92-1.77 (m, 2H), 1.65-1.54 (m, 2H), 1.61 (s, 3H minor), 1.57 (s, 3H major), 1.43-1.33 (m, 2H minor), 1.33-1.04 (m, 4H), 0.89-0.80 (m, 2H minor), 0.64-0.54 (m, 1H minor), 0.58 (t, *J* = 5.0 Hz, 2H major), 0.32 (tt, *J* = 6.9, 4.6 Hz, 1H major). <sup>13</sup>C NMR (100 MHz, CDCl<sub>3</sub>) δ 173.24 (C), 132.95 (C major), 132.86 (C minor), 127.71 (C major), 127.50 (C minor), 57.56 (C major), 57.51 (C minor), 52.87 (CH<sub>3</sub>), 46.04 (CH<sub>2</sub> minor), 45.95 (CH<sub>2</sub> major), 44.17 (CH<sub>2</sub> major), 43.93 (CH<sub>2</sub> minor), 32.77 (CH<sub>2</sub> major), 23.71 (CH<sub>2</sub> major), 22.93 (CH<sub>2</sub> minor), 22.78 (CH<sub>2</sub> minor), 22.68 (CH major), 21.77 (CH<sub>2</sub> major), 19.11 (CH<sub>2</sub> minor), 17.54 (CH minor), 17.22 (CH major), 13.58 (CH<sub>3</sub> minor), 13.44 (CH<sub>3</sub> major), 10.45 (CH minor). HRMS-ESI calcd for C<sub>18</sub>H<sub>26</sub>NaO<sub>4</sub> [M+Na]<sup>+</sup>: 329.1729. Found: 329.1743. The structure of **76b** was confirmed by COSY, HMQC, HMBC, and NOESY experiments

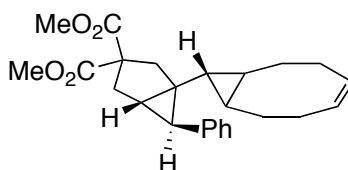
### Cyclopropanes **76c/76c'** (Scheme 31)



Colorless oil, mixture of two isomers (*cis:trans* = 3.3:1). <sup>1</sup>H NMR (500 MHz, CDCl<sub>3</sub>) δ 7.27-7.01 (m, 5H), 5.29 (bs, 1H minor), 5.19 (hept, *J* = 1.8 Hz, 1H major), 3.73-3.68 (m, 6H), 2.98 (bs, 4H minor), 2.95 (hept, *J* = 2.0 Hz, 2H major), 2.87 (part A, AB system, *J* = 16.9 Hz, 1H major), 2.79 (part B, AB system, *J* = 16.9 Hz, 1H major), 2.16 (td, *J* = 8.5, 6.3 Hz, 1H major), 2.20-2.02 (m, 2H minor), 1.90 (dd, *J* = 16.1, 5.6 Hz, 1H major), 1.69-1.61 (m, 1H minor), 1.53 (ddd, *J* = 16.3, 8.3, 1.1 Hz, 1H major), 1.27-1.18 (m, 1H major), 1.17-1.07 (m, 1H minor), 1.03 (td, *J* = 8.3, 5.2 Hz, 1H major), 0.97-0.91 (m, 1H minor), 0.86-0.76 (m, 1H minor), 0.69 (q, *J* = 5.6 Hz, 1H major). <sup>13</sup>C NMR (125 MHz, CDCl<sub>3</sub>) δ 172.98 (C), 172.94 (C), 143.54 (C minor), 141.68 (C major), 141.35 (C minor), 139.19 (C major), 129.33 (CH major), 128.43 (CH major), 128.01 (CH major), 125.98 (CH minor), 125.93 (CH major), 125.78 (CH minor), 125.59 (CH minor), 125.49 (CH minor), 121.02 (CH minor), 120.47 (CH major), 59.36

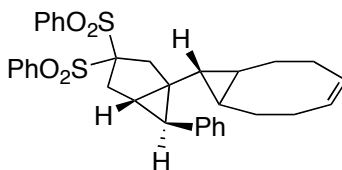
(C minor), 59.26 (C major), 52.91 (CH<sub>3</sub>), 43.47 (CH<sub>2</sub> minor), 43.42 (CH<sub>2</sub> major), 40.83 (CH<sub>2</sub> minor), 40.78 (CH<sub>2</sub> major), 35.49 (CH<sub>2</sub> minor), 29.91 (CH<sub>2</sub> major), 23.34 (CH minor), 21.99 (CH minor), 20.87 (CH major), 17.10 (CH major), 16.26 (CH<sub>2</sub> minor), 9.88 (CH<sub>2</sub> major). HRMS-ESI calcd for C<sub>19</sub>H<sub>22</sub>O<sub>4</sub>Na [M+Na]<sup>+</sup>: 337.1416. Found: 337.1407. The structure of **76c** was confirmed by COSY, HMQC, HMBC, and NOESY experiments.

### Biscyclopropane **75k** (Table 5, entry 1)



Colorless oil. <sup>1</sup>H NMR (CDCl<sub>3</sub>, 400 MHz) δ 7.25-7.21 (m, 2H), 7.13-7.10 (m, 3H), 5.57-5.45 (m, 2H), 3.73 (s, 3H), 3.71 (s, 3H), 2.80 (d, *J* = 13.8 Hz, 1H), 2.58 (d, *J* = 2.9 Hz, 2H), 2.42 (d, *J* = 13.8 Hz, 1H), 2.20-2.12 (m, 1H), 2.10-1.91 (m, 3H), 1.80-1.79 (d, *J* = 4.0 Hz, 1H), 1.80-1.78 (m, 1H), 1.59-1.56 (m, 1H), 1.24-1.10 (m, 2H), 0.77-0.68 (m, 1H), 0.77-0.68 (m, 1H), 0.35-0.28 (m, 1H), 0.22 (t, *J* = 5.3 Hz, 1H). <sup>13</sup>C NMR (CDCl<sub>3</sub>, 100 MHz) δ 173.33 (C), 172.71 (C), 138.97 (C), 130.33 (CH), 130.20 (CH), 129.30 (CH), 127.97 (CH), 125.66 (CH), 60.79 (C), 53.07 (CH<sub>3</sub>), 52.96 (CH<sub>3</sub>), 43.53 (CH<sub>2</sub>), 38.24 (C), 37.13 (CH<sub>2</sub>), 32.80 (CH), 29.69 (CH<sub>2</sub>), 28.68 (CH<sub>2</sub>), 27.24 (CH), 27.17 (CH<sub>2</sub>), 26.90 (CH<sub>2</sub>), 26.82 (CH), 25.46 (CH), 23.13 (CH). HRMS-ESI calcd for C<sub>25</sub>H<sub>30</sub>NaO<sub>4</sub> [M+Na]<sup>+</sup>: 417.2042. Found: 417.2028

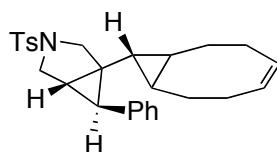
### Biscyclopropane **75l** (Table 5, entry 2)



Pale yellow solid; mp 191-192 °C. <sup>1</sup>H NMR (CDCl<sub>3</sub>, 400 MHz) δ 8.16-8.04 (m, 4H), 7.76-7.69 (m, 2H), 7.65-7.57 (m, 4H), 7.29-7.20 (m, 2H), 7.17-7.10 (m, 1H), 7.10-7.05 (m, 2H), 5.57-5.46 (m, 2H), 3.13 (dd, *J* = 16.2, 6.5 Hz, 1H), 3.03 (d, *J* = 16.2 Hz, 1H), 2.89 (d, *J* = 16.2 Hz, 1H), 2.69 (d, *J* = 5.3 Hz, 1H), 2.30 (d, *J* = 4.1 Hz, 1H), 2.23-1.92 (m, 4H, CH<sub>2</sub>), 1.86-1.80 (m, 1H), 1.86-1.71 (m, 1H), 1.24-1.05 (m, 2H), 0.94-0.84 (m, 1H), 0.73-0.61 (m, 1H), 0.40-0.30 (m, 1H), 0.19 (t, *J* = 5.3 Hz, 1H). <sup>13</sup>C NMR (CDCl<sub>3</sub>, 100 MHz) δ 138.12 (C), 137.00 (C), 136.27 (C), 134.76 (CH), 134.73 (CH),

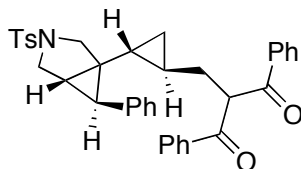
132.00 (CH), 131.63 (CH), 130.46 (CH), 130.23 (CH), 129.00 (CH), 128.88 (CH), 128.82 (CH), 128.12 (CH), 125.91 (CH), 97.65 (C), 42.16 (CH<sub>2</sub>), 41.36 (C<sub>q</sub>), 36.57 (CH<sub>2</sub>), 36.24 (CH), 29.95 (CH<sub>2</sub>), 28.86 (CH), 28.79 (CH<sub>2</sub>), 27.66 (CH), 27.02 (CH<sub>2</sub>), 26.81 (CH<sub>2</sub>), 26.18 (CH), 22.92 (CH). Anal calcd for C<sub>33</sub>H<sub>34</sub>O<sub>2</sub>·H<sub>2</sub>O: C, 68.72; H, 6.29; found: C, 69.11; H, 6.29. HRMS-ESI calcd for C<sub>33</sub>H<sub>34</sub>NaO<sub>4</sub>S<sub>2</sub> [M+Na]<sup>+</sup>: 581.1796. Found 581.1780

### Biscyclopropane 75m (Table 5, entry 3)



Colorless oil. <sup>1</sup>H NMR (CDCl<sub>3</sub>, 400 MHz) δ 7.73-7.69 (m, 2H), 7.36-7.31 (m, 2H), 7.27-7.22 (m, 2H), 7.17-7.11 (m, 1H), 7.09-7.04 (m, 2H), 5.55-5.43 (m, 2H), 3.66 (d, *J* = 9.4 Hz, 1H), 3.60 (d, <sup>2</sup>*J* = 9.2 Hz, 1H), 3.14 (dd, *J* = 9.2, 4.0 Hz, 1H), 3.09 (d, *J* = 9.4 Hz, 1H), 2.44 (s, 3H), 2.19-1.85 (m, 4H), 2.09 (d, *J* = 4.0 Hz, 1H), 1.81-1.71 (m, 1H), 1.61-1.59 (m, *J* = 4.0 Hz, 1H), 1.24-1.11 (m, 2H), 0.80-0.69 (m, 1H), 0.51-0.42 (m, 1H), 0.32-0.24 (m, 1H), 0.16 (t, *J* = 5.3 Hz, 1H). <sup>13</sup>C NMR (CDCl<sub>3</sub>, 100 MHz) δ 143.62 (C), 137.60 (C), 134.22 (C), 130.27 (CH), 130.08 (CH), 129.80 (CH), 129.09 (CH), 128.17 (CH), 127.62 (CH), 126.07 (CH), 54.53 (CH<sub>2</sub>), 50.64 (CH<sub>2</sub>), 36.48 (C), 30.37 (CH), 29.39 (CH<sub>2</sub>), 28.53 (CH<sub>2</sub>), 26.94 (CH<sub>2</sub>), 26.80 (CH<sub>2</sub>), 25.11 (CH), 25.00 (CH), 24.49 (CH), 23.00 (CH), 21.71 (CH<sub>3</sub>). HRMS-ESI calcd for C<sub>27</sub>H<sub>31</sub>NNaO<sub>2</sub>S [M+Na]<sup>+</sup>: 456.1973. Found: 456.1966.

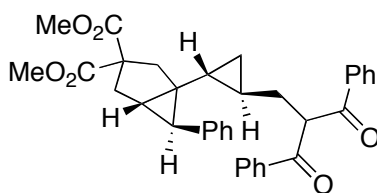
### Biscyclopropane 75o (Table 7, entry 4)



White foam solid, mixture of two diastereoisomers (15:1). <sup>1</sup>H NMR (CDCl<sub>3</sub>, 400 MHz) δ 7.91-7.86 (m, 2H), 7.82-7.77 (m, 2H), 7.61-7.55 (m, 4H), 7.48-7.41 (m, 4H), 7.28-7.20 (m, 4H), 7.18-7.13 (m, 1H), 7.10-7.06 (m, 2H), 5.03 (t, *J* = 6.6 Hz, 1H), 3.60 (d, *J* = 9.4 Hz, 1H), 3.51 (d, *J* = 9.4 Hz, 1H), 3.06 (dd, *J* = 9.2, 3.9 Hz, 1H), 2.85 (d, *J* = 9.4 Hz, 1H), 2.43 (s, 3H), 2.16 (d, *J* = 4.1 Hz, 1H), 1.89-1.82 (m, 1H), 1.76-1.69 (m, 1H), 1.64 (t, *J* = 3.9 Hz, 1H), 0.61-0.49 (m, 2H), 0.18-0.14 (dt, *J* = 8.4, 5.2 Hz, 1H),

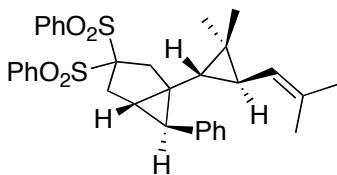
0.08-0.03 (dt,  $J = 8.8, 5.3$  Hz, 1H). Significant signals for the minor diastereoisomer:  $\delta$  4.81 (t,  $J = 6.6$  Hz, 1H), 3.24 (dd,  $J = 9.4, 3.7$  Hz, 1H), 2.95 (d,  $J = 9.4$  Hz, 1H).  $^{13}\text{C}$  NMR ( $\text{CDCl}_3$ , 100 MHz, ppm)  $\delta$  195.87 (C), 143.66 (C), 137.31 (C), 136.17 (CH), 135.92 (C), 133.77 (CH), 133.67 (C), 129.86 (CH), 129.09 (CH), 128.98 (CH), 128.68 (CH), 128.31 (CH), 127.62 (CH), 126.35 (CH), 57.33 (CH), 53.52 ( $\text{CH}_2$ ), 50.53 ( $\text{CH}_2$ ), 35.27 (C), 33.96 ( $\text{CH}_2$ ), 30.29 (CH), 25.45 (CH), 21.73 ( $\text{CH}_3$ ), 17.18 (CH), 16.49 (CH), 12.64 ( $\text{CH}_2$ ). HRMS-ESI calcd for  $\text{C}_{37}\text{H}_{35}\text{NO}_4\text{NaS}$   $[\text{M}+\text{Na}]^+$ : 612.2185. Found: 612.2178.

### Biscyclopropane 75p (Table 7, entry 5)



White foam solid, mixture of two diastereoisomers (8:1).  $^1\text{H}$  NMR ( $\text{CDCl}_3$ , 400 MHz)  $\delta$  7.93-7.89 (m, 2H), 7.83-7.78 (m, 2H), 7.59-7.52 (m, 2H), 7.49-7.38 (m, 4H), 7.25-7.20 (m, 2H), 7.16-7.10 (m, 3H), 5.10 (dd,  $J = 7.1, 5.9$  Hz, 1H), 3.72 (s, 3H), 3.63 (s, 3H), 2.65-2.55 (m, 3H), 2.19 (d, 1H), 1.91-1.75 (m, 3H), 1.64 (t,  $J = 4.4$  Hz, 1H), 0.77-0.68 (m, 1H), 0.56-0.50 (m, 1H), 0.28 (dt,  $J = 8.4, 5.1$  Hz, 1H), 0.05 (dt,  $J = 8.7, 5.1$  Hz, 1H). Significant signal for minor diastereoisomer: 4.85 (t,  $J = 6.6$  Hz, 1H).  $^{13}\text{C}$  NMR ( $\text{CDCl}_3$ , 100 MHz)  $\delta$  196.10 (C), 196.04 (C), 173.26 (C), 172.51 (C), 138.62 (C), 136.36 (C), 136.03 (C), 133.58 (CH), 129.17 (CH), 129.02 (CH), 129.00 (CH), 128.85 (C), 128.76 (CH), 128.29 (CH), 128.16 (CH), 126.03 (CH), 60.77 (C), 57.46 (CH), 53.13 ( $\text{CH}_3$ ), 53.06 ( $\text{CH}_3$ ), 41.13 ( $\text{CH}_2$ ), 37.31 (C), 37.18 ( $\text{CH}_2$ ), 34.32 ( $\text{CH}_2$ ), 33.41 (CH), 27.74 (CH), 19.43 (CH), 16.48 (CH), 12.48 ( $\text{CH}_2$ ). HRMS-ESI calcd for  $\text{C}_{35}\text{H}_{34}\text{O}_6\text{Na}$   $[\text{M}+\text{Na}]^+$ : 573.2253. Found: 573.2238.

### Biscyclopropane 75q (Table 7, entry 11)



Colorless oil.  $^1\text{H}$  NMR ( $\text{CDCl}_3$ , 400 MHz)  $\delta$  8.11-8.03 (m, 4H), 7.76-7.51 (m, 6H), 7.25-7.18 (m, 2H), 7.17-7.11 (m, 1H), 7.02-6.96 (m, 2H), 4.72 (d,  $J = 8.2$  Hz, 1H), 3.11

(dd,  $J = 16.2, 6.4$  Hz, 1H), 3.02 (d,  $J = 16.2$  Hz, 1H), 2.94 (d,  $J = 16.2$  Hz, 1H), 2.74 (d,  $J = 16.2$  Hz, 1H), 2.23 (d,  $J = 4.4$  Hz, 1H), 1.79-1.69 (m, 1H), 1.74 (s, 3H), 1.72 (s, 3H), 1.20 (dd,  $J = 8.2, 5.7$  Hz, 1H), 0.68 (s, 3H), 0.43 (d,  $J = 5.6$  Hz, 1H), 0.37 (s, 3H).  $^{13}\text{C}$  NMR ( $\text{CDCl}_3$ , 100 MHz)  $\delta$  138.82 (C), 137.48 (C), 136.43 (C), 134.80 (CH), 134.64 (CH), 133.08 (C), 131.84 (CH), 131.47 (CH), 128.98 (CH), 128.92 (CH), 128.18 (CH), 127.96 (CH), 125.85 (CH), 124.84 (CH), 97.90 (C), 42.28 ( $\text{CH}_2$ ), 39.31 (C), 38.48 (CH), 37.43 ( $\text{CH}_2$ ), 35.99 (CH), 34.49 (CH), 30.03 (CH), 25.88 ( $\text{CH}_3$ ), 23.33 (C), 23.01 ( $\text{CH}_3$ ), 21.74 ( $\text{CH}_3$ ), 18.66 ( $\text{CH}_3$ ). HRMS-ESI calcd for  $\text{C}_{33}\text{H}_{36}\text{O}_4\text{NaS}_2$   $[\text{M}+\text{Na}]^+$ : 452.1660. Found: 583.1957.

## 4. Gold(I)-Catalyzed Cyclization of 1,7-Enynes

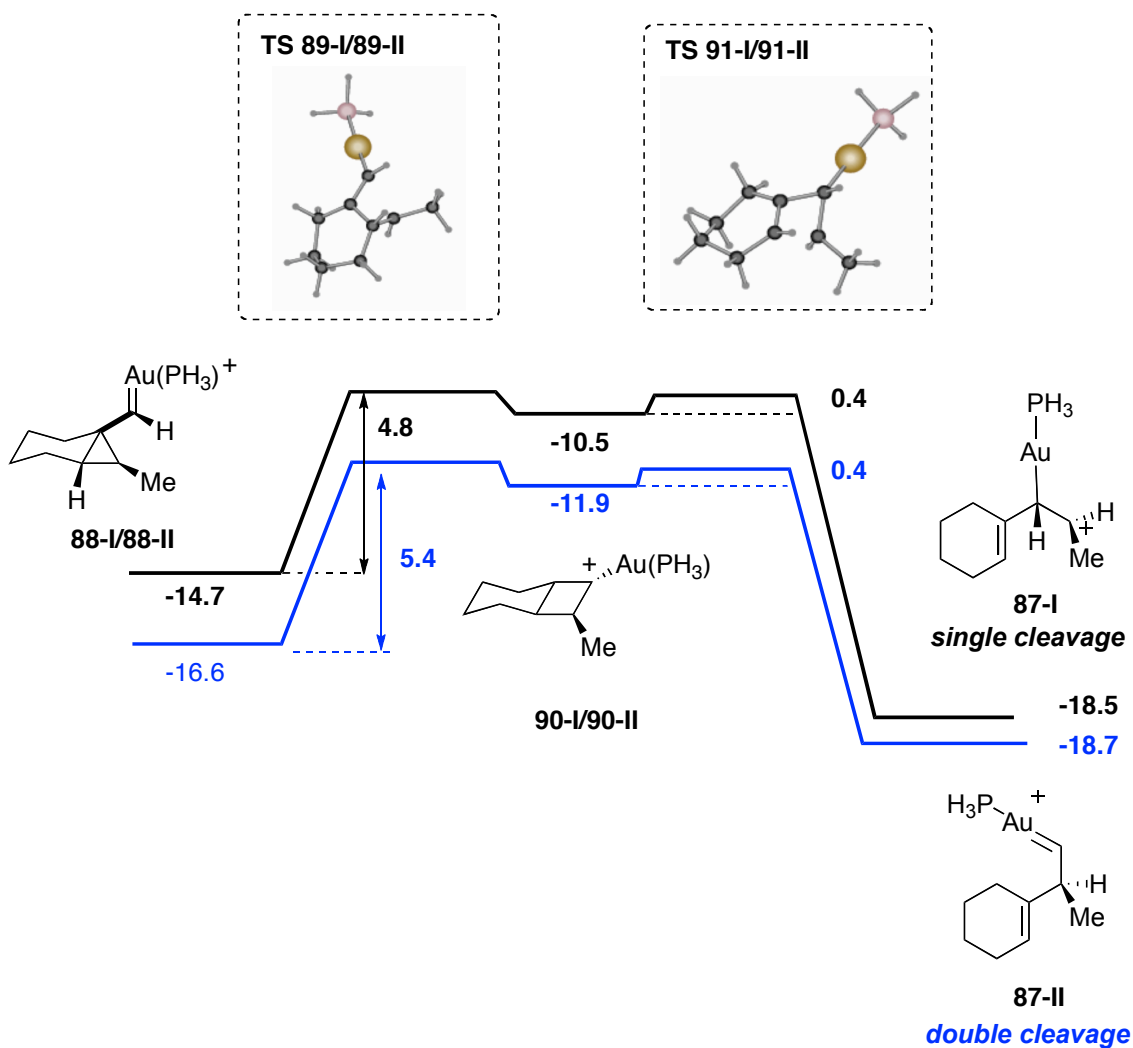
### 4.1. Computational Details

All calculations were performed with Gaussian03.<sup>115</sup> The methods were B3LYP<sup>116</sup> and ONIOM(B3LYP:UFF).<sup>117,118</sup> The inner electrons of Au were described by an effective core potential (LANL2DZ), and the associated double- $\zeta$  basis set was used for the outer electrons.<sup>119</sup> The 6-31G(d) basis set was used for H, C, O, P.<sup>120</sup> The initial calculations on systems, with PH<sub>3</sub> phosphines, were carried out at the B3LYP level with basis set 6-31G(d). For the calculations on systems with the real phosphine ligands, the ONIOM (B3LYP:UFF) approach was used, with the phosphine substituents in the MM region.

- 
- 115 Frisch, M. J.; Trucks, G. W.; Schlegel, H. B.; Scuseria, G. E.; Robb, M. A.; Cheeseman, J. R.; Montgomery, Jr., J. A.; Vreven, T.; Kudin, K. N.; Burant, J. C.; Millam, J. M.; Iyengar, S. S.; Tomasi, J.; Barone, V.; Mennucci, B.; Cossi, M.; Scalmani, G.; Rega, N.; Petersson, G. A.; Nakatsuji, H.; Hada, M.; Ehara, M.; Toyota, K.; Fukuda, R.; Hasegawa, J.; Ishida, M.; Naka jima, T.; Honda, Y.; Kitao, O.; Nakai, H.; Klene, M.; Li, X.; Knox, J. E.; Hratchian, H. P.; Cross, J. B.; Bakken, V.; Adamo, C.; Jaramillo, J.; Gomperts, R.; Stratmann, R. E.; Yazyev, O.; Austin, A. J.; Cammi, R.; Pomelli, C.; Ochterski, J. W.; Ayala, P. Y.; Morokuma, K.; Voth, G. A.; Salvador, P.; Dannenberg, J. J.; Zakrzewski, V. G.; Dapprich, S.; Daniels, A. D.; Strain, M. C.; Farkas, O.; Malick, D. K.; Rabuck, A. D.; Raghavachari, K.; Foresman, J. B.; Ortiz, J. V.; Cui, Q.; Baboul, A. G.; Clifford, S.; Cioslowski, J.; Stefanov, B. B.; Liu, G.; Liashenko, A.; Piskorz, P.; Komaromi, I.; Martin, R. L.; Fox, D. J.; Keith, T.; Al-Laham, M. A.; Peng, C. Y.; Nanayakkara, A.; Challa-combe, M.; Gill, P. M. W.; Johnson, B.; Chen, W.; Wong, M. W.; Gonzalez, C.; and Pople, J. A.; "Gaussian 03, Revision C.02", Gaussian, Inc., Wallingford, CT, 2004.
- 116 (a) Stephens, P. J.; Devlin, F. J.; Chabalowski, C. F.; Frisch, M. J. *J. Phys. Chem.* **1994**, *98*, 11623-11627. (b) Becke, A. D. *J. Phys. Chem.* **1993**, *98*, 5648-5652. (c) Lee, C.; Parr, R. G.; Yang, W. *Phys. Rev.* **1988**, *37*, 785-789.
- 117 (a) Dapprich, S.; Komaromi, I.; Byun, K. S.; Morokuma, K.; Frisch, M. J. *J. Mol. Struct.-Theochem* **1999**, *461*, 1-21. (b) Maseras, F.; Morokuma, K. *J. Comput. Chem.* **1995**, *16*, 1170-1179.
- 118 Rappe, A. K.; Casewit, C. J.; Colwell, K. S.; Goddard, W. A.; Skiff, W. M. *J. Am. Chem. Soc.* **1992**, *114*, 10024-10035.
- 119 (a) Hay, P. J.; Wadt, W. R. *J. Chem. Phys.* **1985**, *82*, 299-310. (b) Wadt, W. R.; Hay, P. J. *J. Chem. Phys.* **1985**, *82*, 284-298.
- 120 (a) Francel, M. M.; Pietro, W. J.; Hehre, W. J.; Binkley, J. S.; Gordon, M. S.; Defrees, D. J.; Pople, J. A. *J. Chem. Phys.* **1982**, *77*, 3654-3665.

The starting phosphine conformation was taken from reported X-ray structures of similar systems.

#### 4.2. Cartesian Coordinates (in Å) and Absolute Energies (in a.u.)



Scheme 58

**Scheme 58:** Cartesian coordinates (Å) of **88-I** (E = -829.748847680 a.u.).

---

---

C	-1.717004	-0.882855	1.325906
C	-2.855508	-2.184316	-0.524065
C	-1.724168	0.364693	0.453918
C	-0.579289	0.891597	-0.117099
C	-2.793221	-1.931372	0.983141
C	-2.824114	0.384185	-0.925667
C	-3.082793	1.116626	0.309438
C	-3.150964	2.634154	0.330332
P	3.609849	-0.545011	-0.000702
Au	1.322269	0.192388	-0.052853
C	-3.402655	-0.966485	-1.296939
H	-0.728482	-1.347072	1.235686
H	-1.822694	-0.563063	2.370688
H	-1.852768	-2.430829	-0.898100
H	-3.497171	-3.042082	-0.747933
H	-0.715076	1.825388	-0.663312
H	-2.548988	-2.856465	1.515055
H	-3.779765	-1.621438	1.353095
H	-2.434875	0.975121	-1.750326
H	-3.810980	0.643853	0.968578
H	-2.465118	3.098428	-0.383964
H	-2.922922	3.017758	1.329341
H	-4.165084	2.953056	0.067184
H	3.878583	-1.854077	-0.441665
H	4.537041	0.187210	-0.764573
H	4.247488	-0.554188	1.253599
H	-4.485715	-0.894255	-1.120383
H	-3.262119	-1.118171	-2.370855

---

---

**Scheme 58:** Cartesian coordinates (Å) of **TS89-I** ( $E = -829.741295031$  a.u.,  $\text{freq} = -87.0354$ ).

---

---

C	-1.802634	-1.511297	-0.003752
C	-4.324481	-1.354046	-0.056674
C	-1.739014	-0.099628	-0.530105
C	-0.550941	0.627183	-0.646487
C	-3.111105	-1.887237	0.711547
C	-2.956650	0.775016	-0.497752
C	-1.972898	1.263726	0.561380
C	-1.627604	2.740692	0.693282
P	3.600579	-0.563468	0.383056
Au	1.345263	0.047524	-0.137590
C	-4.320868	0.181468	-0.105348
H	-1.702079	-2.127532	-0.911669
H	-0.916445	-1.726271	0.604321
H	-4.314388	-1.758157	-1.078066
H	-5.253995	-1.698615	0.407505
H	-0.616938	1.527681	-1.255066
H	-3.157815	-2.976769	0.805553
H	-3.111332	-1.490154	1.736292
H	-3.001278	1.498731	-1.312931
H	-2.008585	0.747023	1.518757
H	-1.618071	3.258032	-0.268106
H	-0.670801	2.894571	1.197647
H	-2.415141	3.189443	1.312203
H	4.584249	-0.213767	-0.560356
H	4.161828	-0.029644	1.558075
H	3.879122	-1.931645	0.558627
H	-4.615172	0.582111	0.872629
H	-5.070497	0.537315	-0.818170

---

---

**Scheme 58:** Cartesian coordinates (Å) of **90-I** (E = -829.742186002 a.u.).

---

---

C	-1.845116	-1.566510	-0.140312
C	-4.361595	-1.280060	0.027624
C	-1.772009	-0.154121	-0.615349
C	-0.583869	0.662944	-0.603648
C	-3.120338	-1.941647	0.636182
C	-2.908177	0.753697	-0.478684
C	-1.702054	1.255946	0.476259
C	-1.604493	2.782356	0.612162
P	3.576822	-0.583147	0.380096
Au	1.326974	0.047289	-0.122195
C	-4.250141	0.252835	0.061753
H	-1.814301	-2.124418	-1.095322
H	-0.924315	-1.840716	0.385567
H	-4.487166	-1.616934	-1.010361
H	-5.260254	-1.593146	0.568211
H	-0.591606	1.450908	-1.359451
H	-3.222769	-3.031166	0.642366
H	-3.010653	-1.635008	1.684907
H	-2.979939	1.521102	-1.250159
H	-1.688152	0.761871	1.447139
H	-1.634247	3.278334	-0.360518
H	-0.669144	3.043792	1.114990
H	-2.443085	3.140306	1.218407
H	4.554444	-0.277807	-0.585353
H	4.166562	-0.026141	1.530452
H	3.841588	-1.949329	0.592014
H	-4.374254	0.611641	1.091791
H	-5.059230	0.705473	-0.518636

---

---

**Scheme 58:** Cartesian coordinates (Å) of **TS91-I** ( $E = -829.741531297$  a.u.,  $\text{freq} = -173.2014$ ).

---

---

C	-1.827478	-1.538477	-0.078208
C	-4.356118	-1.340264	0.006220
C	-1.783044	-0.129880	-0.593780
C	-0.576945	0.720509	-0.554729
C	-3.108254	-1.913096	0.687021
C	-2.937710	0.691781	-0.560858
C	-1.593202	1.238429	0.512429
C	-1.759501	2.750639	0.673701
P	3.584259	-0.608615	0.328606
Au	1.337085	0.062563	-0.114910
C	-4.288883	0.193249	-0.082356
H	-1.744102	-2.142067	-0.998916
H	-0.920262	-1.753372	0.495875
H	-4.447649	-1.758691	-1.004773
H	-5.258043	-1.636839	0.550309
H	-0.565878	1.470888	-1.349276
H	-3.173662	-3.002923	0.762118
H	-3.040125	-1.535546	1.716234
H	-2.948489	1.562419	-1.211728
H	-1.591549	0.717843	1.468851
H	-1.761161	3.270605	-0.286565
H	-0.906282	3.110181	1.259708
H	-2.678152	2.990575	1.217006
H	4.592144	-0.014374	-0.453978
H	4.093783	-0.379486	1.620788
H	3.903073	-1.970129	0.166283
H	-4.499465	0.643793	0.897804
H	-5.060944	0.576540	-0.757614

---

---

**Scheme 58:** Cartesian coordinates (Å) of **87-I** (E = -829.754899222 a.u.).

---

---

C	-1.763860	-1.147371	0.700843
C	-4.020647	-1.795769	-0.218319
C	-1.843118	0.127313	-0.120470
C	-0.552409	0.993749	-0.360298
C	-3.153254	-1.706183	1.044382
C	-2.983138	0.447716	-0.806000
C	-1.249313	1.664355	0.694870
C	-1.888934	3.015987	0.606332
P	3.487380	-0.851285	0.098871
Au	1.308667	0.079079	-0.110033
C	-4.201509	-0.412007	-0.862268
H	-1.197256	-1.882263	0.111385
H	-1.172339	-0.973523	1.607913
H	-3.543852	-2.472484	-0.938901
H	-5.001054	-2.223528	0.012341
H	-0.611848	1.532376	-1.308039
H	-3.046867	-2.692888	1.506213
H	-3.640452	-1.059768	1.787186
H	-3.024398	1.388735	-1.351703
H	-1.163157	1.263577	1.703639
H	-2.060364	3.342967	-0.421926
H	-1.178489	3.722272	1.061847
H	-2.816286	3.082306	1.182791
H	4.383749	-0.608289	-0.958397
H	4.261557	-0.439472	1.199704
H	3.591762	-2.250118	0.214809
H	-5.008380	0.153981	-0.365096
H	-4.530598	-0.488601	-1.908630

---

---

**Scheme 58:** Cartesian coordinates (Å) of **88-II** ( $E = -829.751806808$  a.u.).

---

---

P	-3.635933	-0.550869	-0.004474
Au	-1.346064	0.179508	0.063252
C	1.715189	-0.943468	-1.246748
C	1.699700	0.330428	-0.408292
C	0.557826	0.869420	0.144563
C	3.516333	-0.877006	1.250935
C	2.903545	0.447851	0.874530
C	3.060924	1.153720	-0.375103
C	3.053520	2.669265	-0.444974
H	-4.062022	-1.246193	-1.151185
H	-4.058622	-1.431061	1.008907
H	-4.624274	0.446671	0.082782
H	0.695798	1.798919	0.697896
H	2.537318	1.035477	1.713333
H	3.733559	0.685463	-1.092523
H	2.421932	3.124141	0.323309
H	2.713555	3.013070	-1.426185
H	4.073971	3.036892	-0.290879
C	3.645997	-1.906691	0.119440
C	2.287582	-2.182748	-0.531678
H	4.369858	-1.567774	-0.633495
H	4.055843	-2.828604	0.544234
H	2.374281	-2.995982	-1.259790
H	1.578963	-2.520255	0.237436
H	2.294517	-0.752732	-2.158852
H	0.687726	-1.144795	-1.566864
H	2.936583	-1.305382	2.076960
H	4.505387	-0.630575	1.669050

---

---

**Scheme 58:** Cartesian coordinates (Å) of **TS89-II** (E = -829.743319680 a.u., freq = -95.0697).

---

---

P	3.583872	-0.556581	0.431694
Au	1.337644	0.053928	-0.129507
C	-1.770677	-1.519281	-0.029653
C	-1.730328	-0.113236	-0.589474
C	-0.550692	0.633302	-0.670248
C	-4.296454	0.130720	-0.158778
C	-2.953351	0.750678	-0.540437
C	-1.969659	1.263359	0.509790
C	-1.668107	2.751982	0.619825
H	3.833880	-1.904585	0.749186
H	4.563616	-0.332471	-0.553278
H	4.171710	0.085598	1.537475
H	-0.607303	1.532462	-1.281367
H	-3.026691	1.476725	-1.352665
H	-1.978756	0.752759	1.470018
H	-1.682791	3.256834	-0.348238
H	-0.711261	2.940370	1.112353
H	-2.462708	3.185571	1.240550
C	-4.167513	-1.132841	0.703893
C	-3.182927	-2.117800	0.062417
H	-3.837079	-0.878328	1.720860
H	-5.153901	-1.595326	0.809891
H	-3.136091	-3.051425	0.631850
H	-3.536942	-2.381579	-0.942674
H	-1.277622	-1.526709	0.952445
H	-1.127265	-2.122151	-0.683674
H	-4.816523	-0.122362	-1.090961
H	-4.907988	0.891699	0.339844

---

---

**Scheme 58:** Cartesian coordinates (Å) of **90-II** (E = -829.744385888 a.u.).

---

---

P	3.557685	-0.578005	0.424435
Au	1.317248	0.058261	-0.112611
C	-1.805478	-1.578046	-0.198811
C	-1.762514	-0.163675	-0.682794
C	-0.586698	0.678537	-0.623321
C	-4.236077	0.181460	-0.010907
C	-2.913946	0.714862	-0.541484
C	-1.708512	1.256219	0.424389
C	-1.686880	2.786508	0.542374
H	4.138377	-0.007458	1.572799
H	3.812799	-1.942351	0.659128
H	4.547508	-0.292342	-0.534679
H	-0.571444	1.457352	-1.389064
H	-3.012521	1.497402	-1.294988
H	-1.690490	0.768130	1.397508
H	-1.710862	3.270153	-0.436834
H	-0.775456	3.092447	1.064544
H	-2.553692	3.118082	1.123137
C	-4.081774	-1.113387	0.801570
C	-3.220966	-2.127647	0.036122
H	-3.627310	-0.900510	1.779061
H	-5.071899	-1.531751	1.006637
H	-3.151928	-3.074040	0.581097
H	-3.693461	-2.354722	-0.928008
H	-1.179054	-1.656227	0.701507
H	-1.257412	-2.152686	-0.962742
H	-4.891354	0.000162	-0.872650
H	-4.722576	0.966829	0.580439

---

---

**Scheme 58:** Cartesian coordinates (Å) of **TS91-II** ( $E = -829.743725151$  a.u.,  $\text{freq} = -163.0702$ ).

---

---

P	3.564050	-0.606017	0.379755
Au	1.327274	0.069530	-0.107737
C	-1.786002	-1.545184	-0.106619
C	-1.776777	-0.135996	-0.628015
C	-0.579882	0.734467	-0.578507
C	-4.273201	0.128087	-0.101479
C	-2.949778	0.651143	-0.604277
C	-1.581616	1.275138	0.466930
C	-1.808249	2.780772	0.575617
H	4.163496	-0.080808	1.540187
H	3.809873	-1.979706	0.565235
H	4.546823	-0.297089	-0.579510
H	-0.548412	1.459619	-1.395969
H	-2.994648	1.521647	-1.254109
H	-1.579053	0.775050	1.433402
H	-1.813864	3.271437	-0.400103
H	-0.973439	3.187615	1.158639
H	-2.738492	3.010696	1.103030
C	-4.137090	-1.151785	0.737085
C	-3.192204	-2.145139	0.047892
H	-3.755555	-0.907121	1.737857
H	-5.125466	-1.597913	0.882900
H	-3.126055	-3.078829	0.614769
H	-3.591985	-2.406275	-0.940407
H	-1.227834	-1.574255	0.839845
H	-1.168837	-2.119707	-0.813350
H	-4.900535	-0.060802	-0.984740
H	-4.782612	0.924848	0.455442

---

---

**Scheme 58:** Cartesian coordinates (Å) of **87-II** ( $E = -829.755247502$  a.u.).

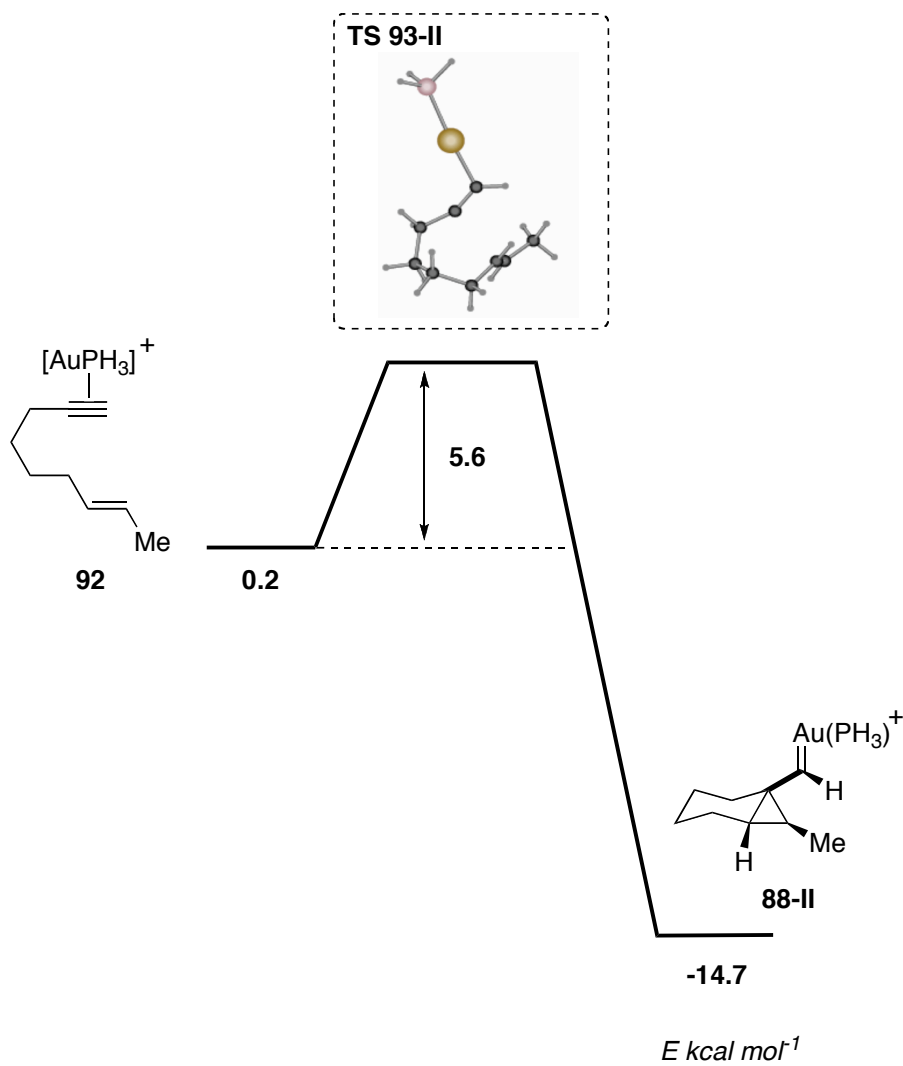
---

---

P	3.315354	-0.889129	0.096825
Au	1.181109	0.160344	-0.118472
C	-1.894357	-0.714509	1.340681
C	-2.040144	0.390412	0.308419
C	-0.582044	1.178533	-0.360595
C	-3.461273	-1.090426	-1.170955
C	-2.799884	0.198330	-0.820070
C	-1.447985	1.797150	0.632619
C	-2.238525	3.061201	0.334469
H	4.120296	-0.483053	1.177054
H	3.342807	-2.287009	0.257766
H	4.209285	-0.728406	-0.977621
H	-0.770785	1.526005	-1.377100
H	-2.927280	1.016565	-1.524912
H	-1.078404	1.753367	1.658182
H	-2.583994	3.105661	-0.702709
H	-1.596704	3.932364	0.504047
H	-3.106073	3.146490	0.996256
C	-3.455448	-2.134872	-0.042578
C	-2.133705	-2.105541	0.737251
H	-4.285931	-1.928661	0.644189
H	-3.637370	-3.128160	-0.464077
H	-2.146771	-2.855472	1.534568
H	-1.299506	-2.364023	0.069676
H	-2.627989	-0.521145	2.136256
H	-0.907521	-0.651917	1.811359
H	-2.942089	-1.471289	-2.067945
H	-4.479727	-0.873211	-1.523494

---

---



Scheme 59

**Scheme 59:** Cartesian coordinates (Å) of **92** ( $E = -829.725414221$  a.u.).

---

---

C	1.148103	1.049333	0.931373
C	3.230195	1.423259	-0.574674
C	0.508564	0.080245	0.052406
C	0.004462	-0.764697	-0.699859
C	2.701555	0.976217	0.791996
C	5.314661	-0.050268	-0.578603
C	6.132800	-0.505394	0.376067
C	6.700381	-1.893864	0.446047
P	-4.306779	0.139108	0.300741
Au	-2.020568	-0.194740	-0.096282
C	4.770730	1.352344	-0.661228
H	0.800785	2.059486	0.681006
H	0.860878	0.839752	1.968865
H	2.797152	0.798074	-1.368869
H	2.903469	2.452695	-0.774359
H	0.060833	-1.554742	-1.428275
H	3.099039	1.627596	1.579544
H	3.041358	-0.038947	1.021614
H	5.013116	-0.727510	-1.381666
H	6.443017	0.179025	1.168470
H	6.341704	-2.520575	-0.377336
H	6.437057	-2.385326	1.392115
H	7.797127	-1.871628	0.401840
H	-4.807251	1.421882	0.020941
H	-5.163322	-0.687513	-0.445477
H	-4.749301	-0.078526	1.616460
H	5.209246	1.971239	0.132739
H	5.072959	1.809783	-1.613576

---

---

*Scheme 59:* Cartesian coordinates (Å) of **TS93-II** ( $E = -829.716434769$  a.u.,  
freq =  $-97.5875$ ).

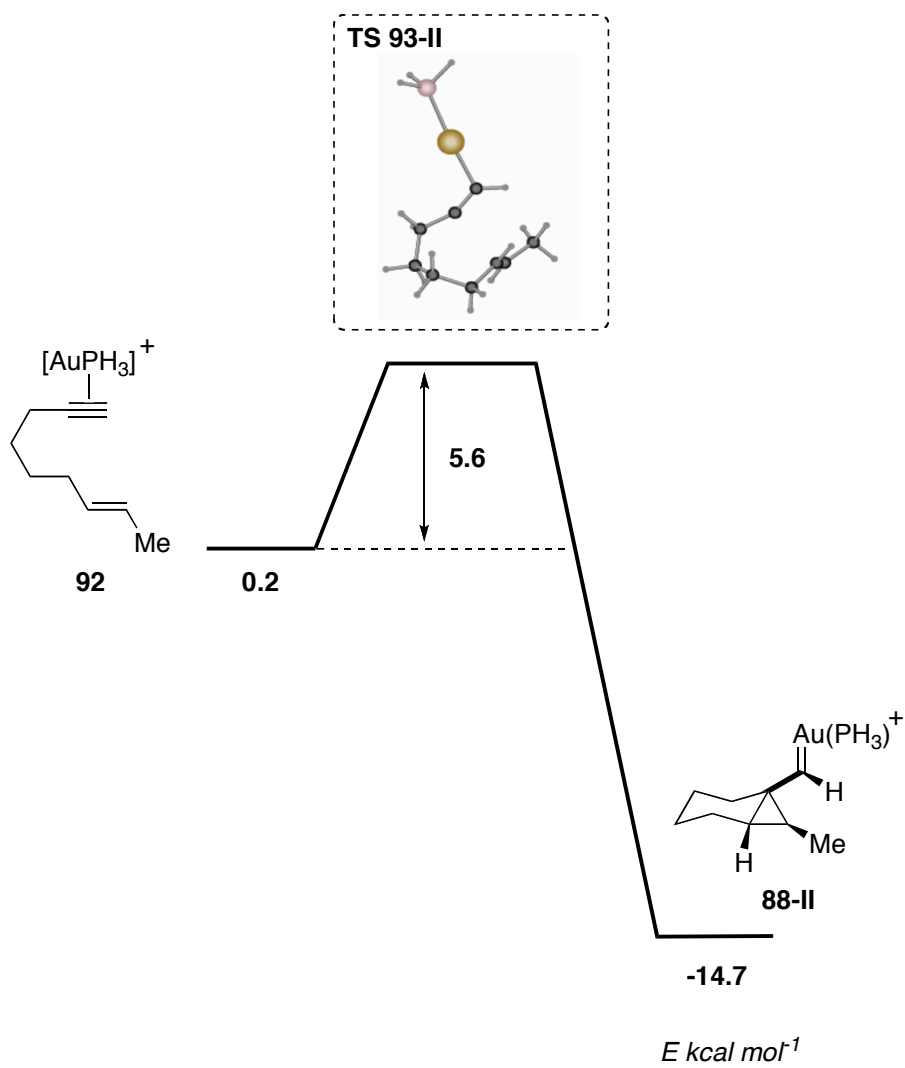
---

---

C	-1.708954	-1.323310	1.084087
C	-3.591423	-1.904944	-0.629648
C	-1.299919	-0.122859	0.348307
C	-0.489275	0.701037	-0.173484
C	-3.112907	-1.929979	0.829702
C	-3.572474	0.663605	-0.754708
C	-3.626815	1.435240	0.357358
C	-3.025572	2.799903	0.507318
P	3.834009	-0.382140	-0.022178
Au	1.529333	0.117741	-0.063596
C	-4.358423	-0.607330	-0.962525
H	-0.957266	-2.074678	0.796654
H	-1.580145	-1.138597	2.158066
H	-2.746070	-2.045693	-1.316392
H	-4.269959	-2.747853	-0.799049
H	-0.648969	1.660185	-0.646301
H	-3.061096	-2.958366	1.200124
H	-3.840329	-1.412861	1.465792
H	-3.000170	1.025467	-1.608726
H	-4.237215	1.092851	1.194552
H	-2.437824	3.094354	-0.368215
H	-2.399466	2.876627	1.404451
H	-3.827160	3.541504	0.623649
H	4.231502	-1.608922	-0.583078
H	4.669694	0.521449	-0.701640
H	4.448788	-0.438346	1.241272
H	-5.260403	-0.579460	-0.338348
H	-4.696815	-0.645286	-2.004461

---

---



Scheme 60

**Scheme 60:** Cartesian coordinates (Å) of **TS93-III** (E= -829.721559087 a.u., freq - 96.5152).

---

---

P	3.794434	-0.371219	0.058750
Au	1.492354	0.133685	-0.072501
C	-1.357480	-0.036177	0.328468
C	-0.515104	0.710556	-0.262219
C	-3.690425	0.578945	-0.516157
C	-3.538906	1.534168	0.432291
C	-3.019907	2.916986	0.190867
C	-1.848874	-1.155791	1.132994
C	-3.503213	-1.940454	-0.731077
C	-2.479174	-2.336165	0.348486
C	-4.394591	-0.742333	-0.346652
H	4.654341	0.501336	-0.631218
H	4.372369	-0.376272	1.340815
H	4.206745	-1.620541	-0.438311
H	-0.675625	1.608235	-0.846107
H	-3.373798	0.810610	-1.534695
H	-3.882119	1.319948	1.445943
H	-2.663029	3.050490	-0.835744
H	-2.216846	3.177588	0.890991
H	-3.823932	3.646918	0.355774
H	-0.980075	-1.517487	1.703470
H	-2.544968	-0.768792	1.884493
H	-2.982009	-1.702494	-1.667299
H	-4.129542	-2.812642	-0.945156
H	-2.955350	-2.977901	1.098574
H	-1.678911	-2.928950	-0.107627
H	-4.779764	-0.849354	0.675476
H	-5.273880	-0.731930	-1.005058

---

---

**Scheme 60:** Cartesian coordinates (Å) of **88-III** (E= -829.746381317 a.u.).

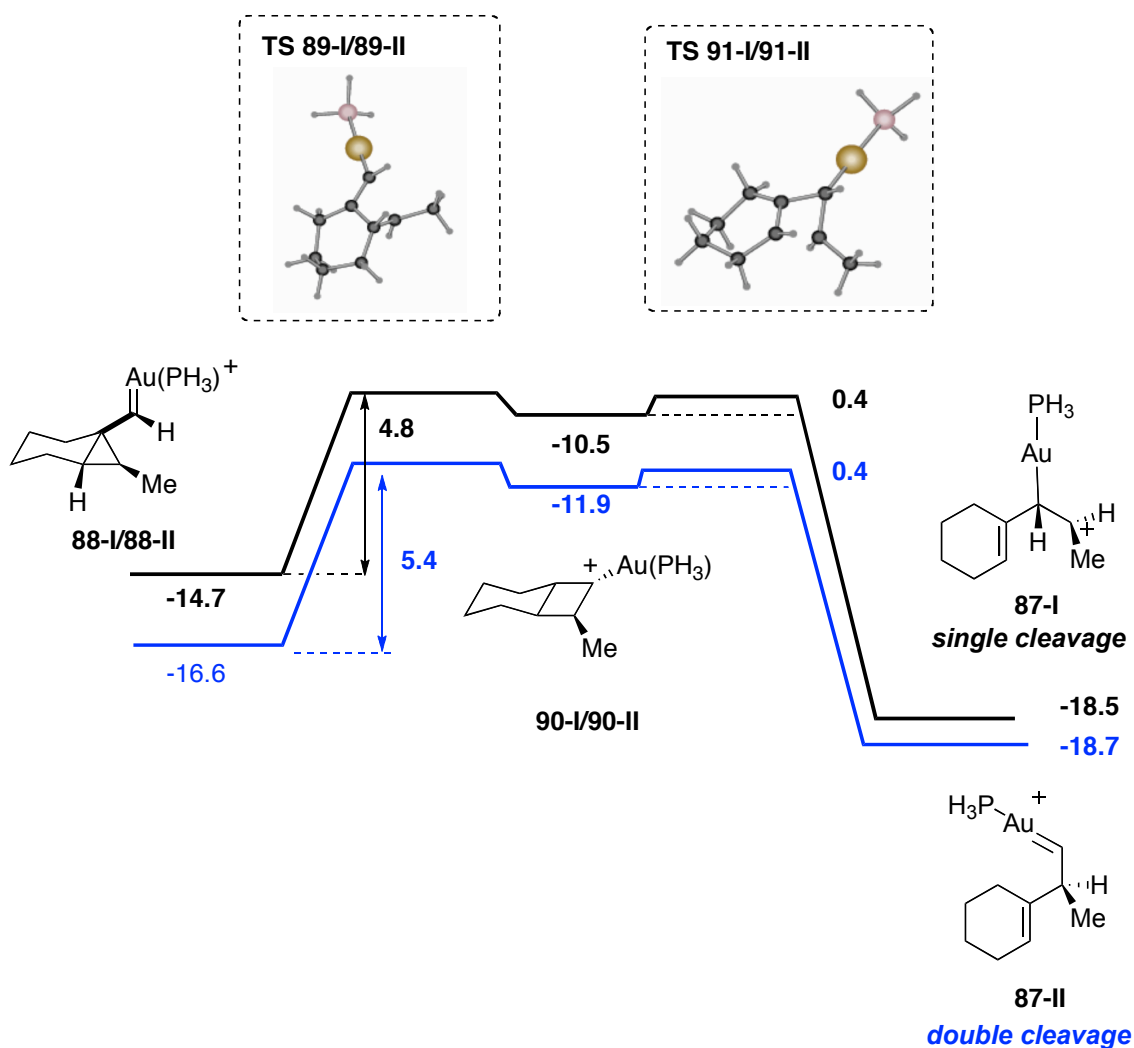
---

---

P	-3.578142	0.426397	0.057475
Au	-1.264598	-0.217095	-0.080913
C	1.770470	-0.337678	0.415346
C	0.660618	-0.825757	-0.234599
C	3.112117	-0.253897	-0.669941
C	3.130811	-1.215875	0.398144
C	3.086937	-2.710015	0.160264
C	1.738694	0.867107	1.343810
C	2.633376	2.228927	-0.671153
C	1.721136	2.217442	0.581739
C	3.717424	1.132965	-0.618270
H	-4.502216	-0.367535	-0.646113
H	-4.163872	0.446050	1.336694
H	-3.921317	1.708877	-0.409118
H	0.841389	-1.656955	-0.917272
H	2.841307	-0.615262	-1.659613
H	3.694414	-0.924023	1.283540
H	2.584180	-2.978480	-0.772952
H	2.596199	-3.228650	0.988919
H	4.116611	-3.079138	0.092510
H	0.857584	0.790356	1.988768
H	2.606305	0.833836	2.010873
H	2.035813	2.076835	-1.578070
H	3.115885	3.204580	-0.780747
H	2.028099	3.001576	1.281848
H	0.693975	2.456124	0.285051
H	4.337188	1.243862	0.278037
H	4.384336	1.223169	-1.484363

---

---



**Scheme 61**

**Scheme 61:** Cartesian coordinates (Å) of **TS94-II** ( $E = -829.741247266$  a.u.,  $\text{freq} = -152.9107$ ).

P	3.610833	-0.492453	0.040131
Au	1.306450	0.188431	-0.079478
C	-1.724051	-0.897034	1.269739
C	-1.738920	0.353534	0.405911
C	-0.605716	0.838446	-0.214267
C	-3.852111	-0.930381	-0.777293
C	-3.051407	0.363628	-0.716930

C	-3.054278	1.267033	0.408683
C	-2.961368	2.771873	0.260648
H	4.215566	-0.482913	1.310539
H	3.924216	-1.794398	-0.392043
H	4.536661	0.263991	-0.701382
H	-0.759396	1.703961	-0.859614
H	-2.732765	0.776555	-1.670141
H	-3.661800	0.945364	1.254466
H	-2.430679	3.078829	-0.644805
H	-2.472947	3.225803	1.127922
H	-3.977560	3.176500	0.193889
C	-3.196203	-2.272582	-0.298518
C	-1.826578	-2.152091	0.387359
H	-3.897320	-2.743507	0.397747
H	-3.112434	-2.952595	-1.150965
H	-1.649912	-3.048933	0.990417
H	-1.021718	-2.115567	-0.358600
H	-2.543346	-0.876016	1.998268
H	-0.791562	-0.907709	1.843122
H	-4.168869	-1.042098	-1.818394
H	-4.764409	-0.761094	-0.195617

---

---

**Scheme 61:** Cartesian coordinates (Å) of **TS94-I** (E= -829.744728197 a.u., freq = -98.9518).

---

---

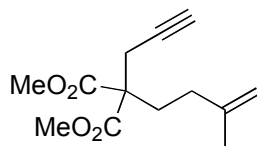
P	-3.592939	0.455286	0.031486
Au	-1.282902	-0.204649	-0.074247
C	1.760601	-0.345294	0.433015
C	0.638142	-0.836900	-0.198040
C	3.026030	-0.322493	-0.779027
C	3.120574	-1.189545	0.368011
C	3.091111	-2.700846	0.256490
C	1.729700	0.845426	1.383945
C	2.606374	2.177965	-0.679055
C	2.159253	2.227331	0.786701
C	3.637059	1.054567	-0.903154
H	-4.505069	-0.292527	-0.735463
H	-4.212213	0.415109	1.294347
H	-3.913105	1.763281	-0.377198
H	0.804246	-1.694318	-0.851308
H	2.680933	-0.771436	-1.707048
H	3.758904	-0.819690	1.170416
H	2.506700	-3.051863	-0.598434
H	2.688582	-3.153735	1.167250
H	4.116638	-3.062545	0.122390
H	0.705030	0.914229	1.759859
H	2.352315	0.613493	2.254400
H	1.750580	2.021948	-1.348315
H	3.054891	3.137186	-0.956158
H	2.983189	2.627857	1.387784
H	1.334054	2.938435	0.889785
H	4.457999	1.162940	-0.184049
H	4.066621	1.128393	-1.908371

---

---

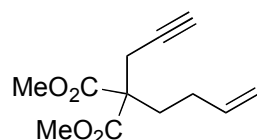
### 4.3. Procedures for the Synthesis of Staring Enynes

#### Dimethyl 2-(3-methylbut-3-enyl)-2-(prop-2-ynyl)malonate (**20h**)



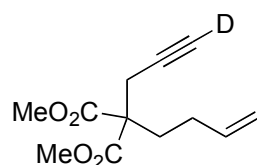
Enyne **20h** was prepared following the general procedure for alkylation<sup>121</sup> using propargylmalonate (Aldrich) and 4-iodo-2-methylbut-1-ene<sup>122</sup> in DMF. The product has been previously described in the literature.<sup>123</sup>

#### Dimethyl 2-(but-3-enyl)-2-(prop-2-ynyl)malonate (precursor of **20g-d<sub>1</sub>**)<sup>68</sup>



The usual procedure was followed starting from methylpropargylmalonate (0.51 g, 3.5 mmol), NaH (0.36 g, 9 mmol) in DMF. After addition of 4-bromo-1-butene (0.4 mL, 3.7 mmol), the mixture was heated overnight at 70 °C. After the usual work-up, purification by flash chromatography (SiO<sub>2</sub>, Hexane:AcOEt, 25:2) afforded the expected compound as a colorless oil in a 30% yield. The product has been previously described in the literature.<sup>124</sup>

#### 2-(But-3-enyl)-2-(3-deuterioprop-2-ynyl)-malonic acid dimethyl ester (**20g-d<sub>1</sub>**)<sup>68</sup>



A two-necked round bottomed flask was dried and equipped with a thermometer and a magnetic stirrer. Enyne **20g** (0.11 g, 0.5 mmol) was introduced in and 5 mL of dry

121 Susana Porcel, *PhD Thesis*, Madrid, 2007.

122 Preparation of 4-iodo-2-methylbut-1-ene: Helmboldt, H.; Köhler, D.; Hiersemann, M. *Org. Lett.* **2006**, *8*, 1573-1576.

123 Ikeda, S.-I.; Sanuki, R.; Miyachi, H.; Miyashita, H.; Taniguchi, M.; Odashima, K. *J. Am. Chem. Soc.* **2004**, *126*, 10331-10338.

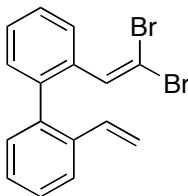
124 Trost, B. M.; Ball, Z. T. *J. Am. Chem. Soc.* **2005**, *127*, 17644-17655.

THF were added under N<sub>2</sub>. The solution was cooled to -78 °C and *n*BuLi (2.5 M in hexanes, 0.19 mL) was added. The reaction mixture was stirred at this temperature for 1h, then allowed to warm to -50 °C and stirred at this temperature for 2 h. 1 mL of D<sub>2</sub>O was added at -50 °C and the mixture was allowed to warm slowly to rt and stirred 30 min at this temperature. The resulting solution was diluted with Et<sub>2</sub>O, dried over MgSO<sub>4</sub> and evaporated. Purification by flash chromatography (SiO<sub>2</sub>, Hexane:AcOEt, 25:2) afforded the expected compound as a colorless oil in 40% yield. <sup>1</sup>H NMR (400 MHz, CDCl<sub>3</sub>) δ 5.84-5.74 (m, 2H), 5.06 (d, *J* = 17.2 Hz, 1H), 4.99 (d, *J* = 10.3 Hz, 1H), 3.74 (s, 6H), 2.85 (s, 2H), 2.19-2.15 (m, 2H), 2.01-1.95 (m, 2H).

### Synthesis of 2-(prop-1-ynyl)-2'-vinylbiphenyl (95)

The synthesis was performed in two steps starting from 2-vinylbenzeneboronic acid (Alfa Aesar). 2'-vinylbiphenyl-2-carbaldehyde was synthesized according to described procedure.<sup>125</sup> Corey-Fuchs reaction of the aldehyde to afford the methyl substituted alkyne was also reported in the literature.<sup>126</sup>

### 2-(2,2-dibromovinyl)-2'-vinylbiphenyl (precursor of 95)



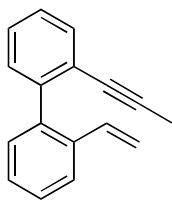
2-(2,2-dibromovinyl)-2'-vinylbiphenyl was obtained as a yellow oil (4.75 g, 97%). <sup>1</sup>H NMR (400 MHz, CDCl<sub>3</sub>) δ 7.74-7.62 (m, 2H), 7.44-7.27 (m, 4H), 7.27-7.20 (m, 1H), 7.14 (dd, *J* = 7.5, 1.4 Hz, 1H), 6.98 (bs, 1H), 6.39 (dd, *J* = 17.5, 11.0 Hz, 1H), 5.67 (dd, *J* = 17.5, 1.1 Hz, 1H), 5.15 (dd, *J* = 11.0, 1.1 Hz, 1H). <sup>13</sup>C NMR (100 MHz, CDCl<sub>3</sub>) δ 140.30 (C), 138.90 (C), 136.87 (CH), 136.48 (C), 135.13 (CH), 130.63 (CH), 130.42 (CH), 128.87 (CH), 128.42 (CH), 128.24 (CH), 127.66 (CH), 127.45 (CH), 125.33 (CH), 115.08 (CH<sub>2</sub>), 91.22 (C). HRMS-APCI calcd for C<sub>16</sub>H<sub>13</sub>Br<sub>2</sub> [M+H]<sup>+</sup>: 364.9364. Found: 364.9369.

---

125 Schmid, G. A.; Borsberg, H. J. *Helv. Chim. Acta.* **2001**, *84*, 388-400.

126 Fürstner, A.; Mamane, V. *J. Org. Chem.* **2002**, *67*, 6264-6267.

## 2-(prop-1-ynyl)-2'-vinylbiphenyl (95)

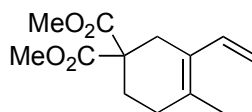


White solid (0,59 g, 82%). mp 37-39 °C.  $^1\text{H}$  NMR (400 MHz,  $\text{CDCl}_3$ )  $\delta$  7.66 (d,  $J = 7.5$  Hz, 1H), 7.53-7.44 (m, 1H), 7.39-7.23 (m, 5H), 7.23-7.16 (m, 1H), 6.54 (dd,  $J = 17.5, 11.0$  Hz, 1H), 5.66 (d,  $J = 17.5$  Hz, 1H), 5.11 (d,  $J = 11.0$  Hz, 1H), 1.81 (s, 3H).  $^{13}\text{C}$  NMR (100 MHz,  $\text{CDCl}_3$ )  $\delta$  143.17 (C), 140.09 (C), 136.20 (C), 135.74 (CH), 132.34 (CH), 130.53 (CH), 130.48 (CH), 127.70 (CH), 127.34 (CH), 127.25 (CH), 127.23 (CH), 124.92 (CH), 123.92 (C), 114.21 ( $\text{CH}_2$ ), 89.47 (C), 78.95 (C), 4.53 ( $\text{CH}_3$ ). HRMS-APCI calcd for  $\text{C}_{17}\text{H}_{15}$   $[\text{M}+\text{H}]^+$ : 219.1174. Found: 219.1178.

### 4.4. Procedure for the Gold(I)-Catalyzed Cyclization of Enyne 20h

Over a solution of gold catalyst **B** (2 mol%) in 1 mL of  $\text{CH}_2\text{Cl}_2$ , enyne **20h** (0.21 mmol) was added solved in 1 mL of  $\text{CH}_2\text{Cl}_2$ . The reaction was stirred at room temperature for 2 h. The reaction was quenched with 1 mL of  $\text{Et}_3\text{N}$  (0.1 M in hexanes). The crude was purified by flash chromatography (silica gel) using hexane:EtOAc mixtures, affording **21h** as a colorless oil in 86% yield.

### Dimethyl 4-methyl-3-vinylcyclohex-3-ene-1,1-dicarboxylate (21h)

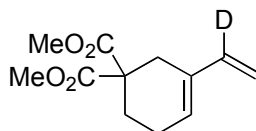


$^1\text{H}$  NMR (400 MHz,  $\text{CDCl}_3$ )  $\delta$  6.78 (dd,  $J = 17.3, 11.1$  Hz, 1H), 5.16 (d,  $J = 17.5$  Hz, 1H), 5.00 (d,  $J = 11.1$  Hz, 1H), 3.73 (s, 6H), 2.69 (bs, 2H), 2.19-2.10 (m, 4H), 1.75 (bs, 3H).  $^{13}\text{C}$  NMR  $\delta$  (100 MHz,  $\text{CDCl}_3$ ) 172.24 (C), 134.32 (CH), 132.08 (C), 125.41 (C), 111.29 ( $\text{CH}_2$ ), 53.50 (C), 52.82 ( $\text{CH}_3$ ), 30.44 ( $\text{CH}_2$ ), 29.90 ( $\text{CH}_2$ ), 27.73 ( $\text{CH}_2$ ), 18.98 ( $\text{CH}_3$ ). HRMS-ESI calcd for  $\text{C}_{13}\text{H}_{18}\text{O}_4\text{Na}$   $[\text{M}+\text{Na}]^+$ : 261.1103. Found: 261.1090.

#### 4.5. Procedure for the gold(I)-catalyzed cyclization of *D*-dimethyl 2-(but-3-enyl)-2-(prop-2-ynyl)malonate (**20g-d<sub>1</sub>**)

Over a solution of gold catalyst **B** (2 mol%) in 1.5 mL of 1,2-dichloroethane at 80 °C, enyne **20g-d<sub>1</sub>** (0.22 mmol) was added solved in 0.5 mL of 1,2-dichloroethane. The reaction was stirred at 80 °C during 1 h, and then quenched using 1 mL of Et<sub>3</sub>N (0.1 M solution in hexanes). The crude was purified by flash chromatography (silica gel) with hexane:EtOAc mixtures. Product **21g-d<sub>1</sub>** was obtained as a colorless oil in 94% yield.

#### *D*-dimethyl 3-vinylcyclohex-3-ene-1,1-dicarboxylate (**21g-d<sub>1</sub>**)<sup>68</sup>

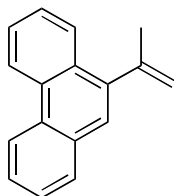


<sup>1</sup>H NMR (400 MHz, CDCl<sub>3</sub>) δ 5.70 (s, 1H), 5.14 (s, 1H), 4.99 (s, 1H), 3.73 (s, 6H), 2.70 (s, 2H), 2.22 (br s, 2H), 2.16-2.12 (m, 2H).

#### 4.6. Procedure for the gold(I)-catalyzed cyclization of enyne **95**

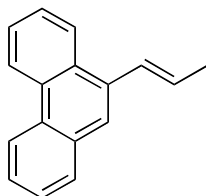
Over a solution of catalyst **G** (5 mol%) in CH<sub>2</sub>Cl<sub>2</sub> or 1,2-dichloroethane, enyne **95** (0.23 mmol) solved in 1 additional mL of the solvent of choice. The reaction was stirred at room temperature or 80°C until TLC showed complete conversion. Crude analysis was made by <sup>1</sup>H NMR. Cyclization products were purified by flash chromatography (silica gel) using hexane as eluent.

#### 9-(prop-1-en-2-yl)phenanthrene (**96**)



This product was previously described in the literature.<sup>127</sup> <sup>1</sup>H NMR (400 MHz, CDCl<sub>3</sub>) δ 8.77-8.58 (m, 2H), 8.11-8.04 (m, 1H), 7.88-7.80 (m, 1H), 7.69-7.51 (m, 5H), 5.42 (bs, 1H), 5.14 (bs, 1H), 2.24 (bs, 3H).

### (*E*)-9-(prop-1-enyl)phenanthrene (97)

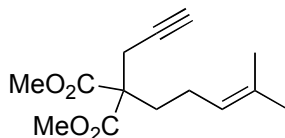


This product was previously described in the literature.<sup>127</sup> <sup>1</sup>H NMR (400 MHz, CDCl<sub>3</sub>) δ 8.77-8.58 (m, 2H), 8.18-8.13 (m, 1H), 7.88-7.80 (m, 1H), 7.69-7.51 (m, 5H), 7.11 (d, *J* = 14.6 Hz, 1H), 6.37-6.25 (m, 1H), 2.02 (d, *J* = 6.6 Hz, 3H).

## 5. Gold-catalyzed [4+2] Cycloaddition of Substituted 1,7-enynes

### 5.1 Procedure for the Synthesis of Starting Enynes

#### Dimethyl 2-(4-Methylpent-3-enyl)-2-(prop-2-ynyl)malonate (20e, precursor of 105a and 105d)<sup>68</sup>

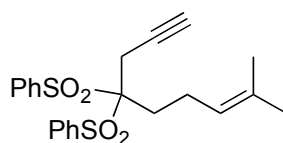


Over a suspension of NaH (7.05 mmol) in DMF at 0 °C, dimethyl propargylmalonate (5.87 mmol) was added and stirred for 30 min. Then, 5-bromo-2-methylpent-2-ene was added and the mixture was stirred at room temperature for five days. The reaction was quenched with water, extracted with Et<sub>2</sub>O/HCl (10%) and purified through chromatography using hexane/EtOAc mixtures to give the title compound in 57% yield. Spectroscopic data of enyne **20e** were available in the literature.<sup>128</sup>

127 Matsumoto, M.; Dobashi, S.; Kondo, K. *Bull. Chem. Soc. Jpn.* **1978**, *51*, 185-187.

128 Nishizawa, M.; Yadav, V. K.; Skwarczynski, M.; Takao, H.; Imagawa, H.; Sugihara T. *Org. Lett.* **2003**, *5*, 1609-1611.

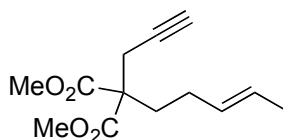
#### 4,4-Bis(phenylsulfonyl)-8,8-dimethyl-7-hepten-1-yne (**20c**, precursor of **105b**)<sup>68</sup>



Step 1: To a suspension of NaH (0.14 g, mmol) in 15 mL of dry DMF was added a solution of bisphenylsulfonylmethane (1.00 g, 3.4 mmol) in 5 mL of DMF at 0 °C. The mixture was stirred for 30 min at 0 °C and 4-methyl-bromopentene (0.45 mL) in 5 mL of DMF was added. The reaction was stirred at rt for 4 days, and after it was quenched with water. Purification by flash chromatography (SiO<sub>2</sub>, Hexane:AcOEt, 3:1 to 2:1) afforded the bis(phenylsulfonyl)-5-methylhex-4-ene in a 71% yield.

Step 2: To a suspension of NaH (80 mg, 1.9 mmol) in 5 mL of dry DMF was added a solution of bis(phenylsulfonyl)-5-methylhex-4-ene (0.60 g, 1.6 mmol) in 15 mL of DMF at 0 °C. The mixture was stirred for 30 min at low temperature and the propargylbromide (0.2 mL) was added. The reaction was stirred at rt for 4.5 days, and quenched with water. Purification by flash chromatography (SiO<sub>2</sub>, Hexane:AcOEt, 8:1 to 6:1) afforded the expected 1,7-enyne in a 70% yield. Enyne **20c** has been previously described.<sup>129</sup>

#### (*E*)-dimethyl 2-(pent-3-enyl)-2-(prop-2-ynyl)malonate (**20d**)<sup>68</sup>



To a suspension of NaH (0.13 g, mmol) in 10 mL of dry DMF was added a solution of dimethylpropargylmalonate (0.44 g, 3.1 mmol) in 5 mL of DMF at 0 °C. The mixture was stirred for 30 min at low temperature and then bromopent-4-ene (0.40 g) in 2 mL of DMF was added. The reaction was stirred at rt for 3 days (80% conversion monitored by <sup>1</sup>H NMR), and quenched with water. Purification by flash chromatography (SiO<sub>2</sub>, Hexane:AcOEt, 7:1) afforded the expected compound as a 9:1 mixture of *E*:*Z* isomers (determined by <sup>1</sup>H NMR) in a 22% yield. Colorless oil. <sup>1</sup>H NMR (400 MHz, CDCl<sub>3</sub>) δ 5.49-5.35 (m, 2 H), 3.74 (s, 6H, *Z* isomer), 3.73 (s, 6 H, *E* isomer), 2.86 (d, *J* = 2.8 Hz, 2H *Z* isomer), 2.83 (d, *J* = 3.0 Hz, 2H *E* isomer), 2.14-2.10 (m, 2H), 2.00 (t, *J* = 2.8 Hz, 1H), 1.93-1.87 (m, 2H), 1.63 (d, *J* = 6.1 Hz, 3H *E* isomer),

---

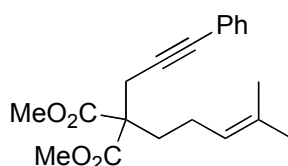
129 Trost, B. M.; Toste, F. D. *J. Am. Chem. Soc.* **2002**, *124*, 5025-5036.

1.63 (d,  $J = 6.7$  Hz, 3H Z isomer).  $^{13}\text{C}$  NMR (100 MHz,  $\text{CDCl}_3$ )  $\delta$  170.64 (C), 129.65 (CH), 125.95 (CH), 78.79 (CH), 71.30 (C), 56.65 (C), 52.72 (CH), 31.87 ( $\text{CH}_2$ ), 27.15 ( $\text{CH}_2$ ), 22.87 ( $\text{CH}_2$ ), 17.88 ( $\text{CH}_3$ ). HRMS-ESI calcd for  $\text{C}_{13}\text{H}_{18}\text{O}_4\text{Na}$  [ $\text{M} + \text{Na}$ ] $^+$ : 261.1103. Found: 261.1099.

## 5.2 General procedure for the Sonogashira coupling

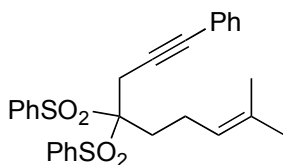
$\text{CuI}$  (0.2 mmol) and  $[\text{PdCl}_2(\text{PPh}_3)_2]$  (0.1 mmol) were suspended in piperidine and the resulting mixture was stirred for 5 min. Iodobenzene (2.6 mmol) and the corresponding enyne (2 mmol) were added sequentially. The reaction was stirred at room temperature until TLC showed total conversion. The crude mixture was quenched with water, extracted with  $\text{Et}_2\text{O}/\text{HCl}$  (10%) and purified through flash chromatography (silica gel) using Hexane/ $\text{EtOAc}$  mixtures.

### Dimethyl 2-(4-methylpent-3-enyl)-2-(3-phenylprop-2-ynyl)malonate (**105a**)



Starting from the enyne **20e** and iodobenzene (98%, Fluka) and following the general procedure for Sonogashira coupling, **105a** was obtained in 68% yield. Colorless oil.  $^1\text{H}$  NMR (400 MHz,  $\text{CDCl}_3$ )  $\delta$  7.38-7.33 (m, 2H), 7.29-7.24 (m, 3H), 5.11 (tq,  $J = 7.1, 1.4$  Hz, 1H), 3.75 (s, 6H), 3.07 (bs, 2H), 2.18-2.11 (m, 2H), 1.98-1.90 (m, 2H), 1.68 (bs, 3H), 1.60 (bs, 3H).  $^{13}\text{C}$  NMR (100 MHz,  $\text{CDCl}_3$ )  $\delta$  171.06 (C), 132.97 (C), 131.85 (CH), 128.37 (CH), 128.14 (CH), 123.45 (C), 123.13 (CH), 84.53 (C), 83.62 (C), 57.33 (C), 52.89 ( $\text{CH}_3$ ), 32.47 ( $\text{CH}_2$ ), 25.86 ( $\text{CH}_3$ ), 23.99 ( $\text{CH}_2$ ), 23.02 ( $\text{CH}_2$ ), 17.77 ( $\text{CH}_3$ ). HRMS-ESI calcd for  $\text{C}_{20}\text{H}_{24}\text{O}_4$  [ $\text{M}$ ] $^+$ : 328.1675. Found: 328.1676.

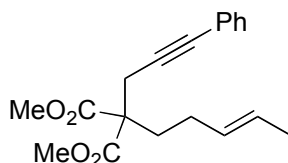
### 4,4-Bis(phenylsulfonyl)-8,8-dimethyl-7-hepten-1-yne (**105b**)



Starting from the enyne **20c** and iodobenzene (98%, Fluka) and following the general procedure for Sonogashira coupling, **105b** was obtained in 45% yield. Yellow

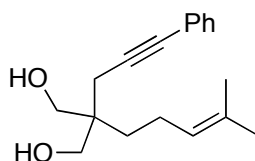
solid; mp: 163-164 °C;  $^1\text{H}$  NMR (400 MHz,  $\text{CDCl}_3$ )  $\delta$  8.12 (d,  $J = 7.3$  Hz, 4H), 7.67 (t,  $J = 7.5$  Hz, 2H), 7.55 (t,  $J = 7.8$  Hz, 4H), 7.33-7.22 (m, 5H), 5.02 (bt,  $J = 7.2$  Hz, 1H), 3.49 (s, 2H), 2.59-2.48 (m, 2H), 2.37-2.29 (m, 2H), 1.66 (bs, 3H), 1.61 (bs, 3H).  $^{13}\text{C}$  NMR (100 MHz,  $\text{CDCl}_3$ )  $\delta$  137.15 (C), 134.80 (CH), 133.76 (CH), 131.77 (CH), 131.59 (CH), 128.80 (CH), 128.58 (CH), 128.39 (CH), 122.78 (C), 122.49 (CH), 90.06 (C), 85.92 (C), 81.80 (C), 29.40 ( $\text{CH}_2$ ), 25.85 ( $\text{CH}_3$ ), 22.93 ( $\text{CH}_2$ ), 21.48 ( $\text{CH}_2$ ), 18.03 ( $\text{CH}_3$ ). HRMS-ESI calcd for  $\text{C}_{28}\text{H}_{28}\text{O}_4\text{NaS}_2$  [ $\text{M}+\text{Na}$ ] $^+$ : 515.1327. Found: 515.1320.

### (*E*)-dimethyl 2-(pent-3-enyl)-2-(3-phenylprop-2-ynyl)malonate (105c)



Colorless oil, mixture of isomers (*trans/cis* = 13:1).  $^1\text{H}$  NMR (400 MHz,  $\text{CDCl}_3$ )  $\delta$  7.39-7.33 (m, 2H), 7.30-7.24 (m, 3H), 5.53-5.36 (m, 2H), 3.75 (s, 6H), 3.05 (bs, 2H), 2.21-2.14 (m, 2H), 1.99-1.92 (m, 2H), 1.63 (dd,  $J = 6.0, 1.0$  Hz, 3H). Significant signals for the *cis* isomer:  $^1\text{H}$  NMR (400 MHz,  $\text{CDCl}_3$ )  $\delta$  3.76 (s, 3 H), 3.08 (bs, 2H), 1.60 (d,  $J = 6.7$  Hz, 3H).  $^{13}\text{C}$  NMR (100 MHz,  $\text{CDCl}_3$ )  $\delta$  171.01 (C), 131.85 (CH), 129.98 (CH), 128.38 (CH), 128.15 (CH), 126.11 (C), 123.43 (C), 84.48 (C), 83.62 (C), 57.27 (C), 52.91 ( $\text{CH}_3$ ), 32.32 ( $\text{CH}_2$ ), 27.45 ( $\text{CH}_2$ ), 24.04 ( $\text{CH}_2$ ), 18.09 ( $\text{CH}_3$ ). HRMS-ESI calcd for  $\text{C}_{19}\text{H}_{22}\text{O}_4\text{Na}$  [ $\text{M}+\text{Na}$ ] $^+$ : 337.1416. Found: 337.1406.

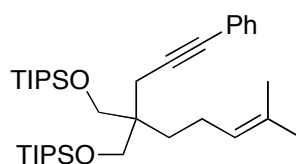
### 2-(4-Methylpent-3-enyl)-2-(3-phenylprop-2-ynyl)propane-1,3-diol (105d)



To a solution of  $\text{LiAlH}_4$  (5.48 mmol) in  $\text{Et}_2\text{O}$  (16 mL) at 0 °C, enyne **105a** (1.83 mmol) was added dropwise. After 4 h of stirring at room temperature, the reaction was quenched with the minimum amount of a 5% solution of aqueous  $\text{NaOH}$  (1 M) in THF.  $\text{MgSO}_4$  was then added and the mixture was filtered through Celite using THF as solvent. The product was purified by flash chromatography (silica gel, 2:1 Hexane-EtOAc). Yield: 47%. White solid, mp: 79-80°C;  $^1\text{H}$  NMR (400 MHz,  $\text{CDCl}_3$ )  $\delta$  7.41-7.36 (m, 2H), 7.31-7.27 (m, 3H), 5.13 (tq,  $J = 7.1, 1.4$  Hz, 1H), 3.76 (part A, AB system,  $J = 10.9$  Hz,  $^3J_{\text{OH}} = 5.6$  Hz, 2H), 3.71 (part B, AB system,  $J = 10.9$  Hz,  $^3J_{\text{OH}} =$

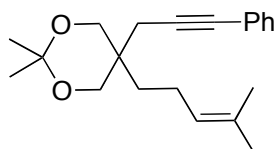
5.6 Hz, 2H), 2.52 (s, 2H), 2.17 (t,  $J = 5.6$  Hz, 2H), 2.03 (dt,  $J = 9.3, 7.4$  Hz, 2H), 1.68 (bs, 3H), 1.62 (bs, 3H), 1.44 (m, 2H).  $^{13}\text{C}$  NMR (100 MHz,  $\text{CDCl}_3$ )  $\delta$  132.23 (C), 131.76 (CH), 128.44 (CH), 127.98 (CH), 124.42 (CH), 123.80 (C), 86.71 (C), 83.12 (C), 68.41 ( $\text{CH}_2$ ), 42.40 (C), 32.05 ( $\text{CH}_2$ ), 25.87 ( $\text{CH}_3$ ), 22.58 ( $\text{CH}_2$ ), 22.03 ( $\text{CH}_2$ ), 17.83 ( $\text{CH}_3$ ). HRMS-ESI calcd for  $\text{C}_{18}\text{H}_{24}\text{O}_2\text{Na}$   $[\text{M}+\text{Na}]^+$ : 295.1674. Found: 295.1675.

### 3,3,9,9-tetraisopropyl-2,10-dimethyl-6-(4-methylpent-3-enyl)-6-(3-phenylprop-2-ynyl)-4,8-dioxa-3,9-disilaundecane (105e)



Over a solution of enyne **105d** (0.37 mmol) and imidazole (99%, 2.22 mmol) in DMF (5 mL) at  $0^\circ\text{C}$ , TIPSCl (97%, 2.22 mmol, 0.481 mL) was added dropwise. The reaction was stirred 16 h at room temperature and quenched with 3 mL of saturated  $\text{NH}_4\text{Cl}$  solution. The crude mixture was extracted with  $\text{Et}_2\text{O}$  (4x10 mL), washed with  $\text{H}_2\text{O}$  (2x10 mL) and dried over  $\text{MgSO}_4$ . The product was purified by flash chromatography (silica gel, 50:1 Hexane- $\text{EtOAc}$ ). Yield: 50%. Colorless oil.  $^1\text{H}$  NMR (400 MHz,  $\text{CDCl}_3$ )  $\delta$  7.41-7.35 (m, 2 H), 7.30-7.25 (m, 3H), 5.11 (t,  $J = 7.1$  Hz, 1H), 3.71-3.59 (m, 4H), 2.70 (bs, 2H), 2.04-1.96 (m, 2H), 1.68 (bs, 3H), 1.62 (bs, 3H), 1.45-1.39 (m, 42H).  $^{13}\text{C}$  NMR (100 MHz,  $\text{CDCl}_3$ )  $\delta$  131.67 (CH), 131.25 (C), 128.30 (CH), 127.50 (CH), 125.27 (CH), 124.54 (C), 88.40 (C), 82.36 (C), 65.18 ( $\text{CH}_2$ ), 44.39 (C), 31.88 ( $\text{CH}_2$ ), 25.91 ( $\text{CH}_3$ ), 22.78 ( $\text{CH}_2$ ), 22.47 ( $\text{CH}_2$ ), 18.29 ( $\text{CH}_3$ ), 17.83 ( $\text{CH}_3$ ), 12.24 (CH). HRMS-ESI calcd for  $\text{C}_{36}\text{H}_{64}\text{O}_2\text{SiNa}$   $[\text{M}+\text{Na}]^+$ : 607.4343. Found: 607.4337.

### 2,2-dimethyl-5-(4-methylpent-3-enyl)-5-(3-phenylprop-2-ynyl)-1,3-dioxane (105f)



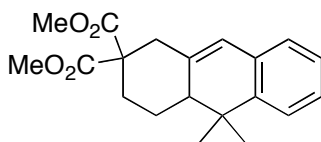
A mixture of enyne **105d** (0.37 mmol) and *p*-toluensulfonic acid (0.32 mmol) in 2,2-methoxy propane was stirred at  $0^\circ\text{C}$  until TLC showed complete conversion. Then, the reaction was quenched with 35  $\mu\text{L}$  of  $\text{Et}_3\text{N}$  and the solvent was evaporated under reduce pressure. The crude mixture was solved again in 10 mL of  $\text{Et}_2\text{O}$  and extracted consecutively with  $\text{NaOH}$  10% aq. (5mL), saturated aqueous  $\text{NaCl}$  solution (5mL),  $\text{H}_2\text{O}$

(5 mL) and dried over MgSO<sub>4</sub>. The product was purified by flash chromatography (silica gel, 2:1 Hexane-EtOAc). Yield: 94%. Yellow oil. <sup>1</sup>H NMR (400 MHz, CDCl<sub>3</sub>) δ 7.41-7.35 (m, 2H), 7.31-7.24 (m, 3H), 5.11 (t, *J* = 7.1, 1H), 3.73 (part A, AB system, *J* = 11.2 Hz, 2H), 3.70 (part B, AB system, *J* = 11.2 Hz, 2H), 2.70 (s, 2H), 2.05-1.95 (m, 2H), 1.68 (bs, 3H), 1.62 (bs, 3H), 1.43 (s, 6H), 1.45-1.38 (m, 2H). <sup>13</sup>C NMR (100 MHz, CDCl<sub>3</sub>) δ 132.15 (C), 131.77 (CH), 128.37 (CH), 127.81 (CH), 124.30 (CH), 124.06 (C), 98.32 (C), 86.93 (C), 83.04 (C), 67.54 (CH<sub>2</sub>), 35.95 (C), 33.22 (CH<sub>2</sub>), 27.10 (CH<sub>3</sub>), 25.87 (CH<sub>3</sub>), 23.25 (CH<sub>2</sub>), 21.67 (CH<sub>2</sub>), 20.91 (CH<sub>3</sub>), 17.80 (CH<sub>3</sub>). HRMS-ESI calcd for C<sub>21</sub>H<sub>28</sub>O<sub>2</sub>Na [M+Na]<sup>+</sup>: 335.1987. Found: 335.1990.

### 5.3 General Procedure for the [4+2] Cycloaddition of Substituted 1,7-Enynes

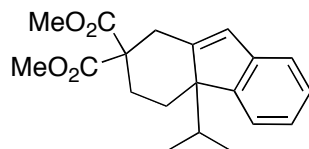
To a solution of gold(I) complex (0.0146 mmol, 5 mol%) and AgSbF<sub>6</sub> (0.0146 mmol, 5 mol%) in dry CH<sub>2</sub>Cl<sub>2</sub>, the enyne was added solved in CH<sub>2</sub>Cl<sub>2</sub>. The reaction was stirred at room temperature until TLC showed complete conversion. The resulting mixture was purified by flash-chromatography (silica gel) using Hexane/EtOAc mixtures.

#### Dimethyl 10,10-dimethyl-3,4,4a,10-tetrahydroanthracene-2,2(1*H*)-dicarboxylate (106a)



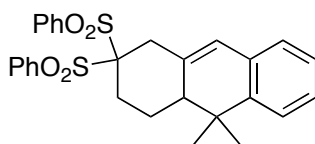
The mixture of **106a** and **107** was separated by semipreparative HPLC using 45:55 H<sub>2</sub>O-MeCN and a Sunfire 100x4.6 mm, 5 mm column for identification purposes. Colorless oil. <sup>1</sup>H NMR (400 MHz, CDCl<sub>3</sub>) δ 7.23-7.00 (m, 1H), 7.11 (quint d, *J* = 7.1, 1.6 Hz, 2H), 6.94 (dd, *J* = 7.1, 1.6 Hz, 1H), 6.17 (s, 1H), 3.72 (s, 3H), 3.68 (s, 3H), 3.11 (dd, *J* = 13.2, 2.1 Hz, 1H), 2.70 (d, *J* = 13.3 Hz, 1H), 2.52-2.42 (m, 1H), 2.03 (dd, *J* = 12.7, 3.9 Hz, 1H), 1.47-1.16 (m, 1H), 1.23 (s, 3H), 1.21 (s, 3H). <sup>13</sup>C NMR (100 MHz, CDCl<sub>3</sub>) δ 172.46 (CH), 171.00 (CH), 142.70 (C), 138.55 (C), 132.53 (C), 127.34 (CH), 126.30 (CH), 123.93 (CH), 122.57 (CH), 58.23 (C), 52.97 (CH<sub>3</sub>), 52.57 (CH<sub>3</sub>), 50.16 (CH), 40.53 (CH<sub>2</sub>), 36.27 (C), 32.12 (CH<sub>2</sub>), 30.78 (CH<sub>3</sub>), 25.61 (CH<sub>2</sub>), 23.78 (CH<sub>3</sub>). HRMS-ESI calcd for C<sub>20</sub>H<sub>24</sub>O<sub>4</sub>Na [M+Na]<sup>+</sup>: 351.1572. Found 351.1555. The structure of **117** was confirmed by COSY, NOESY, HMQC and HMBC experiments.

**Dimethyl 4a-isopropyl-4,4a-dihydro-1H-fluorene-2,2(3H)-dicarboxylate (107)**



White solid.  $^1\text{H}$  NMR (400 MHz,  $\text{CDCl}_3$ )  $\delta$  7.32 d,  $J = 7.3$  Hz, 1H), 7.28-7.24 (m, 1H), 7.20 (td,  $J = 7.4$ , 0.9 Hz, 1H), 7.07 (td,  $J = 7.4$ , 1.0 Hz, 1H), 6.46 (d,  $J = 1.7$  Hz, 1H), 3.76 (s, 3H), 3.63 (s, 3H), 3.36 (dd,  $J = 13.7$ , 2.0 Hz, 1H), 2.74 (dd,  $J = 13.7$ , 1.7 Hz, 1H), 2.47 (dt,  $J = 14.1$ , 3.2 Hz, 1H), 2.37-2.30 (m, 1H), 2.27 (q,  $J = 6.8$  Hz, 1H), 2.13 (td,  $J = 14.0$ , 3.6 Hz, 1H), 1.24 (d,  $J = 7.0$  Hz, 3H), 1.07 (td,  $J = 14.1$ , 3.9 Hz, 1H), 0.28 (d,  $J = 6.7$  Hz, 3H).  $^{13}\text{C}$  NMR (100 MHz,  $\text{CDCl}_3$ )  $\delta$  172.66 (C), 170.64 (C), 151.10 (C), 150.38 (C), 144.62 (C), 126.66 (CH), 125.44 (CH), 123.68 (CH), 123.31 (CH), 121.00 (CH), 58.03 (C), 56.12 (C), 53.11 ( $\text{CH}_3$ ), 52.72 ( $\text{CH}_3$ ), 31.89 ( $\text{CH}_2$ ), 30.81 ( $\text{CH}_2$ ), 28.20 (CH), 27.50 ( $\text{CH}_2$ ), 17.89 ( $\text{CH}_3$ ), 16.36 ( $\text{CH}_3$ ). HRMS-ESI calcd for  $\text{C}_{20}\text{H}_{24}\text{O}_4\text{Na}$   $[\text{M}+\text{Na}]^+$ : 351.1572. Found 351.1559. The structure of **107** was confirmed by COSY, NOESY, HMQC and HMBC experiments.

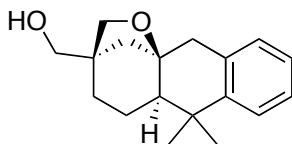
**2,2-Bis(phenylsulfonyl)-10,10-dimethyl-1,2,3,4,4a,10-hexahydroanthracene (106b)**



White solid; mp 154-157 °C;  $^1\text{H}$  NMR (400 MHz,  $\text{CDCl}_3$ )  $\delta$  8.10 (d,  $J = 7.3$  Hz, 2H), 8.03 (d,  $J = 7.6$  Hz, 2H), 7.74-7.51 (m, 6H), 7.27-7.23 (m, 1H), 7.20-7.10 (m, 2H), 7.00-6.93 (m, 1H), 3.31 (part A, AB system,  $J = 16.5$  Hz, 1H), 3.12 (part B, AB system,  $J = 16.5$  Hz, 1H), 2.68 (dt,  $J = 15.8$ , 3.7 Hz, 1H), 2.41 (ddd,  $J = 16.3$ , 12.4, 4.0 Hz, 1H), 2.14-2.07 (m, 1H), 1.93-1.84 (m, 1H), 1.89 (dq,  $J = 13.0$ , 4.2 Hz, 1H), 1.65 (qd,  $J = 12.7$ , 3.7 Hz, 1H), 1.32 (s, 3H), 0.98 (s, 3H).  $^{13}\text{C}$  NMR (100 MHz,  $\text{CDCl}_3$ )  $\delta$  143.92 (C), 136.65 (C), 136.41 (C), 134.80 (CH), 133.64 (C), 132.56 (C), 131.76 (CH), 128.86 (CH), 128.75 (CH), 127.68 (CH), 126.46 (CH), 124.84 (CH), 123.71 (CH), 87.52 (C), 44.74 (CH), 37.06 (C), 33.55 ( $\text{CH}_2$ ), 26.74 ( $\text{CH}_2$ ), 26.17 ( $\text{CH}_3$ ), 23.18 ( $\text{CH}_3$ ), 20.59

(CH<sub>2</sub>). HRMS-ESI calcd for C<sub>30</sub>H<sub>27</sub>O<sub>4</sub>S<sub>2</sub> [M]<sup>+</sup>: 515.1351. Found 515.1357. The structure of **106b** was confirmed by COSY, NOESY, HMQC and HMBC experiments.

### Cyclization product **108**



White solid. <sup>1</sup>H NMR (400 MHz, C<sub>6</sub>D<sub>6</sub>) δ 7.33 (dd, *J* = 7.8, 1.3 Hz, 1H), 7.17-7.12 (m, 1H), 7.08 (td, *J* = 7.3, 1.4 Hz, 1H), 6.99-6.95 (m, 1H), 3.73 (part A, AB system, d, *J* = 7.5, 2.0 Hz, 1H), 3.63 (part B, AB system, *J* = 7.5 Hz, 1H), 3.34 (d, *J* = 17.9 Hz, 1H), 3.12 (s, 2H), 2.98 (d, *J* = 18.0 Hz, 1H), 1.76-1.62 (m, 2H), 1.59 (dd, *J* = 10.8, 2.9 Hz, 1H), 1.52-1.45 (m, 1H), 1.33 (s, 3H), 1.27 (dd, *J* = 11.5, 5.5 Hz, 1H) 1.23 (s, 3H), 1.18-1.09 (m, 2H). <sup>13</sup>C NMR (100 MHz, C<sub>6</sub>D<sub>6</sub>) δ 147.80 (C), 134.48 (C), 128.87 (CH), 126.32 (CH), 125.98 (CH), 124.85 (CH), 82.63 (C), 74.98 (CH<sub>2</sub>), 67.28 (CH<sub>2</sub>), 50.75 (CH), 49.66 (CH<sub>2</sub>), 47.35 (C), 41.28 (CH<sub>2</sub>), 37.34 (C), 32.64 (CH<sub>2</sub>), 27.33 (CH<sub>3</sub>), 25.64 (CH<sub>3</sub>), 21.25 (CH<sub>2</sub>); HRMS-ESI calcd for C<sub>18</sub>H<sub>24</sub>O<sub>4</sub>Na [M+Na]<sup>+</sup>: 295.1674. Found: 295.1684. The structure of **108** was confirmed by COSY, NOESY, HMQC and HMBC experiments.

## 6. Crystallographic Data

### X-ray Structure of Biscyclopropane 75c.

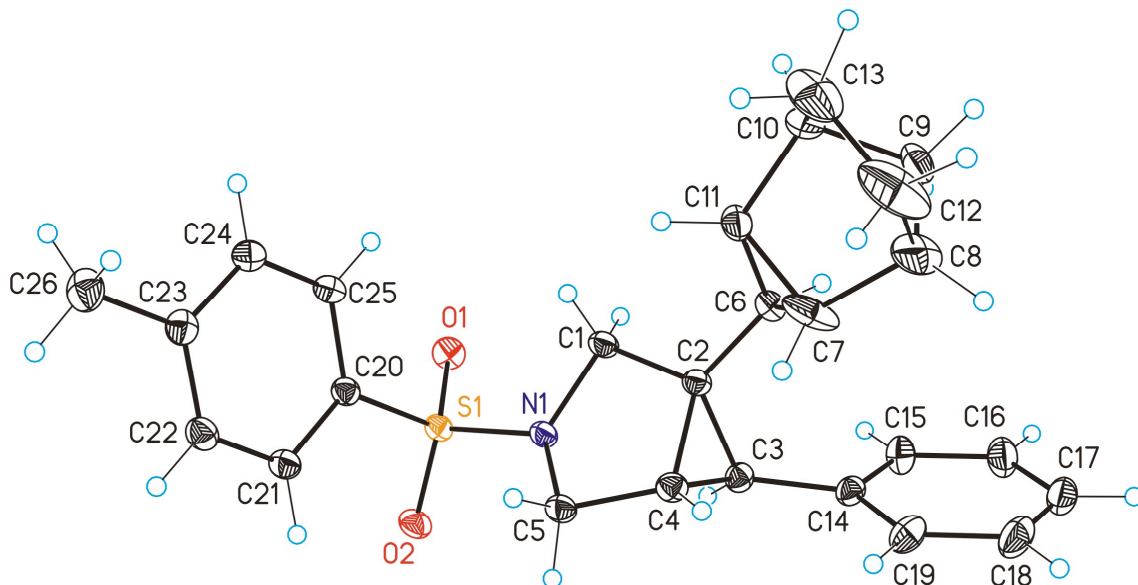


**Table 1.** Crystal data and structure refinement for **75c**.

Empirical formula	$C_{26}H_{29}NO_2S$	
Formula weight	419.56	
Temperature	100(2) K	
Wavelength	0.71073 Å	
Crystal system	Monoclinic	
Space group	P2(1)	
Unit cell dimensions	$a = 13.7052(11)$ Å	$\alpha = 90^\circ$ .
	$b = 5.9989(5)$ Å	$\beta = 111.198(2)^\circ$ .
	$c = 14.0074(11)$ Å	$\gamma = 90^\circ$ .
Volume	$1073.71(15)$ Å <sup>3</sup>	
Z	2	
Density (calculated)	1.298 Mg/m <sup>3</sup>	
Absorption coefficient	0.174 mm <sup>-1</sup>	
F(000)	448	
Crystal size	0.20 x 0.05 x 0.01 mm <sup>3</sup>	
Theta range for data collection	2.60 to 39.65°.	

Index ranges	-24<=h<=24, -9<=k<=7, -25<=l<=19
Reflections collected	19916
Independent reflections	10312 [R(int) = 0.0348]
Completeness to theta = 39.65°	91.9 %
Absorption correction	SADABS (Bruker-Nonius)
Max. and min. transmission	0.9983 and 0.9660
Refinement method	Full-matrix least-squares on F <sup>2</sup>
Data / restraints / parameters	10312 / 25 / 294
Goodness-of-fit on F <sup>2</sup>	1.039
Final R indices [I>2sigma(I)]	R1 = 0.0398, wR2 = 0.1012
R indices (all data)	R1 = 0.0448, wR2 = 0.1061
Absolute structure parameter	-0.01(4)
Largest diff. peak and hole	0.614 and -0.317 e.Å <sup>-3</sup>

**Table 2.** Bond lengths [Å] and angles [°] for **75c**.

S(1)-O(2)	1.4381(8)	C(4)-C(3)-C(2)	60.04(7)
S(1)-O(1)	1.4391(11)	C(3)-C(4)-C(2)	60.89(7)
S(1)-N(1)	1.6221(9)	C(3)-C(4)-C(5)	115.07(9)
S(1)-C(20)	1.7703(10)	C(2)-C(4)-C(5)	107.55(9)
N(1)-C(1)	1.4758(13)	N(1)-C(5)-C(4)	102.18(9)
N(1)-C(5)	1.4796(16)	C(11)-C(6)-C(7')	69.7(4)
C(1)-C(2)	1.5174(14)	C(11)-C(6)-C(7)	61.56(14)
C(2)-C(6)	1.4989(13)	C(7')-C(6)-C(7)	11.6(4)
C(2)-C(4)	1.5177(17)	C(11)-C(6)-C(2)	121.17(11)
C(2)-C(3)	1.5304(12)	C(7')-C(6)-C(2)	124.8(4)
C(3)-C(14)	1.4957(14)	C(7)-C(6)-C(2)	120.22(13)
C(3)-C(4)	1.5026(16)	C(11)-C(6)-C(11')	17.0(3)
C(4)-C(5)	1.5200(14)	C(7')-C(6)-C(11')	56.8(5)
C(6)-C(11)	1.4876(17)	C(7)-C(6)-C(11')	47.1(3)
C(6)-C(7')	1.490(4)	C(2)-C(6)-C(11')	117.1(3)
C(6)-C(7)	1.494(2)	C(6)-C(7)-C(11)	59.01(11)
C(6)-C(11')	1.516(4)	C(6)-C(7)-C(8)	120.0(2)
C(7)-C(11)	1.526(3)	C(11)-C(7)-C(8)	103.9(2)

C(7)-C(8)	1.530(3)	C(9)-C(8)-C(7)	103.84(19)
C(8)-C(9)	1.502(4)	C(9)-C(8)-C(12)	99.8(2)
C(8)-C(12)	1.558(4)	C(7)-C(8)-C(12)	105.3(2)
C(9)-C(10)	1.527(3)	C(8)-C(9)-C(10)	96.00(18)
C(10)-C(11)	1.533(2)	C(9)-C(10)-C(11)	103.77(13)
C(10)-C(13)	1.544(3)	C(9)-C(10)-C(13)	99.60(16)
C(12)-C(13)	1.556(5)	C(11)-C(10)-C(13)	105.09(19)
C(7')-C(11')	1.429(12)	C(6)-C(11)-C(7)	59.43(11)
C(7')-C(8')	1.534(4)	C(6)-C(11)-C(10)	119.05(15)
C(8')-C(9')	1.532(4)	C(7)-C(11)-C(10)	103.46(15)
C(8')-C(12')	1.558(4)	C(13)-C(12)-C(8)	102.82(19)
C(9')-C(10')	1.524(4)	C(10)-C(13)-C(12)	103.10(16)
C(10')-C(11')	1.536(4)	C(11')-C(7')-C(6)	62.5(3)
C(10')-C(13')	1.548(4)	C(11')-C(7')-C(8')	105.7(8)
C(12')-C(13')	1.548(4)	C(6)-C(7')-C(8')	120.2(6)
C(14)-C(15)	1.3932(19)	C(9')-C(8')-C(7')	102.2(6)
C(14)-C(19)	1.3952(17)	C(9')-C(8')-C(12')	103.0(3)
C(15)-C(16)	1.3940(16)	C(7')-C(8')-C(12')	103.0(5)
C(16)-C(17)	1.386(2)	C(10')-C(9')-C(8')	93.3(3)
C(17)-C(18)	1.393(2)	C(9')-C(10')-C(11')	101.3(4)
C(18)-C(19)	1.4016(18)	C(9')-C(10')-C(13')	101.4(4)
C(20)-C(21)	1.3889(17)	C(11')-C(10')-C(13')	108.0(5)
C(20)-C(25)	1.4001(14)	C(7')-C(11')-C(6)	60.7(3)
C(21)-C(22)	1.3977(15)	C(7')-C(11')-C(10')	104.1(6)
C(22)-C(23)	1.3995(16)	C(6)-C(11')-C(10')	124.3(4)
C(23)-C(24)	1.3975(18)	C(13')-C(12')-C(8')	101.6(3)
C(23)-C(26)	1.5092(15)	C(12')-C(13')-C(10')	103.5(3)
C(24)-C(25)	1.3952(15)	C(15)-C(14)-C(19)	118.42(10)
O(2)-S(1)-O(1)	120.41(5)	C(15)-C(14)-C(3)	117.78(10)
O(2)-S(1)-N(1)	106.96(5)	C(19)-C(14)-C(3)	123.73(11)
O(1)-S(1)-N(1)	106.31(5)	C(14)-C(15)-C(16)	121.32(13)
O(2)-S(1)-C(20)	107.03(5)	C(17)-C(16)-C(15)	119.88(15)
O(1)-S(1)-C(20)	107.75(5)	C(16)-C(17)-C(18)	119.72(11)

*Chapter 2. Experimental section*

N(1)-S(1)-C(20)	107.84(5)	C(17)-C(18)-C(19)	120.06(13)
C(1)-N(1)-C(5)	110.72(8)	C(14)-C(19)-C(18)	120.57(14)
C(1)-N(1)-S(1)	120.28(7)	C(21)-C(20)-C(25)	120.75(10)
C(5)-N(1)-S(1)	120.48(7)	C(21)-C(20)-S(1)	119.98(8)
N(1)-C(1)-C(2)	102.58(9)	C(25)-C(20)-S(1)	119.27(9)
C(6)-C(2)-C(1)	117.97(9)	C(20)-C(21)-C(22)	119.22(10)
C(6)-C(2)-C(4)	126.19(9)	C(21)-C(22)-C(23)	121.22(12)
C(1)-C(2)-C(4)	107.47(8)	C(24)-C(23)-C(22)	118.46(10)
C(6)-C(2)-C(3)	118.35(8)	C(24)-C(23)-C(26)	120.85(11)
C(1)-C(2)-C(3)	114.52(7)	C(22)-C(23)-C(26)	120.68(12)
C(4)-C(2)-C(3)	59.07(7)	C(25)-C(24)-C(23)	121.18(10)
C(14)-C(3)-C(4)	123.56(9)	C(24)-C(25)-C(20)	119.16(11)
C(14)-C(3)-C(2)	116.76(8)		

Symmetry transformations used to generate equivalent atoms:

**Table 3.** Torsion angles [ $^{\circ}$ ] for **75c**.

O(2)-S(1)-N(1)-C(1)	162.72(8)
O(1)-S(1)-N(1)-C(1)	32.88(9)
C(20)-S(1)-N(1)-C(1)	-82.46(9)
O(2)-S(1)-N(1)-C(5)	-52.28(9)
O(1)-S(1)-N(1)-C(5)	177.88(8)
C(20)-S(1)-N(1)-C(5)	62.55(9)
C(5)-N(1)-C(1)-C(2)	30.50(11)
S(1)-N(1)-C(1)-C(2)	178.60(7)
N(1)-C(1)-C(2)-C(6)	-167.33(9)
N(1)-C(1)-C(2)-C(4)	-17.09(10)
N(1)-C(1)-C(2)-C(3)	46.25(12)
C(6)-C(2)-C(3)-C(14)	2.24(16)
C(1)-C(2)-C(3)-C(14)	148.52(11)
C(4)-C(2)-C(3)-C(14)	-115.08(11)
C(6)-C(2)-C(3)-C(4)	117.32(11)
C(1)-C(2)-C(3)-C(4)	-96.40(10)
C(14)-C(3)-C(4)-C(2)	103.96(10)

C(14)-C(3)-C(4)-C(5)	-159.12(9)
C(2)-C(3)-C(4)-C(5)	96.92(10)
C(6)-C(2)-C(4)-C(3)	-104.33(10)
C(1)-C(2)-C(4)-C(3)	108.57(8)
C(6)-C(2)-C(4)-C(5)	146.24(9)
C(1)-C(2)-C(4)-C(5)	-0.86(10)
C(3)-C(2)-C(4)-C(5)	-109.43(9)
C(1)-N(1)-C(5)-C(4)	-30.93(10)
S(1)-N(1)-C(5)-C(4)	-178.96(6)
C(3)-C(4)-C(5)-N(1)	-47.10(11)
C(2)-C(4)-C(5)-N(1)	18.36(10)
C(1)-C(2)-C(6)-C(11)	54.90(18)
C(4)-C(2)-C(6)-C(11)	-89.17(16)
C(3)-C(2)-C(6)-C(11)	-159.97(14)
C(1)-C(2)-C(6)-C(7')	140.6(5)
C(4)-C(2)-C(6)-C(7')	-3.4(5)
C(3)-C(2)-C(6)-C(7')	-74.2(5)
C(1)-C(2)-C(6)-C(7)	127.93(18)
C(4)-C(2)-C(6)-C(7)	-16.1(2)
C(3)-C(2)-C(6)-C(7)	-86.94(19)
C(1)-C(2)-C(6)-C(11')	73.9(4)
C(4)-C(2)-C(6)-C(11')	-70.2(4)
C(3)-C(2)-C(6)-C(11')	-141.0(4)
C(7')-C(6)-C(7)-C(11)	132(3)
C(2)-C(6)-C(7)-C(11)	-111.45(14)
C(11')-C(6)-C(7)-C(11)	-11.2(4)
C(11)-C(6)-C(7)-C(8)	-88.7(3)
C(7')-C(6)-C(7)-C(8)	44(2)
C(2)-C(6)-C(7)-C(8)	159.84(19)
C(11')-C(6)-C(7)-C(8)	-99.9(4)
C(6)-C(7)-C(8)-C(9)	28.9(3)
C(11)-C(7)-C(8)-C(9)	-33.1(2)
C(6)-C(7)-C(8)-C(12)	133.3(2)

C(11)-C(7)-C(8)-C(12)	71.3(2)
C(7)-C(8)-C(9)-C(10)	50.7(2)
C(12)-C(8)-C(9)-C(10)	-57.85(19)
C(8)-C(9)-C(10)-C(11)	-50.09(18)
C(8)-C(9)-C(10)-C(13)	58.17(17)
C(7')-C(6)-C(11)-C(7)	-9.1(4)
C(2)-C(6)-C(11)-C(7)	109.96(16)
C(11')-C(6)-C(11)-C(7)	29.0(11)
C(7')-C(6)-C(11)-C(10)	79.8(4)
C(7)-C(6)-C(11)-C(10)	88.92(19)
C(2)-C(6)-C(11)-C(10)	-161.12(15)
C(11')-C(6)-C(11)-C(10)	117.9(12)
C(8)-C(7)-C(11)-C(6)	116.9(2)
C(6)-C(7)-C(11)-C(10)	-116.01(16)
C(8)-C(7)-C(11)-C(10)	0.9(2)
C(9)-C(10)-C(11)-C(6)	-31.3(2)
C(13)-C(10)-C(11)-C(6)	-135.42(18)
C(9)-C(10)-C(11)-C(7)	31.0(2)
C(13)-C(10)-C(11)-C(7)	-73.15(19)
C(9)-C(8)-C(12)-C(13)	35.7(2)
C(7)-C(8)-C(12)-C(13)	-71.7(2)
C(9)-C(10)-C(13)-C(12)	-35.5(2)
C(11)-C(10)-C(13)-C(12)	71.7(2)
C(8)-C(12)-C(13)-C(10)	0.3(2)
C(11)-C(6)-C(7')-C(11')	12.5(3)
C(7)-C(6)-C(7')-C(11')	-31(2)
C(2)-C(6)-C(7')-C(11')	-102.0(5)
C(11)-C(6)-C(7')-C(8')	-80.4(8)
C(7)-C(6)-C(7')-C(8')	-124(3)
C(2)-C(6)-C(7')-C(8')	165.0(5)
C(11')-C(6)-C(7')-C(8')	-92.9(9)
C(11')-C(7')-C(8')-C(9')	-29.6(6)
C(6)-C(7')-C(8')-C(9')	37.4(9)

C(11')-C(7')-C(8')-C(12')	77.0(5)
C(6)-C(7')-C(8')-C(12')	144.0(7)
C(7')-C(8')-C(9')-C(10')	50.9(5)
C(12')-C(8')-C(9')-C(10')	-55.8(5)
C(8')-C(9')-C(10')-C(11')	-54.3(5)
C(8')-C(9')-C(10')-C(13')	56.9(5)
C(8')-C(7')-C(11')-C(6)	116.3(5)
C(6)-C(7')-C(11')-C(10')	-121.7(5)
C(8')-C(7')-C(11')-C(10')	-5.5(6)
C(11)-C(6)-C(11')-C(7')	-136.2(13)
C(7)-C(6)-C(11')-C(7')	8.2(5)
C(2)-C(6)-C(11')-C(7')	115.5(5)
C(11)-C(6)-C(11')-C(10')	-48.8(8)
C(7')-C(6)-C(11')-C(10')	87.4(8)
C(7)-C(6)-C(11')-C(10')	95.6(7)
C(2)-C(6)-C(11')-C(10')	-157.1(5)
C(9')-C(10')-C(11')-C(7')	39.0(5)
C(13')-C(10')-C(11')-C(7')	-67.1(5)
C(9')-C(10')-C(11')-C(6)	-24.9(8)
C(13')-C(10')-C(11')-C(6)	-131.0(6)
C(9')-C(8')-C(12')-C(13')	33.5(6)
C(7')-C(8')-C(12')-C(13')	-72.5(6)
C(8')-C(12')-C(13')-C(10')	2.7(6)
C(9')-C(10')-C(13')-C(12')	-38.2(6)
C(11')-C(10')-C(13')-C(12')	67.8(6)
C(4)-C(3)-C(14)-C(15)	-163.18(10)
C(2)-C(3)-C(14)-C(15)	-92.85(12)
C(4)-C(3)-C(14)-C(19)	13.59(16)
C(2)-C(3)-C(14)-C(19)	83.91(14)
C(19)-C(14)-C(15)-C(16)	-2.06(17)
C(3)-C(14)-C(15)-C(16)	174.88(11)
C(14)-C(15)-C(16)-C(17)	0.34(19)
C(15)-C(16)-C(17)-C(18)	1.45(19)

C(16)-C(17)-C(18)-C(19)	-1.50(19)
C(15)-C(14)-C(19)-C(18)	2.00(17)
C(3)-C(14)-C(19)-C(18)	-174.75(10)
C(17)-C(18)-C(19)-C(14)	-0.25(19)
O(2)-S(1)-C(20)-C(21)	20.13(10)
O(1)-S(1)-C(20)-C(21)	150.97(8)
N(1)-S(1)-C(20)-C(21)	-94.65(9)
O(2)-S(1)-C(20)-C(25)	-158.81(8)
O(1)-S(1)-C(20)-C(25)	-27.96(9)
N(1)-S(1)-C(20)-C(25)	86.42(9)
C(25)-C(20)-C(21)-C(22)	0.75(15)
S(1)-C(20)-C(21)-C(22)	-178.17(8)
C(20)-C(21)-C(22)-C(23)	-0.09(16)
C(21)-C(22)-C(23)-C(24)	-0.64(16)
C(21)-C(22)-C(23)-C(26)	179.66(10)
C(22)-C(23)-C(24)-C(25)	0.74(16)
C(26)-C(23)-C(24)-C(25)	-179.56(10)
C(23)-C(24)-C(25)-C(20)	-0.10(16)
C(21)-C(20)-C(25)-C(24)	-0.66(15)
S(1)-C(20)-C(25)-C(24)	178.27(8)

---

Symmetry transformations used to generate equivalent atoms.

### X-ray Structure of Biscyclopropane 75f

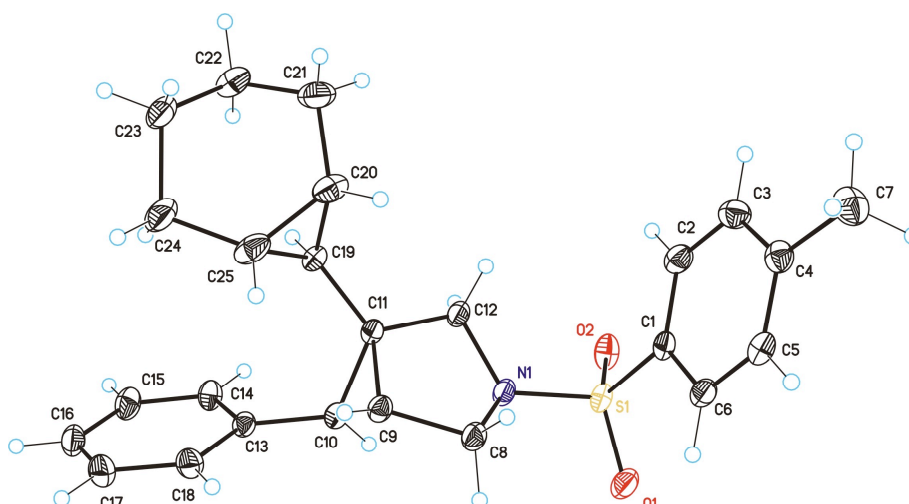


**Table 1.** Crystal data and structure refinement for **75f**.

Empirical formula	$C_{26.50}H_{30.50}C_{11.50}O_2S$	
Formula weight	466.2	
Temperature	100(2) K	
Wavelength	0.71073 $\approx$	
Crystal system	Monoclinic	
Space group	$C2/c$	
Unit cell dimensions	$a = 35.8601(11) \approx$	$a = 90^\circ$ .
	$b = 6.0216(2) \approx$	$b =$
	$111.9790(10)^\circ$ .	
	$c = 23.1924(6) \approx$	$g = 90^\circ$ .
Volume	$4644.1(2) \approx^3$	
Z	8	
Density (calculated)	1.334 $Mg/m^3$	
Absorption coefficient	0.334 $mm^{-1}$	
F(000)	1976	
Crystal size	0.40 x 0.20 x 0.20 $mm^3$	
Theta range for data collection	3.44 to 31.51 $^\circ$ .	
Index ranges	$-52 \leq h \leq 42, -6 \leq k \leq 8, -32 \leq l \leq 34$	
Reflections collected	15608	
Independent reflections	7482 [R(int) = 0.0315]	
Completeness to theta = 31.51 $^\circ$	96.7 %	

Absorption correction	SADABS (Bruker-Nonius)
Max. and min. transmission	0.9362 and 0.8781
Refinement method	Full-matrix least-squares on F <sup>2</sup>
Data / restraints / parameters	7482 / 0 / 317
Goodness-of-fit on F <sup>2</sup>	1.046
Final R indices [I>2sigma(I)]	R1 = 0.0650, wR2 = 0.1894
R indices (all data)	R1 = 0.0829, wR2 = 0.2052
Largest diff. peak and hole	1.504 and -0.922 e. <sup>-3</sup>

**Table 2.** Bond lengths [Å] and angles [°] for **75f**.

S(1)-O(1)	1.4320(16)	C(3)-C(4)-C(7)	121.2(2)
S(1)-O(2)	1.4373(17)	C(5)-C(4)-C(7)	120.3(2)
S(1)-C(8)	1.6278(16)	C(6)-C(5)-C(4)	121.35(19)
S(1)-C(1)	1.763(2)	C(5)-C(6)-C(1)	118.95(18)
C(1)-C(2)	1.389(3)	C(12)-C(8)-C(9)	110.28(15)
C(1)-C(6)	1.400(3)	C(12)-C(8)-S(1)	119.76(14)
C(2)-C(3)	1.395(3)	C(9)-C(8)-S(1)	119.24(12)
C(3)-C(4)	1.392(3)	C(8)-C(9)-C(10)	102.25(15)
C(4)-C(5)	1.395(3)	C(13)-C(10)-C(9)	115.26(16)
C(4)-C(7)	1.506(3)	C(13)-C(10)-C(11)	60.32(12)
C(5)-C(6)	1.391(3)	C(9)-C(10)-C(11)	107.92(15)
C(8)-C(12)	1.475(2)	C(20)-C(11)-C(12)	117.64(16)
C(8)-C(9)	1.482(3)	C(20)-C(11)-C(10)	125.10(16)
C(9)-C(10)	1.517(2)	C(12)-C(11)-C(10)	106.88(14)
C(10)-C(13)	1.511(3)	C(20)-C(11)-C(13)	119.76(15)
C(10)-C(11)	1.519(3)	C(12)-C(11)-C(13)	114.90(15)
C(11)-C(20)	1.489(2)	C(10)-C(11)-C(13)	59.59(12)
C(11)-C(12)	1.518(3)	C(8)-C(12)-C(11)	102.97(15)
C(11)-C(13)	1.522(3)	C(14)-C(13)-C(10)	122.25(16)
C(13)-C(14)	1.495(2)	C(14)-C(13)-C(11)	118.65(15)
C(14)-C(19)	1.391(3)	C(10)-C(13)-C(11)	60.10(12)
C(14)-C(15)	1.398(3)	C(19)-C(14)-C(15)	118.40(17)

C(15)-C(16)	1.394(3)	C(19)-C(14)-C(13)	122.94(17)
C(16)-C(17)	1.387(3)	C(15)-C(14)-C(13)	118.65(17)
C(17)-C(18)	1.379(3)	C(16)-C(15)-C(14)	121.05(19)
C(18)-C(19)	1.402(3)	C(17)-C(16)-C(15)	120.0(2)
C(20)-C(26)	1.501(3)	C(18)-C(17)-C(16)	119.61(18)
C(20)-C(21)	1.508(3)	C(17)-C(18)-C(19)	120.6(2)
C(21)-C(26)	1.512(3)	C(14)-C(19)-C(18)	120.36(19)
C(21)-C(22)	1.521(3)	C(11)-C(20)-C(26)	122.78(17)
C(22)-C(23)	1.511(6)	C(11)-C(20)-C(21)	121.84(16)
C(22)-C(23')	1.593(5)	C(26)-C(20)-C(21)	60.31(15)
C(23)-C(24)	1.538(8)	C(20)-C(21)-C(26)	59.63(13)
C(23')-C(24')	1.515(7)	C(20)-C(21)-C(22)	119.83(19)
C(24)-C(25)	1.577(6)	C(26)-C(21)-C(22)	119.97(18)
C(24')-C(25)	1.572(6)	C(23)-C(22)-C(21)	112.8(3)
C(25)-C(26)	1.519(3)	C(23)-C(22)-C(23')	31.0(3)
C(1S)-Cl(3S)	1.707(8)	C(21)-C(22)-C(23')	111.8(3)
C(1S)-Cl(2S)	1.749(6)	C(22)-C(23)-C(24)	104.5(4)
C(1S)-Cl(1S)	1.812(8)	C(24')-C(23')-C(22)	111.4(3)
O(1)-S(1)-O(2)	120.18(10)	C(23)-C(24)-C(25)	109.8(4)
O(1)-S(1)-C(8)	107.24(9)	C(23')-C(24')-C(25)	104.9(4)
O(2)-S(1)-C(8)	106.36(9)	C(26)-C(25)-C(24')	113.3(2)
O(1)-S(1)-C(1)	107.43(9)	C(26)-C(25)-C(24)	109.3(3)
O(2)-S(1)-C(1)	107.51(10)	C(24')-C(25)-C(24)	35.5(3)
C(8)-S(1)-C(1)	107.55(9)	C(20)-C(26)-C(21)	60.06(14)
C(2)-C(1)-C(6)	120.77(18)	C(20)-C(26)-C(25)	119.5(2)
C(2)-C(1)-S(1)	119.59(15)	C(21)-C(26)-C(25)	120.45(19)
C(6)-C(1)-S(1)	119.63(15)	Cl(3S)-C(1S)-Cl(2S)	114.8(4)
C(1)-C(2)-C(3)	119.07(19)	Cl(3S)-C(1S)-Cl(1S)	111.9(4)
C(4)-C(3)-C(2)	121.37(19)	Cl(2S)-C(1S)-Cl(1S)	107.7(4)
C(3)-C(4)-C(5)	118.47(19)		

---

Symmetry transformations used to generate equivalent atoms.

**Table 3.** Torsion angles [°] for **75f**.

O(1)-S(1)-C(1)-C(2)	156.01(15)
O(2)-S(1)-C(1)-C(2)	25.35(17)
C(8)-S(1)-C(1)-C(2)	-88.83(16)
O(1)-S(1)-C(1)-C(6)	-22.51(17)
O(2)-S(1)-C(1)-C(6)	-153.17(14)
C(8)-S(1)-C(1)-C(6)	92.65(16)
C(6)-C(1)-C(2)-C(3)	1.3(3)
S(1)-C(1)-C(2)-C(3)	-177.23(15)
C(1)-C(2)-C(3)-C(4)	-0.3(3)
C(2)-C(3)-C(4)-C(5)	-1.3(3)
C(2)-C(3)-C(4)-C(7)	176.87(19)
C(3)-C(4)-C(5)-C(6)	1.9(3)
C(7)-C(4)-C(5)-C(6)	-176.26(18)
C(4)-C(5)-C(6)-C(1)	-1.0(3)
C(2)-C(1)-C(6)-C(5)	-0.7(3)
S(1)-C(1)-C(6)-C(5)	177.83(14)
O(1)-S(1)-C(8)-C(12)	-168.16(15)
O(2)-S(1)-C(8)-C(12)	-38.39(18)
C(1)-S(1)-C(8)-C(12)	76.56(17)
O(1)-S(1)-C(8)-C(9)	50.80(17)
O(2)-S(1)-C(8)-C(9)	-179.43(15)
C(1)-S(1)-C(8)-C(9)	-64.48(17)
C(12)-C(8)-C(9)-C(10)	30.9(2)
S(1)-C(8)-C(9)-C(10)	175.32(13)
C(8)-C(9)-C(10)-C(13)	47.1(2)
C(8)-C(9)-C(10)-C(11)	-17.9(2)
C(13)-C(10)-C(11)-C(20)	106.92(19)
C(9)-C(10)-C(11)-C(20)	-143.69(18)
C(13)-C(10)-C(11)-C(12)	-109.39(16)
C(9)-C(10)-C(11)-C(12)	0.0(2)
C(9)-C(10)-C(11)-C(13)	109.39(17)
C(9)-C(8)-C(12)-C(11)	-31.1(2)

S(1)-C(8)-C(12)-C(11)	-175.31(13)
C(20)-C(11)-C(12)-C(8)	164.89(16)
C(10)-C(11)-C(12)-C(8)	18.05(19)
C(13)-C(11)-C(12)-C(8)	-45.7(2)
C(9)-C(10)-C(13)-C(14)	156.04(17)
C(11)-C(10)-C(13)-C(14)	-106.93(19)
C(9)-C(10)-C(13)-C(11)	-97.04(17)
C(20)-C(11)-C(13)-C(14)	-2.8(3)
C(12)-C(11)-C(13)-C(14)	-151.55(17)
C(10)-C(11)-C(13)-C(14)	112.78(19)
C(20)-C(11)-C(13)-C(10)	-115.62(19)
C(12)-C(11)-C(13)-C(10)	95.67(17)
C(10)-C(13)-C(14)-C(19)	-28.8(3)
C(11)-C(13)-C(14)-C(19)	-99.7(2)
C(10)-C(13)-C(14)-C(15)	152.48(18)
C(11)-C(13)-C(14)-C(15)	81.6(2)
C(19)-C(14)-C(15)-C(16)	-0.5(3)
C(13)-C(14)-C(15)-C(16)	178.21(18)
C(14)-C(15)-C(16)-C(17)	0.8(3)
C(15)-C(16)-C(17)-C(18)	-0.1(3)
C(16)-C(17)-C(18)-C(19)	-0.7(3)
C(15)-C(14)-C(19)-C(18)	-0.3(3)
C(13)-C(14)-C(19)-C(18)	-179.03(18)
C(17)-C(18)-C(19)-C(14)	1.0(3)
C(12)-C(11)-C(20)-C(26)	-140.40(19)
C(10)-C(11)-C(20)-C(26)	-0.2(3)
C(13)-C(11)-C(20)-C(26)	71.7(2)
C(12)-C(11)-C(20)-C(21)	-67.5(2)
C(10)-C(11)-C(20)-C(21)	72.8(3)
C(13)-C(11)-C(20)-C(21)	144.65(19)
C(11)-C(20)-C(21)-C(26)	-112.3(2)
C(11)-C(20)-C(21)-C(22)	138.3(2)
C(26)-C(20)-C(21)-C(22)	-109.4(2)

C(20)-C(21)-C(22)-C(23)	48.5(4)
C(26)-C(21)-C(22)-C(23)	-21.5(4)
C(20)-C(21)-C(22)-C(23')	82.0(3)
C(26)-C(21)-C(22)-C(23')	12.0(4)
C(21)-C(22)-C(23)-C(24)	56.4(5)
C(23')-C(22)-C(23)-C(24)	-38.3(4)
C(23)-C(22)-C(23')-C(24')	49.2(5)
C(21)-C(22)-C(23')-C(24')	-49.1(5)
C(22)-C(23)-C(24)-C(25)	-75.3(5)
C(22)-C(23')-C(24')-C(25)	70.3(5)
C(23')-C(24')-C(25)-C(26)	-55.5(4)
C(23')-C(24')-C(25)-C(24)	35.4(4)
C(23)-C(24)-C(25)-C(26)	53.8(5)
C(23)-C(24)-C(25)-C(24')	-49.6(4)
C(11)-C(20)-C(26)-C(21)	110.8(2)
C(11)-C(20)-C(26)-C(25)	-139.0(2)
C(21)-C(20)-C(26)-C(25)	110.2(2)
C(22)-C(21)-C(26)-C(20)	109.1(2)
C(20)-C(21)-C(26)-C(25)	-108.7(2)
C(22)-C(21)-C(26)-C(25)	0.4(3)
C(24')-C(25)-C(26)-C(20)	-48.7(4)
C(24)-C(25)-C(26)-C(20)	-86.7(3)
C(24')-C(25)-C(26)-C(21)	21.9(4)
C(24)-C(25)-C(26)-C(21)	-16.1(4)

---

**X-ray structure of complex 75l.**

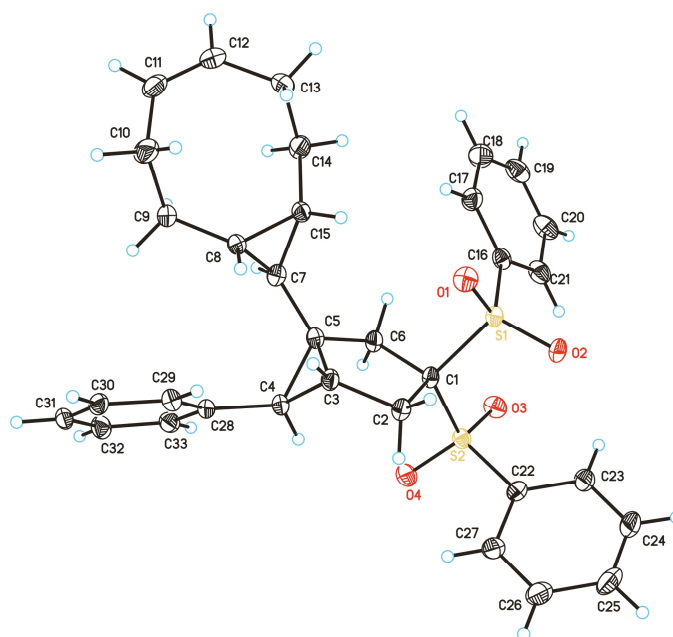


Table 1. Crystal data and structure refinement for **75l**.

Empirical formula	$C_{33}H_{34}O_4S_2$	
Formula weight	558.72	
Temperature	273(2) K	
Wavelength	0.71073 Å	
Crystal system	Triclinic	
Space group	P-1	
Unit cell dimensions	$a = 10.7285(12)$ Å	$\alpha = 111.389(5)^\circ$ .
	$b = 10.9833(12)$ Å	$\beta = 92.772(5)^\circ$ .
	$c = 13.0463(12)$ Å	$\gamma = 103.536(6)^\circ$ .
Volume	$1376.4(2)$ Å <sup>3</sup>	
Z	2	
Density (calculated)	1.348 Mg/m <sup>3</sup>	
Absorption coefficient	0.232 mm <sup>-1</sup>	
Crystal size	0.20 x 0.10 x 0.10 mm <sup>3</sup>	
Theta range for data collection	2.79 to 27.9 °.	
Index ranges	-15 ≤ h ≤ 12, -10 ≤ k ≤ 15, -18 ≤ l ≤ 18	
Reflections collected	7467	
Independent reflections	5081 [R(int) = 0.0825]	
Completeness to theta = 30.29 °	0.905 %	

Absorption correction	Empirical
Max. and min. transmission	0.9772 and 0.9551
Refinement method	Full-matrix least-squares on F <sup>2</sup>
Data / restraints / parameters	7467 / 0 / 352
Goodness-of-fit on F <sup>2</sup>	1.056
Final R indices [I>2sigma(I)]	R1 =0.0729 , wR2 = 0.1838
R indices (all data)	R1 = 0.1108 , wR2 =0.2100
Largest diff. peak and hole	0.539 and -0.600 e.Å <sup>-3</sup>

**Table 2.** Bond lengths [Å] and angles [°] for **75l**.

S1-O2	1.439(2)	O4-S2-C22	107.16(14)
S1-O1	1.442(2)	O3-S2-C22	108.42(15)
S1-C16	1.765(3)	O4-S2-C1	104.11(13)
S1-C1	1.84(3)	O3-S2-C1	108.34(13)
C1-C6	1.558(4)	C22-S2-C1	109.19(14)
C1-C2	1.563(4)	C3-C2-C1	106.2(3)
C1-S2	1.833(3)	C5-C3-C4	60.64(19)
S2-O4	1.439(2)	C5-C3-C2	109.8(2)
S2-O3	1.44(2)	C4-C3-C2	115.1(2)
S2-C22	1.764(4)	C28-C4-C3	123.6(2)
C2-C3	1.519(4)	C28-C4-C5	121.1(3)
C3-C5	1.506(5)	C3-C4-C5	59.40(19)
C3-C4	1.515(4)	C7-C5-C3	124.8(2)
C4-C28	1.498(4)	C7-C5-C4	120.6(2)
C4-C5	1.525(4)	C3-C5-C4	60.0(2)
C5-C7	1.494(4)	C7-C5-C6	116.3(3)
C5-C6	1.531(4)	C3-C5-C6	108.8(2)
C7-C8	1.515(4)	C4-C5-C6	114.4(2)
C7-C15	1.519(4)	C5-C6-C1	106.4(2)
C8-C15	1.507(4)	C5-C7-C8	124.5(3)
C8-C9	1.513(4)	C5-C7-C15	121.1(3)
C9-C10	1.547(4)	C8-C7-C15	59.55(18)

C10-C11	1.513(5)	C15-C8-C9	123.2(3)
C11-C12	1.323(4)	C15-C8-C7	60.39(18)
C12-C13	1.501(5)	C9-C8-C7	119.6(3)
C13-C14	1.558(5)	C8-C9-C10	114.0(3)
C14-C15	1.518(4)	C11-C10-C9	113.4(3)
C16-C17	1.39(4)	C12-C11-C10	126.0(3)
C16-C21	1.395(4)	C11-C12-C13	125.4(3)
C17-C18	1.383(5)	C12-C13-C14	111.8(3)
C18-C19	1.39(5)	C15-C14-C13	112.5(3)
C19-C20	1.386(5)	C8-C15-C14	121.6(3)
C20-C21	1.388(5)	C8-C15-C7	60.06(18)
C22-C23	1.394(4)	C14-C15-C7	122.0(3)
C22-C27	1.407(4)	C17-C16-C21	121.0(3)
C23-C24	1.384(6)	C17-C16-S1	117.8(2)
C24-C25	1.386(6)	C21-C16-S1	120.9(3)
C25-C26	1.394(5)	C18-C17-C16	119.9(3)
C26-C27	1.379(5)	C17-C18-C19	119.6(3)
C28-C33	1.392(4)	C20-C19-C18	120.2(3)
C28-C29	1.396(4)	C19-C20-C21	121.0(3)
C29-C30	1.396(4)	C20-C21-C16	118.3(3)
C30-C31	1.386(5)	C23-C22-C27	120.6(3)
C31-C32	1.389(5)	C23-C22-S2	119.6(3)
C32-C33	1.392(4)	C27-C22-S2	119.8(2)
O2-S1-O1	118.63(15)	C24-C23-C22	118.7(3)
O2-S1-C16	109.47(14)	C23-C24-C25	121.0(3)
O1-S1-C16	105.86(14)	C24-C25-C26	120.2(4)
O2-S1-C1	108.63(13)	C27-C26-C25	119.7(3)
O1-S1-C1	103.94(12)	C26-C27-C22	119.7(3)
C16-S1-C1	110.04(14)	C33-C28-C29	118.6(3)
C6-C1-C2	107.4(2)	C33-C28-C4	117.9(3)
C6-C1-S2	108.54(19)	C29-C28-C4	123.5(3)
C2-C1-S2	111.1(2)	C28-C29-C30	120.3(3)
C6-C1-S1	109.42(19)	C31-C30-C29	120.5(3)

*Chapter 2. Experimental section*

---

C2-C1-S1	107.14(19)	C30-C31-C32	119.4(3)
S2-C1-S1	113.08(14)	C31-C32-C33	120.0(3)
O4-S2-O3	119.28(14)	C32-C33-C28	121.1(3)

---

Symmetry transformations used to generate equivalent atoms.

**Table 3.** Torsion angles [°] for **75l**.

O2-S1-C1-C6	-159.12(19)
O1-S1-C1-C6	73.7(2)
C16-S1-C1-C6	-39.3(2)
O2-S1-C1-C2	84.7(2)
O1-S1-C1-C2	-42.5(2)
C16-S1-C1-C2	-155.5(2)
O2-S1-C1-S2	-38.0(2)
O1-S1-C1-S2	-165.22(17)
C16-S1-C1-S2	81.8(2)
C6-C1-S2-O4	-55.1(2)
C2-C1-S2-O4	62.8(2)
S1-C1-S2-O4	-176.73(17)
C6-C1-S2-O3	72.8(2)
C2-C1-S2-O3	-169.3(2)
S1-C1-S2-O3	-48.8(2)
C6-C1-S2-C22	-169.30(18)
C2-C1-S2-C22	-51.4(2)
S1-C1-S2-C22	69.09(19)
C6-C1-C2-C3	-10.9(3)
S2-C1-C2-C3	-129.5(2)
S1-C1-C2-C3	106.6(2)
C1-C2-C3-C5	6.5(3)
C1-C2-C3-C4	72.5(3)
C5-C3-C4-C28	-109.1(3)
C2-C3-C4-C28	151.3(3)
C2-C3-C4-C5	-99.6(3)
C4-C3-C5-C7	108.3(3)

---

C2-C3-C5-C7	-143.4(3)
C2-C3-C5-C4	108.4(2)
C4-C3-C5-C6	-107.9(2)
C2-C3-C5-C6	0.5(3)
C28-C4-C5-C7	-1.8(4)
C3-C4-C5-C7	-115.1(3)
C28-C4-C5C3	113.3(3)
C28-C4-C5-C6	-148.3(3)
C3-C4-C5-C6	98.4(3)
C7-C5-C6-C1	140.0(2)
C3-C5-C6-C1	-7.3(3)
C4-C5-C6-C1	-72.1(3)
C2-C1-C6-C5	11.2(3)
S2-C1-C6-C5	131.42(19)
S1-C1-C6-C5	-104.8(2)
C3-C5-C7-C8	-7.7(4)
C4-C5-C7-C8	65.0(4)
C6-C5-C7-C8	-149.2(3)
C3-C5-C7-C15	64.6(4)
C4-C5-C7-C15	137.3(3)
C6-C5-C7-C15	-76.9(4)
C5-C7-C8-C15	108.8(3)
C5-C7-C8-C9	-137.5(3)
C15-C7-C8-C9	113.7(3)
C15-C8-C9-C10	-74.3(4)
C7-C8-C9-C10	-146.4(3)
C8-C9-C10-C11	102.4(4)
C9-C10-C11-C12	-73.1(5)
C10-C11-C12-C13	1.0(6)
C11-C12-C13-C14	74.6(5)
C12-C13-C14-C15	-107.6(3)
C9-C8-C15-C14	3.4(5)
C7-C8-C15-C14	111.3(3)

C9-C8-C15-C7	-107.9(3)
C13-C14-C15-C8	71.4(4)
C13-C14-C15-C7	143.6(3)
C5-C7-C15-C8	-114.4(3)
C5-C7-C15-C14	134.8(3)
C8-C7-C15-C14	-110.7(3)
O2-S1-C16-C17	-139.6(2)
O1-S1-C16-C17	-10.6(3)
C1-S1-C16-C17	101.1(3)
O2-S1-C16-C21	35.0(3)
O1-S1-C16-C21	163.9(2)
C1-S1-C16-C21	-84.4(3)
C21-C16-C17-C18	1.0(5)
S1-C16-C17-C18	175.5(3)
C16-C17-C18-C19	-0.6(5)
C17-C18-C19-C20	0.2(5)
C18-C19-C20-C21	0.0(5)
C19-C20-C21-C16	0.3(5)
C17-C16-C21-C20	-0.8(5)
S1-C16-C21-C20	-175.1(2)
O4-S2-C22-C23	150.4(2)
O3-S2-C22-C23	20.4(3)
C1-S2-C22-C23	-97.5(3)
O4-S2-C22-C27	-26.8(3)
O3-S2-C22-C27	-156.8(2)
C1-S2-C22-C27	85.3(3)
C27-C22-C23-C24	-1.8(5)
S2-C22-C23-C24	-179.0(3)
C22-C23-C24-C25	-0.1(5)
C23-C24-C25-C26	1.6(5)
C24-C25-C26-C27	-1.2(5)
C25-C26-C27-C22	-0.7(5)
C23-C22-C27-C26	2.2(5)

S2-C22-C27-C26	179.4(3)
C3-C4-C28-C33	170.7(3)
C5-C4-C28-C33	98.9(3)
C3-C4-C28-C29	-10.2(5)
C5-C4-C28-C29	-81.9(4)
C33-C28-C29-C30	-1.4(4)
C4-C28-C29-C30	179.5(3)
C28-C29-C30-C31	1.9(5)
C29-C30-C31-C32	-1.3(5)
C30-C31-C32-C33	0.1(5)
C31-C32-C33-C28	0.4(5)
C29-C28-C33-C32	0.2(5)
C4-C28-C33-C32	179.4(3)

---

Symmetry transformations used to generate equivalent atoms

UNIVERSITAT ROVIRA I VIRGILI

GOLD(I)-CATALYZED CYCLIZATIONS OF 1,6- AND 1,7-ENYNES: NEW GOLD COMPLEXES AND CYCLOPROPANATION REACTIONS

Elena Herrero Gómez

ISBN: 978-84-692-5924-5/DL:T-1663-2009

UNIVERSITAT ROVIRA I VIRGILI

GOLD(I)-CATALYZED CYCLIZATIONS OF 1,6- AND 1,7-ENYNES: NEW GOLD COMPLEXES AND CYCLOPROPANATION REACTIONS

Elena Herrero Gómez

ISBN: 978-84-692-5924-5/DL:T-1663-2009

UNIVERSITAT ROVIRA I VIRGILI

GOLD(I)-CATALYZED CYCLIZATIONS OF 1,6- AND 1,7-ENYNES: NEW GOLD COMPLEXES AND CYCLOPROPANATION REACTIONS

Elena Herrero Gómez

ISBN: 978-84-692-5924-5/DL:T-1663-2009